2-1-2012

Biosorption of uranium and its effect on uranium transport in groundewater

Jeanette Leavitt

Jeanette Leavitt

Candidate

Civil Engineering

Department

This dissertation is approved, and it is acceptable in quality and form for publication:

Approved by the Dissertation Committee:

Kerry Howe , Chairperson

Steve Cabaniss

Bruce Thomson

Andrew Schuler

Paul Reimus

BIOSORPTION OF URANIUM AND ITS EFFECT ON URANIUM TRANSPORT IN GROUNDWATER

by

JEANETTE LEAVITT

B.S., Chemical engineering, New Mexico State University, 2001
M.S., Civil engineering, University of New Mexico, 2006
Ph.D., Engineering, University of New Mexico, 2011

DISSERTATION

Submitted in Partial Fulfillment of the
Requirements for the Degree of

Doctor of Philosophy
Engineering

The University of New Mexico
Albuquerque, New Mexico

December, 2011

DEDICATION

To my husband Aaron, thank you for supporting my decision to walk away from different high-paying jobs over the years in my quest for higher education. Most of all, thank you for all the love and emotional support you have given me as I have ventured through this quest.

To my daughter Kelsey, may this inspire you to have the strength to follow your heart, walk your own path, and achieve your dreams.

To my Dad, thank you for teaching me the value of hard work and for stressing the value of education. You have instilled in me the courage to walk my own path and the strength to never give up, even in the toughest of times. I wish you were here to see me get this final degree and share in my joy.

To Dr. Kerry Howe and Dr. Steve Cabaniss, thank you both for having the patience to teach me the things I should have already known and for your abilities to impart, in a manner I could understand, the knowledge I needed to achieve my goal of obtaining a Ph.D. Throughout my life, I will feel your influence on my professional development and education and I greatly appreciated it.

THE EFFECTS OF BISORPTION ON URANIUM TRANSPORT IN A BIO-REMEDIATED AQUIFER

by

Jeanette Leavitt

B.S., chemical engineering, New Mexico State University, 2001

M.S., civil engineering, University of New Mexico, 2006

Ph.D., Engineering, University of New Mexico, 2011

ABSTRACT

In past years, microbial reduction has been explored as a remediation method for uranium-contaminated groundwater at U.S. Department of Energy sites with promising results. Although transport models have been improved to include variations in geochemical concentrations, reductive microbial processes, and adsorption of uranium to minerals, they do not incorporate the presence of microorganisms as sorption sites that may influence the overall transport of uranium.

The main objective of this research was to determine the effects of uranium biosorption on the overall transport of uranium by understanding the solution chemical equilibrium and its effects on modeling sorption. This was done by first evaluating the uncertainty associated with uranium equilibrium speciation and its effect on the prediction of uranium sorption to minerals. Then, the partition coefficient between U(VI) and the microbial species *Geobacter uraniireducens* and *Acholeplasma palmae* were experimentally determined. The experimentally obtained partition coefficients were used to incorporate biosorption into a thermodynamic model that describes the distribution of uranium in a system with microorganisms available as sorption sites.

When considering mineral adsorption equilibrium, modeling predictions were robust with respect to adsorbed U(VI) concentration, as indicated by the resulting normal Gaussian distributions. Modeling predictions also indicated the amplification of uncertainty with background levels of total U(VI) and higher estimates of input uncertainty (spatial and

temporal variability), as indicated by the resulting bi-modal Gaussian distributions. Experimental results indicate that U(VI) sorbs more strongly, approximately 300 times, to *G. uraniireducens* under low-dissolved inorganic carbon (DIC) conditions and decreases as DIC increases. Under low-DIC conditions, the K_D obtained for uranium sorption to *G. uraniireducens* is 7985 ± 1024 L kg^{-1}, which is larger than the K_D of 1850 ± 1.8 L kg^{-1} determined for uranium sorption to the surface of *A. palmae*.

Beamline analysis on sorption tests with *G. uraniireducens* detected reduction had occurred in these experiments without the addition of an external electron source, indicating that the obtained K_D values are overestimated for *G. uraniireducens*. While the partition coefficients of the bacteria in high-DIC waters are comparable to reported U(VI)- mineral sorption, when combined with the bacterial concentration during and after remediation, the amount of uranium sorbed to the microorganisms is not large enough to produce a noticeable effect on the transport of uranium in a bioremediated aquifer. Finally, the reactions that describe sorption as captured by the experimentally obtained partition coefficients were best described by the sorptive site reacting with uranium and one or two carbonate groups.

Contents

List of Figures viii
List of Tables ix
Chapter 1: Introduction 1
Objective 6
Chapter 2: Background 8
Modeling Uncertainty 8
Biosorption 12
Chapter 3: Evaluation of Modeling Error 21
Methods 21
Determinate Error 22
Indeterminate Error (Uncertainty) 32
Results and Discussion 38
Determinate Error 38
Indeterminate Error (Uncertainty) 45
Chapter 4 Evaluation of Biosorption 56
Materials and Methods 56
Microorganisms 56
Artificial Groundwater (AGW) 60
Sorption experiments 65
Analytical techniques 68
Results and Discussion 71
Sorption Isotherms 71
Images of uranium sorption by bacteria 81
Speciation 87
SCM Parameter for Uranium Sorption to *G. uraniireducens* 94
Chapter 5: Conclusions 99
Modeling 99
Determinate Error 99
Indeterminate Error 100
Biosorption 100

Acknowledgments..... 101
References.....103
Appendix A……...……....112
Appendix B……...……....130

List of Figures

Figure 1: Old Rifle site bounded to the south by the Colorado River [8]. 21
Figure 2: Old Rifle site [8]. 22
Figure 3: Representation of how activity coefficients deviate as a function of increasing ionic strength and different ionic strength correction approaches [52]. 29
Figure 4: Old Rifle site area [70].. 37
Figure 5: Carbonic acid speciation concentration as a function of pH done with VisualMINTEQ using 1.4 uM uranium difference that are captured between atmospheric and 2% P_{CO2}. 45
Figure 6: Log concentrations of calculated sorbed and dissolved U(VI) as a function of total U(VI) in the system. 47
Figure 7: Sensitivity (first derivative) analysis for effects of uncertainty on three key U(VI) species concentrations for 11 analytical constraints in a dissolved-only system. 48
Figure 8: Monte Carlo simulations of System I (dissolved-only), showing frequency of result versus log concentration. 49
Figure 9: Sensitivity (first derivative) analysis for effects of uncertainty on U(VI) species concentrations for 14 analytical constraints in dissolved-solid partitioning system. 51
Figure 10: Monte Carlo simulations of System II (dissolved and sorbed) with 8.65 µM total U(VI) showing the frequency of result versus log concentration 52
Figure 11: Monte Carlo simulations of System II (dissolved and sorbed) with 3.50 µM total U(VI) showing the frequency of result versus log concentration 54
Figure 12: Bacteria growth charts 57
Figure 13: Cryo-EM image of *A. palmae* showing intact cells after rinse and re-disbursement into experimental solution. 59
Figure 14: Cryo-EM image of *G. uraniireducens* presenting intact cells with some membrane disturbance after rinse and re-disbursement into experimental solution. 59
Figure 15: Changes in soluble DIC concentrations as a function of P_{CO2} at pH 7. System modeled using VisualMINTEQ. 60
Figure 16: Effects on the DIC distribution for water exposed to 2% P_{CO2} a function of solution pH. System modeled by VisualMINTEQ. 61
Figure 17: Preparation for bulk solution to set pH at desired $P_{CO2.}$ 64
Figure 18: Final experimental preparation. 67
Figure 19: Uranium sorption to *G. uraniireducens* under atmospheric P_{CO2} at pH 6.95 ±0.05 with 6.5 mM calcium and 8.5 mM sulfate. 72
Figure 20: Uranium sorption isotherm to *G. uraniireducens* under 2% P_{CO2} at pH 7±0.2 with 6.5 mM calcium and 8.5 mM sulfate. 72

Figure 21: Uranium sorption to *G. uraniireducens* under atmospheric P_{CO2} at pH 6.95 ±0.05 with 6.5 mM calcium and 8.5 mM sulfate.. 74
Figure 22: Comparison of sorption capacity of both types of bacteria within similar ranges 75
Figure 23: Uranium sorption isotherm to *A. palmae* at atmospheric P_{CO2} at pH 7 ± 0.2 with 6.5 mM calcium and 8.5 mM sulfate. 77
Figure 24: Cryo-EM images of uranium sorption to *G. uraniireducens* OM under 2% P_{CO2} and 1.4 □M U. Uranium is indicated by the darkened areas of the cellmembrane. 82
Figure 25: EDX analysis of patchy deposits on the OM of geobacter, which confirms uranium sorption. 82
Figure 26: Cryo-ET of uranium sorption to *G. uraniireducens* under 2% P_{CO2} and 50 uM uranium 84
Figure 27: Experimentally obtained sorption (System II, contains solution and bacteria) compared to modeled (System I contains solution only) uranium carbonate concentration. Modeling performed with VisualMINTEQ. 90
Figure 28: Calcium sweep of Old Rifle site critical components pH 7 to evaluate the effects on uranyl distribution. 92
Figure 29: Sulfate sweep of Old Rifle site critical components pH 7 to evaluate the effects on uranyl distribution. 93
Figure 30: U(VI) sweep of Old Rifle site critical components at pH 7 to evaluate the effects on uranyl distribution. 94

List of Tables

Table 1: Input parameters used to define the Old Rifle site for thermodynamic equilibrium calculations [76]. This input file results in an ionic strength of 0.0382. 23
Table 2: Equilibrium programs used to evaluate model error 23
Table 3: List of thermodynamic constraints that were used in equilibrium simulations and uncertainty calculations. Formation constants written using H^+, UO_2^{2+}, Ca^{2+}, Mg^{2+}, Sr^{2+}, Na^+, K^+, CO_3^{2-}, SO_4^{2-}, NO_3^-, Cl^- and H_2O as components. Uncertainty values were determined from those listed in the NIST database or set by the user, as explained in the text above. 26
Table 4: Parameters used to determine sorption site concentration and equilibrium calculations. All sorption reactions were taken from Fang et al. [24]. 34
Table 5: Critical input concentrations as defined by first-derivative analyses used in Monte Carlo simulations. All other inputs parameters are standard as listed. 37
Table 6: Percent distribution of U(VI) among the aqueous species using default databases with various thermodynamic equilibrium programs. 39
Table 7: Calculated ion strength using the different ionic strength corrections with the different programs. 41
Table 8: Difference is the species concentration determined input parameters of 480 mg L^{-1} $CaCO_3$ alkalinity and 531 mg L^{-1} carbonate and those listed in Table 1. 44
Table 9: Summary statistics of distributions in Figure 8 (System I) 49
Table 10: Summary statistics of distributions in Figure 10 (System II, 8.65 µM total U(VI)) 52
Table 11: Summary statistics of distributions for system with low uranium concentration in Figure 11 (System II, 3.50 µM total U(VI)) 53

Table 12: Uranyl distribution at pH = 6.95, Ca^{2+} = 6.5 mM, SO_4^{2-} = 8.5 mM using VisualMINTEQ using complete database listed in Table 3 of Chapter 3. A shift in uranyl distribution from approximately 99% calcium-uranyl-triscarbonato species only occurs between atmospheric and 2% P_{CO2}. 62
Table 13: Available surface area based on bacteria mass assuming a density of 1 g cm^{-3}. This analysis is on the test performed under atmospheric P_{CO2} conditions. 75
Table 14: Experimental K_D converted for direct surface-area comparison using data presented in the previous table. 76
Table 15: Comparison of K_D values for material exposed to elevated DIC. [a] references to values obtained from this work, [b] values obtained from [17], [c] value obtained from [82], [d] value obtained from [42] 79
Table 16: The concentration of bacteria at the Old Rifle site in the pore water and sediment used to calculate the concentration in the aquifer. The Old Rifle site sediment density was used to determine the number of bacteria per volume of sediment, and the site porosity was used to obtain the final value listed. 80
Table 17: Percent uranium distribution under different CO_2 partial pressures at an ionic strength of 0.04, a pH of 6.95 with 6.5 mM calcium, 8 mM sulfate, 1.4 μM $U(VI)^{+2}$ 88
Table 18: Summary of simulated results lisiting log K values, which result in equivalent experimental uranium distribution at atmospheric P_{CO2} and the corresponding K_D values at 2% P_{CO2}. 97
Table 19: Soluble uranium distribution at equilibrium in the modeled system that accounts for sorption. Results obtained from using sorption equations 1 and 2 with associated log K values. . 97

Chapter 1: Introduction

Uranium exists naturally in the earth's crust and hydrosphere [1]. While it is a natural constituent of the environment, elevated concentrations as a result of mining are concerning due to the radioactivity, toxicity, and solubility of uranium. In 1978, the Uranium Mill Tailings Radiation Control Act (UMTRCA) established a uranium concentration limit of 44 $\mu g\ L^{-1}$ as safe for public health and the environment, which was enforced by the U.S. Environmental Protection Agency (EPA) [2]. The EPA further reduced this limit to 30 $\mu g\ L^{-1}$ in 2000 through the Radionuclide Rule listed in the Safe Drinking Water Act (SDWA) [3, 4]. The uranium concentration in natural waters at contaminated sites has been measured well in excess of these recommended levels for potential drinking water [4, 5]. As a result of the high levels of uranium detected in the environment and the defined regulations, the U.S. Department of Energy (DOE) has identified and begun the remediation of 120 different uranium contaminated areas, covering more than 7,280 square kilometers, in 36 states and territories [6].

The Old Rifle site is the location of a former vanadium and uranium processing mill, which operated from 1924 to 1958. The mill was located on 24 acres of land, atop an alluvial floodplain directly above an impermeable boundary. This land is on the north side of the Colorado River and is approximately 0.3 mile east of Rifle, Colorado. Due to contamination resulting from former milling activities, the site became a Uranium Mill Tailings Remedial Action (UMTRA) site as dictated by the 1978 UMTRCA legislation. This categorization resulted in remediation activities to address surface contamination in 1996, leaving only groundwater contamination as the unresolved issue [7].

In the late 1990s, the DOE decided to implement a groundwater remediation strategy consisting of natural attenuation with administrative controls, such as limited access and groundwater monitoring at the Old Rifle site [8]. The alluvial aquifer flushes into the Colorado River because it is surrounded in all other directions by the impermeable Wasatch formation. Numerical modeling of groundwater flow and contaminant transport

indicated that concentrations of uranium will decrease to UMTRCA standards or background concentrations, which also meet the 2000 EPA SDWA standards, during a 100-year natural flushing period [8].

Two oxidation states of uranium are generally considered geochemically relevant when predicting its fate and transport in the natural environment. 1) Hexavalent uranium, U(VI), is highly soluble in water, while 2) tetravalent uranium, U(IV), is sparingly soluble and easily precipitates to form the mineral uraninite, UO_2 (s). Pentavalent uranium, U(V), is soluble in solution but it quickly disproportionates to U(VI) and U(IV), therefore is not addressed when estimating the transport of uranium in the natural environment [9]. The degree of mobility of U(VI) in groundwater is highly influenced by its speciation, which is described below.

In low pH waters, pH less than 5, the mobility of U(VI) is decreased due to the dominate speciation represented by the UO_2^{+2} cation and its adsorption behavior with subsurface minerals [10]. In the presence of high-carbonate concentrations, the major species shift to uranyl-carbonates, resulting in decreased adsorption to the minerals and allowing U(VI) to remain mobile [11, 12]. In the mid-1990s, the calcium-uranyl-triscarbonato species was identified as the major species in the presence of high-carbonate waters and alkaline earth metals. The formation of this species further decreases uranium-mineral adsorption [13-18]. Before this discovery, the major species were expected to be uranyl-carbonates in the presence of high-carbonate waters and alkaline earth metals and the decreased uranium-mineral adsorption due to the formation of this recently discovered species was not accounted for.

Because uranium speciation directly correlates to the affinity of uranium to surrounding minerals, uranium equilibrium speciation and associated uncertainties must be understood to predict its fate and transport in natural waters. Soluble uranium, U(VI), species concentrations and sorption over an entire contaminated area are variable due to the spatial and temporal variability of natural systems. Traditionally, multiple and representative *in situ* measurements of these areas to determine the total soluble uranium

concentration are prohibitively difficult and expensive [19]. While progress has been made that lessens the cost and difficulties with *in situ* measurements through the application of passive flux membranes [20], aqueous thermodynamic equilibrium codes remain the preferred tool in predicting transport of and bioavailability of contaminants [19]. Though the mathematical predictions of solution equilibria will have inherent uncertainty associated with the complexity of natural systems [21], chemical transport models coupled with aqueous thermodynamic equilibrium speciation modeling have been employed to estimate *in situ* speciation and concentrations of contaminants of concerns for large areas of contamination [11, 22-24].

The calculations to predict aqueous speciation can be performed by various thermodynamic equilibrium codes, such as VisualMINTEQ[25], PHREEQC[26], and TITRATOR[27]. These codes rely upon a database of reactions, associated reaction energies (thermodynamic constraints, such as equilibrium coefficients), and a set of measured or postulated concentrations (analytical constraints, such as total concentrations of each constituent solution). The algorithms used by these codes predict the speciation and concentration at equilibrium for a given area by iteratively solving a mass balance using the previously mentioned parameters. However, the similarity of the predicted concentrations to field conditions is subject to potential problems related to the user-defined thermodynamic and analytical constraints [21, 28].

While natural attenuation with administrative controls is the chosen remediation approach at the Old Rifle site [8], the DOE has sponsored an investigation into the more time-efficient strategy of bioremediation of uranium at the site. The approach of bioremediation was evaluated in a field study that examined the effect of stimulating subsurface microorganisms growth to remove soluble uranium from solution. While microorganisms cannot destroy uranium, the oxidation states of uranium can be manipulated by enzymatically reducing soluble U(VI) to insoluble U(IV) to limit the bioavailability of the element. This new strategy may not only remediate the site faster than natural attenuation, but it may also influence the transport of uranium by adding sorption to biological materials not previously considered in the current transport model of the Old Rifle site [29].

In the early 1990s, the standing belief that U(VI) reduction in natural environments was solely an abiotic process spurred by the reaction of U(VI) with organic compounds, molecular hydrogen, and sulphides [30-32] was changed by Lovley and colleagues [33]. The Lovley group was the first to establish the enzymatic reduction of uranium by two different iron-reducing bacteria: *Shewanella putrefaciens* and the *Geobacter* species, GS-15 [33]. This research proved these microorganisms obtained energy for growth by electron transport to U(VI). The results of these experiments were obtained under anaerobic conditions using acetate as the electron donor for GS-15 and hydrogen as the electron donor for *S. putrefaciens*. The Lovley group not only proved microbial mediated reduction of U(VI) can occur, it also provided a possible explanation for uranium deposits found in aquifers and related sediments [33]. As a result of these findings, scientists began examining enzymatic U(VI) reduction as a new method for remediating uranium contaminated areas.

To further explore the enzymatic reduction of U(VI) as a possible remediation process, the ability of the microorganism to precipitate uranium from solution had to be confirmed. This ability was proven by Gorby and Lovley using a GS-15 culture and acetate as the electron donor [34]. During their anaerobic laboratory experiments, U(VI) was removed from solution as a black precipitate appeared. X-ray diffraction analysis of this black precipitate determined that the material was the U(IV) mineral, uraninite (UO_2), which is the most commonly occurring U(IV) mineral in anoxic sediments and aquifers [31, 35]. The presence of this material proved that uranium could not only be reduced by microorganisms, but also could be precipitated from solution.

Given that enzymatic reduction and precipitation of uranium from solution was proven, many studies were done to further understand the microbial reduction of uranium. These further investigations found some sulfate-reducing microorganisms that can reduce iron can also reduce uranium, although they do not obtain energy from either of these enzymatic reductions [36, 37]. As investigations progressed on the subject, it was determined that most microorganisms can recover energy to support growth by oxidizing organic compounds or hydrogen with the reduction of iron can also reduce U(VI) [38].

Because many different iron-reducing and sulfate-reducing microorganisms may facilitate uranium reduction, Finneran et al. expanded the investigation of U(VI) microbial reduction with the use of naturally existing microorganisms found in field sediment and groundwater [39]. In these studies, Finneran et al. used different organic oxidizing compounds with sediment and groundwater obtained from a DOE UMTRA site located in Shiprock, New Mexico. Different organic compounds were added to the sediment-groundwater mixture in efforts to stimulate the growth of the existing indigenous microorganisms and evaluate any subsequent uranium reduction. Their results demonstrated that acetate amendments can successfully promote the reduction and removal of uranium from the groundwater through the facilitated growth of native organisms. They also found that reduction was associated with the growth of iron-reducing microorganisms belonging to the *Geobacteraceae* family that are closely related to the laboratory-pure culture, GS-15. Additionally, it was determined that sulfate reducers are probably not important participants in reduction [39].

To determine whether results of laboratory sediment incubation could be extrapolated to field conditions, Anderson et al. further evaluated the process of uranium bioremediation at a field level [40]. This was done by applying acetate amendments to a uranium contaminated aquifer in Rifle, Colorado until the geochemical environment shifted from an iron-reducing environment to a sulfate-reducing environment. Within 50 days of acetate injections, the soluble uranium concentration declined below the prescribed treatment level. It was also determined that the initial removal of uranium from the treatment area was related to the enrichment of *Geobacter* species. This research supports that microbial reduction of uranium is an effective remediation process and demonstrates that the process can be optimized to support the long-term activity of the *Geobacter* species [40].

While the research conducted by Anderson et al. [40] provided more support for microbial reduction to be used as a remediation process, it also exposed weaknesses associated with the process. Vrionis et al. began investigations on how to improve the bioremediation process by examining microbial communities at the Old Rifle site and the related geochemistry in both the groundwater and sediment [41]. The results of their

investigation demonstrated that reduction was highly impacted by the heterogonous nature of the aquifer. Heterogeneity of the solid phase may have resulted in different exposure to geochemical conditions that influence both the activity and diversity of reducing microorganisms. These findings suggest that the electron donor amendments be done in a manner that accounts for the site heterogeneity. The Vrionis group also recommends close interval sampling for future studies to better understand microbial composition of the aquifer and to improve models of the process influencing *in situ* uranium bioremediation [41].

While issues associated with maintaining the bioremediation process at the Old Rifle site were investigated, a positive unexpected phenomenon as a result of this process was captured through long-term groundwater monitoring. After bioremediation activities ceased at the site, uranium concentrations in the groundwater continued to decrease. Upon further examination of this unexpected phenomenon, N'Guessan et al. postulated that the continued uranium removal may be associated with U(VI) adsorption to the enhanced biomass of the natural microbial community resulting from remediation [29].

Objective

While the field research at the Old Rifle site demonstrated the effective microbial reduction of uranium, it emphasized that the effects associated with site heterogeneity must be examined. It also identified the need to understand how the artificially increased concentrations of microorganisms affected uranium transport. Uranium sorption to minerals in uranium-contaminated sites has been successfully studied and modeled [23, 42], but sorption to biomaterials has not been considered in such models. Given the identified knowledge gap, it is necessary to examine uncertainties with speciation due to aquifer heterogeneity, which affects uranium sorption to any material, before examining the issue of uranium biosorption. Once this is accomplished, evaluating biosorption under the Old Rifle site conditions can determine the effect on uranium transport.

The first part of this research evaluates the impact of thermodynamic and analytical uncertainty on the speciation of U(VI) in high-carbonate groundwater, such as that of the Old Rifle site. First-derivative sensitivity analyses and Monte Carlo simulations were

performed to determine the uncertainty in U(VI) speciation resulting from typical levels of analytical uncertainty, spatial variability, and temporal variability. Once uncertainty was analyzed, the sensitivity analysis was used to define artificial groundwater composition to investigate the effects of increased biomass on uranium transport after bioremediation at the Old Rifle site.

The study of U(VI) sorption to the microorganisms, *Geobacter uraniireducens* and *Acholeplasma palmae*, began by determining partition coefficients under Old Rifle site conditions between uranium and the different bacteria. Once the partitioning coefficients characterized the affinity for uranium sorption to the different bacteria, the physical location of sorbed uranium was investigated using cryo-electron microscopy (EM), energy dispersive x-ray spectroscopy (EDS), and beamline x-ray spectroscopy. A comparison of uranium sorption capacity between the two bacteria species and mineral sorption was also performed. The effects of critical components as identified by the sensitivity analysis on experimental sorption were reviewed. Finally, experimentally obtained partitioning coefficients were used to develop equilibrium constants, which were incorporated into the surface complexation model that describes solid-dissolved uranium partitioning under Old Rifle site geochemistry.

Chapter 2: Background

Modeling Uncertainty

Thermodynamic equilibrium modeling is one part of a multifaceted transport model used to predict contaminant fate and transport [24, 42]. In equilibrium modeling, there are two types of errors that propagate uncertainty in a calculated prediction. These errors can be termed as determinate and indeterminate. Determinate errors result from uncertainties associated with ill-defined model parameters, such as flawed input concentrations or inaccurate equilibrium constants. Indeterminate errors are uncertainties associated with equipment limitations or techniques used to determine the concentration of input parameters. Eliminating determinate errors and identifying indeterminate errors can result in a simulation with defined bounds of uncertainty.

Omitted chemical reactions and/or incorrectly defined reactions are factors that can lead to determinate errors in thermodynamic simulations. Serkiz et al. found that errors in solutions produced using the thermodynamic equilibrium program, MINTEQA2, would arise due to reactions not properly expressed in terms of MINTEQA2 components [43]. In 1996, Bernhard et al. identified the formation of the di-calcium-uranyl-triscarbonato complex, $Ca_2UO_2(CO_3)_3$ (aq) [13]. In 2001, they also identified the formation of the calcium-uranyl-triscarbonato complex, $CaUO_2(CO_3)_3^{-2}$ [14]. These complexes account for the largest distribution of uranium in high dissolved inorganic carbon (DIC) waters with alkaline earth metals. Before this research, the reactions and the associated equilibrium coefficients to produce these complexes were not included in equilibrium programs. Research performed before 2001 with the previously mentioned conditions resulted in erroneous equilibrium solutions because the reactions related to the formation of the calcium-uranyl-triscarbonato species were not included. The omission of reactions can be due to lack of knowledge, an oversight on the user's part, or due to the fact that the reaction was yet to be confirmed as the case of the calcium-uranyl-triscarbonato species. Regardless of the source of omission, the result of obtaining an erroneous equilibrium prediction is still the same.

Not correcting the thermodynamic equilibrium constants to specified reference states can also be a source of determinate error. Serkiz et al. found in their analysis that solutions

generated with equilibrium constants, log K values, that were not corrected to zero ionic strength or standard temperature resulted in avoidable error [43]. An example of this error can be seen when examining the log K values of the aqueous calcium-uranyl-triscarbonato species, $CaUO_2(CO_3)_3^{2-}$ and $Ca_2UO_2(CO_3)_3^0$ formed from the reaction of Ca^{2+} with $UO_2(CO_3)_3^{4-}$ (equation 1 and 2).

$$K_1 = \frac{[Ca_2UO_2(CO_3)_3^0]}{[M^{2+}]^2[UO_2(CO_3)_3^{4-}]} \quad (1)$$

$$K_2 = \frac{[Ca_2UO_2(CO_3)_3^0]}{[M^{2+}][UO_2(CO_3)_3^{4-}]} \quad (2)$$

The log K values for these species obtained by Dong and Brooks [16] are the most recent and were obtained from the best fit of experimental data at an ionic strength of 0.1 M, which was then corrected to zero ionic strength. The experimentally obtained values were, on average, two log units smaller (3.63 ±0.04 and 6.29± 0.04) than values corrected by the Davies equations to an ionic strength of zero (5.34 ±0.04 and 8.86±0.04) [16].

Another determinate error associated with the ionic strength correction of a thermodynamic constant can be caused by the choice of ionic strength correction approach. The log K value for the $Ca_2UO_2(CO_3)_3^0$ complex in terms of calcium, the free uranyl ion, and carbonate reacting in solution (equation 3) was determined to be 29.8 ± 0.7 at zero ionic strength by Kalmykov and Choppin using the specific ion interaction theory (SIT) [44]. This value was in agreement with the value originally stated in 1996 by Bernhard et al. [13], but lower than the latest values produced in 2001 by the Berhard et al. study [14] and in 2006 by Dong and Brooks [16]. The log K value for the $Ca_2UO_2(CO_3)_3^0$ complex produced by Dong and Brooks [16] is 30.7 ± 0.5 at zero ionic strength, which is similar to the value of 30.6 ± 0.3 at zero ionic strength determined by the 2001 Bernhard et al. study [14]. The log K values from all studies are similar when considering the associated uncertainty, but most thermodynamic equilibrium programs only use a specifically defined value for input constraints. Therefore, the use of log K values chosen by the ionic strength correction approach can change the value by approximately one log unit for the $Ca_2UO_2(CO_3)_3^0$ complex. This difference in log K values will result in erroneous uranium equilibrium speciation.

$$XM^{2+} + UO_2^{+2} + 3CO_3^{2-} = M_xUO_2(CO_3)_3^{(2x-4)} \quad (3)$$

The equilibrium constant for the $CaUO_2(CO_3)_3^{-2}$ complex was updated by research results obtained by Dong and Brooks [16]. Their log K value was 1.58 orders of magnitude different than the original value obtained by the 2001 Bernhard et al. study [14]. The difference in the values was attributed to the binding constants of Ca^{2+} to $UO_2(CO_3)_3^{4-}$ and $CaUO_2(CO_3)_3^{2-}$. The 2001 Bernhard et al. study [14] indicated that the binding constant of Ca^{2+} to $CaUO_2(CO_3)_3^{2-}$ is much larger than that of Ca^{2+} to $UO_2(CO_3)_3^{4-}$, while Dong and Brooks [16] determined the opposite. The equilibrium constant, as determined by Dong and Brooks [16], is in agreement with the expected trend in the stepwise formation constant, resulting in the binding of Ca^{2+} to $UO_2(CO_3)_3^{4-}$ to be larger than that of Ca^{2+} to $CaUO_2(CO_3)_3^{2-}$. Given this information, the log K value for the $CaUO_2(CO_3)_3^{2}$ complex was updated to the value determined by Dong and Brooks [16]. Using the value as determined by the 2001 Bernhard et al. study [14] instead of the latest value determined by Dong and Brooks [16] will result in determinate error.

Determinate errors can also arise from missing or out-of-date log K values. Unsworth et al. compared thermodynamic equilibrium solutions using original thermodynamic data provided with different speciation models [45]. Using the unaltered default databases, they identified a different uranyl species as the major species for each model. This error can also be seen in the use of the equilibrium constant for the $CaUO_2(CO_3)_3^{-2}$ complex as expressed by equation 3 before 2006, which uses a value that is 1.58 orders of magnitude lower than the current value determined by Dong and Brooks [16].

Another type of determinate error that may misrepresent uranium speciation in a modeled system is the choice of approximations used to represent complex phenomena. These approximations are associated with predicting ion behavior as a function of ideal and non-ideal systems (e.g., ionic strength correction or adsorption model). Davis and Curtis found that assuming a constant ionic strength over an entire site resulted in the overestimation of uranium complexes that sorb when compared to using simulations that considered variable ionic strength [11]. The overestimation in sorption could be from a

decreased activity between the sorption site and soluble species or from misleading soluble speciation due to errors in calculated activity. Weber et al. found that at dilute solutions, using default ionic strength correction approaches as dictated by the program, resulted in comparable results. But as ionic strength increases to that of fresh water levels, the correction methods used to calculate constants tended to result in more uncertain solutions [46].

Indeterminate errors that can impact aqueous speciation modeling results are associated with the uncertainty of thermodynamic constraints (equilibrium constants) and with uncertainties of critical input concentrations. While equilibrium constants are calculated in a controlled system, such as a laboratory environment, applying this constant in environmental systems has an associated inherent deviation from the true value [28]. The thermodynamic value associated with $CaUO_2(CO_3)_3^{2-}$ is a good example of this type of issue. While the underestimation of 1.58 log units in the thermodynamic equilibrium value of the species, $CaUO_2(CO_3)_3^{2-}$ between values obtained by the 2001 study of Bernhard [14] and Dong and Brooks [16] is a determinate error in the viewpoint that two values exist and the best value must be chosen, the value obtained before 2001 is an example of an indeterminate error. Before 2001, the value was the best available value but had an inherent error due to a misunderstanding in the relationship between species formation and the expected trend of the stepwise formation constants, resulting in a deviation from the true value. This misunderstanding resulted in an inherent deviation from the true value.

Indeterminate error can also result when uncertainties associated with constraints are averaged, which neglects the natural heterogeneity of an aquifer. The average value associated with the input concentration is commonly used in modeling for simplification purposes and to control expense [19]. This simplification neglects changes in critical component concentrations due to spatial and temporal differences. Uncertainty in the critical component concentration has been examined in past research, which provides support for the necessity of including a standard deviation or uncertainty associated with the input value in simulations to better understand error associated with the final solutions due to the natural variability [21, 47, 48].

Quantifying the reliability of model predictions is not routine [21, 46, 49, 50]. Provided that determinate errors (model parameter values that can be corrected) are adequately addressed, first-derivative sensitivity analyses and Monte Carlo simulations can suggest bounds of reliability or uncertainty for the calculated speciation results of a defined system. First-derivative sensitivity analyses can be used to identify critical input parameters by evaluating the effect of each input constraint (thermodynamic or analytical) on calculated equilibrium concentrations. Monte Carlo simulations can estimate the effects of thermodynamic and analytical uncertainties of known distribution on calculated equilibrium concentrations [21, 28, 46-49]. For the Monte Carlo simulations, the equilibrium system is solved for P trials in which different values of input constraints are selected randomly from the uncertainty distributions of those constraints. The resulting distribution of calculated concentrations as P approaches infinity represents the predicted uncertainty in that concentration. If the resulting distribution is approximately Gaussian (normal), a mean and standard deviation can be specified. Sometimes non-Gaussian distributions, such as a bimodal distribution, may occur, resulting in a mean and standard deviation that cannot be adequately determined [48, 49], thus indicating that values have some degree of error and should be used with care, if at all. While this approach is valid for equilibrium models because they assume reactions have gone to completion, it may not be directly applicable when considering redox and precipitation/dissolution reactions.

Biosorption

Because sorption is known to be the controlling factor in uranium transport, it is important to understand the distribution of the resulting chemical speciation and affinity of that speciation to sorb to surfaces within the aquifer. If a sorptive site has a demonstrated affinity for uranium, its presence can change the thermodynamic speciation of a system. Therefore, it is necessary to evaluate all possible sorptive sites in a system, such as microbial material which was suggested by N'Guessan et al. [29] to truly predict transport and fate of uranium.

The affinity of a given solute for a specific sorbent is determined by a partitioning coefficient that relates the equilibrium between the concentration of sorbate in solution (mass per volume) and its sorbed concentration (mass sorbate per mass sorbent). In the simplest case, the partitioning coefficient is the linear slope obtained from graphing the previously mentioned parameters. In more complicated situations where the graphed data has a linear slope that changes to zero as it approach a maximum; the partitioning is described from sorption isotherms and not as a simple ratio. Commonly used isotherms are the Langmuir and Freundlich isotherms; both are based on the same graphical relationship described above but differ by the application of additional parameters used to fit the experimental data. The fitting parameters are related to assumptions that are inherent to each isotherm.

The simplest partitioning coefficient, K_D, is determined from the graphical method as described above with no fitting parameters as shown by equation 4.

$$K_D = \frac{q_A}{c_A} \tag{4}$$

Where q_a is the equilibrium sorbent-phase concentration of sorbate A and C_A is the equilibrium concentration of sorbate A in solution.

The Langmuir isotherm incorporates two parameters to describe the partitioning between solid and liquid phases. These constants are the maximum sorption density and the affinity of the sorbent for the sorbate and are based on the following assumptions: 1) site energy for sorption is the same for all sorption sites, and 2) the largest sorption capacity corresponds to only monolayer sorption behavior [51]. The Langmuir isotherm is presented by equation 5.

$$q_a = \frac{Q_m K_L C_A}{1+K_L C_A} \tag{5}$$

Where q_a is the equilibrium sorbent-phase concentration of sorbate A, Q_m is the maximum sorbent-phase concentration of sorbate when surface sites are saturated with sorbent, and C_A is the equilibrium concentration of sorbate A in solution.

The Freundlich isotherm produces a partitioning coefficient, K_f, for sorption to heterogeneous sorbents with a fitting parameter to describe how the binding strength changes as the sorption density changes and is shown by equation 6 [52].

$$q_a = K_f C_A^{\frac{1}{n}} \quad (6)$$

Where q_a is the equilibrium sorbent-phase concentration of sorbate A, K_f is the Freudlich sorption capacity parameter, C_A is the equilibrium concentration of sorbate A in solution and 1/n is the intensity parameter.

Regardless of the approach used to describe sorption, the resulting partitioning coefficient values depend on the chemical composition of the aqueous solutions, and do not take into account temporal and spatial geochemical differences known to exist in aquifers [53]. Therefore, an approach to describe sorption in a manner that removes the known error inherent to the direct use of partition coefficients was necessary. Hence, the surface complexation theory was derived, which describes sorption in terms of chemical reactions between dissolved species and surface function groups using mass action equations and equilibrium coefficients within a general geochemical framework [54]. The four fundamental tenets of this theory are as follows: 1) Specific functional groups are on the surfaces of minerals that reacted with solutes in solutions to form surface species. 2) Sorption reactions are described by mass action equations with corrections factors if necessary to account for electrostatic interactions. 3) The partitioning coefficient is related to thermodynamic constants that represent the formation of complexes formed at the surface of the sorption site. 4) At the surface of a sorption site, the electrical charge is determined by chemical reactions of the functional groups [42].

Using the fundamental tenants of the surface complexation theory, a Surface Complexation Model (SCM) can be developed to describe sorption to natural materials using two different approaches known as the component additivity (CA) approach and the general composite (GC) approach [55, 56]. The CA approach assumes that the sorption of a complex mixture can be predicted from the sum of the contributions from

individual sorptive components. The GC approach is a semi-empirical process that experimentally fits data for the mineral assemblage as a whole by using mass law equations written with "generic" surface functional groups, stoichiometry, and formation constants and eliminates the need to quantify the electrical field and surface charge of the sorptive site [42].

Applying the SCM approach to describe sorption allows the effect of variable aqueous geochemical conditions to be coupled with sorption processes controlled by a limited number of sites. Specifically, applying the SCM GC approach results in a practical approach to simulating non-linear uranium sorption and transport applied at field scale [11]. To expand the SCM GC approach applied by Fang et al. [24] at the Old Rifle site to include microorganisms as sorptive sites, possible functional groups on the surface of the microorganisms for binding uranium and partitioning coefficients must be determined.

Microorganisms, such as fungi, have variable densities of metal-binding functional groups, such as phosphoryl, carboxyl, and amines, present on their cell walls. These functional groups can interact with the surrounding aqueous solution and sequester soluble metals solution [57]. Fungi are eukaryotic organisms, such as yeast and molds. The main component of the fungal cell walls is chitin, which is a long-chain polymer of N-acetylglucosamine. Chitin has carboxylate- and amine-surface functional groups that metals in solution can interact with. Proteins on the fungi surface also provide a source of phosphoryl- and hydroxyl-functional groups that can sequester metals [58].

Bacteria are another type of microorganism that posses surface functional groups capable of metal sequestration. These prokaryotic organisms can be divided into two major groups based on cell wall compositions, which are termed as Gram negative and Gram positive bacteria. In Gram positive bacteria, as much as 90% of the cell wall consists of peptidoglycan (PG), which is a crystal lattice structure made up of linear chains of alternating amino sugars. Free carboxyl groups, amino groups of non-crosslinked amino acids, amides, and hydroxyl groups are potential coordination sites for metal ions [59]. Gram negative bacteria have cell walls consisting of only about 10% peptidoglycan. Most of the cell wall consists of the outer membrane (OM), which is effectively a second lipid bilayer, the lipopolysaccharide layer (LPS). Metal binding may occur to hydroxyl,

phosphoryl, carboxyl, and amino groups that are integrated throughout the LPS [60]. It should also be noted that bacteria that originated from Gram negative or Gram positive bacteria can lack cell walls. Bacteria of this nature include prokaryotic bacteria, mycoplasmas, and thermoplasma groups. These bacteria have rigid cytoplasmic membranes or live in osmotically protected habitats and have rigid membranes that are strengthened by sterols or various lipids providing hydroxyl groups to interact with metals [61].

As with minerals, the sorption of metals to microbial surfaces depends on the functional groups present on the surface and aqueous speciation for the contaminant of concern. In natural systems, the geochemical conditions that have the largest effect on uranium sorption to minerals are pH[42], P_{CO2}[12, 62], and increased P_{CO2} with high calcium concentrations [17]. Although studies have shown uranium sorption to microorganisms, the general focus of these studies was to prove sorption of radionuclides and metals to biological materials or to examine the effects of sorption on microbial growth; therefore, experimental conditions were not designed to capture the effects of parameters, such as elevated P_{CO2} with calcium present, pH, and $P_{CO2,}$ on sorption to microorganisms.

Experimental investigations of uranium sorption to different microorganisms have been performed in low pH solutions. In moderately low pH solutions, the principal uranyl species is uncomplexed uranyl ion, UO_2^{+2}, which has strong affinity to many minerals because of its corresponding negative surface charge except at very low solution pH values. The speciation associated with low pH solutions simplifies the process to prove the occurrence of uranyl sorption to the surface of microorganisms. These studies not only demonstrate that uranium biosorption occurs, but that that maximum sorption occurs at approximately pH 5 for a variety of bacterial species [63-65].

Below pH 5, uranium sorption to microorganisms has been investigated by many research groups. Sarri and et al. used three strains of yeast to investigate uranium biosorption at a solution pH of 4.5 [66]. They found that various species of yeast examined could effectively sorb uranium from a uranium nitrate solution, resulting in a range of K_D values of approximately 800 to 2,000 L kg^{-1}. These values were estimated

from the linear portion of the sorption isotherm presented in Figure 1 of the study [66]. Fowle et al. examined uranium sorption at pH interval of 1.5 -5 using *Bacillus subtilis*, a gram positive bacteria, in a sodium perchlorate solution [65]. The K_D value estimated from Figure 1 presented in the study for 1.5 g L^{-1} bacterial solution at pH 5 was approximately 6,300 L kg^{-1} [65]. Uranium sorption investigations by Hass et al. using the gram negative bacteria, *Shewanella putrefaciens*, resulted in an estimated K_D of 5,000 kg L^{-1} obtained from Figure 4 at pH 5 for 1.72 g L^{-1} of biomass [64]. These low pH studies produced K_D values within in a small range, 1,000 to 7,000 L kg^{-1}, and indicate that the yeast are slightly less sorptive by weight than the gram negative and gram positive bacteria, which have similar sorptive capacity by weight. It is important to note that all studies were performed in an open atmosphere.

Above pH 5, the principal speciation is no longer dominated by the free uranyl ion, UO_2^{+2}, resulting in a more complicated system to evaluate sorption. This is because the free uranyl ion may have a preferential reaction with soluble ligands as opposed to those on a sorptive site, resulting in decreased sorption. An example of this occurrence is when carbonate is present in neutral to alkaline pH solutions representative of environmental conditions. Uranyl sorption to mineral surfaces is greatly reduced due to the stability of aqueous uranyl-carbonato complexes [42].

While it is true that the presence of carbonates in solution reduces uranium sorption to minerals, it may not have the same effect on the sorption of uranium to biological surfaces. Acharya et al. demonstrated that uranium was removed from solution in an open system at mid pH levels in carbonate solutions void of phosphate [67]. They found that at pH 7.8, *Synechococcus elongatus* strain BDU/75042, a gram negative bacteria, removed soluble uranium from a uranyl carbonate solution and that the bound uranium was associated mostly with the extracellular polysaccharides (EPS). They also suggested that amide groups and the deprotonated carboxyl groups on the cyanobacterial cell surface were involved in uranium sorption. This study resulted in a range of estimated K_D values of 4,500 to 8,000 L kg^{-1} [67]. These K_D values obtained from solution in which carbonate is an available ligands are within the range of those obtained from low

pH solution experiments with gram negative bacteria (K_D ~5,000 L kg^{-1}) where the uranly ion is the major species.

The presence of carbonate in solution did not greatly affect uranly biosorption, as demonstrated by an unpublished study by N'Guessan et al. [68]. This study provided a K_D value for uranium sorption to *G. uraniireducens* of approximately 200 L kg^{-1} of protein in a sodium chloride solution at pH 7 and a K_D of approximately 230 L kg^{-1} of protein in a bicarbonate solution at pH 7. When comparing these K_D values, it does not appear that the presence of carbonate in solution greatly affect uranium biosorption. It should be noted that the sodium chloride solution experiments were performed in open atmosphere conditions, which may provide similar carbonate concentrations between all experiments due to carbon dioxide (CO_2) water chemistry.

Other partitioning coefficients were also estimated for biosorption in the unpublished study by N'Guessan et al. providing more insight to uranium biosorption [29]. The partition coefficient obtained from sorption experiments in a sodium chloride solution at pH 7 was approximately 200 L kg^{-1} of protein for both *G. uraniireducens* and *D. Meridiei,* which are both gram negative species. A K_D value obtained under the same conditions for *A .palmae* (a bacteria species that lacks a cell wall) was determined to be 800 L kg^{-1} of protein. While these values are in range of each other (200 to 800 L kg^{-1} of protein), the study indicates that the *A. palmae* may be four times more sorptive than the other two bacteria species.

A study that examined the effects of calcium and atmospheric P_{CO2} concentrations on uranium bacterial sorption was done by Gorman-Lewis et al. [69]. They examined the sorption of uranium onto the gram positive species, *B. subtilis,* in the presence or absence of carbonate and calcium at a range of pH values. They found greater than 90% of the uranium was sorbed to bacterial concentrations of 0.25 g L^{-1} and 0.125 g L^{-1} exposed to 4.2 μM uranium, atmospheric carbonate concentrations and 10 mM calcium in solution. For solutions with the same bacteria concentrations exposed to 4.2 um uranium and atmospheric carbonate concentrations in solution, approximately 80% of the uranium

were sorbed. This study indicated that the presence of calcium in solution with carbonate will increase uranium sorption.

The effects of calcium in solution with carbonate on uranium biosorption were also observed in results obtained by N'Guessan et al. [68]. In their unpublished study, the group obtained an isotherm for uranium sorption in the Old Rifle site groundwater that has an average carbonate concentration of greater than 3 mM and an average calcium concentration of 6.5 mM [70]. This isotherm resulted in a K_D of approximately 57 L kg^{-1} of protein for G. When compared to the partitioning coefficient obtained for *G. uraniireducens* in a bicarbonate solution void of calcium, 230 L kg^{-1} of protein for G, there is an approximate four time decrease in estimated K_D values [68]. This indicates that uranium biosorption is decreased in the presence of calcium and carbonate in solution.

A difference in K_D values was not the only observation noted during experiments focused on uranium sorption to biomass. The locations of sorbed uranium were noticed to be variable. It has been observed that uranium can sorb to the surface of bacteria [69, 71] or inside the cell membrane of the bacteria [72, 73]. While uranium has been seen in the membrane of bacteria that are capable of enzymatic reduction, it has also been seen within the membrane of fungi [58, 74, 75], which do not perform reduction. Uranium sorption within the cell, as well as on the cell surface, may make it difficult to accurately determine partitioning coefficients and to directly compare the surface sorption affinity of the different types of bacteria.

As summarized above, a significant amount of research has been performed, investigating uranium sorption to biomass. While this work provides supporting data for the occurrence of uranium sorption to the surface of biomass, the results obtained from these studies cannot be directly correlated to predict uranium sorption to biomass under the condition of the Old Rifle site aquifer. Many of the studies were done at a pH lower than that found in the aquifer at the Old Rifle site [64-67]. Of the studies that were performed at the proper pH range, only those done by N'Guessan et al. [68] and Gorman-Lewis et al. [69] captured the effects of calcium and DIC in solution; although, the levels of DIC were lower than that found at the Old Rifle site. Also, the study by N'Guessan et

al. [68] and Gorman-Lewis et al. [69] determined opposing results regarding the effect of calcium and DIC on uranium sorption to biomass. Given that the previous literature has limited sorption results with the representative geochemical components and pH range similar to that of the Old Rifle site aquifer and that previous work to evaluate the effects of calcium and carbonate on uranium sorption has resulted in opposing conclusions, more work must be done.

Chapter 3: Evaluation of Modeling Error

Methods

The specific site of interest is the UMTRA Old Rifle site in Rifle, Colorado. It covers approximately 24 acres of land surrounded to the north, west, and east by the Wasatch Formation and bounded by the Colorado River to the south (Figure 1). This site consists of an alluvial floodplain 6 to 7.5 m deep directly above an impermeable boundary (Figure 2). Aqueous U(VI) concentrations at this site, considering spatial and temporal variability, ranged between 0.32 and 1.48 μM with DIC levels in the average range of 7.8 to 8.6 mM [23, 70]. Solution chemistry at this site is believed to be typical of high-DIC groundwaters at other contaminated sites [11].

Figure 1: Old Rifle site bounded to the south by the Colorado River [8].

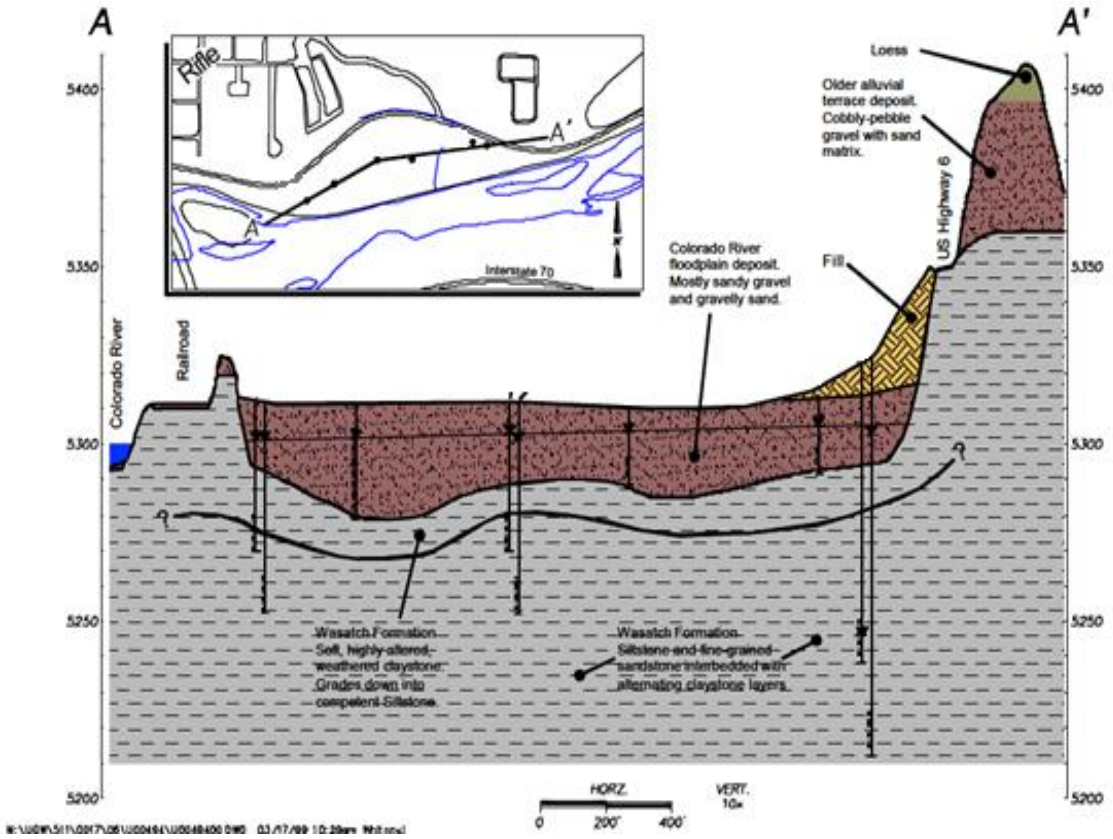

Figure 2: Old Rifle site cross section from east to west shows the alluvial aquifer directly above the Wasatch Formation [8].

Determinate Error

Determinate error associated with equilibrium modeling may stem from missing or inaccurate equilibrium coefficients and associated reactions, ionic strength correction approaches, and the manner in which the DIC concentration is specified by the user. To evaluate determinate error, a standard input file was used to define the Old Rifle site system (Table 1) with the four different thermodynamic equilibrium programs (Table 2). This was done because a standard set of analytical constraints, given that the thermodynamic constraints are the same, should produce the same equilibrium prediction regardless of the program used; since all thermodynamic equilibrium programs operate on the same theoretical and mathematical principles. Therefore, any difference in equilibrium predictions can be traced to differences in defined analytical or thermodynamic constraints.

Component	Mean (M)	Component	Mean (M)
Ca^{+2}	6.54E-03	Cl^{-}	5.42E-03
Na^{+}	8.79E-03	NO_3^{-}	1.94E-04
Mg^{+2}	5.27E-03	UO_2^{+2}	8.37E-07
SO_4^{-2}	8.26E-03	K^{+}	3.07E-04
CO_3^{-2}	8.85E-03	Sr^{+2}	3.42E-05
Temperature (^{o}C)	25	pH	7.18

Table 1: Input parameters used to define the Old Rifle site for thermodynamic equilibrium calculations [76]. This input file results in an ionic strength of 0.0382.

Program	Comments
VisualMINTEQ	Built on the EPA's MINTEQA2 software by Jon Petter Gustafsson at the KTH Royal Institute of Technology. He also maintains it. It is a free program and is available at http://www2.lwr.kth.se/English/OurSoftware/vminteq/index.html
PHREEQC	Maintained by David L Parkhurst at the U.S. Geological Survey (USGS). Based on the USGS Fortran program PHREEQE. It is a free program and is available at http://wwwbrr.cr.usgs.gov/projects/GWC_coupled/phreeqc/index.html
MINTEQA2 for Windows	Maintained by Jerry Allison of Allison Geoscience Consultants. Based on EPA (DOS version) of MINTEQA2. Cost range from $89.95 to $750 and is available at Inc. http://www.allisongeoscience.com/MINTEQ.htm
TITRATOR	Developed and maintained by Steve Cabaniss at the University of New Mexico. It is a free program and is available at http://code.google.com/p/titrator/

Table 2: Equilibrium programs used to evaluate model error.

The first source of determinate error evaluated was due to the use of default thermodynamic databases associated with the various programs to generate equilibrium predictions. With the exception of TITRATOR, ver 2.5, all the other programs downloaded with default thermodynamic database(s). VisualMINTEQ had a comprehensive default database that could be easily altered by the user from the program interface. The VisualMINTEQ, ver 2.40b and ver 2.53 had different versions of the default database, which reflected the best available data when the program update occurred. PHREEQC for Windows, Ver 2.15.07 downloaded with several different

thermodynamic database files, which could not be easily changed from the program interface. MINTEQA2 for Windows Academic, ver 1.50 downloaded with one comprehensive default database that could be easily altered by the user from the program interface.

After the equilibrium predictions generated from the different programs (using their default thermodynamic database with the standard input file) were compared, the default databases were cross referenced in efforts to identify inconsistencies within the thermodynamic equilibrium constants. Once the source of errors stemming from the use of unaltered default databases were identified, the thermodynamic databases were updated with data taken from Guillaumont et al. [77] and the U.S. National Institute of Standards and Technology (NIST) standard reference database 46 ver 8.0 [78]. When standard deviations were unavailable, a value of 0.1 log unit was assumed. This value is at the lower end of the range for metal-ligand formation constants, slightly larger than most well-studied systems [78] but smaller than the values estimated for more complex constants and less well-studied systems [79]. The final thermodynamic equilibrium constants, log K, and standard deviations used for modeling the Old Rifle site are shown in Table 3.

Species	Log K	Uncertainty	Source
$(UO_2)_2(OH)_2^{+2}$	-5.62	0.04	Guillaumont et al. [77]
$(UO_2)_2CO_3(OH)_3^{-}$	-0.858	0.851	Guillaumont et al. [77]
$(UO_2)_2OH^{+3}$	-2.7	1	Guillaumont et al. [77]
$(UO_2)_3(CO_3)_6^{-6}$	54	1	Guillaumont et al. [77]
$(UO_2)_3(OH)_4^{+2}$	-11.9	0.3	Guillaumont et al. [77]
$(UO_2)_3(OH)_5^{+}$	-15.55	0.12	Guillaumont et al. [77]
$(UO_2)_3(OH)_7^{-}$	-32.2	0.8	Guillaumont et al. [77]
$(UO_2)_4(OH)^{7+}$	-21.9	1	Guillaumont et al. [77]
$UO_2(CO_3)_2^{-2}$	16.61	0.09	Guillaumont et al. [77]
$UO_2(CO_3)_3^{-4}$	21.84	0.04	Guillaumont et al. [77]
$UO_2(OH)_{2\ (aq)}$	-12.15	0.07	Guillaumont et al. [77]

$UO_2(OH)_3^-$	-20.25	0.42	Guillaumont et al. [77]
$UO_2(OH)_4^{-2}$	-32.4	0.68	Guillaumont et al. [77]
$UO_2(SO_4)_2^{-2}$	4.14	0.07	Guillaumont et al. [77]
UO_2Cl^+	0.17	0.02	Guillaumont et al. [77]
$UO_2Cl_{2\ (aq)}$	-1.1	0.4	Guillaumont et al. [77]
$UO_2CO_{3\ (aq)}$	9.94	0.03	Guillaumont et al. [77]
$UO_2NO_3^+$	0.3	0.15	Guillaumont et al. [77]
UO_2OH^+	-5.25	0.24	Guillaumont et al. [77]
$UO_2SO_{4\ (aq)}$	3.15	0.02	Guillaumont et al. [77]
$UO_2(SO_4)_3^{-4}$	3.02	0.38	Guillaumont et al. [77]
$Ca_2UO_2(CO_3)_{3\ (aq)}$	30.7	0.05	Dong and Brooks [16]
$CaUO_2(CO_3)_3^{-2}$	27.18	0.06	Dong and Brooks [16]
$Mg_2UO_2(CO_3)_{3\ (aq)}$	28.36	0.2	Dong and Brooks [16]
$MgUO_2(CO_3)_3^{-2}$	26.11	0.04	Dong and Brooks [16]
$SrUO_2(CO_3)_3^{-2}$	26.86	0.04	Dong and Brooks [16]
$Ca(NO_3)_{2\ (aq)}$	-4.5	0.1	Gustafson [25]
$CaCl^+$	0.4	0	NIST [78]
$CaCO_{3\ (aq)}$	3.22	0.07	NIST [78]
$CaHCO_3^+$	11.529	0.1	NIST [78]
$CaNO_3^+$	0.5	0.2	NIST [78]
$CaOH^+$	-12.7	0.1	NIST [78]
$CaSO_{4\ (aq)}$	2.36	0.07	NIST [78]
$H_2CO_3{}^*{}_{(aq)}$	16.681	0.006	NIST [78]
HCO_3^-	10.329	0.009	NIST [78]
HSO_4^-	1.99	0.01	NIST [78]
$KCl_{(aq)}$	-0.3	0.1	NIST [78]
$KNO_{3\ (aq)}$	-0.19	0.08	NIST [78]
$KOH_{(aq)}$	-13.757	0.1	NIST [78]
KSO_4^-	0.85	0.01	NIST [78]

$Mg_2CO_3^{+2}$	3.59	0.1	NIST [78]
$MgCl^+$	0.6	0.1	NIST [78]
$MgCO_{3\ (aq)}$	2.92	0.07	NIST [78]
$MgHCO_3^+$	11.339	0.06	NIST [78]
$MgOH^+$	-11.417	0.03	NIST [78]
$MgSO_{4\ (aq)}$	2.26	0.07	NIST [78]
$NaCl_{\ (aq)}$	-0.3	0	NIST [78]
$NaCO_3^-$	1.27	0.1	NIST [78]
$NaHCO_{3\ (aq)}$	10.029	0.01	NIST [78]
$NaNO_{3\ (aq)}$	-0.55	0	NIST [78]
$NaOH_{\ (aq)}$	-13.897	0.03	NIST [78]
$NaSO_4^-$	0.79	0.09	NIST [78]
OH^-	-13.997	0.003	NIST [78]
$SrCl^+$	0.22	0.05	NIST [78]
$SrCO_{3\ (aq)}$	2.81	0	NIST [78]
$SrHCO_3^+$	11.539	0.03	NIST [78]
$SrNO_3^+$	0.6	0.2	NIST [78]
$SrOH^+$	-13.177	0.1	NIST [78]
$SrSO_{4\ (aq)}$	2.3	0.1	NIST [78]

Table 3: List of thermodynamic constraints that were used in equilibrium simulations and uncertainty calculations. Formation constants written using H^+, UO_2^{2+}, Ca^{2+}, Mg^{2+}, Sr^{2+}, Na^+, K^+, CO_3^{2-}, SO_4^{2-}, NO_3^-, Cl^- and H_2O as components. Uncertainty values were determined from those listed in the NIST database or set by the user, as explained in the text above.

Ionic Strength Correction

Error associated with ionic strength was investigated using the different ionic strength correction approaches available in the different thermodynamic equilibrium programs. This investigation was done using the standard input file as listed in Table 1 with the updated thermodynamic database as listed in Table 2. In a solution with very low ionic strength, ions behave independently of each other and result in a measured concentration reflective of the ion activity of the solutions. In more concentrated solutions, increased electrostatic interaction between ions decreases the activity to less than the measured concentration. This change is accounted for by the activity coefficient of an ion which is

determined from the various ionic strength correction approaches discussed later in detail. The activity coefficients which account for deviations from an ideal to a non ideal system, do so by relating the concentration of the species to the activity of the species in solution (equation 7).

$$\gamma_i = \frac{\{i\}}{[i]} \tag{7}$$

Where {i} is the activity of species i, [i] is the concentration of species i, and γ is the activity coefficient.

Errors associated with the calculation of activity coefficient can greatly affect the generated equilibrium solution because these coefficients are used to calculate the activity of species in solutions that are related to the applicable thermodynamic equilibrium coefficients (equation 8). These coefficients help determine the species equilibrium concentrations in a system.

$$K = \frac{\{C\}^c\{D\}^d}{\{A\}^a\{B\}^b} = \frac{\gamma_c[C]^c\gamma_d[D]^d}{\gamma_a[A]^a\gamma_b[B]^b} \tag{8}$$

Where K is the thermodynamic equilibrium coefficient that relates the activities of the reactants, {A} and {B}, to the activity of the products, {C} and {D}. The activity, {}, of the reactants and products are related to the concentration, [ ], by the activity coefficient, γ. The stoichiometric coefficients, a, b, c, and d, are defined by the reaction of A + B, which yields C + D, as shown by equation 9.

$$aA + bB = cC + dD \tag{9}$$

The calculated concentrations of species in a solution are used to determine the ionic strength of that solution (equation 10), which defines the ionic strength correction approach to be used when calculating the activity coefficient.

$$I = \frac{1}{2}\sum_i C_i Z_i \tag{10}$$

Where I is the ionic strength of the solution, C_i is the concentration of a given species, and Z_i is the charge of that given species.

But, the different ionic strength corrections are only applicable up to a maximum ionic strength. As shown by Figure 3a, increases in ionic strength result in the activity coefficient of an ion deviating further from the value of 1, which represents an ideal system. The choice of the correction approach for ionic strength (discussed further below) affects the speciation prediction because the various approaches can result in different values for the activity coefficients as the ionic strength of a solution increases above 0.1 M (Figure 3b).

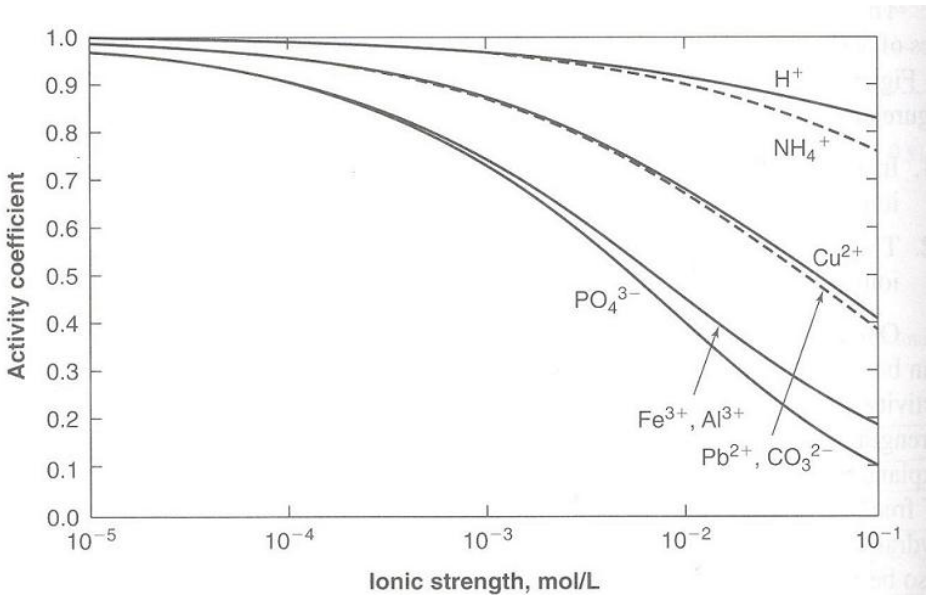

(a)

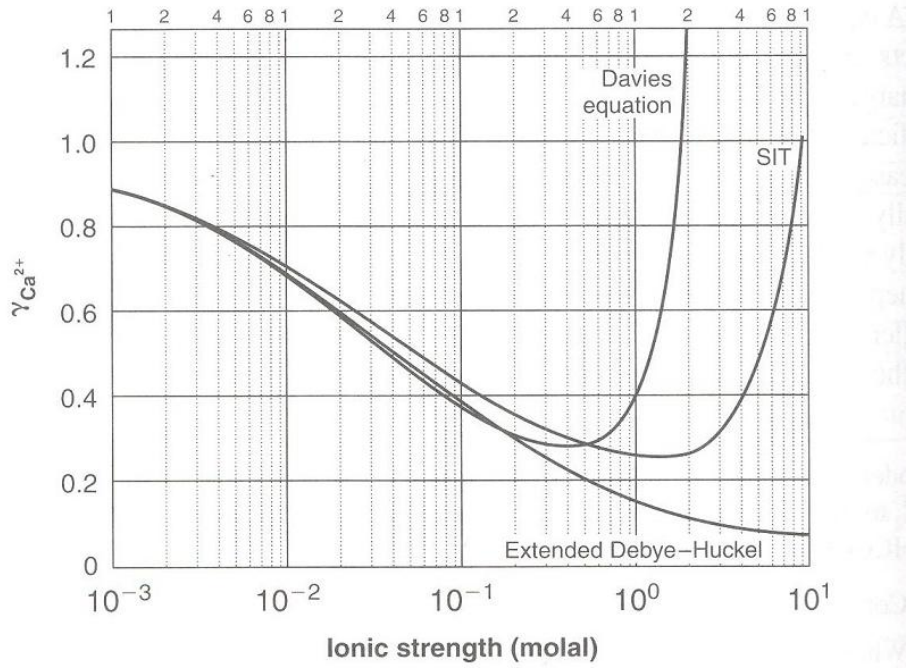

(b)

Figure 3: Representation of how activity coefficients deviate as a function of increasing ionic strength and different ionic strength correction approaches [52]. (a) Extended Debye-Huckel activity coefficients of various ions. (b) The activity coefficient of Ca_2^{+2} in solution according to the three listed models, prepared by dissolution of $CaCl_2$.

The errors associated with ionic strength correction approach were examined by using the following four approaches: 1) SIT, 2) Extended Debye-Huckel, 3) Davies, and 4) Guntelberg Approximation. The SIT approach is applicable for higher ionic strength solutions (greater than 1M), while the latter are applicable for lower ionic strength solutions [52, 80]. All approaches listed are derived from the Debye-Huckel limiting law in which all ions are treated as point charges that can approach infinitely closely to one another in a continuous solution. This law is only valid for solutions with ionic strength less than 0.005 M. The Extended Debye-Huckel (equation 11) incorporates the size of ions to the limiting law and assumes the ion of interest and the shielding ions are the same size. This approach is valid for solutions with ionic strengths less than 0.1M. The Davies approach (equation 12) extended the Extended Debye-Huckel approach further by adding empirical terms to improve the fit between the equation and the experimental observation. This approach is only valid for solutions with ionic strength less than 0.5 M. The Guntelberg approach (equation 13) simplifies the Extended Debye-Huckel with the assumption all ions were the same in size and is only valid for solutions with ionic strength less than 0.5 M.

$$\log \gamma_{Ext.D-H} = -Az^2 \left(\frac{\sqrt{I}}{1 + Ba\sqrt{I}} \right) \tag{11}$$

$$\log \gamma_{Davies} = -Az^2 \left(\frac{\sqrt{I}}{1 + \sqrt{I}} - bI \right) \tag{12}$$

$$\log \gamma_{Guntelberg} = -Az^2 \left(\frac{\sqrt{I}}{1 + \sqrt{I}} \right) \tag{13}$$

Where I is ionic strength, z is the charge of the ion, and b is an empirical parameter that ranges from 0.3 to 0.2. $A = 1.82 \text{ X } 10^6 (\varepsilon T)^{\frac{-2}{3}}$, a is the ion size parameter, $B = 50.3(\varepsilon T)^{\frac{1}{2}}$, and ε is the dielectric constant of the medium.

Although the SIT approach is also derived from the Debye-Huckel limiting law, it accounts for ion size and the non-continuous characteristic of a highly concentrated solution by considering interactions between given ions. The Bronsted-Guggenhein-Scatchard version of the SIT (equation 14) assumes a constant ion size and is valid for ionic strengths greater than 0.1.

$$\log \gamma_i = -A \cdot z_i^2 \left(\frac{\sqrt{I}}{1+1.5\sqrt{I}} \right) + \sum_k \varepsilon(i,k) \cdot m_k \qquad (14)$$

Where $A = 1.82 \text{ X } 10^6 (\varepsilon T)^{\frac{-2}{3}}$, z is the charge of the species, $\varepsilon(i,k)$ is the aqueous species interaction coefficient that determines the specific short-range interactions between species i and k, and m_k is the molality of species i.

Dissolved Inorganic Carbon (DIC) Concentration

Determinate error can result from how the DIC concentration associated with the system is defined by the user. DIC concentration can be determined from an alkalinity measurement or from a user-stated DIC concentration input. Alkalinity is commonly defined as the amount of strong acid needed to titrate a solution to a preselected pH near 4.7 [52] and in natural waters is mainly attributable to carbonate dissociation, with small influences by species such as silicates, borates, ammonia, phosphates, and organic bases [81] as shown by equation 15. Thus accounting for alkalinity contributions from non-carbonate components, an alkalinity measurement should be interchangeable with a user defined DIC concentration when specifying the DIC concentration of a system in a model.

$$Alkalinity = \left[HCO_3^-\right] + 2\left[CO_3^{2-}\right] + \left[OH^-\right] - \left[H^+\right] + \sum_i^{N_{aq}} b_{alk,i} n_i \qquad (15)$$

Where $\left[HCO_3^-\right] + 2\left[CO_3^{2-}\right] + \left[OH^-\right] - \left[H^+\right]$ is alkalinity (eq L^{-1}) due to total carbonate and the weak acid character of water, $b_{alk,i}$ is the alkalinity contribution of all other aqueous species i (eq mol^{-1}), and n_i is the concentration in (mol L^{-1}) of the component associated with the given alkalinity contribution.

Indeterminate Error (Uncertainty)

After determinate errors were resolved, indeterminate errors or uncertainties associated with thermodynamic equilibrium programs were investigated. First derivative sensitivity analyses and Monte Carlo simulations were used to examine the uncertainty in equilibrium calculations for the system of interest. All calculations were done using TITRATOR ver 3.0.

Equilibrium Systems and Speciation

Two equilibrium systems were considered in this indeterminate error analysis. System I used only dissolved species and System II used both dissolved and sorbed species. Both systems used input parameters identified in Table 1. Each system required a set of analytical constraints, such as total concentration of input species determined by the sensitivity analysis and pH, as well as the representative set of thermodynamic constraints (equilibrium reactions with formation constants). Given the two different systems, the speciation of the final equilibrium solutions will be different because speciation drives the final distribution of uranium and the degree of error propagation related to the simulations is also different.

System I

System I represented only dissolved species and used the analytical constraints in Table 1. Total concentrations, not free ion concentrations are given for all input values except pH. Total dissolved uranium concentration, U(VI), is equal to 0.837 μM. Thermodynamic constants for dissolved uranium species are given in Table 3.

System II

System II represents both dissolved and sorbed U(VI) species. Because sorption is believed to be the controlling factor in uranium transport, it is important to understand the distribution of the resulting chemical speciation and affinity of that speciation to sorb to surfaces within the aquifer. As discussed in Chapter 2, sorption of contaminants such as U(VI) has been described using partition coefficient, K_D (equation 16), which describes the affinity for sorption to a given sorbent and is highly dependent on the chemical composition of the aqueous solutions. Because the geochemistry of aquifers is variable, the use of partition coefficients derived from laboratory experiments can result in a large

degree of error when calculating sorption [53]. In efforts to minimize the error associated with laboratory-obtained partition coefficients, sorption of U(VI) to sediment surfaces was modeled using the Surface Complexation Model (SCM) General Composite (GC) approach of Curtis, Davis, and co-workers [11, 82] as implemented by Fang et al. [24].

$$K_D = \frac{U_{sorbed}}{U_{aqueous}} \tag{16}$$

As explained in detail in Chapter 2, the SCM model describes solution speciation and the sorptive affinity for the contaminant in terms of chemical reactions between dissolved species and surface function groups using mass action equations and equilibrium coefficients within a general geochemical framework [54]. The GC derivative of the SCM approach does not include electrostatic terms and assumes sorption occurs on generic surface sites representative of average surface properties rather than specific mineral surfaces. This approach is semi empirical and allows the coupling of variable aqueous geochemical conditions with sorption processes controlled by a limited number of sorption sites [11].

The SCM GC model, as applied to the Old Rifle site specifically, calculated sorption of U(VI) over a restricted range of pH (near pH 7) and ionic strength represented by a set of three surface sites of varying concentrations and formation constants. Sorption sites are represented by a ratio of weak sites (WOH), strong sites (SOH) and very strong sites (SSOH) of 10000:10:1 in the sediment, as shown in Table 4. Calculations based on this model are consistent with observed overall sorption constants for the Old Rifle site [24, 82]. The labile U(VI) concentration $U(VI)_{lab}$, the amount of uranium desorbable from soil, was estimated to be 7.81 μM by assuming 5.25 nmol U(VI) g^{-1} of less than 2 mm sediment taken from the contaminated area within the site [82, 83]. It was assumed that the less than 2 mm sediment was 20% of the total sediment and that this fraction was the only sediment that contained labile U(VI) as done by Fang et al. [24]. For System II, the total concentration of soluble uranium is defined as the conetration of labile uranium plus the concentratio of dissolved uranium, $U(VI)_{Tot} = U(VI)_{lab} + U(VI)_{diss}$.

Particle Density (kg/L)	2.75	Very strong binding sites (SSOH) (%)	0.01
Porosity	0.23	Strong binding sites (SOH) (%)	0.1
Particle fraction <2 mm	0.27	Weak binding sites (WOH) (%)	99.89
Concentration of Sorption Sites (μmol/g <2mm)		16.34	
Sorption Species		Equilibrium data (log K)	
$SSOUO_2^+$		12.28	
$SOUO_2^+$		6.95	
$WOUO_2^+$		2.74	
SSOUOOH		0.033	
SOUOOH		-2.12	
WOUOOH		-5.01	

Table 4: Parameters used to determine sorption site concentration and equilibrium calculations. All sorption reactions were taken from Fang et al. [24].

Uncertainty Calculations

Sensitivity Analysis

A sensitivity analysis was performed by calculating the first derivatives for each resulting equilibrium species concentration with respect to each input parameter with associated constraints in analytical and thermodynamic uncertainties. This analysis was used to identify critical input parameters for the system of interest by evaluating how changes in a constraint will affect calculated equilibrium concentrations. Recommendations were made as to what input parameters, termed critical parameters, must be precisely measured to minimize indeterminate error.

A simple graphical approach to this analysis is to plot a response variable (one of the calculated equilibrium species) versus various values of a given constraint (input parameters and related thermodynamic equilibrium value, both with defined uncertainties). The resulting plot of a flat line indicates little effect; a smooth, steep slope in either direction indicates a large effect; and a more complicated response indicates that

sensitivity is variable. A more quantitative alternative is to compute a sensitivity matrix S in which the value of the jth row and ith column, $S_{i,j}$, is the first derivative of the concentration of the ith chemical species with respect to the jth constraint (equation 17). Because the concentrations may vary dramatically in magnitude, it is convenient to compute this as a log/log derivative (i.e., the change in the log concentration of species i with respect to the log value of constraint j).

$$S_{i,j} = \frac{d \log[C_i]}{d \log X_j} \tag{17}$$

Where X_j is the logarithm of the jth constraint: log K for a thermodynamic constraint and log concentration or activity for an analytical constraint.

TITRATOR calculates sensitivity matrices using a simple numerical derivative method in which the log derivative $S_{i,j}$ is determined by equation 18.

$$S_{i,j} = \frac{\log[C_i]_{+\Delta x} - \log[C_i]_{-\Delta x}}{2\,\Delta x} \tag{18}$$

Where $[C_i]_{\pm\Delta x}$ is the calculated concentration of the ith species when the jth constraint has its given value $\pm\Delta x$, and Δx is a user settable interval in log X. $2\Delta x$ is the small interval over which the derivative is calculated [47]. Here, $\Delta x = 0.01$ log units.

Monte Carlo Analysis

Monte Carlos simulations were performed by TITRATOR, ver 3.0. For the Monte Carlo simulation, the equilibrium systems were solved with many trials, which are different input constraints (measurements or thermodynamic values) selected randomly from the uncertainty distributions of those constraints. If all constraints are given random values (full Monte Carlo), then the resulting distribution of calculated concentrations as the number of trials approaches infinity represents the predicted uncertainty in that concentration. If the resulting distribution is approximately Gaussian (normal), equilibrium species concentrations can be expressed with a mean and standard deviation.

All simulations were performed with 10,000 trials because it has been shown that the resulting Gaussian distribution is not significantly different with more trials [47].

For Monte Carlo simulations, each constraint was assigned a standard deviation in log molar units, $S_{\log M.}$ This is related to the relative standard deviation in measured concentration (RSD_M) by the approximate 'rule of thumb' $RSD_M = 2.303\ S_{\log M}$ [84]. Thus, a standard deviation in log concentration $S_{\log M} = 0.007$ corresponds to a relative error of 0.016, or 1.6% in molar concentration. The assumption of log normal analytical uncertainty thus corresponds to a constant relative error, which corresponds reasonably well to observation.

The Monte Carlo simulations for both equilibrium systems dissolved only (System I) and dissolved with sorbed species (System II), used three different levels of uncertainty in the analytical constraints (Table 5). The DIC concentration was specified as total carbonate, not alkalinity, and ionic strength corrections used the Guntelberg approximation [80]. Based on the derivative calculations of the sensitivity analysis, pH and total calcium, U(VI), DIC, sulfate concentrations were selected as 'critical parameters' for which a standard deviation was calculated at each level; standard deviations for other parameters remained constant.

The three levels of uncertainty in the Monte Carlo simulations are instrumental or analytical, temporal, and spatial. Instrumental uncertainty represents laboratory measurement uncertainty, and is the minimum achievable level. The instrumental or analytical uncertainties listed in Table 5 are based on water quality data taken from well B1(655) in 2009 and equipment limitations [76]. Temporal uncertainty represents seasonal variability at a single well, and can be thought of as the uncertainty from using a few samples per year to represent annual concentrations. The average concentrations and temporal standard deviations were calculated using 10 years of data (1998 to 2008 [70]) from well 655. Spatial uncertainty represents variability due to the location of wells within the subsurface uranium plume, ignoring background areas, and can be thought of as the uncertainty due to sampling a large plume in only a few locations. The average concentrations and spatial standard deviations were calculated from data obtained in 2007 for wells 305, 655, and 654 (Figure 4) [70].

Critical Parameter	Analytical Uncertainty		Temporal Uncertainty		Spatial Uncertainty	
	Mean (M)	Standard Deviation (Log M)	Mean Mean(M)	Standard Deviation (Log M)	Mean (M)	Standard Deviation (Log M)
Ca^{+2}	6.54E-03	0.007	4.94E-03	0.096	4.74E-03	0.096
SO_4^{-2}	8.26E-03	0.007	8.25E-03	0.017	6.32E-03	0.161
CO_3^{-2}	8.85E-03	0.043	8.37E-03	0.083	7.82E-03	0.113
UO_2^{+2}	8.37E-07	0.007	5.96E-07	0.078	4.04E-07	0.326
pH	7.18	0.02	7.04	0.12	7.13	0.16

Table 5: Critical input concentrations as defined by first-derivative analyses used in Monte Carlo simulations. All other inputs parameters are standard as listed.

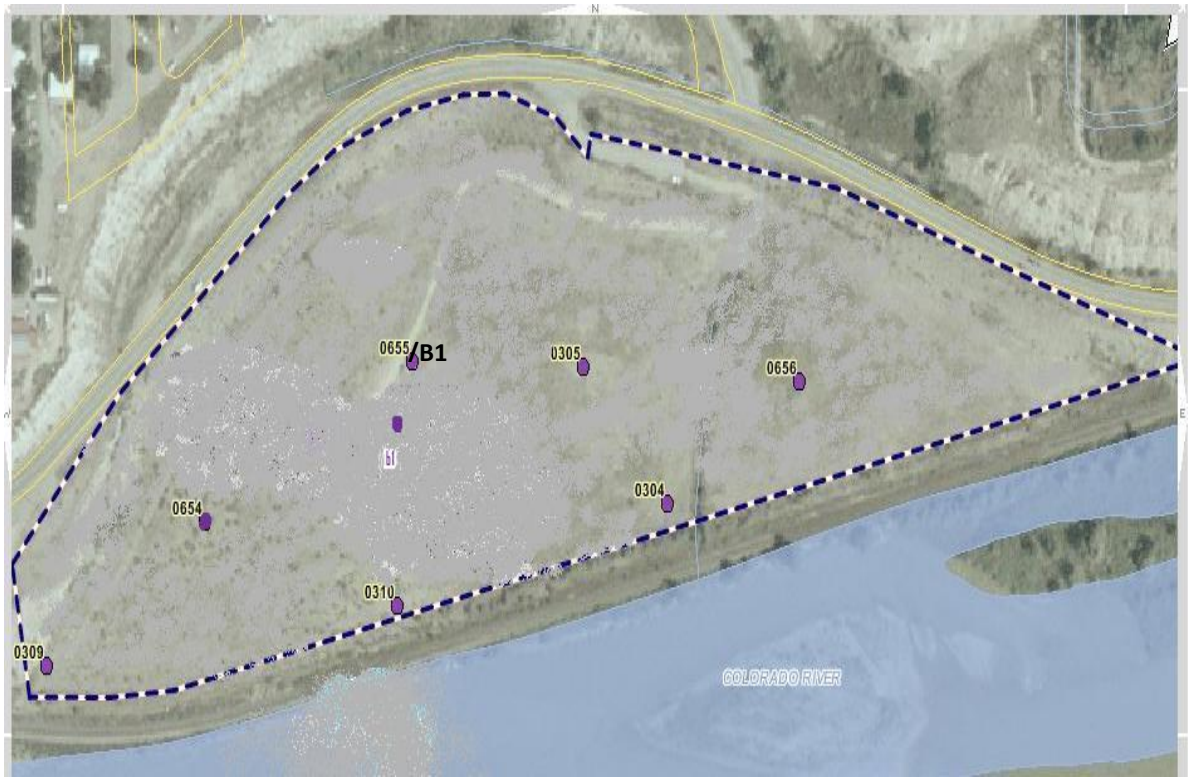

Figure 4: Old Rifle site area [70]. Wells pictured are data sources for Monte Carlo analyses.

For the Monte Carlo simulations, which include sorption reactions, concentrations for $U(VI)_{Tot}$ are equal to $U(VI)_{lab}$ = 7.81 µM (described earlier) plus the soluble

concentrations for each uncertainty level listed in Table 5. Uncertainties in the total uranium concentration were assumed to be the same as in System I. Because the site concentrations are fixed by the model (for a given sediment composition and porosity), they were assumed to have zero uncertainty in the Monte Carlo simulations. As explained earlier, standard deviations in the log formation constants are taken from the same source as the constants [77, 78] when available. When standard deviations were unavailable, as in the case of the thermodynamic equilibrium values for sorption in Table 5, a value of 0.1 log unit was assumed.

Results and Discussion

Determinate Error

Inconsistencies in Thermodynamic Data

Four programs were used to simulate thermodynamic equilibrium conditions related to a groundwater sample obtained from the Old Rifle site: 1) MINTEQ for Windows, 2) PHREEQC, 3) VisualMINTEQ, and 4) TITRATOR. Of the default databases reviewed, a little more than half of them had thermodynamic data associated with uranium. Use of programs with unaltered default databases resulted in significantly different equilibrium predictions (Table 6). TITRATOR results are not present because the program does not have a default thermodynamic database. Differences in equilibrium predictions are attributed to the exclusion of critical reactions and/or inconsistent thermodynamic equilibrium constant values. The calcium-uranyl-triscarbanato species, which accounts for 80% to 99% (depending on the equilibrium coefficients used) of the uranyl ion distribution is missing from all but two of the databases evaluated.

Aqueous Species	Default Database					
	Visual MINTEQ Ver 2.53	MINTEQ For Windows	LLNL and ISO.dat	MINTEQ .dat	Minteq.V4 .dat	Wateq4f .dat
$UO_2(CO_3)_2^{-2}$	< 0.1 %	66%	61%	73%	55%	63%
$UO_2(CO_3)_3^{-4}$	< 0.1 %	31%	36%	24%	44%	36%
$UO_2(OH)_2$ (aq)	< 0.1 %	> 0.1 %	2%	> 0.1 %	> 0.1 %	> 0.1 %
UO_2CO_3 (aq)	< 0.1 %	3%	1%	3%	1%	1%
$Ca_2UO_2(CO_3)_3$ (aq)	80%	-	-	-	-	-
$CaUO_2(CO_3)_3^{-2}$	20%	-	-	-	-	-
Total	100%	100%	100%	100%	100%	100%

Table 6: Percent distribution of U(VI) among the aqueous species using default databases with various thermodynamic equilibrium programs.

Simulations were performed using the two different versions different versions of VisualMINTEQ, but only predictions obtained from VisualMINTEQ ver 2.53 were compared in Table 6. This is because the difference within the default database is solely reflective of a program update and the program does not intended to offer the use of two different default databases. But, it should be noted that the use of the default databases associated with the different versions resulted in different equilibrium predictions. Using the database supplied with version 2.40b, the major species, $Ca_2UO_2(CO_3)_3$ (aq), accounted for 99% of the uranyl ion distribution, while using the database supplied with version 2.53 resulted in the major species only accounting for 80% of the uranyl ion distribution. This disparity is mainly attributable to the different thermodynamic equilibrium values, log K, for the $CaUO_2(CO_3)_3^{-2}$ species. The equilibrium constant for the $CaUO_2(CO_3)_3^{-2}$ in the two versions of the default database differed by almost two log units. VisualMINTEQ ver 2.53 had the most current value of the thermodynamic values for the calcium-uranyl-triscarbonato species [16] and produced the best results as to the expected equilibrium solution before altering the databases for completeness.

The significant differences in equilibrium prediction indicate that it is common for the default databases not to have the most current equilibrium constants for the uranium system. To minimize determinate error, it is necessary to investigate and incorporate current equilibrium constants before using any of these programs to predict uranium speciation. The constants shown in Table 3 are currently (as of September 2011) the most accurate equilibrium constants for conditions similar to those from the Old Rifle site.

Ionic Strength

Ionic strength predictions as a result of various approaches to determine activity coefficients were compared. These simulations were performed using the thermodynamic equilibrium information listed in Table 3 and standard input file listed in Table 1. When modeling a system, equilibrium concentrations are calculated in part by the activity coefficient. The approach used to calculate the activity coefficient (i.e., the Davis vs. Debye-Huckel) is determined by ionic strength in theory; but, in a simulation it is determined by the user without knowledge of solution ionic strength. Ionic strength is then determined from the calculated concentrations of species that are in part determined from the activity coefficient. The error can be identified by comparing ionic strengths from simulations performed with each ionic strength correction approach.

The ionic strength of the system, which was estimated using the different approaches, provided similar results ranging from 3.8 E-02 to 3.9E-02 M and are listed in Table 7. Because VisualMINTEQ and MINTEQ for Windows are different interfaces to the MINTEQA2 program, MINTEQ for Windows was not used for additional analysis. The calculated ionic strength using the various approaches to determine activity coefficients were very close to the average Old Rifle site ionic strength of 0.04 M [24] . The similarity of the results is attributable to the low ionic strength of the Old Rifle site and indicates that all correction approaches are valid when modeling this system. This can been seen in Figure 3b; at the ionic strength of 0.04M, the activity coefficients resulting from applying the Davis, SIT, and Extended Debye-Huckel are approximately equal to each other (~0.5). Therefore, determinate error associated with ionic strength correction

approaches for this system is assumed to be minimal due to the similarity of obtained values (Table 7).

Simulation Program	Davies	Debye-Huckel	SIT	Guntelberg Debye Huckel
Visual MINTEQ Ver 2.53	0.0382	0.0378	0.0379	N/A
Visual MINTEQ Ver 2.40b	0.0380	0.0377	N/A	N/A
MINTEQ for Windows	0.0382	0.0379	N/A	N/A
TITRATOR	N/A	N/A	N/A	.0386
PHREEQC	0.0379	0.0379	N/A	N/A

Table 7: Calculated ion strength using the different ionic strength corrections with the different programs.

The slight differences between calculated ionic strength can be explained by the manner in which each program uses the various ionic strength correction approaches throughout the entire calculation. TITRATOR uses the Guntelberg approach to calculate ionic strength throughout the entire equilibrium calculation. PHREEQC and VisualMINTEQ have the ability to use different approaches to solve for the activity coefficient.

VisualMINTEQ allows the user to specify which ionic strength correction approach is to be used. This is done through the default parameter section of the user interface, which prompts the user to select the SIT, Davies, or Extended Debye-Huckel approach. When the Davies approach is chosen, the VisualMINTEQ program interface allows the user to specify the empirical value, which by default is 0.3 and uses the approach consistently through the entire solution equilibrium calculation. When the SIT approach is specified, the Bronsted-Guggenhein-Scatchard version of the SIT is used throughout the entire calculation, and if interaction values are not listed in the database, the VisualMINTEQ program estimates them using the approach defined by Grenth et al. [85]. But, when the use of the Extended Debye-Huckel approach is specified in VisualMINTEQ, the approach may not be consistently used throughout the equilibrium calculation. In cases where the Debye-Huckel parameters are not available in the thermodynamic database for a specific species, the program uses the Davies approach to calculate activity coefficients

for the species missing the necessary Debye-Huckel parameters. The change in approaches is done without the user's knowledge.

PHREEQC also has the options of using the Davies or Extended Debye-Huckel approach to calculate activity coefficients but the specification of which calculation approach to use is not straightforward. The default approach in the PHREEQC program for ionic strength correction is the Davies equation. This parameter is not defined at the interface level of the program but at the thermodynamic database level, which is an attached file not obviously available to those not well experienced with the program. To use the default approach, the user must remove any Extended Debye-Huckel information from the thermodynamic file before the Davies equation is used throughout the entire calculation. Also, to specify the use of the Extended Debye-Huckel approach, the user must specify it at the thermodynamic-file level and input the necessary parameters need for the calculations in the associated file. Species that do not have these parameters will automatically be corrected with the Davies approach, even though the Extended Debye-Huckel approach was specified. Thus, the results obtained from using a defined Extended Debye-Huckel approach may have activities reflective of a mixture of ionic strength correction approaches.

Dissolved Inorganic Carbon (DIC) Concentration and Alkalinity

The manner in which the DIC concentration is identified within the model can result in determinate error. The DIC concentration can be specified by the user directly as an input parameter or it can be specified using an alkalinity entry in PHREEQC and VisualMINTEQ. TITRATOR only allows the total DIC concentration to be defined as an input, so it is not considered in this discussion. Alkalinity is typically expressed in terms of mass calcium carbonate per volume (g $CaCO_3$ L^{-1}) [86]. The units in which alkalinity are expressed technically represent a DIC concentration because calcium carbonate is dissolved inorganic carbon. But, the alkalinity measurement is not equal to the total DIC concentration of a system because alkalinity includes all species that have buffering capacity, such as borates, phosphates, or silicates. The terminology associated with alkalinity and that used by the program can cause confusion for a user, resulting in determinate error.

When defining the DIC concentration from an alkalinity measurement, errors can arise when converting to different units, as specified in VisualMINTEQ and PHREEQC. Both programs allow alkalinity to be specified in units other than calcium carbonate per volume (g $CaCO_3$ L^{-1}). When using the PHREEQC program with the Wateq4f database, alkalinity is listed by the database in units of mass carbonate per volume, [CO_3^{2-}]. Further details associated with this term are that it has an equivalence of 1 eq mol^{-1}, and a formula weight of 50 g L^{-1}. It may be obvious that the carbonate concentration, [CO_3^{2-}], referred to is equal to the value of calcium carbonate concentration and no other conversion is necessary. But it is possible a mistake can be made by using the carbonate concentration, [CO_3^{2-}], to be that which has a formula weight of 60 g L^{-1} and 2 eq mol^{-1}. Therefore, users need to use consistent units in each code as they all have slightly different methods for entering values for alkalinity.

Error associated with terminology and conversions can also occur when using the VisualMINTEQ program. The program prompts the user to specify "dissolved inorganic carbon" when entering an alkalinity value. As stated earlier, alkalinity is not equivalent to the DIC concentration of the system. The program also allows for alkalinity to be specified in terms of bicarbonate, which has the same associated equivalents but a different formula weight. The confusion associated with this terminology can result in an incorrect value for the DIC concentration to be entered, resulting in an equilibrium prediction that does not represent the intended system. Again, an error could be made if users do not ensure the use of consistent units when entering an alkalinity value into a program.

As stated earlier, alkalinity is used as a program input that determines the DIC concentration of a system because alkalinity measurements are easily obtained. The use of an alkalinity measurement to determine the system's DIC concentration is a reasonable approach based on the calculation of alkalinity as defined by equation 15. However, this approach is only without error if all species that have buffering capacity are defined or if the buffering capacity of the solution is purely due to carbonate concentrations. Once the DIC input is properly defined in units that accurately describe the total dissolved

inorganic carbon in solution, error associated with the use of alkalinity measurements due to neglecting the buffering capacity of non-carbonate equilibrium species can occur.

Species that contribute to the buffering capacity of a system must be specified with an alkalinity factor in the thermodynamic database of all programs that allow alkalinity to determine DIC concentration. An example of an alkalinity factor is given by the species H_2CO_3, which has an alkalinity factor of 2. This species gains two protons as it approaches the titration end point, thus explaining the value of the associated alkalinity factor. The error associated with correctly accounting for the buffering capacity of all species in the alkalinity measurement as compared to directly entering DIC concentration can be seen from the comparison of the resulting free uranyl ion concentration from the two systems presented in Table 8. System I predictions were generated by specifying the DIC concentration. This DIC concentration was determined from the sum of all carbonate species listed in a prediction that was generated from a given alkalinity measurement. System II predictions were generated from specifying the alkalinity entry used to define the DIC concentration in System I. The comparison of the results identified a difference of approximately 0.1 log unit in the free uranyl ion concentration (Table 8) through the use of the two different approaches to specify the same DIC concentration. While the difference is small, it does represent an additional source of determinate error that can be eliminated by proper specification of inputs to the models. For further analysis in this research, the DIC concentration is not calculated from an alkalinity value, but specified as a total DIC concentration in the input file.

Variable	System I (M)		System II (M)	
	PHREEQC	Visual MINTEQ		PHREEQC
Free UO_2^{+2}	-15.2	-15.3	Free UO_2^{+2}	-15.2

Table 8: Difference is the species concentration determined input parameters of 480 mg L^{-1} $CaCO_3$ alkalinity and 531 mg L^{-1} carbonate and those listed in Table 1.

Another source of determinate error resulting from the use of an alkalinity measurement to determine the total DIC concentration of a solution is associated with sampling procedures. The concentration of DIC in a groundwater sample is determined by aquifer properties. The Old Rifle site groundwater is supersaturated with CO_2 with respect to the

atmosphere; thus, exposure of an Old Rifle site groundwater sample to the atmosphere will result in a decrease of DIC concentration in that sample. This decrease in DIC concentration will result in an increase of solution pH, shifting the equilibrium speciation (Figure 5). To correctly correlate alkalinity to the DIC concentration, the pH of the system before degassing occurs must be known. Therefore, alkalinity measurements of groundwater in a laboratory environment may not be fully reflective of the solution alkalinity due to erroneous pH values resulting from degassing, which may have occurred during sampling.

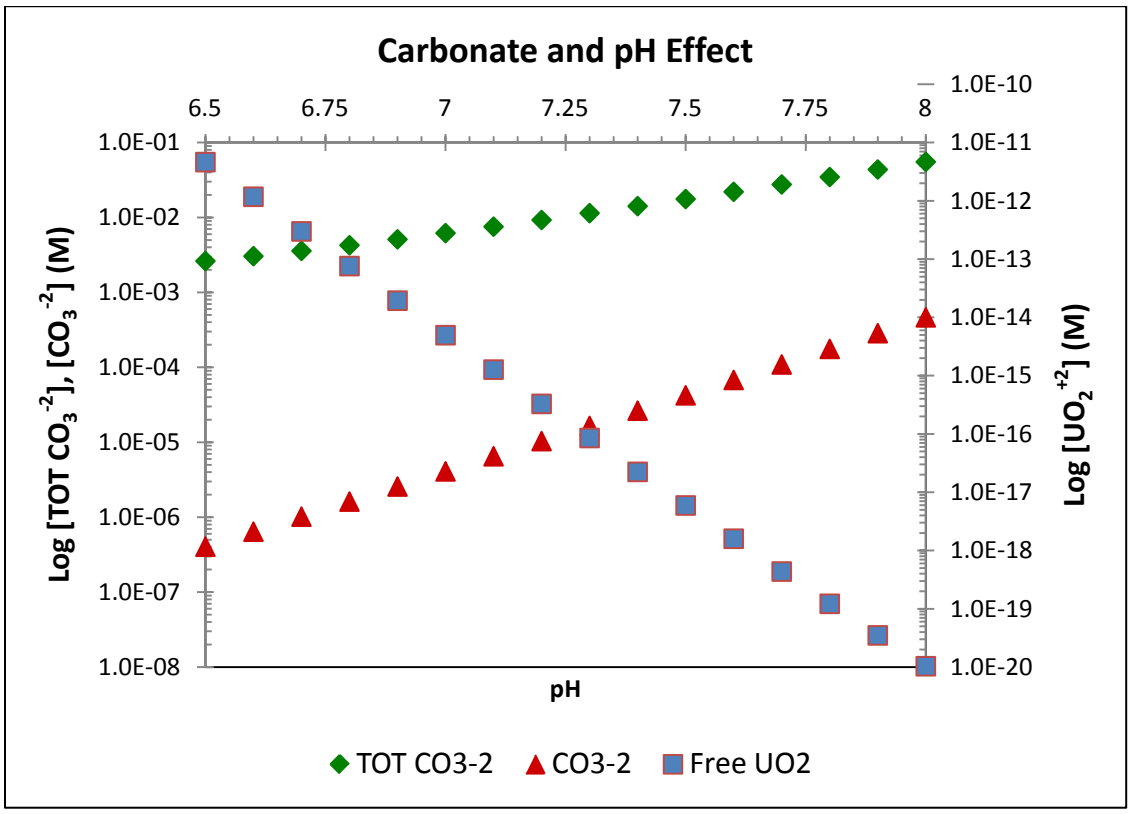

Figure 5: Carbonic acid speciation concentration as a function of pH done with VisualMINTEQ using 1.4 µM uranium difference that are captured between atmospheric and 2% P_{CO2}.

Indeterminate Error (Uncertainty)

After minimizing sources of determinate error for the system of interest, the program TITRATOR, ver 3.0 was used to evaluate uncertainty propagation for both Old Rifle site systems: dissolved species only (System I) and dissolved with sorbed species (System II). First, the equilibrium speciation was evaluated to determine the uranyl distribution for both systems, followed by a sensitivity analysis to determine critical parameters and

Monte Carlo analysis to determine the mean and standard deviation for equilibrium species.

Speciation

In both System I and System II, dissolved U(VI) speciation is dominated by the calcium-uranyl-triscarbonato species. $Ca_2(CO_3)_3UO_2$ (aq) is the highest concentration species, approximately 80% of dissolved U(VI), while $Ca(CO_3)_3UO_2^{2-}$ accounts for most of the remaining 20% of the U(VI). The free uranyl ion is only approximately $10^{-15.4}$ M, not a significant fraction of the total soluble uranium but is a key modeling parameter because uranium sorption, precipitation and complexation constants are typically expressed in terms of this concentration.

In System II, most of the total U(VI) is sorbed, but the fraction dissolved depends strongly on the total U(VI). At low total U(VI) (less than 3 μM), dissolved uranium accounts for less than 1% and as little 0.01% of the total (Figure 6), while at total U(VI) above 4 μM the fraction dissolved is greater than 10%. This dramatic change in the partitioning of uranium between sorbed and dissolved species is due to the 'titration' of strong sorption sites (SSOH) with UO_2^{2+} and has a significant effect on uncertainty propagation as shown in Figure 6.

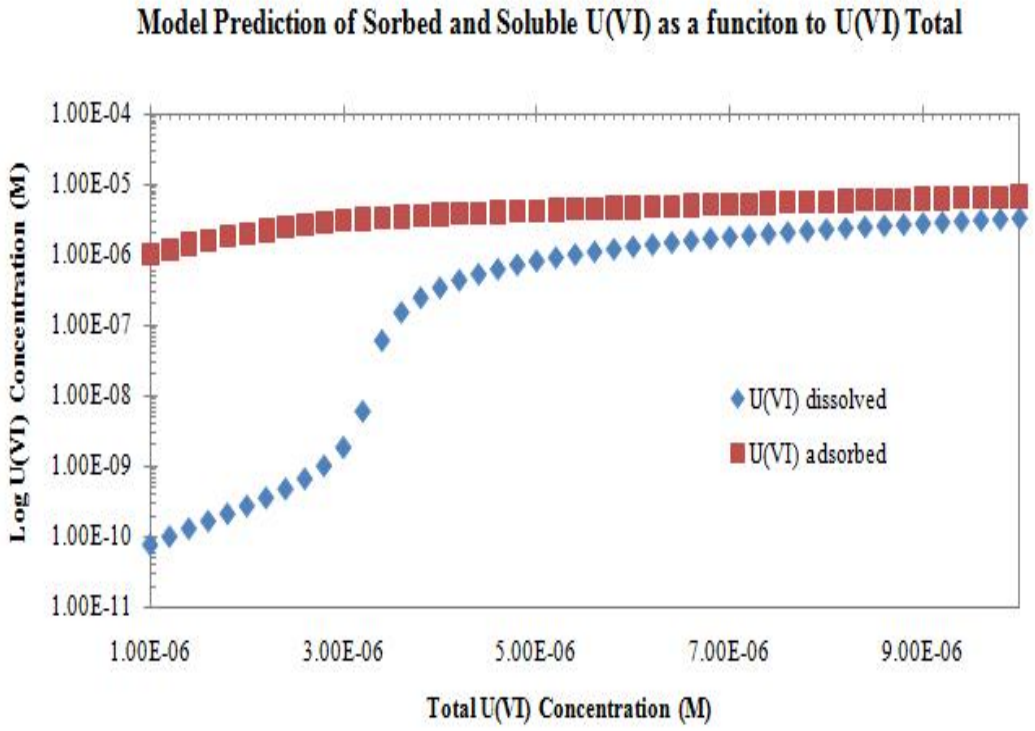

Figure 6: Log concentrations of calculated sorbed and dissolved U(VI) as a function of total U(VI) in the system. Note that although the concentration of sorbed uranium is a smooth function of total U(VI), the concentration of dissolved uranium is not, showing a steep 'endpoint' corresponding to the concentration of the strongest sorption sites (~3.3 µM).

Uncertainty in System I

The two dominant calcium- uranyl-triscarbonato species were less sensitive (lower derivative values) to changes in input constraints than the free uranyl ion concentration, as expected from their much greater stability as reflected by the associated equilibrium coefficients. Analytical input constraints with the largest effect on calculated U(VI) speciation are the system pH, DIC, and concentrations of total Ca(II), U(VI), and (to a lesser extent) sulfate (Figure 7). The first four of these all have a direct role in the formation of the calcium- uranyl-triscarbonato species, while sulfate affects the speciation less directly by complexing Ca(II). Based on this analysis, these five constraints were selected as critical parameters for the Monte Carlo simulations.

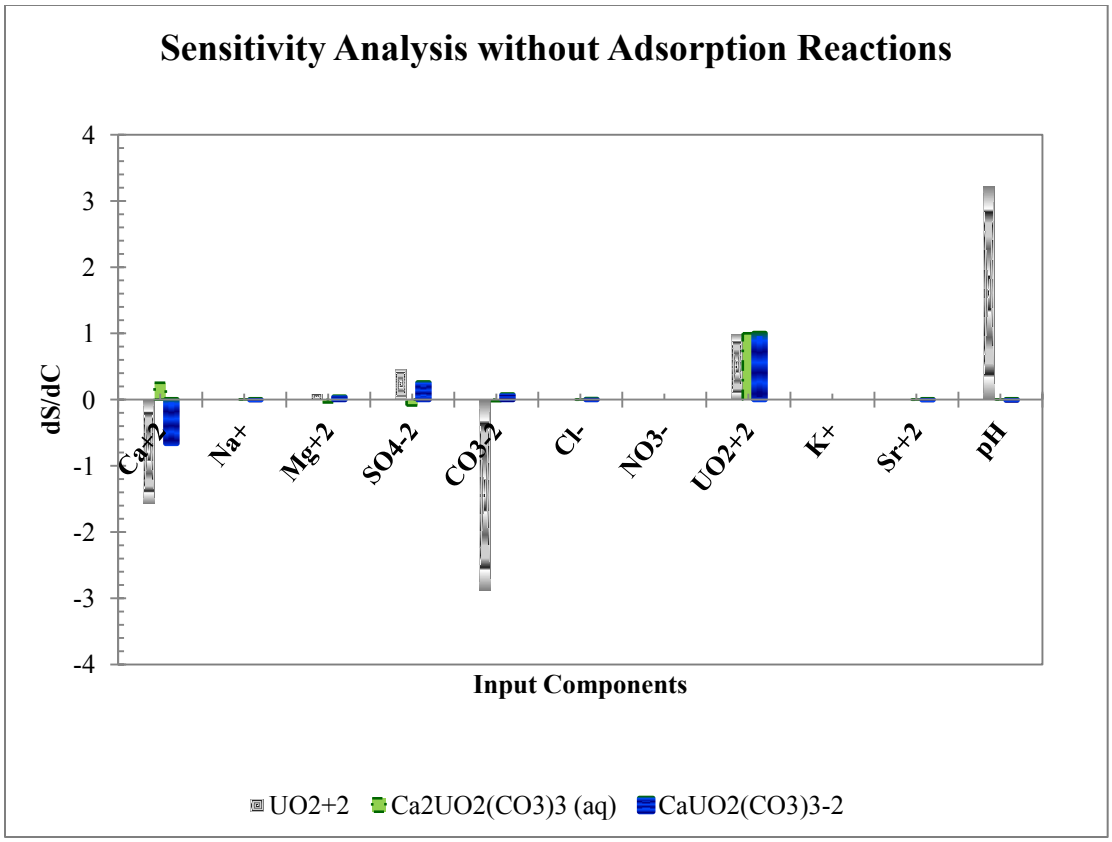

Figure 7: Sensitivity (first derivative) analysis for effects of uncertainty on three key U(VI) species concentrations for 11 analytical constraints in a dissolved-only system. dS/dC is the change in equilibrium speciation as a result in the change of parameter input concentration. Note the major roles played by total Ca(II), total U(VI), DIC, and pH.

Distributions of calculated species concentrations for 10,000 Monte Carlo trials at all uncertainty levels are monomodal (normally distributed) and approximately symmetrical, consistent with a Gaussian distribution of propagated uncertainty (Figure 8). For each level of uncertainty, calculated standard deviations for the dominant species concentrations of $Ca_2UO_2(CO_3)_{3(aq)}$ and $CaUO_2(CO_3)_3^{-2}$ listed in Table 9 are similar to the input uncertainty associated with temporal and spatial conditions for total U(VI) (from Table 4), indicating minimal amplification of uncertainty in the calculation. However, the standard deviation of the free uranyl ion concentration [UO_2^{2+}] is much higher. Extending the range of the total U(VI) to higher and lower values (0.1 to 2.0 µM total U(VI)) gives the same critical species, the same monomodal distributions, and the same elevated amplification of uncertainty for uranyl ion concentration.

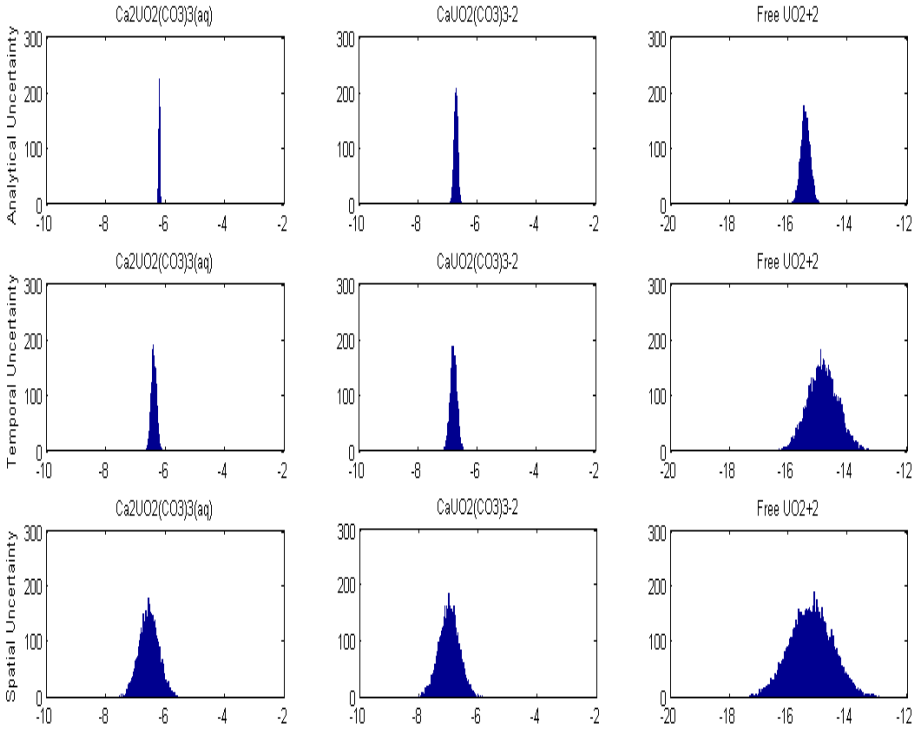

Figure 8: Monte Carlo simulations of System I (dissolved-only), showing frequency of result versus log concentration. Top row is lowest uncertainty (analytical); bottom row is highest uncertainty (spatial). Plots normalized for consistent heights, not areas.

Error without sorption reactions						
	Analytical Uncertainty		Temporal Uncertainty		Spatial Uncertainty	
Species	Mean (Log M)	Standard Deviation (Log M)	Mean (Log M)	Standard Deviation (Log M)	Mean (Log M)	Standard Deviation (Log M)
UO_2^{+2}	-15.4	0.152	-14.9	0.501	-15.3	0.723
$Ca_2UO_2(CO_3)_3(aq)$	-6.2	0.02	-6.39	0.088	-6.55	0.328
$CaUO_2(CO_3)_3^{-2}$	-6.73	0.061	-6.8	0.113	-6.98	0.338

Table 9: Summary statistics of distributions in Figure 8 (System I).

If the chief purpose of the calculation is to predict principal species concentrations, this system is robust. However, because the uranyl ion concentration is used in the calculation of sorption and precipitation, the substantial amplification of uncertainty (the

output uncertainty in log [UO_2^{2+}] is more than double the log $U(VI)_{Tot}$ input uncertainty) may be problematic. Large uncertainty in sorption and precipitation of uranium directly affects the reliability for a transport program to predict how long it will take the Old Rifle site to reach UMTRA and EPA uranium concentration limits.

Uncertainty in System II

First derivative calculations using 8.65 μM total U(VI) are somewhat similar to System I with the addition of significant sensitivity to strong (SOH) and very strong (SSOH) surface site concentrations. The solution pH, DIC, and total concentrations of calcium and U(VI) have the largest effects; although, the magnitude of these derivatives is smaller than in System I (compare Figures 7 and 9). One notable difference is the sensitivity of the calcium- uranyl-triscarbonato species concentrations to DIC concentration and solution pH, which is much greater than in System I. The SOH and SSOH concentrations also have important effects; although, the system is not very sensitive to WOH concentration.

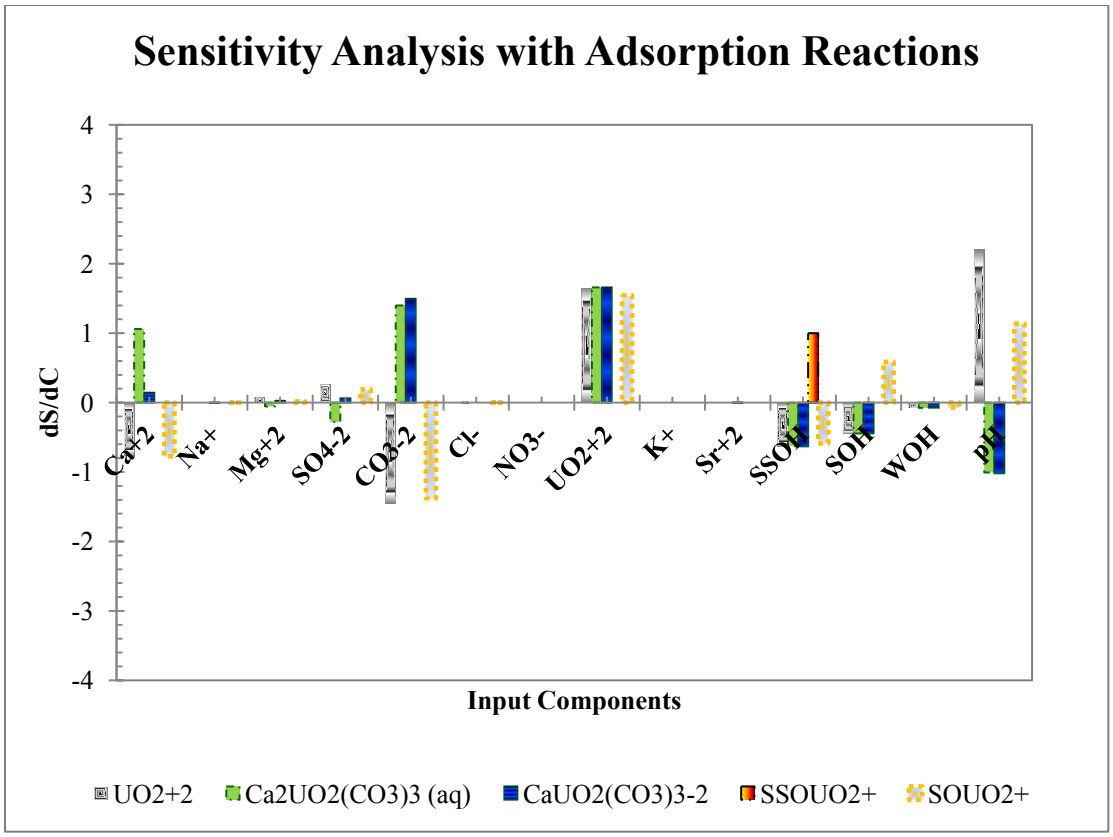

Figure 9: Sensitivity (first derivative) analysis for effects of uncertainty on U(VI) species concentrations for 14 analytical constraints in dissolved-solid partitioning system. dS/dC is the change in equilibrium speciation as a result in the change of parameter input concentration. Note the major roles played by total Ca(II), total U(VI), DIC, and pH and the relatively modest effect of total surface sites (SSOH and SOH) under these conditions of high total U(VI).

Monte Carlo simulations of System II with 8.65 µM total U(VI) show normally distributed Gaussian distributions of calculated concentrations at the lower levels of uncertainty (analytical uncertainty and temporal variation). However, at the highest level of uncertainty, represented by spatial conditions specified in Table 10, asymmetric bimodal distributions are apparent (Figure 10). With high uncertainty inputs, the standard deviation in log concentration of calculated U(VI) species is four times the log standard deviation in $U(VI)_{Tot}$ (Table 10).

Species	Analytical Uncertainty		Temporal Uncertainty		Spatial Uncertainty	
	Mean (Log M)	Standard Deviation (Log M)	Mean (Log M)	Standard Deviation (Log M)	Mean (Log M)	Standard Deviation (Log M)
UO_2^{+2}	-14.9	0.091	-14.6	0.268	-15.2	1.33
$Ca_2UO_2(CO_3)_3(aq)$	-5.72	0.085	-6.18	0.346	-6.52	1.35
$CaUO_2(CO_3)_3^{-2}$	-6.23	0.098	-6.59	0.325	-6.94	1.35
$SSOUO_2^{+}$	-5.48	0	-5.48	0	-5.5	0.066
$SOUO_2^{+}$	-5.68	0.091	-5.52	0.171	-6.01	1.26

Table 10: Summary statistics of distributions in Figure 10 (System II, 8.65 µM total U(VI))

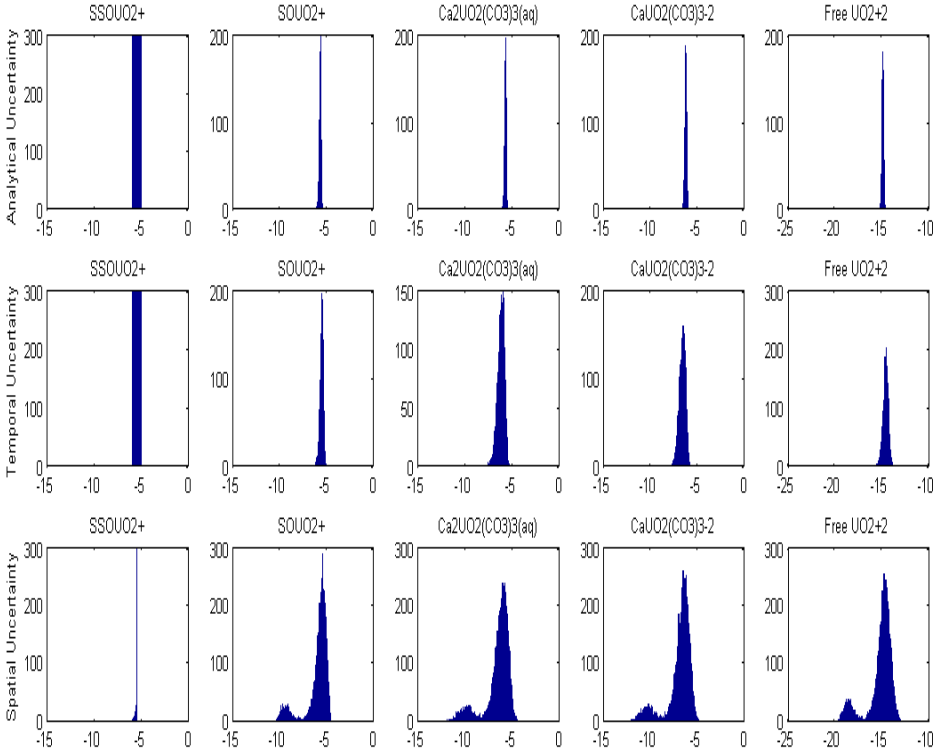

Figure 10: Monte Carlo simulations of System II (dissolved and sorbed) with 8.65 µM total U(VI) showing the frequency of result versus log concentration. Top row is lowest uncertainty (analytical); bottom row is highest uncertainty (spatial). Note the pronounced bimodal distributions at the higher uncertainty levels. Plots normalized for consistent heights, not areas.

Unlike the System I simulations, varying total U(VI) concentration in calculations with sorption has a pronounced effect on both the shape of the output distributions and the uncertainty amplification. At lower $U(VI)_{Tot}$ concentrations, output distributions of U(VI) are highly non-Gaussian and uncertainty amplification is larger. As an example, Figure 11 presents distributions from System II simulations with $U(VI)_{Tot}$ = 3.50 µM, corresponding to an uncontaminated portion of the Old Rifle site. Output distributions are bi-modal for all but the lowest (instrumental) uncertainty levels in Table 11, and the uncertainties are significantly amplified for all dominant species except $SSOUO_2^+$ and for aquo UO_2^{2+} (Table 11). Under these conditions of lower $U(VI)_{Tot}$ and higher uncertainty in analytical constraints, the equilibrium calculation cannot be considered robust.

	Analytical Uncertainty		Temporal Uncertainty		Spatial Uncertainty	
Species	Mean (Log M)	Standard Deviation (Log M)	Mean (Log M)	Standard Deviation (Log M)	Mean (Log M)	Standard Deviation (Log M)
UO_2^{+2}	-16.4	0.134	-16.5	1.16	-16.9	1.89
$Ca_2UO_2(CO_3)_3(aq)$	-7.12	0.138	-8.07	1.2	-8.23	1.92
$CaUO_2(CO_3)_3^{-2}$	-7.64	0.146	-8.48	1.2	-8.66	1.92
$SSOUO_2^+$	-5.49	0	-5.5	0.04	-5.6	0.18
$SOUO_2^+$	-7.05	0.136	-7.38	1.15	-7.67	1.86

Table 11: Summary statistics of distributions for system with low uranium concentration in Figure 11 (System II, 3.50 µM total U(VI)).

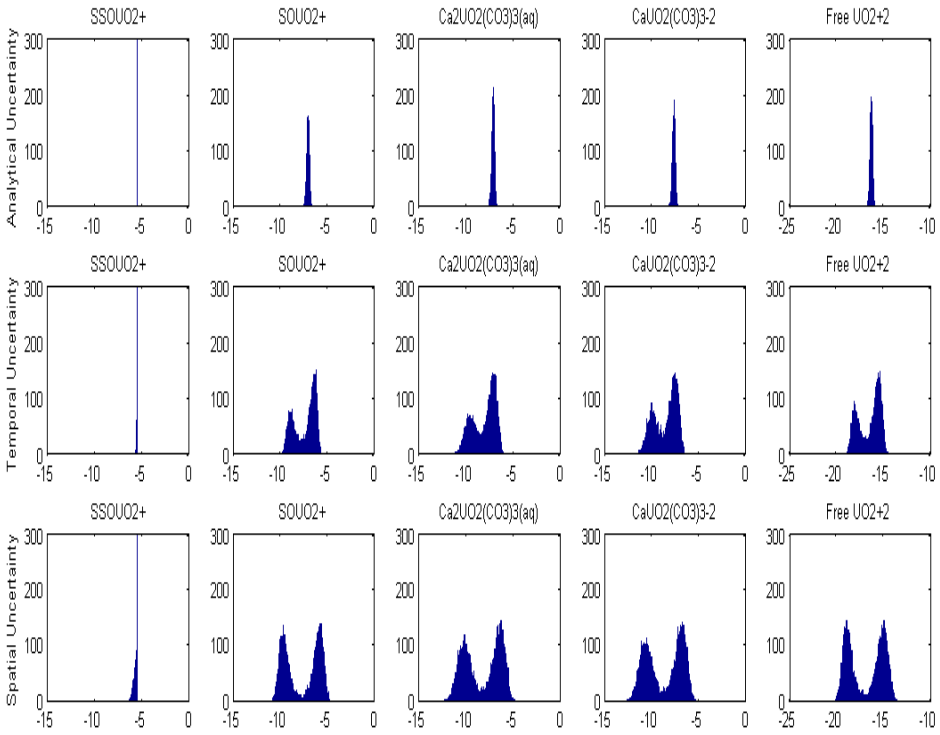

Figure 11: Monte Carlo simulations of System II (dissolved and sorbed) with 3.50 µM total U(VI) showing the frequency of result versus log concentration. Top row is lowest uncertainty (analytical); bottom row is highest uncertainty (spatial). Note the pronounced bimodal distributions at the higher uncertainty levels. Plots normalized for consistent heights, not areas.

The source of the asymmetrical, bimodal distributions and the concomitant amplification of uncertainty is the relationship between the total U(VI) concentration and the abundance of the strongest binding sites. Although the surface complexation model represents sorbed uranium in a smooth fashion, the total dissolved uranium (sum of all dissolved species concentrations) has a steep slope near 3.3 µM total U(VI) concentration, corresponding to the concentration of the strongest binding sites (Figure 6). The bimodal distributions are a result of uncertainty associated with the free uranyl ion.

The results obtained from this analysis are traditionally used within a transport code to estimate the uranium concentration in the entire contamination plum considering all chemical phenomena, such as sorption. But, for our purposes, this analysis will be used to determine the constituents of the artificial groundwater. It also provides an understanding to solution speciation and insight to error associated with modeling

uranium speciation to minerals and sediment. Understanding the error associated with uranium sorption behavior to minerals and sediment and the resulting uranium speciation may be useful in understanding or explaining uranium sorption to biological materials.

Chapter 4 Evaluation of Biosorption

Materials and Methods

Microorganisms

The two types of microorganisms used in the uranium sorption experiments were the *G. uraniireducens* strain Rf4 and *A. palmae*. The *G. uraniireducens* microorganism was chosen because it is the most populous species at the Old Rifle site during active remediation [40]. The *A. palmae* microorganism was chosen because it is closely related to a mollicute species found to be the most populous species after bioremediation ceased [29]. Sulfate-reducing bacteria are also present in large concentrations when the geochemical conditions of the Old Rifle site shift from iron-reducing environments to sulfate-reducing environments due to the remediation effort. Preliminary work listed in Appendix B and done by N'Guessan et al. [68] shows that this type of bacteria, through the use of *D. meridiei* in laboratory sorption tests using Old Rifle groundwater, spiked with 12 μM uranium had minimal, if any uranium sorption capacity. Because sulfate-reducing bacteria were determined to have very minimal uranium sorption capacity in previous tests, they were not considered in these experiments.

The *G. uraniireducens* culture was obtained from University of Massachusetts, Department of Microbiology. The laboratory culture was grown under an anaerobic atmosphere with 5 mM acetate as an electron donor in a bicarbonate-buffered defined medium [87]. Incubation of bacteria occurred under an 80% nitrogen (N_2): 20% CO_2 atmosphere. The *A. palmae* culture was obtained from the ATCC (ATCC 49389) and grown aerobically on 1106 PPLO broth with bovine serum. While *A. palmae* can successfully grow under aerobic or anaerobic atmospheres, the culture was grown aerobically to increase the yield of bacterial mass for experiments. Bacteria were harvested during the stationary growth phase to represent a natural growing culture in the field with some live and some dead bacteria present. *G. uraniireducens* grew faster than the aerobically grown *A. palmae* as indicated by the optical density (OD) of a 10% inoculation for both bacteria as shown in Figure 12. *G. uraniireducens* were harvested at 5 to 7 days, while *A. palmae* were harvested at 7 to 10 days.

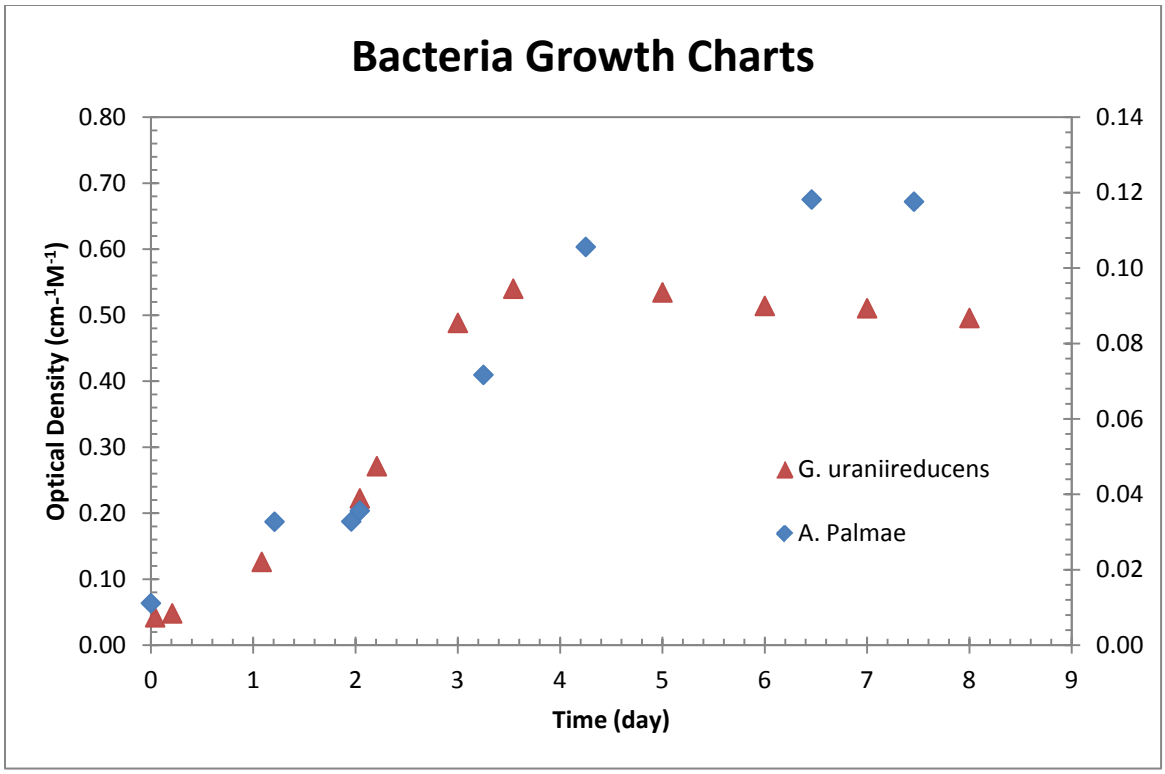

Figure 12: Bacteria growth charts. *G. uraniireducens* growth OD was obtained at 600 nm wavelength while *A. palmae* OD was obtained at 710 nm.

Because *G. uraniireducens* are capable of metabolic uranium reduction, the bacteria were rinsed to remove all growth solution in efforts to prevent or minimize any affinity for uranium reduction during the experiment. This protocol allows for the valid assumption that any decrease of the U(VI) concentration in the test solution is mainly a result of uranium biosorption and not enzymatic uranium reduction. Although *A. palmae* cannot perform enzymatic reduction of uranium, the microorganisms were also rinsed in the same manner as the *G. uraniireducens*. A 0.1 M sodium chloride solution was chosen as the rinse solution to remove growth media because the dissolved ions of sodium and chloride have very minimal complexing affinity with uranly ions (Table 3 of Chapter 3); therefore, any remaining rinse solution associated with the bacteria will not influence uranium sorption during the experiments. The concentration of 0.1 M was selected to provide an intermediate osmotic pressure that would prevent cell lysis. It is assumed that rinsing a bacteria pellet two to three times removes all growth media [89]. Therefore, the harvested bacteria were rinsed four times in 0.1 mM NaCl solution in efforts to ensure the removal of all growth solution from the pellet.

The rinse process began by harvesting a bacterial pellet from the growth media by centrifugation at 5,000 RPM for 20 minutes. The growth solution was decanted from the bacterial pellet, and any remaining visible liquid around the pellet was removed with a pipette tip. After all visible liquid was removed from the pellet; the bacteria were re-dispersed into an aliquot of rinse solution by inducing a vortex using vortex equipment at high until the mixture was completely homogenized. This homogenized mixture was diluted to 50 ml with rinse solution, mixed again, and centrifuged for 20 minutes at 5,000 RPM. This was repeated until four rinses were achieved. After the final rinse and centrifuge, all visible liquid around the pellet was removed using a pipette tip, and the centrifuge tube wall was dried using a KimWipe. A wet weight for the bacteria pellet was taken three times, and the average weight was recorded. A dry weight was also obtained by exposing bacteria pellets with known wet weight to 70^{o}C for 24 hours. The ratio of dry weight to wet weight was determined to be 0.13.

Because bacteria were harvested at the stationary growth phase and because both live and dead bacteria were expected in solution, a live/dead stain could not be easily used to verify the cell membrane integrity. It was not until analysis of experiments that cryo-EM imaging was used to determine whether the cells were damaged during experimental preparation. Figure 13 is an image taken of *A. palmae* upon completion of an experiment. The image shows minimal, if any, disturbance to the cell membrane caused by the rinse. The cryo-EM images of the *G. uraniireducens* cells (Figure 14) show the rinsing process did irritate the cell membrane, resulting in some areas of membrane distortion, but the process did not destroy the cell membrane integrity. Overall, the cell membrane for both types of microorganisms was intact and any irritation to the membrane caused by the collection and rinsing process should not significantly affect the experimental results.

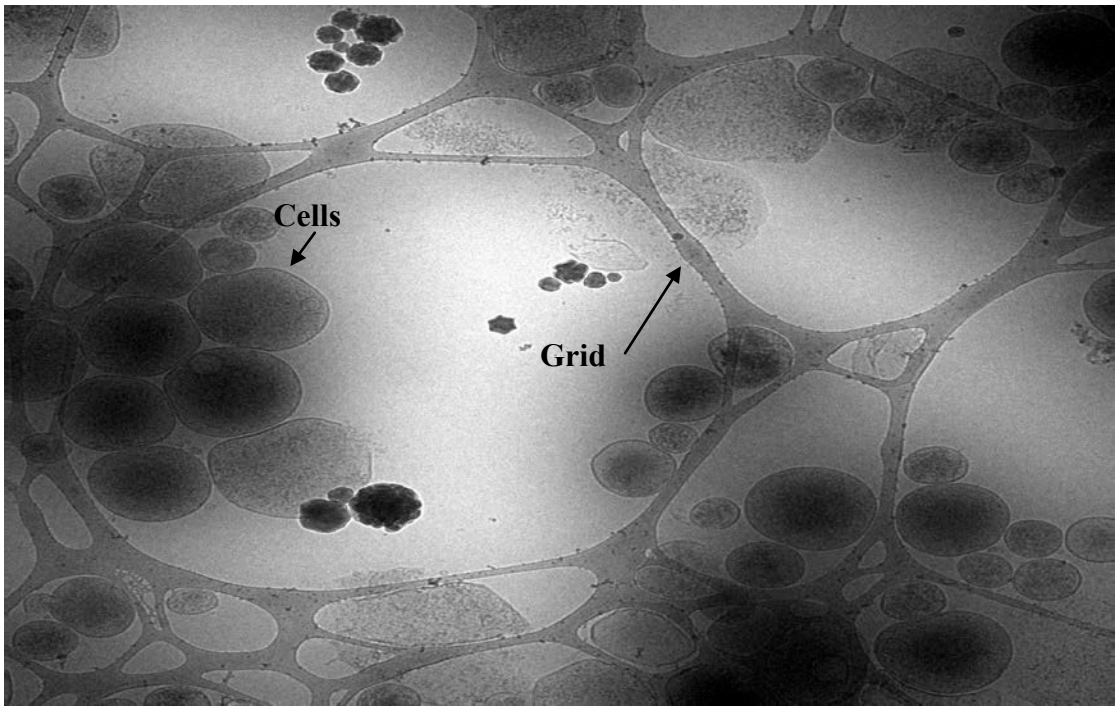

Figure 13: Cryo-EM image of *A. palmae* showing intact cells after rinse and re-disbursement into experimental solution.

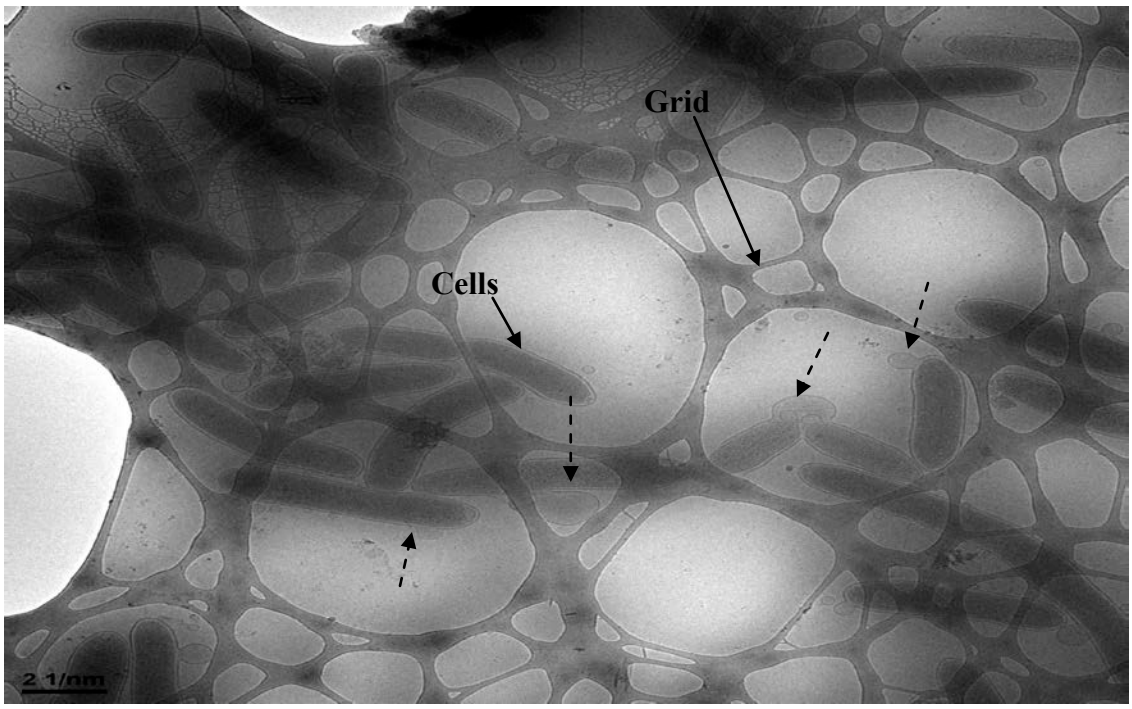

Figure 14: Cryo-EM image of *G. uraniireducens* presenting intact cells with some membrane disturbance (examples indicated by dashed arrows pointing at lighter colored bulge) after rinse and re-disbursement into experimental solution.

Artificial Groundwater (AGW)

In geochemical literature, it is common to report DIC concentrations as the partial pressure of CO_2 (P_{CO2}) that would be in equilibrium with the carbonic acid, H_2CO_3, concentration based on Henry's Law. The relationship between DIC and P_{CO2} as shown by Figure 15 was calculated by VisualMINTEQ. The equilibrium between H_2CO_3 and DIC concentrations depends on the pH of the solution as shown by Figure 16.

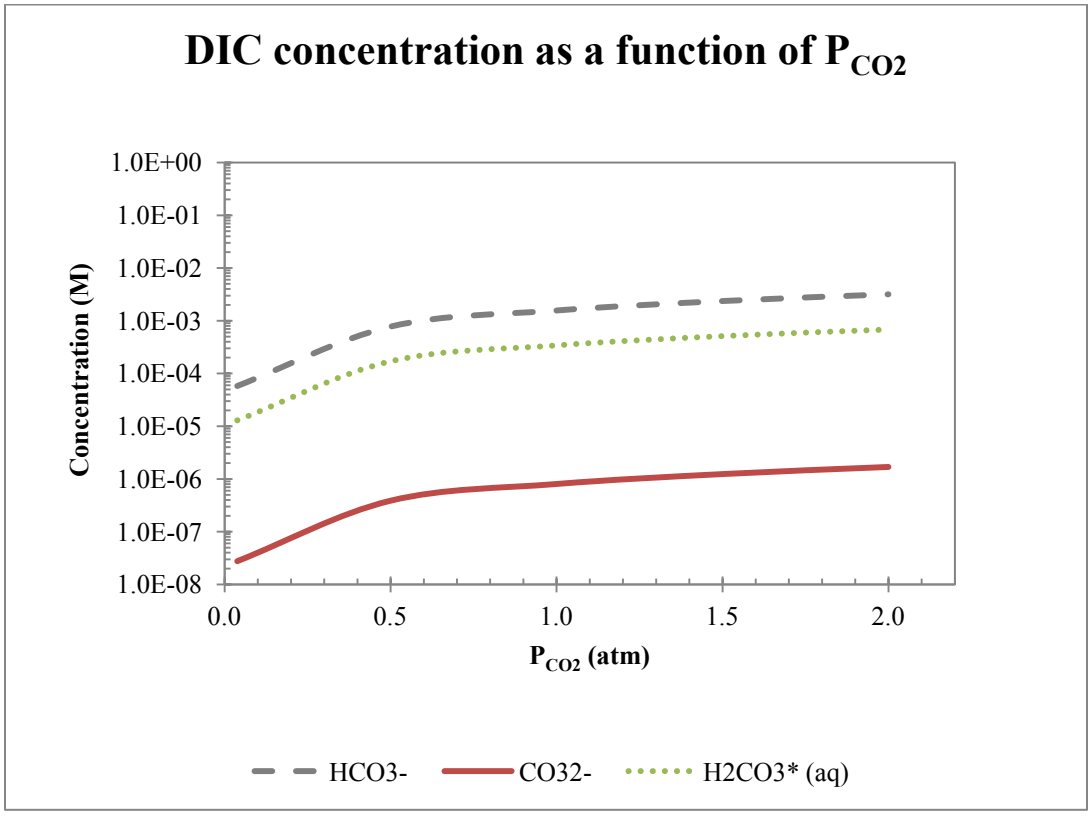

Figure 15: Changes in soluble DIC concentrations as a function of P_{CO2} at pH 7. System modeled using VisualMINTEQ.

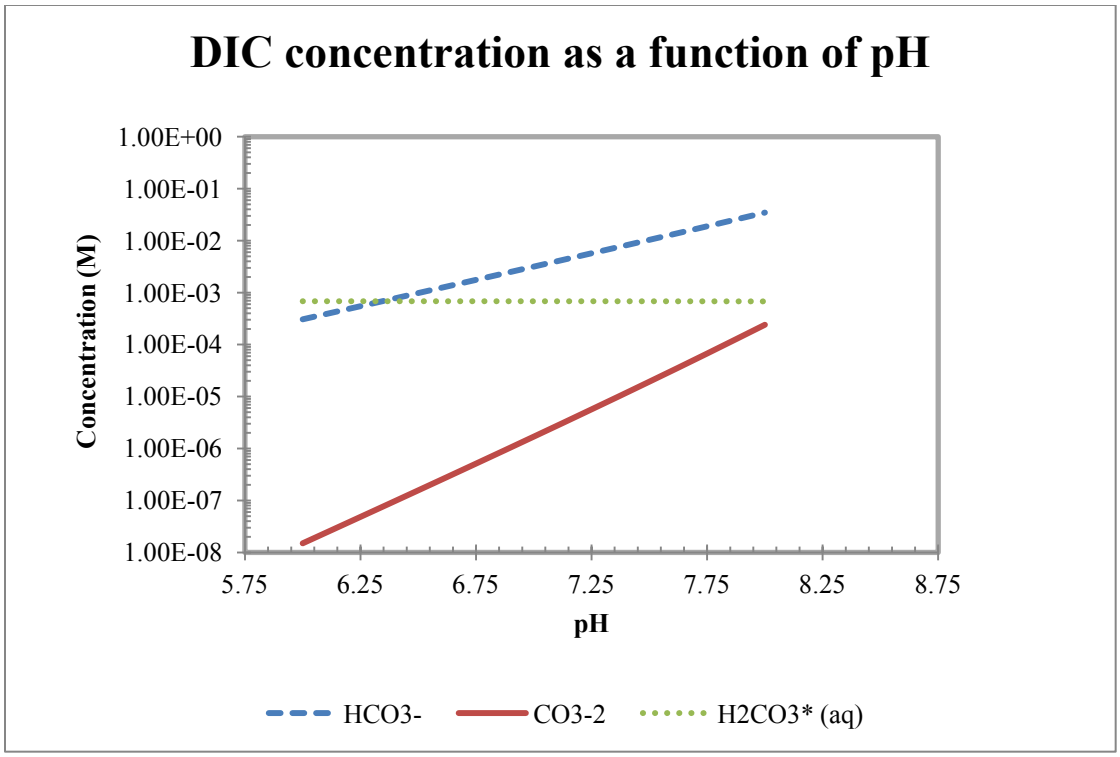

Figure 16: Effects on the DIC distribution for water exposed to 2% P_{CO2} a function of solution pH. System modeled by VisualMINTEQ.

With a total atmospheric pressure of 1 atm, the P_{CO2} can be reported as a percent of total pressure. Typical aquifer P_{CO2} may range from 1% to 5% [11]. This type of variability in P_{CO2} is also seen at the Old Rifle site, with an average P_{CO2} slightly more than 3% [23, 70]. While it is known that increased P_{CO2} decreases uranium sorption to minerals and sediment [11, 17, 55], the major uranyl speciation distribution does not differ significantly from approximately 99% of uranyl distribution to the calcium-uranyl-triscarbonato species for groundwater with P_{CO2} greater than 2% and calcium concentration equal to 6.5 mM, as shown in Table 12. For sorption experiments, artificial groundwater (AGW) was exposed to a maximum of 2% P_{CO2} and atmospheric P_{CO2} (380 ppm) to achieve the DIC concentrations of approximately 0.07 mM (atmospheric P_{CO2}) and 3.3 mM (2% P_{CO2}). Experiments with AGW exposed to 0.2% P_{CO2} were desired but could not be achieved with the gassing station, which is discussed further below.

Species	Percent Uranium distribution as a function of P_{CO2}		
	5%	2%	Atmospheric
$Ca_2UO_2(CO_3)_3$ (aq)	67.4	81.4	10.6
$CaUO_2(CO_3)_3^{-2}$	31.6	18.2	2.3
UO_2CO_3 (aq)	>1.0	>1.0	6.2
$UO_2(CO_3)_2^{-2}$	>1.0	>1.0	1.1
$(UO_2)_2CO_3(OH)_3^-$	>1.0	>1.0	75.2
UO_2OH^+	>1.0	>1.0	1.9
$UO_2(OH)_2$ (aq)	>1.0	>1.0	1.9

Table 12: Uranyl distribution at pH = 6.95, Ca^{2+} = 6.5 mM, SO_4^{2-} = 8.5 mM using VisualMINTEQ using complete database listed in Table 3 of Chapter 3. A shift in uranyl distribution from approximately 99% calcium-uranyl-triscarbonato species only occurs between atmospheric and 2% P_{CO2}.

A gas-mixing manifold was constructed to provide the gassing capabilities necessary to produce the different CO_2 environments required for experiments and for culturing *G. uraniireducens*. The station allowed the gasses to be mixed at the injection point and was calibrated using a 2 L graduated cylinder and a large tub of water. The calibration was done using a graduated cylinder that was inverted in a large the tub of water above a tube with flowing gas. The gas flow pushed water into the inverted cylinder for a given amount of time. The volume of water pushed into this graduated cylinder divided by the time span in which this occurred provided a gas flow rate. This was done in triplicate for at least three different points on each flow meter. The CO_2 flow meter was calibrated with an r^2 value of 0.9987, and the N_2 gas flow meter calibration resulted in an r^2 value of 0.9995.

These two flow meters were able to produce a 2% and 20% P_{CO2} environment without issue. A smaller CO_2 flow meter was purchased in efforts to achieve a 0.2% P_{CO2} atmosphere and was calibrated with an r^2 value of 0.9952. While this flow meter was successfully calibrated, it was not used due to back pressure issues experienced at the injection mixing point. The large flow from the N_2 meter of approximately 2,000 ml min^1 did not allow for reliable mixing of the small flow of CO_2 (~4 ml min^{-1}). Because it was difficult to consistently produce a 0.2% P_{CO2} environment, it was decided that this test condition could be dropped from the testing matrix because a comparison between

atmospheric P_{CO2} and 2% P_{CO2} would still provide the necessary information to evaluate biosorption and the effects of P_{CO2}. A premade, laboratory-certified gas with 380 ppm CO_2 was used to perform the atmospheric P_{CO2} experiments.

The AGW was originally prepared in a bulk solution using a 600 ml Nalgene beaker and 18 MΩ dionized water with 6.5 mM calcium, 8.5 mM sulfate, and variable U(VI) concentrations, which were determined from Old Rifle site values listed in Table 1 of Chapter 3. These ions were chosen because they are the critical components of the Old Rifle site system as indicated by the sensitivity analysis presented in Chapter 3. A uranium nitrate (1.4% HNO_3 v/v) standard was the source of U(VI) in solution. After all AGW components were added to the solution, the 600 ml Nalgene beaker was covered with parafilm and gassed to achieve the desired atmosphere (Figure 17). The predetermined pH was reached by correcting the solution pH with the addition of base or acid until the solution reached equilibrium with the target P_{CO2} atmosphere. After the target pH of the test solution was reached, the ionic strength of the solution was calculated by VisualMINTEQ and adjusted to approximately 0.04 adding sodium chloride to the solution.

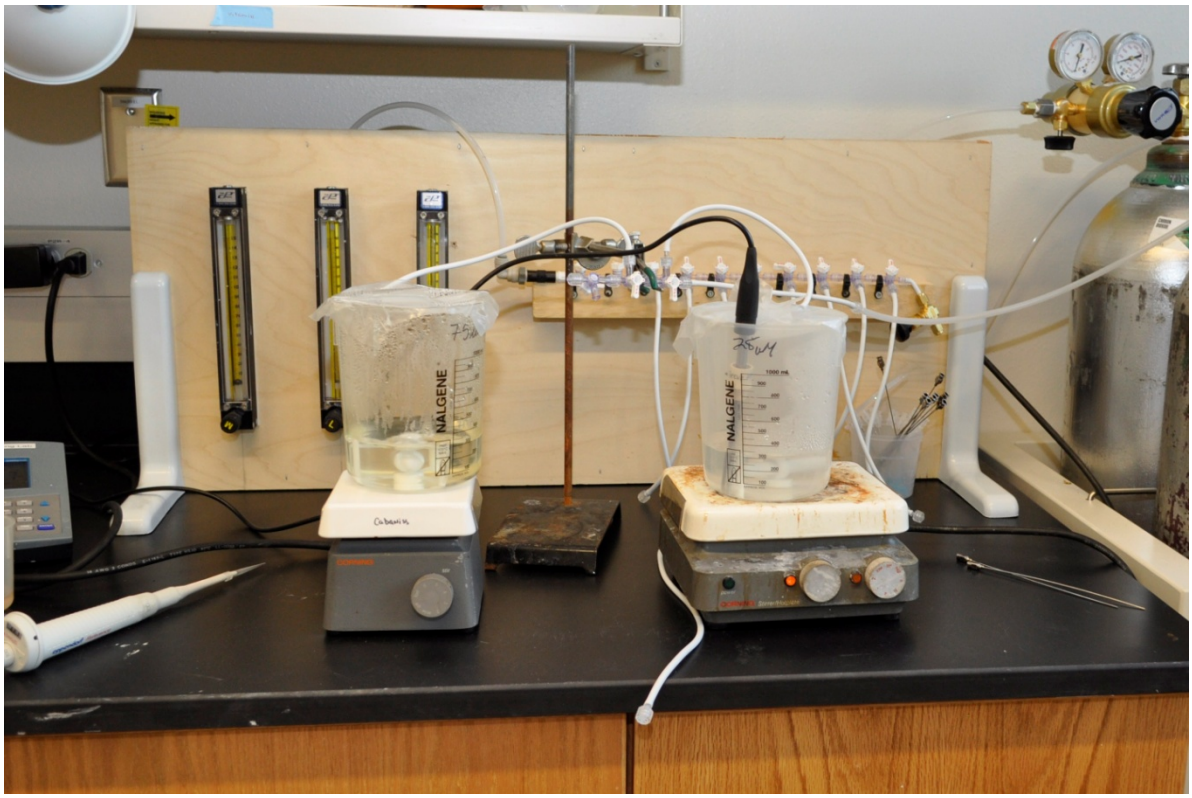

Figure 17: Preparation for bulk solution to set pH at desired P_{CO2}.

The 2% P_{CO2} AGW atmosphere was achieved by gassing the solution with a calibrated N_2:CO_2 (98:2) gas flow while adding acid/base to achieve the desired pH of 6.95 ± 0.05. While the Old Rifle site average pH is 7.2 at this P_{CO2}, a higher pH would be supersaturated with respect to calcite in the experimental solutions. Atmospheric AGW solutions were bubbled with laboratory-certified 380 ppm CO_2 until the desired pH was reached by the addition of base and/or acid, followed by open atmosphere equilibration with another slight acid/base adjustment to correct for any pH drift. For experiments exposed to atmospheric P_{CO2}, the solution pH was controlled to 7.0, so the results would be directly comparable to those obtained under 2% P_{CO2} conditions. Due to the low buffering capacity of the atmospheric P_{CO2} AGW solution, the pH could only be controlled to ± 0.2 of the target pH. Once the desired pH was reached in the bulk AGW solution, it was aliquoted for testing.

Sorption experiments

The weight of the collected bacteria pellet was used to determine the volume of the AGW for each experiment to obtain a known bacterial concentration in the solution. The concentration of *G. uraniireducens* used during testing ranged from approximately 200 g L^{-1} to 5 g L^{-1}, and the concentration of uranium used during those tests ranged between 70 μM to 0.4 μM (Appendix B). The concentration of *A. palmae* used during testing ranged from 30 g L^{-1} to 8.5 g L^{-1}, and the concentration of uranium used during those test ranged between 50 μM and 0.7 μM (Appendix B). The desired volume of the solution was added to the bacteria pellet and redistributed by vortex mixing. The tube was capped with a septum (Figure 18a), re-gassed to return the solution to the desired atmosphere obtained during bulk preparation (Figure 18b), and put into a rotation device during the experiment to achieve a fully mixed solution during the sorption experiment (Figure 18c). All test solutions were allowed to mix slowly for no less than 4 hours, typically 19 hours. This equilibrium time was chosen based on the unpublished work done by N'Guessan et al. (Appendix B) who determined that greater than 95% of the uranium sorption to biomass occurred within the first 4 hours [68].

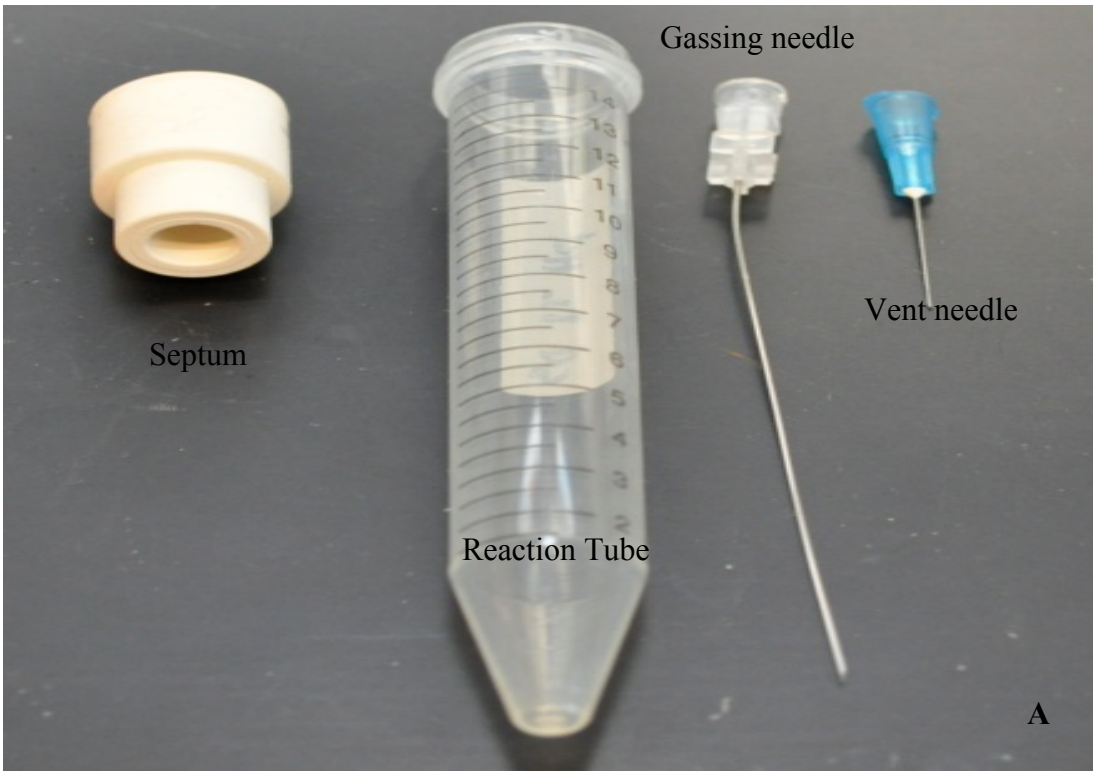
Gassing needle
Septum
Vent needle
Reaction Tube
A

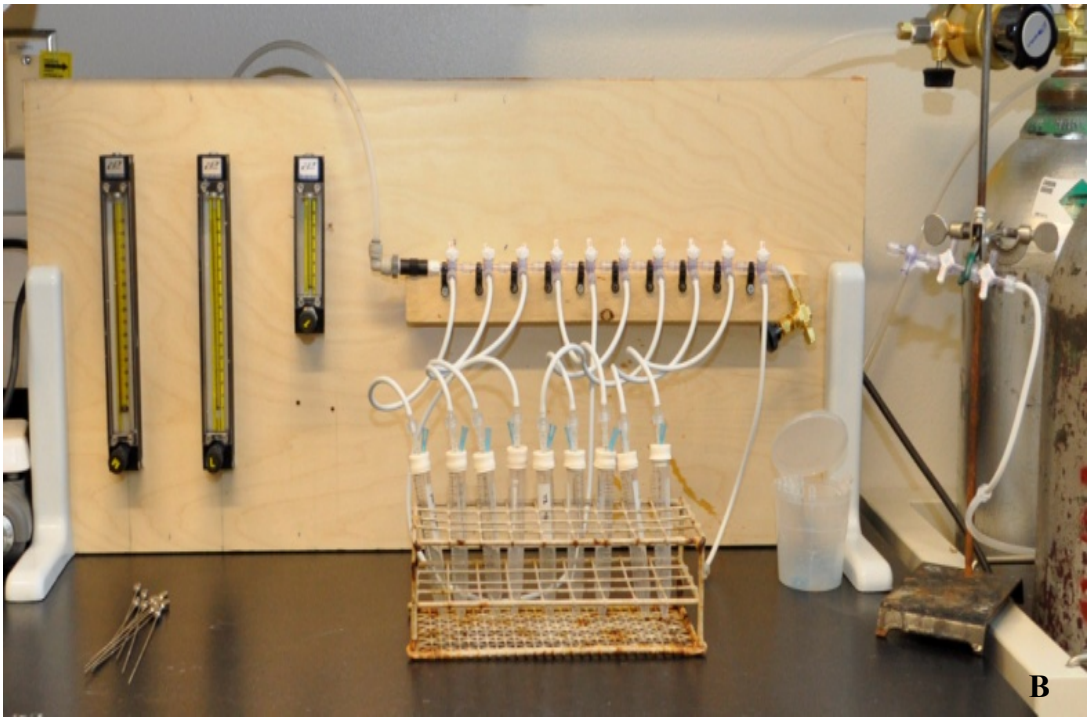
B

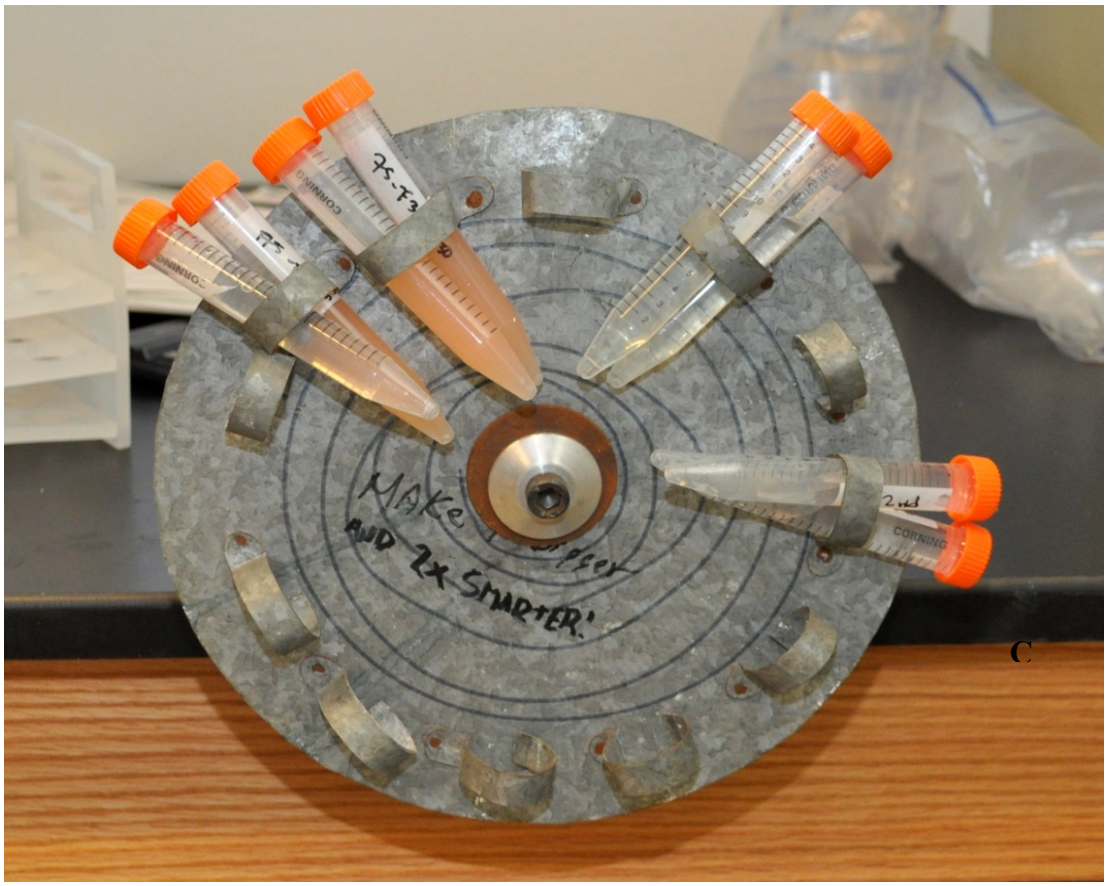

Figure 18: Final experimental preparation. a) Individual test container with septum and needles to gas solution, b) gassing of experiment to achieve desired P_{CO2}, and c) rotation device to ensure full mixing during experiment.

Experiments were prepared to measure three conditions for each sorption test: 1) to obtain conformation of initial uranium concentration of the bulk solution (U_{total}) and indicated whether any uranium was lost to the container wall; 2) to determine the pH at the end of testing, which ensured DIC content and monitored for degassing; and 3) to determine the uranium concentration remaining in solution after the AGW reached equilibrium with the bacteria (U_{aq}). The uranium sorption density on the bacteria was determined by subtracting the mass of U_{aq} from the mass of U_{total} and dividing by the mass of bacteria (BM), as described by equation 19.

$$U_{sorbed} = \frac{U_{total} - U_{aq}}{BM} \tag{19}$$

While uranium loss to the container walls was not an issue for experiments performed under 2% P_{CO2} conditions, uranium did sorb to the wall of the containers used during

atmospheric P_{CO2} test. Under atmospheric P_{CO2} conditions, a loss of uranium to the container walls occurred and was variable even when the tests were performed in the same material made by different manufacturers. To eliminate some variability associated with uranium sorption to the container walls, only one type of centrifuge tube made by a single manufacturer was used. After this modification to the experimental protocol was made, uranium losses to the container wall were assumed to be similar to all centrifuge tubes. Thus, the loss of uranium to the walls was neglected in the sorption calculation. To account for loss of uranium to the container walls, the inductively coupled plasma-mass spectroscopy (ICP-MS) analysis of the initial concentration of the bulk solution, U_{total}, was used to determine the initial uranium available for sorption to bacteria.

At the end of testing, the solutions exposed to bacteria were centrifuged for 20 minutes at 5,000 RPM. The solutions used to determine U_{total} and U_{aq} were filtered through 0.2 μm syringe-driven Millex-VF PVDF filters, immediately acidified with nitric acid for ICP-MS analysis, and stored in acid-washed polypropylene tubes. The pH values of the other aliquots were measured using a Hach 280g meter with a stainless steel solid state probe outfitted with a septum top to prevent degassing of the solution during measurement. The final pH of the test solution decreased due to the addition of bacteria to the solution. The addition of bacteria to the solution caused a drift of 0.1 pH units for 2% P_{CO2} experiments and up to 0.5 pH units for atmospheric P_{CO2} experiments. Given that these drifts in pH were artifacts of the experiments themselves and not preventable by experimental design, the solution pH before the addition of bacteria was considered to be the system pH.

Analytical techniques

Inductively Coupled Plasma-Mass Spectroscopy (ICP-MS)

Uranium concentrations were measured using either a Thermo X-Series II or Perkin Elmer Elan 6100 ICP-MS. Samples were diluted volumetrically with 1% optima-grade nitric acid to minimize matrix effects and to keep expected uranium concentrations within the range of the standards. Standards ranging from 0.1 to 100 ppb were prepared in 1% nitric acid. Each sample and standard was introduced to the plasma using a Gilson peristaltic pump with a tracer standard to monitor instrumental drift. A check standard was run every 10 samples to verify performance within 10% of the expected value. This

analysis was done at the Earth and Planetary Science Department of the University of New Mexico and at the Colorado School of Mines.

Cryo-Transmission Electron Microscopy (TEM) Specimen Preparation

For cryo-transmission electron microscopy (TEM), aliquots of 5 µL were taken directly from the in-vitro cultures and placed onto lacey carbon grids (Ted Pella 01881, Ted Pella Inc., Redding, CA) that were pre-treated by glow-discharge. The Formvar support was not removed from the lacey carbon. The grids were manually blotted with filter paper and plunged into liquid ethane by a compressed air piston, then stored in liquid N_2. This preparation was done at the Lawrence Berkeley National Laboratory.

Cryo-TEM Imaging

Images were acquired at the Lawrence Berkeley National Laboratory on a JEOL–3100 electron microscope equipped with a FEG electron source operating at 300 kV, an Omega energy filter, a Gatan 795 2Kx2K CCD camera (Gatan Inc., Pleasanton, CA), and cryo-transfer stage. The stage was cooled with liquid N_2 to 80 K during acquisition of all data sets.

To have a statistically relevant survey, more than 60 images were recorded using magnifications of 136 kx, 86 kx, 44 kx, and 25 kx at the CCD giving a pixel size of 0.22 nm, 0.34 nm, 0.68 nm, or 1.2 nm at the specimen, respectively. Underfocus values ranged between 2.0 µm ± 0.5 µm to 12 µm ± 0.5 µm, and energy filter widths were typically around 22 eV ± 2 eV.

Electron Tomography

Four tomographic data sets were acquired at the Lawrence Berkeley National Laboratory. Tomographic tilt series were acquired under low-dose conditions, typically over an angular range between +65° and -65°, ± 5° with increments of 1° or 2°. Between 70 and 124 images were recorded for each tilt series, acquired semi-automatically with the program Serial-EM (http://bio3d.colorado.edu/) adapted to JEOL microscopes.

For these tilt series data sets, all images were recorded using nominal magnifications of 20 kx and 40 kx at the CCD giving a pixel size of 1.2 nm or 0.68 nm at the specimen, respectively. Underfocus values ranged between 6 µm ± 0.5 µm to 12 µm ± 0.5 µm,

depending on the goal of the data set. Energy filter widths ranged between 22 to 28 eV, also depending on the data set. For all data sets, the maximum dose used per complete tilt series was approximately 140 $e^-/Å^2$, with typical values of approximately 100 $e^-/Å^2$.

All tomographic reconstructions were obtained with the program Imod (http://bio3d.colorado.edu/) (Kremer et al. 1996) and acquired at the Lawrence Berkeley National Laboratory. The program ImageJ (NIH, http://rsb.info.nih.gov/ij/) was used to analyze the 2D image projections. Volume rendering and image analysis of tomographic reconstructions was performed using the open-source program ParaView (http://www.paraview.org/). All movies were created with the open source package ffmpeg (http://www.ffmpeg.org/). The inner membranes of two cells of each species were segmented by hand using the program Imod.

Energy-Dispersive X-ray (EDX) spectroscopy

High-spatial resolution chemical analysis of cell membranes of air-dried samples were carried out in the JEOL 2100-F 200 kV Field-Emission Analytical TEM equipped with Oxford INCA EDS x-ray detection system at the Molecular Foundry at the Lawrence Berkeley National Laboratory. High-angle annual dark field (HAADF) scanning transmission electron microscopy (STEM) images and x-ray elemental line scans were acquired with a 1 nm probe at 200 kV. The specimens were tilted 10 degrees toward the x-ray detector to optimize the x-ray detection geometry. Collection times were 300 live seconds for each line scan.

The EDS linescans on the high-contrast regions of the OM clearly demonstrate the localized uranium in this membrane responsible for the increased contrast in the STEM HAADF images.

Beamline X-ray Spectroscopy

Samples were transferred into AI sample holders under anaerobic conditions (~2% hydrogen, 98% N_2). 1 mL aliquots of sample were centrifuged, and the supernatant was discarded. Pellets were pooled into a single microfuge tube prior to loading. Loaded sample holders were maintained under anoxic conditions until loaded into a liquid N2 cryostat and then placed under a vacuum at beam line 11-2. The Si(220) monochromators

were detuned by 15% of its maximum transmission to reject harmonics. Energy calibration was maintained continuously using a yttrium foil. Fluorescence x-ray absorption near edge structure (XANES) spectra were measured at the ULIII-edge. XANES spectra were then background subtracted and processed using ARTEMIS. This analysis was done at Stanford Synchrotron Radiation Laboratory.

Results and Discussion

Sorption Isotherms

G. uraniireducens exposed to atmospheric P_{CO2} (Figure 19) resulted in the largest capacity for U(VI) sorption with a K_D value of 7985 ± 1024 L kg^{-1}. *A. palmae* exposed to atmospheric P_{CO2} (Figure 20) produced a lower K_D value of 1850 ± 1.8 L kg^{-1}. The K_D values are within range on a mass basis of values estimated from results for *B. subtilis* [69] and to *S. elongatus* strain BDU/75042 [67], both exposed to atmospheric P_{CO2}. Direct comparison of the K_D values determined on a mass basis and obtained for uranium sorption to the two different bacteria implies *G. uraniireducens* are approximately four times more sorptive than *A. palmae*.

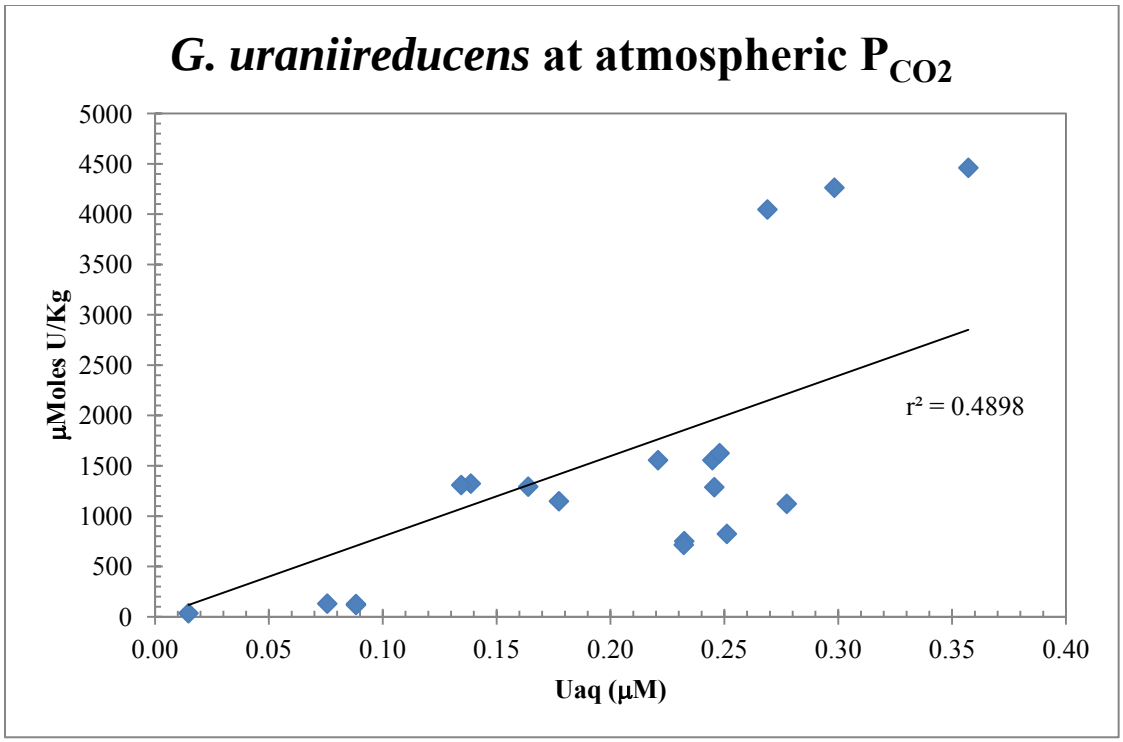

Figure 19: Uranium sorption to *G. uraniireducens* under atmospheric P_{CO2} at pH 6.95 ±0.05 with 6.5 mM calcium and 8.5 mM sulfate.

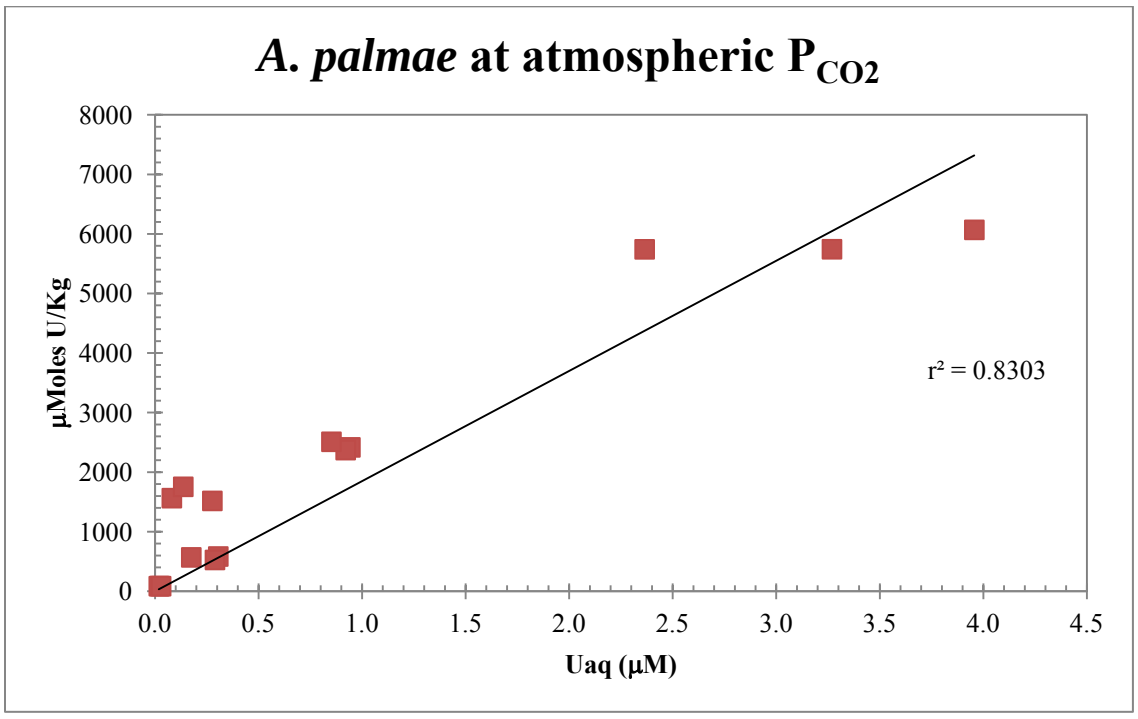

Figure 20: Uranium sorption isotherm to *G. uraniireducens* under 2% P_{CO2} at pH 7±0.2 with 6.5 mM calcium and 8.5 mM sulfate.

The r^2 value of 0.43 obtained from the isotherm of the uranium sorption to *G. uraniireducens* under atmospheric P_{CO2} indicates the available mass of bacteria accounts for slightly less than half of the variance associated in the statistical model of uranium sorption to the surface of the bacteria. Also, if some of the end data points shown in Figure 19 were removed, it is possible to fit the data to a Langmuir or Freundlich isotherm because it appears a maximum sorption capacity is reached around 1200 or 1450 μMoles kg^1, depending on what data are removed (options shown by red curves in Figure 21). But, data was not removed from the analysis to explore the possibility of a Langmuir or Freudlich isotherm because of cryo-imaging of *G. uraniireducens* presented in the upcoming image section. Briefly, these images presented in the upcoming section of "Images of uranium sorption by bacteria "showed that cells exposed to very high concentrations of uranium, 50 μM, the uranium sorbed in a patchy pattern to the surface of the bacteria and inside the OM of the cell. The patchy uranium sorption to the surface of the cell indicated that the surface was not saturated. Therefore, eliminating data points and fitting the remaining data to an isotherm equation does not represent the true sorption phenomena that occurs, even though it may result in a better statistical fit (r^2 = 0.59 Appendix B). The low r^2 value could be a result error propagation related to the standard deviation between replicates which was between 5 – 20% (Appendix B) or a result of the statistical model not accounting for the ability for the uranium to sorb to the inner surface of the cell membrane.

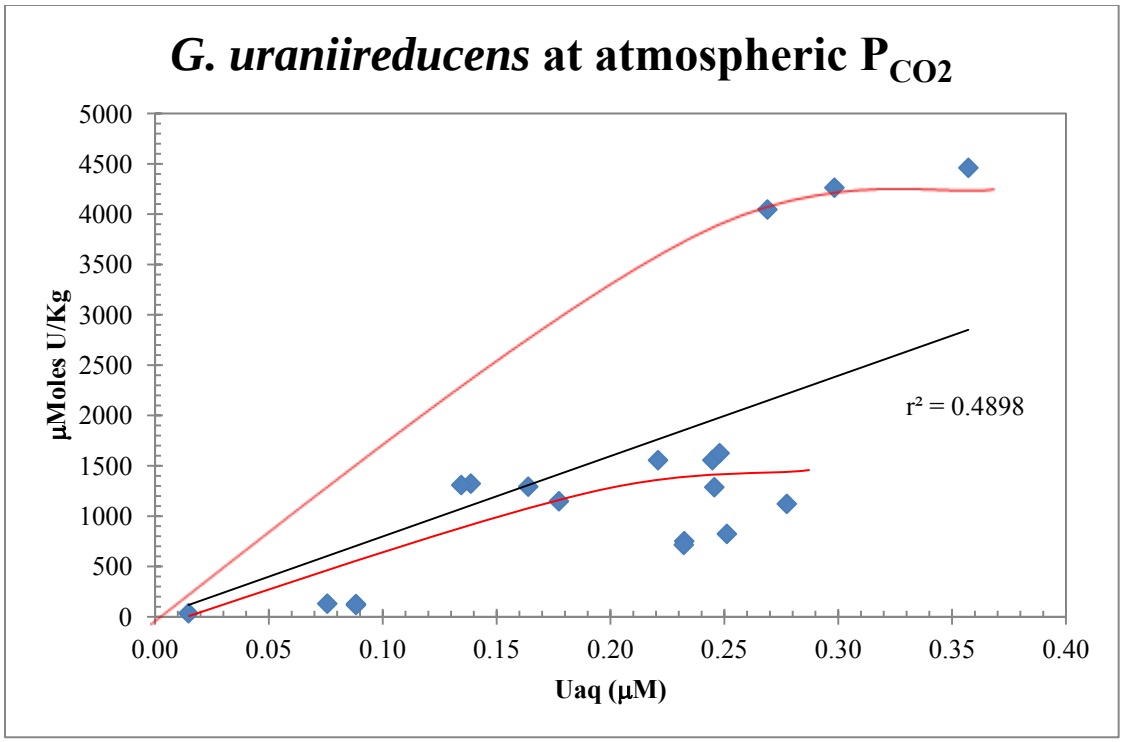

Figure 21: Uranium sorption to *G. uraniireducens* under atmospheric P_{CO2} at pH 6.95 ±0.05 with 6.5 mM calcium and 8.5 mM sulfate. This is the same sorption isotherm shown by Figure 19, but presents possible option for Langmuir or Freudlich isotherm application.

While the difference in experimental uncertainty associated with the plots (r^2 values between 0.43 and 0.83) is acknowledged, comparing uranium sorption capacity was done as defined by the K_D approach represented by equation 4. Before a direct comparison of K_D values obtained for both types of bacteria was done, ranges that were directly comparable for the two different types of bacteria were graphed together to more closely examine the mass comparison of uranium sorption. This required truncation of the experimental data. As seen in Figure 22, the sorptive capacities for the two types of bacteria at the lower end of the isotherm appear to be equivalent on a mass basis. To obtain a better estimate of the difference in uranium sorption affinity between the bacteria, a comparison was done based on the surface area of the different bacteria.

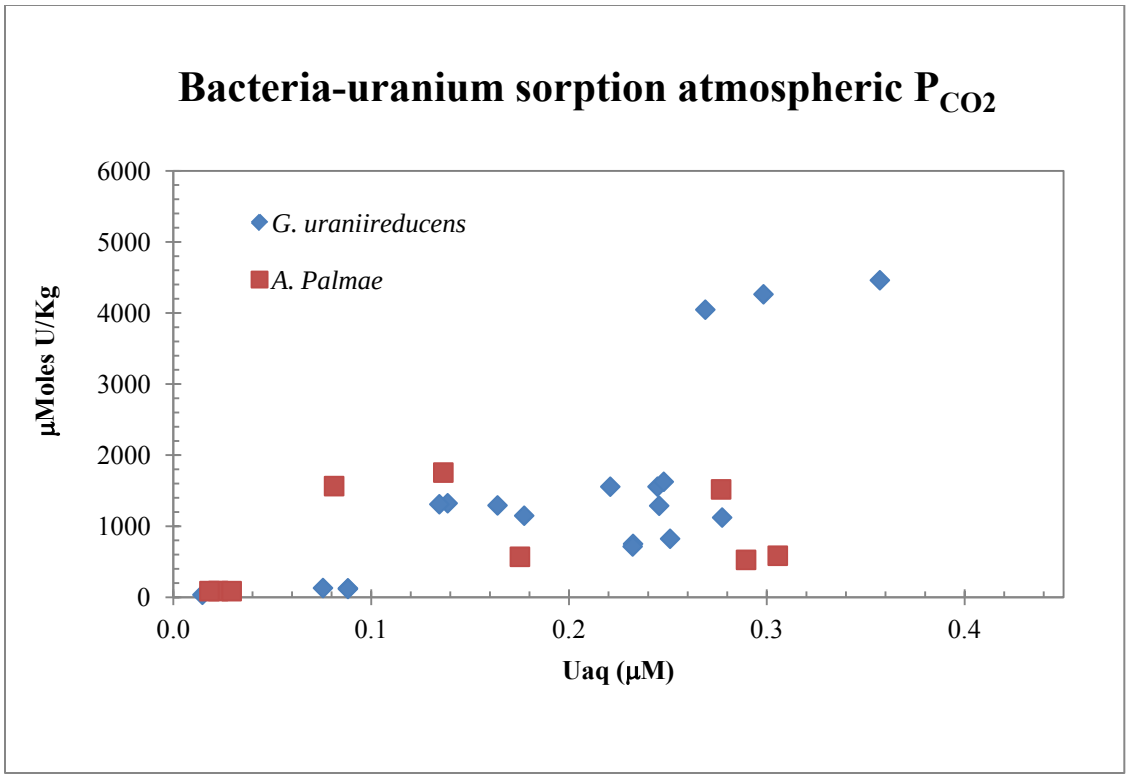

Figure 22: Comparison of sorption capacity of both types of bacteria within similar ranges

While the density of the different type of bacteria can be assumed to be equivalent, the surface areas are different due to the different shapes and sizes of the bacteria. *G. uraniireducens* cells are rod shaped, and *A. palmae* cells are spherical. Using average values for radius and length [88, 89], the geometry of the different bacteria and an estimated bacteria density of 1 g cm^{-3}, the *G. uraniireducens* cell resulted in approximately 2.4 times less surface area than the *A. palmae* cell (Table 13). Assuming the sorption capacity on a mass basis is equivalent, the sorption capacity for *G. uraniireducens* based on surface area is 2.4 times greater than that of *A. palmae*.

Bacteria	Radius (µm)	Length (µm)	Area (μm^2 $cell^{-1}$)	Volume (μm^3 $cell^{-1}$)	Mass (g $cell^{-1}$)	surface area (m^2 g^{-1})
G. uraniireducens	0.50	2	7.85	1.57	6.37E+11	5
A. palmae	0.25	-	0.79	0.07	1.53E+13	12

Table 13: Available surface area based on bacteria mass assuming a density of 1 g cm^{-3}. This analysis is on the test performed under atmospheric P_{CO2} conditions.

The comparison of sorption capacity on a surface area basis was also done using the complete experimentally obtained data set under atmospheric P_{CO2} conditions and its resulting K_D values (Figures 19 and 20). This was done by converting the experimentally determined K_D (L kg^{-1}) obtained under atmospheric P_{CO2} conditions to a value based on the surface area, K_D'(L m^{-2}), allowing for the equivalent comparison of sorptive capacity based on the available surface area found for each type of microorganisms. Comparing the K_D' (L m^{-2}) (Table 14), *G. uraniireducens* were determined to be approximately eight times more sorptive than *A. palmae,* which is twice the sorptive affinity captured by the mass comparison. Based on the comparison of uranium sorption capacity on a surface area basis, a difference in uranium sorption capacity does exist between the two different types of bacteria. The difference in sorption could be due to the different functional groups found on the cells, the different concentration of functional groups per area of cell wall, or the different sorption processes such as sorption within the OM or "passive reduction" associated with uranium sorption to the different bacteria.

Bacteria	Surface area (m^2 g^{-1})	K_D (L kg^{-1})	K_D' (L m^{-2})
G. uraniireducens	5	7985	1.6
A. palmae	12	1850	0.2

Table 14: Experimental K_D converted for direct surface-area comparison using data presented in the previous table.

The effect of increased DIC concentration due to exposure to different P_{CO2} environments resulted in decreased uranium biosorption for both types of bacteria. As shown in Figure 23, exposing *G. uraniireducens* to 2% P_{CO2} decreased the K_D significantly from 7985 ± 1024 L kg^{-1} to 25 ± 1.8 L kg^{-1}. The r^2 value associated with this analysis is 0.63 which is larger than the r^2 value obtained from the analysis of data collected under atmospheric P_{CO2}. Although both r^2 values associated with the two *G. uraniireducens* isotherms are not as high as one would like for reliable predictive purposes, theses models indicate that the mass of the bacteria accounts for approximately half of the variance associated within the statistical model of uranium sorption to *G. uraniireducens*. These results indicate that the mass of *G. uraniireducens* present is an important factor, but not the only factor influencing uranium sorption; there is another phenomenon occurring during uranium

sorption associated with *G. uraniireducens*, such as the ability for uranium to penetrate the OM or the ability for *G. uraniireducens* to reduce uranium without an external electron donor. These possibilities are discussed later in the document with further detail and supporting analysis.

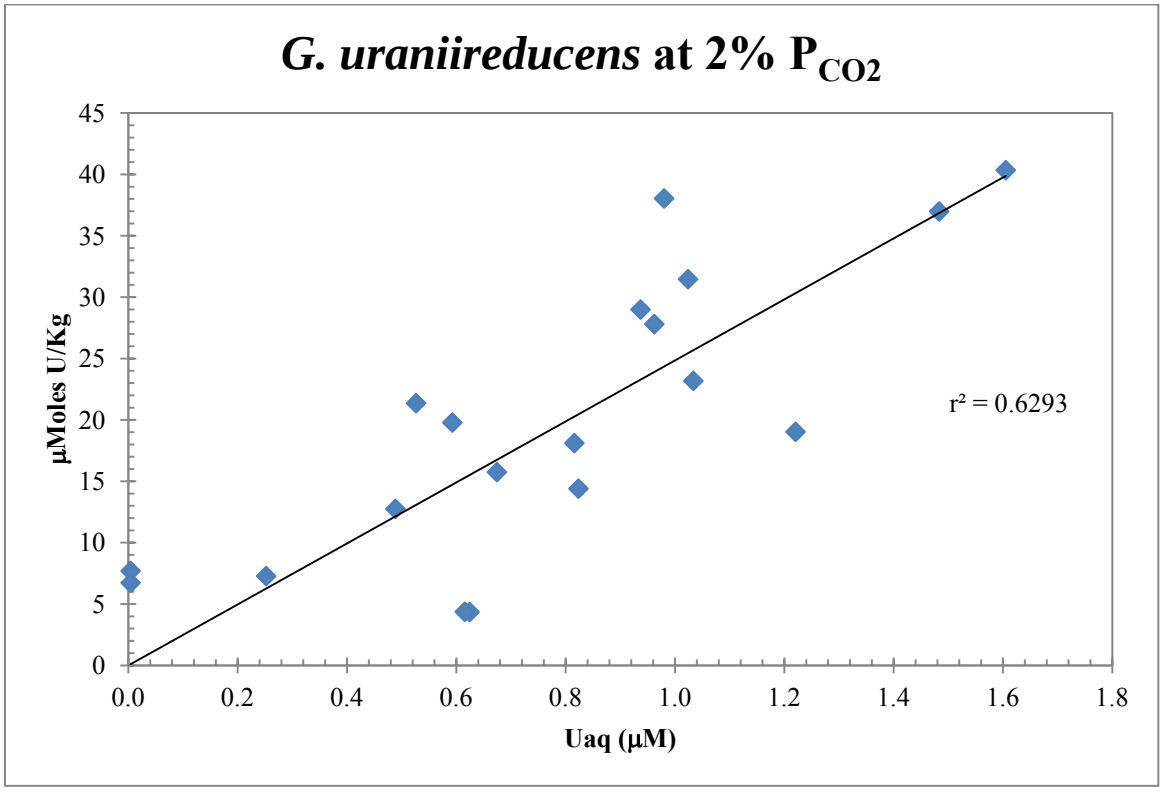

Figure 23: Uranium sorption isotherm to *A. palmae* at atmospheric P_{CO2} at pH 7 ± 0.2 with 6.5 mM calcium and 8.5 mM sulfate.

The isotherm obtained under 2% P_{CO2} conditions is presented in Figure 23. An isotherm for *A. palmae* exposed to 2% P_{CO2} was not collected due to experimental problems, but a point comparison of sorption to *A. palmae* versus sorption to *G. uraniireducens* using a 25 g L^{-1} bacterial solution exposed to 1.4 µM U(VI) was performed. *G. uraniireducens*, on a mass basis, sorbed up to 10 times more uranium from the solution than the *A. palmae*. While the sorption difference between the two types of bacteria under 2% P_{CO2} conditions appears larger than the difference determined from the comparison of K_D values (four times) of the two different bacteria obtained at atmospheric P_{CO2}, a single point comparison provides limited confidence in the results. Therefore, it can only be concluded that uranium sorption to *A. palmae* is significantly decreased under 2% P_{CO2}

conditions as compared to sorption under atmospheric P_{CO2} conditions. The decrease in sorption due to increased DIC content experienced by both types of bacteria is consistent with the reduction of K_D results for uranium biosorption [68] and sorption to iron oxides [42].

While the K_D value obtained at atmospheric P_{CO2} for uranium sorption to *G. uraniireducens* is very large, it is not representative of Old Rifle site average geochemical conditions. The K_D value obtained under 2% P_{CO2} conditions is closer to that of the aquifer and is similar to uranium-mineral sorption K_D values obtained by Stewart et al. [17]. The Stewart group examined uranium sorption to goethite-coated sand and two different natural sediments in an artificial groundwater, which resulted in similar uranium speciation to that of our experiment (greater than 99% calcium-uranyl-triscarbonato complexes and 3.8 mM HCO_3 at pH 7). As seen in Table 14, the K_D values obtained by the Stewart group were all in range of the *G. uraniireducens*-uranium K_D obtained at 2%. The K_D for uranium sorption to *G. uraniireducens* at 2% P_{CO2} was greater than the K_D determined for sorption to the Naturita sediments, which are from a site similar to the Old Rifle site. It is also greater than the K_D determined for uranium sorption to ferrihydrite exposed to 1% P_{CO2}, where sorption to a surface should be increased as compared to 2% P_{CO2} conditions due to the lower DIC content. It should be noted that the K_D values for the minerals and sediments listed in Table 15 reflect the latest literature results that capture DIC and calcium effects on uranium sorption, so they may be different from those found in earlier literature, which does not incorporate these parameters.

Sorbent	K_D (L/kg)	Log K_D
G. uraniireducens (2% CO_2) [a]	25	1.4
Iron Sand (1mM Ca, 3.8 mM DIC) [b]	17	1.23
Hanfor Sediment (1mM Ca, 3.8 mM DIC) [b]	29	1.5
Oak Ridge Sediment (1mM Ca, 3.8 mM DIC) [b]	51	1.71
Naturita Sediments (Field) [c]	0.5-40	-0.3 - 1.6
Ferrihydrite (1% CO_2) [d]	0.2	-0.7

Table 15: Comparison of K_D values for material exposed to elevated DIC. [a] references to values obtained from this work, [b] values obtained from [17], [c] value obtained from [82], [d] value obtained from [42]

Although the uranium-*G. uraniireducens* K_D value at 2% P_{CO2} is comparable to uranium-mineral K_D values obtained under similar conditions, the K_D value for uranium sorption to *G. uraniireducens* does not provide enough information to determine whether biosorption affects the overall transport of uranium in a bioremediated aquifer. While the K_D value indicates a high affinity for uranium to sorb to the bacteria, the concentration of sorption sites as defined by the bacteria concentration at the Old Rifle site must be used in conjunction with the K_D value to estimate the effect of biosorption on uranium transport at the site. Only the concentration of *G. uraniireducens* will be used to determine the overall effects of biosorption on uranium transport. This is because the *G. uraniireducens* species are eight times more sorptive than the *A. palmae* species and more populous during remediation. While the *A. palmae* species is the most populous after remediation, they are slow growers; therefore, the concentration of the *A. palmae* species during and after remediation is assumed to be lower than the concentration of the *G. uraniireducens* at the height of remediation.

The concentration of *G. uraniireducens* at the height of bioremediation at the Old Rifle site was converted to a mass concentration and compared against the average mass concentration used in the experimental work. Analysis done at the University of Massachusetts indicated that at the height of remediation, there were approximately 10^7 bacteria cells per milliliter of solution in the pore space and roughly 10^6 bacteria cells per gram of sediment [89]. Using the mass for a *G. uraniireducens* cell listed in Table 13, the concentration of bacteria in the Old Rifle site pore water is approximately 0.01 g L^{-1}.

This concentration is about 2,000 times less than the average concentration of bacteria (20 g L^{-1}) used in the experiments.

The concentration of bacteria used in the laboratory experiments was also compared to the concentration of bacteria available in a volume of the Old Rifle site aquifer, which includes the bacteria found on the sediment and that available in the pore water. Using the Old Rifle site porosity of 0.27 [24], the concentration of bacteria in the Old Rifle site aquifer in sediment and pore water is approximately 0.005 g L^{-1} (Table 16), which is about 4,000 times less than the average concentration of bacteria (20 g L^{-1}) used in the experiments. While the K_D values for uranium biosorption are significant, the amount of bacteria present in natural system as listed in Table 16 is very small when compared to those used in laboratory experiments.

Bacterial concentration	Pore Water	Sediment
Number of bacterial cell per gram	N/A	1.00E+06
Number of cells per ml	1.00E+07	2.75E+06
mg of bacteria per ml	1.00E-02	2.75E-03
mg of bacteria per ml of aquifer	2.70E-03	2.01E-03
Total bacteria concentration in aquifer (mg per ml)	0.005	

Table 16: The concentration of bacteria at the Old Rifle site in the pore water and sediment used to calculate the concentration in the aquifer. The Old Rifle site sediment density was used to determine the number of bacteria per volume of sediment, and the site porosity was used to obtain the final value listed.

It is also important to note that the mass of bacteria in the aquifer is much less than the mass of sediment in the aquifer. Using the sediment density and the knowledge that only 27% of the sediment has sorption capacity [24], an approximate concentration of sorptive sediment is 500 g L^{-1}. When compared to the available bacteria concentration of 0.005 g L^{-1}, there is approximately 100,000 more sorptive sediment than sorptive biomass. Although the K_D values for sorption to bacteria and sediment are similar in magnitude, the lower concentration of bacteria means it will sorb less uranium. Therefore, it is unlikely that uranium sorption to *G. uraniireducens* will have a large impact on soluble uranium concentrations during bioremediation due to the low surface site availability.

Images of uranium sorption by bacteria

To provide further support that uranium is sorbing to the bacterial surfaces, cryo-EM images and EDX spectroscopy analyses were performed on bacteria taken from experimental solutions. The displayed images are a result of multiple images taken of an intact cell at a variety of angles. A computer program incorporated these images into a final computer-generated image that may show a volumetric or "slice" image of an intact cell. It is important to understand that while the images may be presented as a "slice" image, the cells have not been physically sliced. The cryo-EM images showed uranium located on or integrated into the OM of *G. uraniireducens* exposed to environmentally relevant conditions (1.4 μM uranium and 2% P_{CO2}) as shown by Figure 24. While gold beads are included in the imaging for reference of the presence of heavy metals, the presence of uranium on the cell was confirmed by scanning transmission EDX analysis (Figure 25, red arrow shows path of EDX analysis). Uranium is indicated by the darkened areas on the OM and is patchy and nonuniform. Upon evaluation of the EDX analysis presented in Figure 25, the element of uranium is detected at maximum concentrations, as indicated by the maximum peak height, where the beam path crosses the cell wall. While calcium is also detected by the scanning transmission EDX with a maximum at the cell wall similar to uranium, it is also detected within the cell wall and uranium was not. Since calcium is detected inside the cell wall where there are no dark patchy areas, it can be concluded that uranium, not calcium, is the source of the dark patches. Also further EDX analyses of the areas that do not have the dark patchy occurrences do not detect the presence of uranium but do detect the presence of calcium (Appendix B).

Uranium sorption to the OM, as shown by Figure 24, is in agreement with previous research of uranium sorption to both reductive and nonreductive species [72, 73, 90]. It is more difficult to see the sorbed uranium in the cryo-EM image of the *A. palmae;* therefore, a cryo-EM image is not shown or discussed here. The images of *A. palmae* can be found in Appendix B

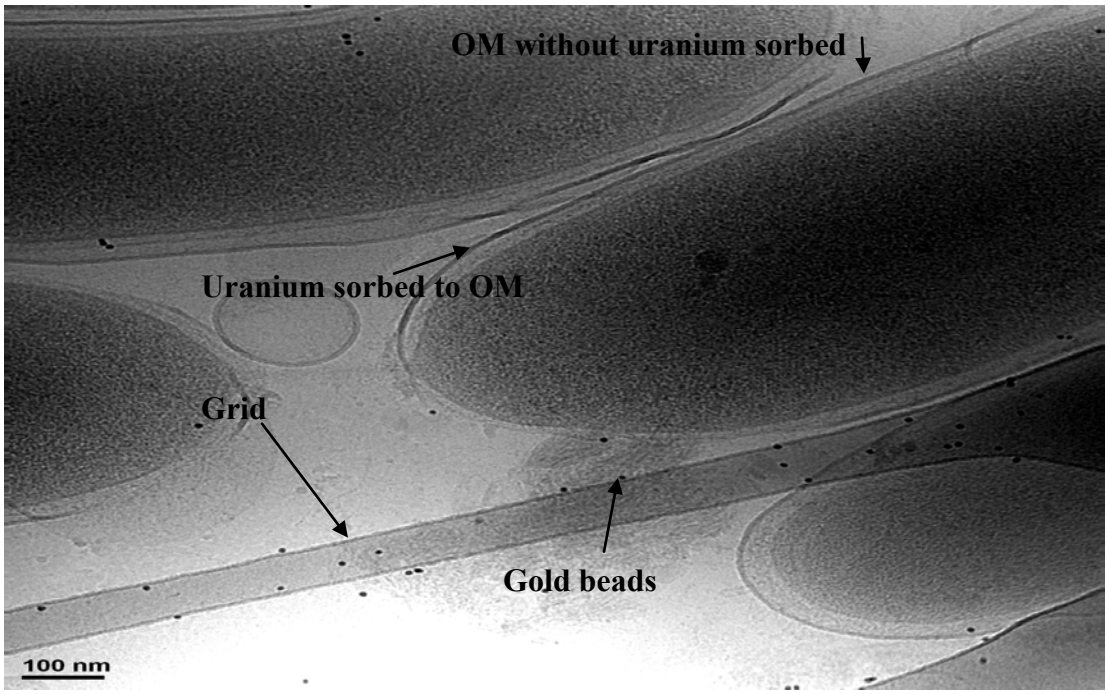

Figure 24: Cryo-EM images of uranium sorption to *G. uraniireducens* OM under 2% P_{CO2} and 1.4 μM U. Uranium is indicated by the darkened areas of the cell membrane.

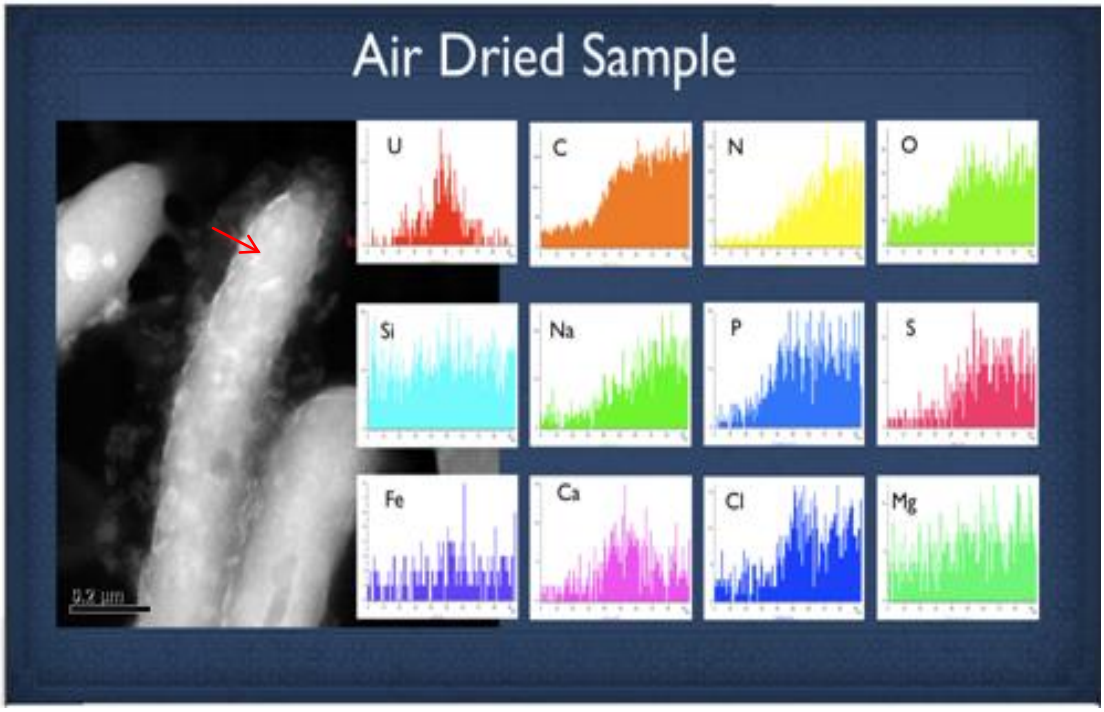

Figure 25: EDX analysis of patchy deposits on the OM of geobacter, which confirms uranium sorption.

The cryo-EM analysis of *G. uraniireducens* exposed to higher concentrations of uranium, 50 μM, and atmospheric P_{CO2} results in a different trend in uranium sorption. While the uranium deposits are patchy and non-uniform on the OM, uranium is also observed on the inside of the OM in the periplasmic space of the bacteria. This distribution is shown in Figure 26.

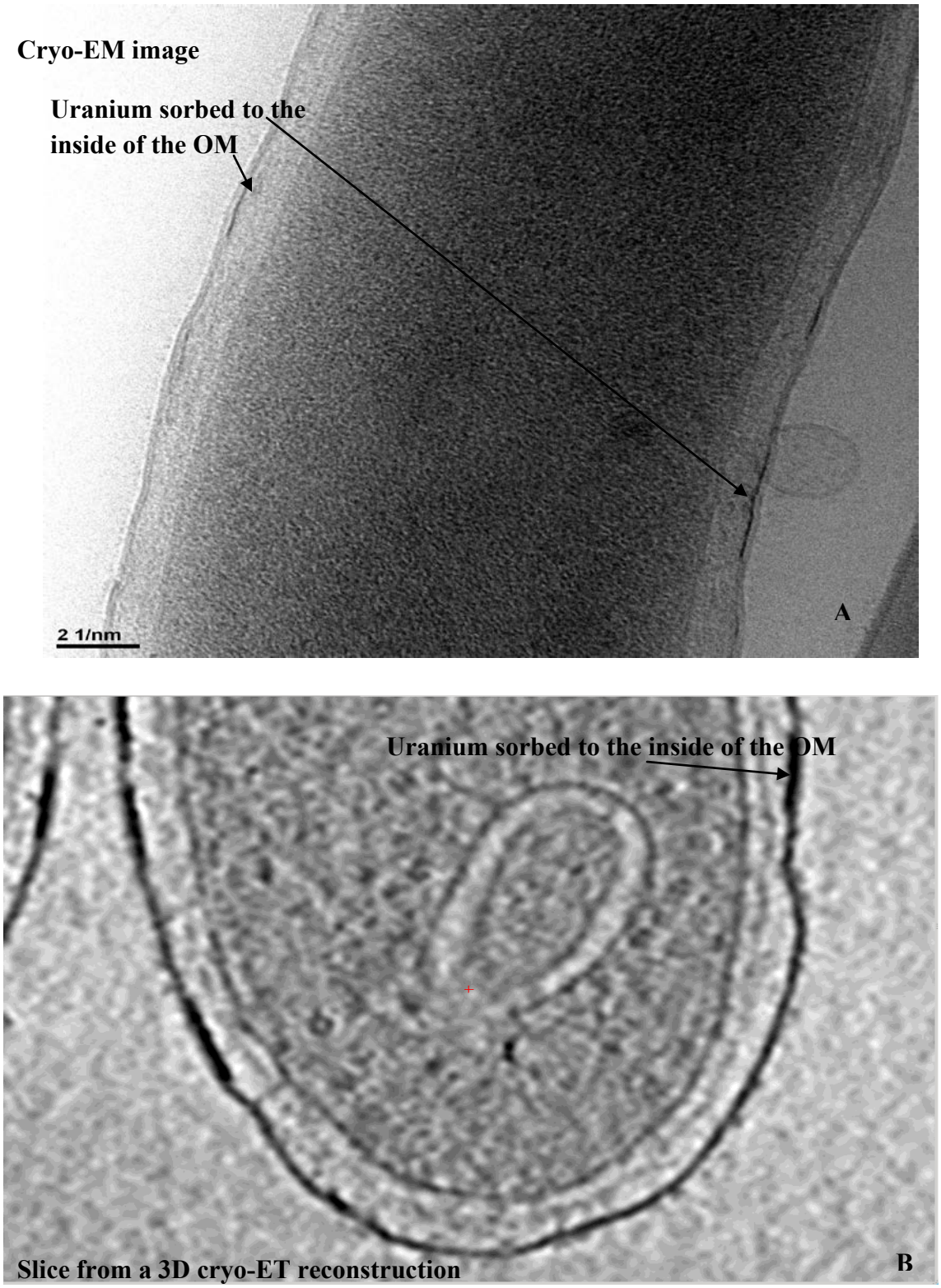

Figure 26: Cryo-ET of uranium sorption to *G. uraniireducens* under 2% P_{CO2} and 50 μM uranium

Experimental conditions were specifically designed to discourage or prevent any uranium reduction by the *G. uraniireducens*. As a result of the experimental design, it is expected the uranium detected on the surface of the bacteria should be U(VI). This is not an unrealistic expectation because uranium was shown sorbed to the surface of the non-reductive species of *A. palmae* (this research) and *B. subtilis* [91, 92]. While uranium sorbed to the surface of *A. palmae* was not confirmed by EDX analysis, uranium sorbed to the surface of the *B. subtilis* was confirmed by TEM-EDS and XANES analysis done by Ohnuki et al. [91].

The same types of uranium deposits on the OM and inside the periplasm as seen in these results were also seen by Shelobolina et al. in a mutant *G. Sulfurreducens* [73]. This species was unable to reduce uranium because the path of electron transfer in the periplasm was deleted. Shelobolina and colleges postulated that the accumulation of uranium in the periplasmic space of the bacteria may reflect the ability of uranium to penetrate the OM and react with substances in the periplasm that may promote formation of U(VI) precipitates and not the reductive ability of this area.

Metal-reducing bacteria have redox active biomolecules within the periplasm. These biomolecules have the ability to store electrons for use during times of famine; this has been demonstrated by the c-Type cytochromes of the *G. Sulfurreducens* when examined by Esteve-Nunez et al [93]. They showed that periplasmic and OM cytochromes of the *G. sulfurreducens* act as capacitors and can store approximately 10^7 electrons per cell [93]. Because bacteria have the capability of storing electrons for use during times of famine and given that uranium has the ability to travel within the cell membrane as seen by cryo-EM analysis, the oxidation state of the observed uranium on and within the *G. uraniireducens cells* (Figures 24 and 26) is not certain. Any U(VI) that diffused into the OM may have contacted a charged cytochrome and subsequently been "passively" reduced. Therefore, the accumulation of uranium in the periplasmic space may be U(IV).

To investigate the above possibility, beamline x-ray spectroscopy was performed on a pellet of bacteria collected from a uranium-*G. uraniireducens* sorption experiment in which no electron donor was present. The bacteria were exposed to 2% P_{CO2} and 50 μM uranium for more than 24 hours. The results from the beamline analysis (Appendix B)

indicate approximately 40% of the uranium associated with the cell pellet was U(IV), which confirmed U(VI) reduction had occurred in the absence of an electron donor. This result indicates that uranium biosorption captured in our experiments represents a mixture of U(VI) complexation and U(IV) through "passive" reduction.

Given that *G. sulfurreducens* have 10^7 haem per cell [93] and each haem stores one electron[94], it would require approximately 12.4 E 12 cells L^{-1} of solution to perform the 40% uranium reduction that occurred. Yet, there were approximately 13.2 E 13 cells L^{-1} in solution during the test that was done to obtain the bacterial pellet for the beamline analysis. The difference between the reduction expected to occur and the reduction that did occur due to electron storage per cell could be due to the difference in growth conditions between that of these tests and Esteve-Nunez et al [95] or it could be due to the large concentration of uranium used in the test. The uranium concentration in the test prepared for beamline analysis is approximately 50 times larger than environmentally relevant concentrations and may have resulted in larger amounts of uranium entering into the cell (due to a concentration gradient), which encounter charged biomolecules and were subsequently reduced.

Examination of the cryo-EM image (Figure 24) of *G. uraniireducens* in AGW exposed to environmentally relevant conditions (2% P_{CO2} and 1.4 μM U(VI)) shows uranium only on the cell wall. The cryo-EM images (Figure 26) of *G. uraniireducens* exposed to 2% P_{CO2} AGW spiked with 50 μM U(VI) show uranium on the cell wall and inside the periplasm. The difference between these images may be due to the different concentration of uranium in the two sorption tests. Because it is unknown whether the amount of U(VI) reduction identified by the beamline analysis is an artifact of the experiment or whether it truly represents an active bioprocess, this result can only confirm reduction occurred in these sorption experiments when no electron donor was present. The degree to which the reduction occurred is not certain. Based on the beamline analysis, it is likely that the K_D values for uranium sorption to *G. uraniireducens* obtained from the previous experiments provide an overestimation in sorption capacity and provides evidence that there is a degree of continuing reduction at bio-remediated sites after active reduction has ceased.

Speciation

Uranium sorption to *G. uraniireducens* is approximately 300 times larger under atmospheric P_{CO2} than under 2% P_{CO2}. The aqueous speciation resulting from the two different DIC concentrations are presented in Table 17. For AGW exposed to 2% P_{CO2}, the calcium-uranyl-triscarbonato species, $Ca_2UO_2(CO_3)_3$ (aq) and $CaUO_2(CO_3)_3^{-2}$, accounted for more than 99% of the uranyl distribution. Sorption experiments under these conditions resulted in markedly lower biosorption. For sorption experiments at atmospheric P_{CO2}, the calcium-uranyl-triscarbonato species only accounted for approximately 19% of the uranyl distribution and produced the largest amount of biosorbed uranium. Under the atmospheric P_{CO2} conditions, the non-calcium uranyl-carbonate species accounted for 77% of the uranyl distribution, with the largest percentage of uranium distributed among the $(UO_2)_2CO_3(OH)_3^-$ species at approximately 70%.

Species	Uranyl Percent Distribution	
	2% P_{CO2}	Atm P_{CO2}
$Ca_2UO_2(CO3)_3$ (aq)	81.81%	15.69%
$CaUO_2(CO3)_3^{-2}$	17.81%	3.26%
$(UO_2)_2CO_3(OH)_3^-$	0.00%	70.26%
UO_2CO_3 (aq)	0.02%	5.64%
$UO_2(OH)_2$ (aq)	0.00%	1.70%
UO_2OH^+	0.00%	1.56%
$UO_2(CO_3)_2^{-2}$	0.17%	1.26%
$UO_2(CO_3)_3^{-4}$	0.19%	0.03%
$UO_2(OH)_3^-$	0.00%	0.16%
$UO_2(SO_4)_2^{-2}$	0.00%	0.01%
UO_2^{+2}	0.00%	0.04%
UO_2SO_4 (aq)	0.00%	0.12%
$(UO_2)_2(OH)_2^{+2}$	0.00%	0.01%
$(UO_2)_3(OH)_5^+$	0.00%	0.27%
$(UO_2)_4(OH)_7^+$	0.00%	0.01%

Table 17: Percent uranium distribution under different CO_2 partial pressures at an ionic strength of 0.04, a pH of 6.95 with 6.5 mM calcium, 8 mM sulfate, 1.4 µM $U(VI)^{+2}$.

When comparing the uranium speciation presented by Table 17 and the K_D values obtained from the experimental work, the non-calcium uranyl-carbonate complexes appear to be the sorbing species and the calcium-uranyl-triscarbonato species (calcium uranyl-carbonates) appear to decrease sorption. This conclusion is in agreement with sorption of uranium to minerals. Steward et al. found that the concentration of the uranyl-carbonate species in a solution can provide a valid prediction of uranyl sorption to artificial and natural sediments within that solution [17]. Fox et al. also found that the presence of calcium uranyl-carbonates decreased uranium sorption to minerals [18]. Bargar et al. showed that uranyl carbonates sorbed to iron oxide, hematite, by examination with EXAFS and electrophoretic measurements and concluded that soluble

uranium can sorb with carbonate to decrease uranium transport in oxic aquifers through a wide range of pH [96].

To evaluate the theory that distribution of uranium among the calcium and non-calcium uranyl carbonates could be used to predict or estimated uranium biosorption under Old Rifle site conditions, the effects of changing solution pH, which changes speciation, was also examined. To begin this examination, sorption experiments were performed with variable pH at 2% P_{CO2} with a constant bacterial concentration and the U(VI) concentration equal to 1.4 μM. The concentration of sulfate and calcium were held constant to the values listed in Table 1 of Chapter 3. Upon completion of these sorption experiments, thermodynamic equilibrium simulations were performed to determine the solution speciation at equilibrium given similar constraints without accounting for sorption. The results obtained from both analyses, System A (the simulated system) and System B (the experimental system) were compared to determine whether the distribution of uranium among the calculated calcium and non-calcium uranyl-carbonates species in System A would correlate to experimental sorption in System B (i.e., high concentrations of calcium uranyl-carbonate in System A would correlate with low uranium sorption in System B or high concentrations of non-calcium uranyl-carbonates in System A would correlate with high uranium sorption in System B).

As shown in Figure 27 the distribution of uranium sorbed to the biomass decreases from 100% to approximately 15% in System B as the distribution of uranium associated with the non-calcium uranyl carbonates in System A decreases from 60% to approximately 10%. As this occurred, the uranium distributed among the calcium uranyl-carbonates in System A increased from approximately 40% to more than 90%. While the trends in Figure 27 provide more support for the theory that uranium distribution among the calcium and non-calcium uranyl carbonates can be used to predict or estimated uranium biosorption, they do not match exactly. This is not unexpected because there are thermodynamic differences between Systems A and B. System B (the experimental system) has an extra constraint, a sorptive site, while the simulated system, System A, does not. In System B, the formation of uranyl complexes at the sorption site and their related reactions will affect the final uranyl distribution among the various species in the

solution, while the uranium distribution in System A is not influenced by those interactions.

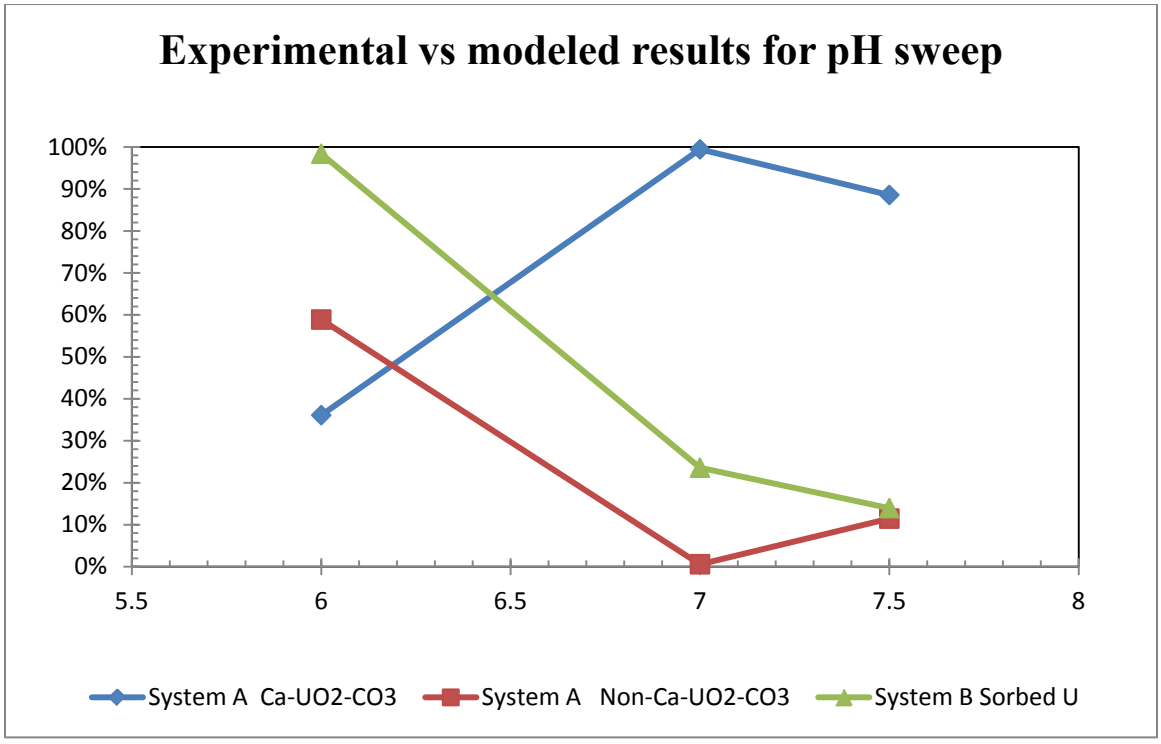

Figure 27: Experimentally obtained sorption (System II, contains solution and bacteria) compared to modeled (System I contains solution only) uranium carbonate concentration. Modeling performed with VisualMINTEQ.

The distribution uranium among the calcium and non-calcium uranyl-carbonates can be used to predict uranium sorption, but their presence does not provide information as to how the uranium complexes with the sorptive site. It is unknown whether a specific uranyl carbonate sorbs to the site or whether uranium sorbs to the site followed by the attachment of carbonates. This will be explored further in the SCM result section. All that can be determined from this analysis so far is that in the Old Rifle site solution, the presence of non-calcium uranyl carbonates indicates sorption will occur and the presence of calcium uranyl-carbonates decreases uranium sorption.

Determining uranium biosorption by the distribution of uranium among the non-calcium and calcium uranyl-carbonates under Old Rifle site conditions can be used to estimate the effect of the other critical components in the Old Rifle groundwater. The effects of the other critical components with respect to uranium distribution as identified in Chapter 3

were examined. This was done by sweeping the final three critical components—concentration of calcium, sulfate, and uranium—against the constant values listed in Table 1 of Chapter 3. Because the distribution of uranium among the uranyl-carbonates was linked to sorption, these sweeps were done in two different P_{CO2} atmospheres to evaluate how these three critical components may affect uranium sorption by influencing the formation of soluble uranyl-carbonates and the distribution of uranium among the calcium and non-calcium uranyl-carbonates at pH 6.95. Prior to the sweeps, the maximum concentration of the component to be swept (Calcium = 7 mM, sulfate =10 mM, uranium =20 μM) at both P_{CO2} atmospheres was modeled to ensure precipitation did not occur (Appendix B). In the simulations that ensured precipitation did not occur, counter ions of sodium and chloride were used to maintain a charge imbalance of less than 10%. These ions were shown by the sensitivity analysis preformed in Chapter 3 to have negligible effects on uranium distribution. During the sweeps, counter ions were not present, so a charge balance was not maintained.

All sweeps using the final three critical components under both DIC concentrations resulted more than 90% of the uranyl ion distribution to be among the uranyl carbonates (Figures 28 through 30). Figure 28 shows the results of sweeping the calcium concentration from 0 to 7 mM under 2% and atmospheric P_{CO2}. Under 2% P_{CO2} conditions, the largest change of uranium distribution between the non-calcium and the calcium uranyl-carbonates occurred at a calcium concentration between 0 and 1 mM, where the distribution of uranium among the non-calcium uranyl-carbonates decreased from 70% to 10% and the distribution of uranium among the calcium uranyl-carbonates increased from 30% to 90%. This predicts that sorption under 2% P_{CO2} will be very sensitive to small concentrations of calcium. Under atmospheric P_{CO2} conditions shown in Figure 27, the effect of calcium on the distribution of uranyl carbonates is not as great, resulting in only a slight decrease of uranium distributed among the non-calcium uranyl carbonates (~90% to 75%) and a slight increase of uranium distributed among the calcium uranyl-carbonates (0% to ~25%) over the entire range of the sweep.

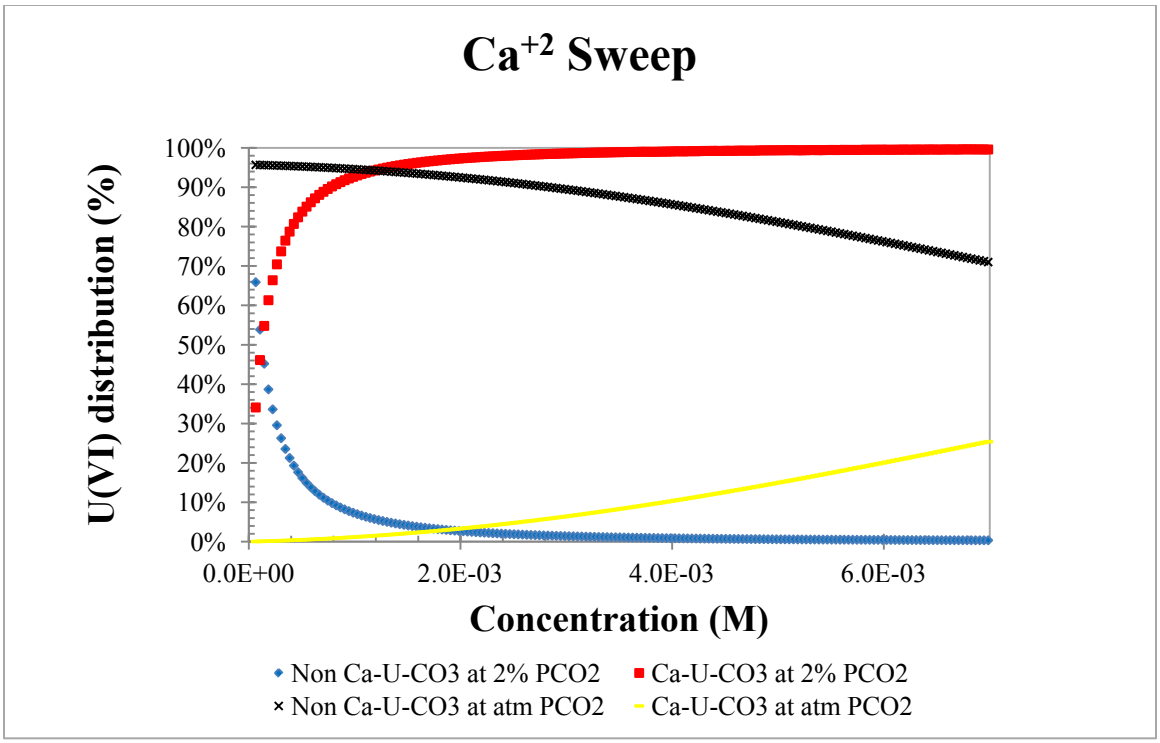

Figure 28: Calcium sweep of Old Rifle site critical components pH 7 to evaluate the effects on uranyl distribution.

While sweeping the sulfate concentration under atmospheric P_{CO2} does not appear to influence the distribution of uranium among the calcium and non-calcium uranyl carbonates, sweeping it under 2% P_{CO2} does (Figure 29). The fraction of calcium uranyl-carbonate that accounts for the uranyl distribution decreases from 65% to approximately 30% as the sulfate concentration increase from 0 to 10 mM. The effect of sulfate on uranium sorption is likely a reflection of how sulfate affects the free calcium concentration available to interact with uranium. This can be seen in a manner that the calcium and sulfate sweep mirrors each other under both DIC concentrations and the fact that urany-sulfates are not a major part of the speciation as identified by Table 17. Therefore, sorption is predicted to be affected by the change in sulfate concentration only if calcium is also in solution.

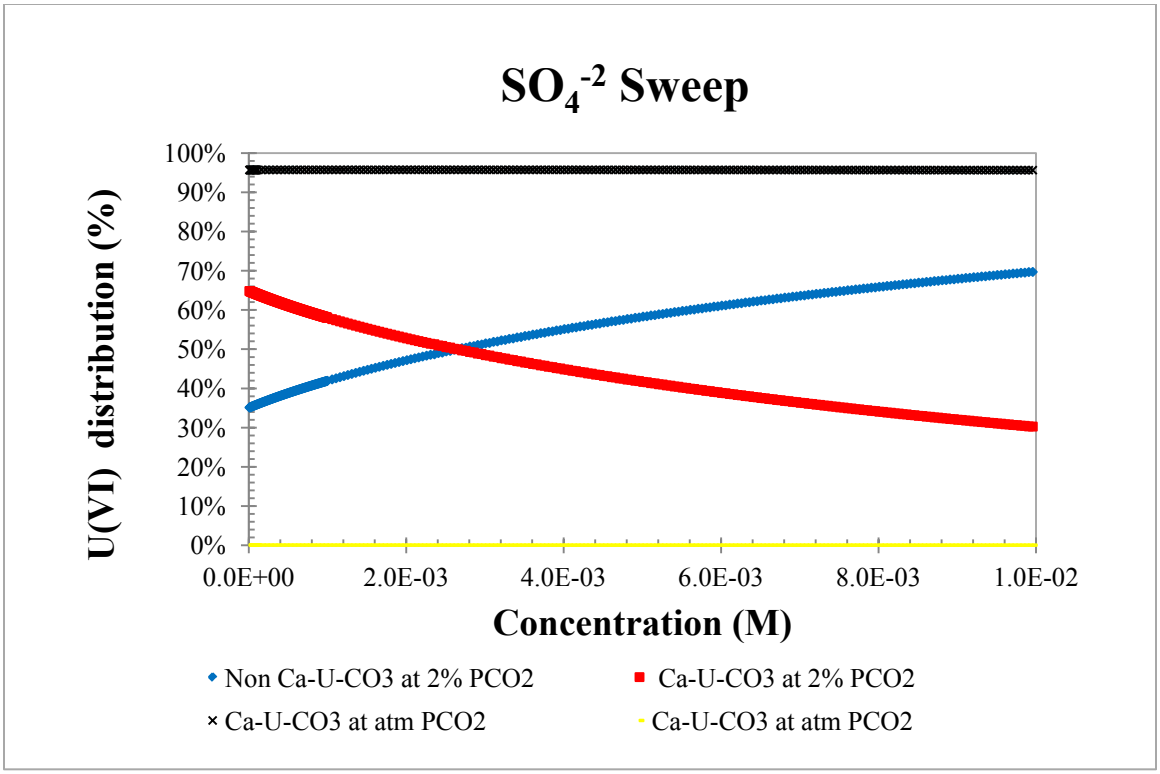

Figure 29: Sulfate sweep of Old Rifle site critical components pH 7 to evaluate the effects on uranyl distribution.

Sweeping the uranium concentration under 2% P_{CO2} does not appear to influence the distribution of uranium among the calcium and non-calcium uranyl carbonates, but sweeping it under atmospheric P_{CO2} does (Figure 30). Under 2% P_{CO2} conditions, the calcium uranyl-carbonates account for greater than 99% of the uranium distribution. Under atmospheric P_{CO2}, changing the uranium concentration from 0 to 5 mM results in a decreased uranium distribution among the calcium uranyl-carbonates from 50% to almost 0% while increasing the distribution of uranium among the non-calcium uranyl-carbonates from 50% to approximately 80%. As the concentration of uranium increases above 5 μM, there is very little change in uranium distribution among the different uranyl-carbonate groups under both DIC conditions. Therefore, it is assumed that uranium sorption is more strongly affected by uranium concentrations under atmospheric P_{CO2} conditions than 2% P_{CO2}.

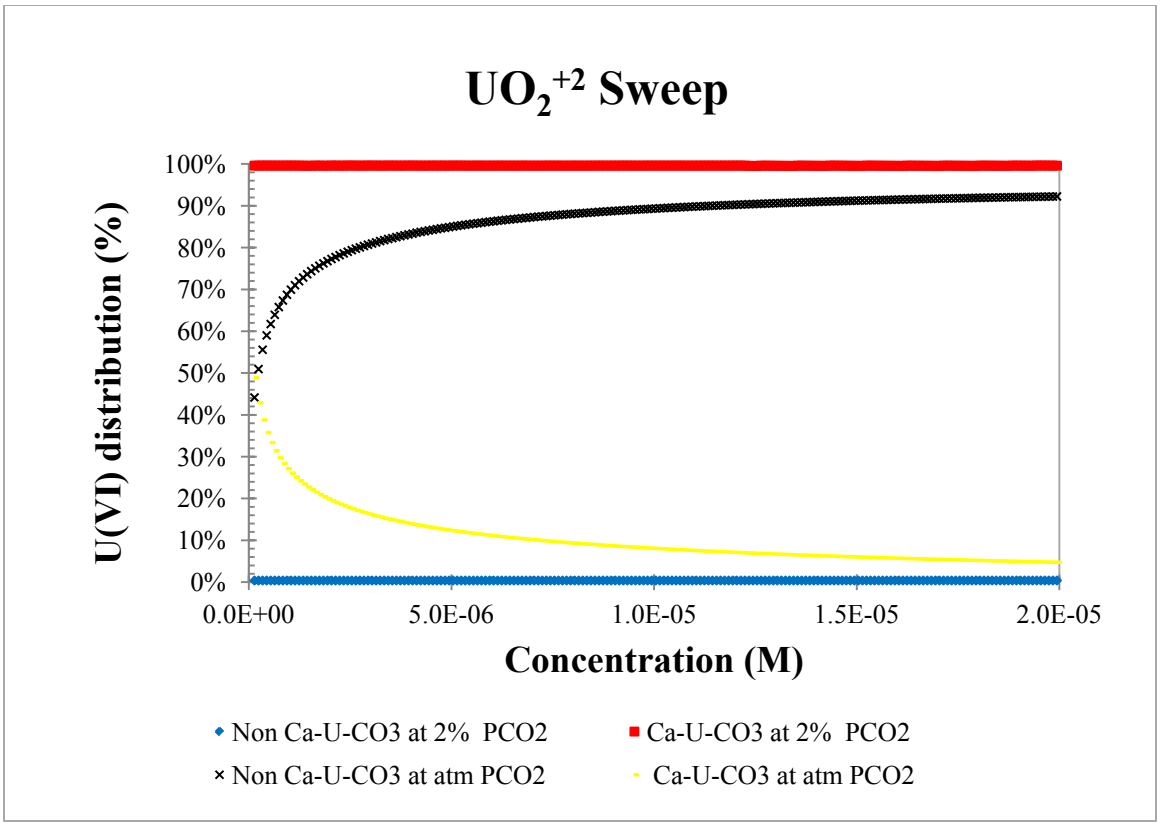

Figure 30: U(VI) sweep of Old Rifle site critical components at pH 7 to evaluate the effects on uranyl distribution.

While all components swept are identified as critical components under Old Rifle site conditions with respect to uranium, they are not all critical components when applied to the framework of sorption. Upon review of the sweep results, solution pH and concentrations of DIC and calcium effect the distribution of uranyl ion among the non-calcium and calcium uranyl-carbonates under both atmospheric and 2% P_{CO2} conditions. Sulfate and uranium concentrations only affect the distribution of the uranyl carbonates under one of the two P_{CO2} conditions. Consequently, solution pH and the concentrations of DIC and calcium are critical components when considering uranium sorption to *G. uraniireducens*.

SCM Parameter for Uranium Sorption to *G. uraniireducens*

Using the SCM approach as applied by Davis et al. [42], the measured K_D values were converted to thermodynamic equilibrium coefficients (log K values) using the surface complexation reactions that could describe uranium sorption to the *G. uraniireducens*.

The conversion was performed using TITRATOR with the input parameters equivalent to the experimental values. The density of sorption sites used in the simulations was 50 μMoles g^{-1}. This concentration was derived from sorption experiments under 2% P_{CO2} where less than 20% of uranium in the solution was sorbed to the given bacterial mass. Because a majority of uranium remained in the solution, it was assumed that the sorption sites on the bacteria were significantly saturated. The sorption site density used in the simulation is only an estimate, but is within the range of the sorption density considered in the Old Rifle site transport model of 16.34 μM g^{-1} [24]. The fact that this sorption density is only an estimate must be stressed because it provides another critical component that has a large effect on the distribution of uranium in the system. The resulting SCM thermodynamic values, which describe sorption, are directly correlated to the site density concentration. Because the site density is an estimate, the resulting log K must be viewed as an estimate as well.

While sorption to weak and strong sites are used to account for the non linear sorption isotherms commonly observed for U(VI) sorption, strong sites only account for 0.1% in the SCM approach as applied by Davis et al. [42]. To simplify the application of the SCM approach, only the reactions for the weak sorption sites, which describe the majority of sorption (99% of sites), were used in the following thermodynamic model. As done by Davis et al., it was assumed that sorption could be described with three or fewer surface reactions, resulting in the simplest model possible to explain the major features of sorption as chemical conditions are varied over field-relevant ranges.

Because it is apparent that sorption is correlated to the formation of uranyl carbonates, reactions relating sorption of different uranyl carbonates was considered (equations 19 through 21). Sorption reactions used by Fang et al. [24] to describe mineral sorption to weak sites at the Old Rifle site were also considered a possible surface reactions (equations 22 and 23).

$$WOH + UO_2^{+2} + CO_3^{-2} = WOUO_2CO_3^{-} + H^+ \quad (19)$$

$$WOH + UO_2^{+2} + 2CO_3^{-2} = WOUO_2(CO_3)_2^{-3} + H^+ \quad (20)$$

$$WOH + UO_2^{+2} + 3CO_3^{-2} = WOUO_2(CO_3)_3^{-5} + H^+ \quad (21)$$

$$WOH + UO_2^{+2} = WOUO_2^{+} + H^+ \quad (22)$$

$$WOH + UO_2^{+2} + H_2O = WOUOOH + 2H^+ \quad (23)$$

The sorption reactions were first evaluated individually using the above-listed stochiometery. The predicted sorbed concentration of uranium was divided by the average mass of bacteria used in the experiments (20 mg mL^{-1}) to obtain K_D values in units equivalent to those used to express partitioning for the experimental results. The log K value for sorption that produced solution concentrations equivalent to that obtained under experimental conditions at atmospheric P_{CO2}, K_D = 7985 ± 1024 L kg^{-1} , was then used to obtain the K_D value at 2% P_{CO2} system. The K_D values obtained from this exercise of obtaining simulated K_D under both CO_2 atmospheres (Table 18) were then compared to the experimentally obtained K_D values. Upon evaluation of the simulated K_D values as compared to the experimentally determined K_D values, uranium sorption to *G. uraniireducens* could not be described well with only a single reaction as described by equations 19 through 23. Therefore, a combination of reactions was used in simulations to describe uranium sorption. The resulting simulated K_D values obtained using equations 19 and 20 were equivalent to the experimental K_D values of 7985 ± 1024 L kg^{-1} at atmospheric P_{CO2} and 25 ± 1.8 L kg^{-1} at 2% P_{CO2}. Equations 19 and 20 equate sorption to the formation of uranyl carbonate and uranyl dicarbonate species at the sorption site.

Reaction defined by equation	Log K	K_D at Atmospheric P_{CO2}	K_D at 2% P_{CO2}
19	10.182	8,034	6
20	17.22	7,975	291
21	23.755	7,909	14,783
22	2.64	7,976	0.14
23	-4.23	8,071	0.14
19,20	10.15, 16.03	7,985	25
22,23	-2.638,-4.23	8,071	0.14
22,23	4.9,-4.23	1,518,720	26

Table 18: Summary of simulated results lisiting log K values, which result in equivalent experimental uranium distribution at atmospheric P_{CO2} and the corresponding K_D values at 2% P_{CO2}.

Using the sorption reactions shown in equations 19 and 20 and their associated log K values to predict equilibrium in the old Rifle site system resulted in K_D values equal to those obtained in laboratory experiments. These simulations results, which match experimentally determined K_D results, indicate that approximately 100% of the soluble uranium is distributed among the uranyl-carbonates, with greater than 99% of the uranium distributed among calcium uranyl-carbonates under both the examined P_{CO2} atmospheres (Table 19). This is in agreement with the conclusion that the sorbing uranyl-carbonates are non-calcium carbonates and the calcium carbonates decreases sorption.

	Uranium distribution among soluble uranium	
Soluble concentration (M)	Atmospheric P_{CO2}	2% P_{CO2}
Non-calcium Uranyl carbonates	0.2%	0.4%
Calcium uranyl carbonates	99.8%	99.6%

Table 19: Soluble uranium distribution at equilibrium in the modeled system that accounts for sorption. Results obtained from using sorption equations 1 and 2 with associated log K values.

The model obtained from this exercise was also tested under 2% P_{CO2} conditions at pH 6 to determine whether the model would produce results similar to those obtained

experimentally. As shown by Figure 27, it was experimentally determined that greater than 90% of soluble uranium would sorb to bacteria in solution. The model prediction using equations 19 and 20 with their associated log K values predicted that approximately 85% of uranium in solution sorbed to the bacteria.

The reaction considered by Fang et al. and Davis et al. did not result in a K_D ratio similar to our experimental system. Although the solution geochemistry is similar to that of our system, the system modeled by Fang et al. and Davis et al. is more complex because they account for equilibrium with precipitated minerals, such as calcite minerals in the thermodynamic equilibrium. These more complex input parameters result in a very different system at equilibrium as compared to our simple system. Also, the model by Fang et al. only considers DIC concentrations in the ranges of 6 to 14 meq L^{-1}[24], which results in the formation of mainly calcium uranyl-carbonates. Although the K_D values for uranium sorption to minerals are similar to that of uranium sorption to biomass, the sorption mechanism between biological materials and minerals may be different.

Chapter 5: Conclusions

Modeling

Determinate Error

When modeling uranium speciation, default databases associated with equilibrium speciation programs should not be used for modeling of any system. Although a default database is a good starting point, background work should be done to ensure that the user identified constraints are from the latest literature research and all reactions related to the input parameters are included. Blind use of databases in equilibrium speciation codes can result in unrealistic simulations of a system, greatly affecting the credibility of any work in which it is used.

A significant difference was not detected in solution speciation as a result of ionic strength correction factors; therefore choosing one ionic strength correction approach over another is not critical for the Old Rifle site model. But the choice of ionic strength correction approaches may be a critical factor for solutions of ionic strength greater than 0.1M. While it is important to choose an applicable ionic strength correction approach for lower ionic strength solutions, the errors associated with using the different approaches is lower because the values for activity coefficients obtained from those different approaches are similar under those conditions. While the error associated with lower ionic strength solution and using different approaches is small, understanding the details of how the program applies ionic strength correction approaches to determine the activity coefficient is important to minimize errors to the best of the user's ability.

Very careful consideration should be taken if using alkalinity to determine DIC concentrations of a model or DIC concentration should be entered into the program as total inorganic carbon concentrations as opposed an alkalinity measurement. Allowing the equilibrium program to calculate the DIC concentration can result in unnecessary error propagation due to issues related to the units of measurement and conversion to final DIC concentration. Sampling related to the DIC input parameter must be precise, especially for systems that are very sensitive to DIC concentrations such as the Old Rifle site. If a DIC concentration is not directly obtainable by a P_{CO2} measurement, care should

be taken to prevent alteration of the carbonate equilibrium because this can propogate error throughout the simulation. Also, all alkalinity factors in the thermodynamic database must be present to minimize error.

Indeterminate Error

The total concentration of calcium, DIC, U(VI) and solution pH were determined to be the critical input parameters that have the greatest effect on the predicted distribution of uranium species. Care should be taken to ensure error associated with sampling and measuring of these parameters is as small as possible. Minimization of determinate error associated with these parameters allows the bounds of uncertainty associated with the distribution of U(VI) to be defined as best as possible.

Uncertainty propagation is straightforward in calculations of dissolved speciation only, but more problematic when sorption is considered. In the former case, and at low levels of uncertainty and high total U(VI) concentrations, calculated species concentrations have Gaussian output distributions and modest uncertainty amplification. In systems including sorption reactions with higher levels of uncertainty (temporal and spatial) and/or lower total U(VI) concentrations, distributions of calculated concentrations are often bimodal and amplification of uncertainty is significant. These behaviors are related to a steep slope or 'endpoint' behavior in concentrations of dissolved U(VI) due to the filling of all the strong sorption sites. Because the bimodal distributions represent system instability with respect to uncertain inputs, the sorption model may be unreliable when used under these conditions. Users should avoid predicting solid-dissolved partitioning of U(VI) based upon this sorption model at lower total uranium concentrations (less than 4 μM) and levels of uncertainty corresponding to spatial and temporal variability of the system. On the other hand, predictions of U(VI) speciation in the contaminant 'plume' appear to be robust as indicated by the resulting mono-modal normal Gaussian distributions, as are dissolved-phase calculations at all uranium levels.

Biosorption

Uranium sorption to *G. uraniireducens* is approximately 300 times higher under low-DIC conditions and decreases as DIC increases. Under low-DIC conditions, the K_D for U(VI) sorption to the surface of *G. uraniireducens* is 7985 ± 1024 L kg^{-1}, which is larger than

the K_D of 1850 ± 1.8 L kg^{-1} determined for uranium sorption to the surface of *A. palmae* . The K_D for *G. uraniireducens* under high-DIC conditions is comparable to reported K_D values for U(VI)- mineral surface sorption in high-DIC waters.

Cryo-EM and EDX analyses confirmed uranium sorbed to the cell wall of the *G. uraniireducens*, and beamline results indicate that reduction had occurred without an electron donor present. Therefore, the experimentally obtained K_D values for the *G. uraniireducens* are likely overestimated. While the partition coefficients of the bacteria in high-DIC waters is comparable in strength to reported U(VI)- mineral sorption, when combined with the bacterial concentration during and after remediation, the concentration of uranium sorbed to biomass is not large enough to produce a noticeable effect on the transport of uranium in a bioremediated aquifer. Therefore, not including *G. uraniireducens* as uranium-sorption sites in the current Old Rifle site transport model will not affect the predicted solution, regardless of the identified uncertainties associated with the thermodynamics of the model.

The difference in biosorption as a result of exposure to different P_{CO2} values is attributable to the distribution of uranium among the non-calcium and calcium uranyl-carbonate species. The calcium uranyl-carbonates hinder sorption while the non-calcium uranyl-carbonates support it. Therefore, the distribution of uranium among the non-calcium and calcium uranyl-carbonate species can be used to estimate the amount of uranyl sorption that will occur to biomass at the Old Rifle site. The sorption of uranium to biomass in the sorption experiments was described well by the SCM GC approach as applied by Fang et al. [24] and Davis et al. [42]. The sorption reactions and related thermodynamic equilibrium constants that fit the SCM GC model were represented by the sorptive site reacting with uranium and two or three carbonate groups.

Acknowledgments

This work was funded by DOE Environmental Remediation Science Program DE-FG02-08ER64585 “Novel Sensor for the In Situ Measurement of Uranium Fluxes.” Various sources of intellectual and/or analytical support were made by the following: Steve Cabaniss, Kerry Howe, Yamane Asmerom, Victor Polyak, Bruce Thomsone, and Andrew Schuler (University of New Mexico); Kirk Hatfield and Mark Newman (University of

Florida); Jim Ranville and Valerie Stucker (Colorado School of Mines); Lucie N'Guessan (Exon); Aaron Peacock (Haley Aldrich); Steve Yabusaki and Philip Long (Pacific Northwestern National Laboratory); Ken Williams, Luis Comolli, Birgit Luef, and Roseann Csencsits (Lawrence Berkeley National Laboratory); Melissa Barlett, Roberto Ornella, and Derek Lovley (University of Massachusetts); John Bargar, Don Pham, and Noémie Janot (SLAC National Accelerator Laboratory); and Paul Reimus (Los Alamos National Laboratory).

References

1. Latimer, W.M. (1939). *A system of chemical analysis (qualitative and semi-quantitative) for the common elements*. Upper Saddle River, NJ: Prentice-Hall, Inc.

2. U.S. Department of Energy (DOE) (2011). *Laws we use (summaries).* Retrieved from http://www.epa.gov/radiation/laws/laws_sum.html#umtrca

3. Environmental Protection Agency (EPA) (2000). *Basic information about the Radionuclides Rule*. Retrieved from http://water.epa.gov/lawsregs/rulesregs/sdwa/radionuclides/basicinformation.cfm

4. EPA (2000). *National primary drinking water regulations. Radionuclides final rule.* Retrieved from http://www.federalregister.gov/articles/2000/12/07/00-30421/national-primary-drinking-water-regulations-radionuclides-final-rule

5. World Health Organization (WHO) (2004). Uranium in Drinking-water. *Summary statement Extract from Chapter 12 - Chemical fact sheets of WHO Guidelines for Drinking-water Quality* (3rd edition). Retrieved from http://www.who.int/water_sanitation_health/dwq/chemicals/uraniumsum.pdf

6. McCullough, J., Hazen, T., & Benson, S. (1999). *Bioremediation of metals and radionuclides: What it is and how it works* (p. LBNL-42595). Berkeley, CA: Lawrence Berkeley National Laboratory.

7. U.S. Energy Information Administration (EIA) (2005). *Nuclear & uranium, Rifle Mill Sites*. Retrieved from http://www.eia.gov/cneaf/nuclear/page/umtra/rifle_mills_title1.html

8. DOE (1999). *Final Site observational work plan for the UMTRA project Old Rifle site* (GJO–99–88–TAR). Grand Junction, CO: U.S. Department of Energy.

9. Cotton, F.A., & Wilkinson, G. (1930). *Advanced inorganic chemistry, a comprehensive text* (3rd ed). Hoboken, NJ: John Wiley & Sons.

10. Davis, J.A., Payne, T.E., & Waite, T.D. (2002). *Geochemistry of Soil Radionuclides* (pp. 61-86). Madison, WI: Soil Science Society of America.

11. Davis, J.A. & Curtis, G.P. (2003). *Application of surface complexation modeling to describe uranium(VI) adsorption and retardation at the Uranium Mill Tailing site at Naturita*. Menlo Park, Ca:US Nuclear Regulatory Commission.

12. Barnett, M.O., Jardine, P.M., Brooks, S.C., & Selim, H.M. (2000). Adsorption and transport of uranium(VI) in subsurface media. *Soil Science Society of America Journal*, 64 (3), pp. 908-917.

13. Bernhard, G., Geipel, G., Brendler, G.V., & Nitsche, H. (1996). Speciation of uranium in seepage waters of a mine tailing pile studied by Time-Resolved Laser-Induced Fluorescence Spectroscopy (TRLFS). *Radiochimica Acta*, 75 (4), pp. 87-91.

14. Bernhard, G., Geipel, G., Reich, T. Brendler,S., Amayri, S., & Nitsche, H. (2001). Uranyl(VI) carbonate complex formation: Validation of the Ca2UO2(CO3)3 (aq.) species. *Radiochimica Acta*, 89 (8), pp. 511-518.

15. Bernhard, G., Geipel, G., Brendler, V., & Nitsche, H. (1998). Uranium speciation in waters of different uranium mining areas. *Journal of Alloys and Compounds*, 271, pp. 201-205.

16. Dong, W.M. and Brooks, S.C. (2006) Determination of the formation constants of ternary complexes of uranyl and carbonate with alkaline earth metals (Mg^{2+}, Ca^{2+}, Sr^{2+}, and Ba^{2+}) using anion exchange method. *Environmental Science & Technology*, 40 (15), pp. 4689-4695.

17. Stewart, B.D., Mayes, M.A., & Fendorf, S. (2010). Impact of Uranyl-Calcium-Carbonato Complexes on Uranium(VI) Adsorption to Synthetic and Natural Sediments. *Environmental Science & Technology*, 44 (3), pp. 928-934.

18. Fox, P.M., Davis, J.A., & Zachara, J.M. (2006). The effect of calcium on aqueous uranium(VI) speciation and adsorption to ferrihydrite and quartz. *Geochimica Et Cosmochimica Acta*, 70 (6), pp. 1379-1387.

19. Janssen, C.R., Heijerick, D.G., De Schamphelaere, K.A., & Allen, H.E. (2003). Environmental risk assessment of metals: tools for incorporating bioavailability. *Environment International*, 28 (8), pp. 793-800.

20. Klammler H., Newman, M.A., Szilagyi, E., Padowski, J.C., Hatfield, K., Jawitz, J.W., & Annable, M.D. (2007). Initial test results for a passive surface water fluxmeter to measure cumulative water and solute mass fluxes. *Environmental Science & Technology*, 41 (7), pp. 2485-2490.

21. Criscenti, L.J., Laniak, G.F., & Erikson, R.L. (1996). Propagation of uncertainty through geochemical code calculations. *Geochimica Et Cosmochimica Acta*. 60 (19), pp. 3551-3568.

22. Abdelouas, A., Lutze, W., & Nuttall, E. (1998). Chemical reactions of uranium in ground water at a mill tailing site. *Journal of Contaminant Hydrology*, 34 (4), pp. 343-361.

23. Yabusaki, S.B., Fang,Y., Long, P.E., Resch, C.T., Peacock, A.D., Komlos, J., Jaffe, P.R., Morrison, S.J., Dayvault, R.D., White, D.C., & Anderson, R.T. (2007). Uranium removal from groundwater via in situ biostimulation: Field-scale modeling of transport and biological processes. *Journal of Contaminant Hydrology*, 93 (1-4), pp. 216-235.

24. Fang, Y., Yabusaki, S.B., Morrison,S.J., Amonettea, J.P., & Long, P.E. (2009). Multicomponent reactive transport modeling of uranium bioremediation field experiments. *Geochimica et Cosmochimica Acta*, 73 (20), pp. 6029-6051.

25. Gustafsson, J.P. (2009) *VisualMINTEQ* [Software]. Retrieved from http://www.lwr.kth.se/English/OurSoftware/vminteq/

26. U.S. Geological Survey (USGS) (2009). *PHREEQC* [Software]. Retrieved from http://wwwbrr.cr.usgs.gov/projects/GWC_coupled/phreeqc/

27. Cabaniss, S.E. (2009) *Titrator* [Software]. Retrieved from sites.google.com/site/titratordownload/

28. Nitzsche, O., G. Meinrath, & B. Merkel (2000). Database uncertainty as a limiting factor in reactive transport prognosis. *Journal of Contaminant Hydrology*, 44 (3), pp. 223-237.

29. N'Guessan, A.L., Vrionis, H.A., Resch,C.T., Long, P.E., & Lovley, D.R. (2008). Sustained removal of uranium from contaminated groundwater following stimulation of dissimilatory metal reduction. *Environmental Science & Technology*, 42 (8), pp. 2999-3004.

30. Jensen, M.L. (1958). Sulphur isotopes and the origin of sandstone-type uranium deposits. *Economic Geology*, 53 (5), pp. 598-616.

31. Langmuir, D. (1978). Uranium solution-mineral equilibria at low temperatures with applications to sedimentary ore deposits. *Geochimica et Cosmochimica Acta*, 42 (6), pp. 547-569.

32. Maynard, J.B. (1983). *Geochemistry of Sedimentary Ore Deposits*. New York, NY: Springer.

33. Lovley, D.R., Phillips, E. J. P.,Gorby, Y. A., & Landa, E. R. (1991). Microbial reduction of uranium. *Nature*, 350(6317): p. 413-416.

34. Gorby, Y.A. & Lovley, D.R. (1992). Enzymatic uranium precipitation. *Environmental Science & Technology*, 26 (1), pp. 205-207.

35. Durrance, E.M. (1986). *Radioactivity in Geology*. Hoboken, NJ: John Wiley & Sons.

36. Lovley, D.R., Roden, E.E., Phillips, E.J.P., & Woodward, J.C. (1993). Enzymatic iron and uranium reduction by sulfate-reducing bacteria. *Marine Geology*, 113, pp. 41-53.

37. Lovley, D.R. & Phillips, E.J.P. (1992). Bioremediation of uranium contamination with enzymatic uranium reduction. *Environmental Science & Technology*, 26 (11), pp. 2228–2234.

38. Lovley, D.R. & Anderson, R.T. (2000). Influence of dissimilatory metal reduction on fate of organic and metal contaminants in the subsurface. *Hydrogeology Journal*, 8 (1), pp. 77-88.

39. Finneran, K.T., Anderson, R.T., Nevin, K.P., & Lovley, D.R. (2002). Potential for bioremediation of uranium-contaminated aquifers with microbial U(VI) reduction. *Soil and Sediment Contamination*, 11 (3), pp. 339-357.

40. Anderson, R.T., Vrionis, H.A., Ortiz-Bernad, I., Resch, C.T., Long, P.E., Dayvault, R., Karp, K., Marutzky, S., Metzler, D.R., Peacock, A., White, D.C., Lowe, M., & Lovley, D.R. (2003). Stimulating the in situ activity of Geobacter species to remove uranium from the groundwater of a uranium-contaminated aquifer. *Applied and Environmental Microbiology*, 69 (10), pp. 5884-5891.

41. Vrionis, H.A., Anderson, R.T., Bernad-Ortiz, I., O'Neill, K.R., Resch, C.T., Peacock, A.D., Dayvault, R., White, D.C., Long, P.E., & Lovley, D.R. (2005). Microbiological and Geochemical Heterogeneity in an In Situ Uranium Bioremediation Field Site. *Applied and Environmental Microbiology*, 71 (10), pp. 6308-6318.

42. Davis, J.A.,Meece, D.E., Kohler, M., & Curtis, G.P. (2004). Approaches to surface complexation modeling of uranium(VI) adsorption on aquifer sediments. *Geochimica Et Cosmochimica Acta*, 68 (18), pp. 3621-3641.

43. Serkiz, S.M., Allison, J.D., perdue, E.M., Allen, H.E., & Brown, D.S. (1996). Correcting errors in the thermodynamic database for the equilibrium speciation model MINTEQA2. *Water Research*, 30 (8), pp. 1930-1933.

44. Kalmykov, S.N. & Choppin, G.R. (2000). Mixed $Ca^{2+}/UO_2^{2+}/CO_3^{2-}$complex formation at different ionic strengths. *Radiochimica Acta*, 88 (9-11), pp. 603-606.

45. Unsworth, E.R., Jones, P., & Hill, S.J. (2002). The effect of thermodynamic data on computer model predictions of uranium speciation in natural water systems. *Journal of Environmental Monitoring*, 4, pp. 528-532.

46. Weber, C.L., Vanbriesen, J.M., & Small, M.S. (2006). A stochastic regression approach to analyzing thermodynamic uncertainty in chemical speciation modeling. *Environmental Science & Technology*, 40 (12), pp. 3872-3878.

47. Cabaniss, S.E. (1997). Propagation of uncertainty in aqueous equilibrium calculations: non-gaussian output distributions. *Analytical Chemistr*y, 69, pp. 3658-3664.

48. Cabaniss, S.E. (1998). Uncertainty propagation in geochemical calculations: non-linearity in solubility equilibria. *Applied Geochemistry*, 14 (2), pp. 255-262.

49. Denison, F.H. & Garnier-Laplace, J. (2004). The effects of database parameter uncertainty on uranium(VI) equilibrium calculations. *Geochimica Et Cosmochimica Acta*, 69 (9), pp. 2183-2191.

50. Meinrath, G., Lis, S., Piskula, Z., & Glatty, Z (2006). An application of the total measurement uncertainty budget concept to the thermodynamic data of uranyl(VI) complexation by sulfate. *Journal of Chemical Thermodynamics*, 38 (11), pp. 1274-1284.

51. Sawyer, C.N., McCarty, P.L., & Parkin, G.F. (2003). *Chemistry for environmental engineering and science*. New York, NY: McGraw-Hill.

52. Benjamin, M. (2002). *Water chemistry*. New York, NY: McGraw-Hill.

53. Bethke, C.M. & Brady, P.V. (2000). How the K_d approach undermines ground water cleanup. *Ground Water*, 38 (3), pp. 435-443.

54. Davis, J.A. & Kent, D.B. (1990). Surface complexation modeling in aqueous geochemistry. *Reviews in Mineralogy*, 23 (1), pp. 177-260.

55. Curtis, G.P., Fox, P., Kohler, M., & Davis, J.A. (2004). Comparison of in situ uranium K-D values with a laboratory determined surface complexation model. *Applied Geochemistry*, 19 (10), pp. 1643-1653.

56. Hyun, S.P., Fox, P.M., Davis, J.A., Campbell, K.M., Hayes, K.F., & Long, P.E. (2009). Surface complexation modeling of U(VI) adsorption by aquifer sediments from a former mill tailings site at Rifle, Colorado. *Environmental Science & Technology*, 43 (24), pp. 9368-9373.

57. Nakajima, A., Horikoshi, T., & Sakaguchi, T. (1982). Studies on the accumulation of heavy-metal elements in biological-systems .21 recovery of uranium by immobilized microorganisms. *European Journal of Applied Microbiology and Biotechnology*, 16 (2-3), pp. 88-91.

58. Sakamoto, F., Ohnuki, T., Fuhii, T., & Lefuji, H. (2010). Response of saccharomyces cerevisiae to heavy element stress: Lead vs. uranium. *Geomicrobiology Journal*, 27 (3), pp. 240-244.

59. Barkleit, A., Moll, H., & Bernhard, G. (2009). Complexation of uranium(VI) with peptidoglycan. *Dalton Transactions*, (27), pp. 5379-5385.

60. Beveridge, T.J. & Doyle, R.J. (1989). *Metal ions and bacteria*. Hoboken, NJ: John Wiley & Sons.

61. Madigan, M.T., Martinko, J.M., Dunlap, P.V., & Clark, D.P. (2009) *Biology of microorganisms* (12th ed). New York, NY: Pearson Benjamin Cummings.

62. Wazne, M., Korfiatis, G.P., & Meng, X.G. (2003). Carbonate effects on hexavalent uranium adsorption by iron oxyhydroxide. *Environmental Science & Technology*, 37 (16), pp. 3619-3624.

63. Kazy, S.K., D'Souza, S.F., & Sar, P. (2009). Uranium and thorium sequestration by a Pseudomonas sp.: Mechanism and chemical characterization. *Journal of Hazardous Materials*, 163 (1), pp. 65-72.

64. Haas, J.R., Dichristina, T.J., & Wade, R. (2001). Thermodynamics of U(VI) sorption onto Shewanella putrefaciens. *Chemical Geology*, 180 (1-4), pp. 33-54.

65. Fowle, D.A., Fein, J.B., & Martin, A.M. (2000). Experimental study of uranyl adsorption onto Bacillus subtilis. *Environmental Science & Technology*, 34 (17), pp. 3737-3741.

66. Sarri, S., Misaelides, P., Papanikolaou, M., & Zamboulis, D. (2009). Uranium removal from acidic aqueous solutions by S*accharomyces cerevisiae, Debaryomyces hansenii, Kluyveromyces marxianus and Candida colliculosa*. *Journal of Radioanalytical and Nuclear Chemistry*, 279 (3), pp. 709-711.

67. Acharya, C., Joseph, D., & Apte, S.K. (2009). Uranium sequestration by a marine cyanobacterium, *Synechococcus elongatus* strain BDU/75042. *Bioresource Technology*, 100 (7), pp. 2176-2181.

68. N'Guessan, A.L., & Lovley, D.R. (2006). *Biosorption: Removal of U(VI) in the absence of acetate*. Amherst, MA: University of Massachusetts.

69. Gorman-Lewis, D., Elias, P.E., & Fein, J.B. (2005). Adsorption of aqueous uranyl complexes onto *Bacillus subtilis* cells. *Environmental Science & Technology*, 39 (13), pp. 4906-4912.

70. DOE (2009). *Geospatial environmental mapping system: Rifle Old, CO* [Processing Site]. Retrieved from gems.lm.doe.gov/imf/imf.jsp?site=rifleoldprocessing&title=Rifle Old, CO, Processing Site

71. Kelly, S.D., Boyanov, M.I., Bunker, B.A., Fein, J.B., Fowle, D.A., Yee, N. & Kemner, K.M. (2001). XAFS determination of the bacterial cell wall functional groups responsible for complexation of Cd and U as a function of pH. *Journal of Synchrotron Radiation*, 8, pp. 946-948.

72. Senko, J.M., Kelly, S.D., Dohnalkova, A.C., McDonough, J.T., Kemner, K.M., & Burgos, W.D. (2007). The effect of U(VI) bioreduction kinetics on subsequent reoxidation of biogenic U(IV). *Geochimica Et Cosmochimica Acta*, 71 (19), pp. 4644-4654.

73. Shelobolina, E.S., Maddalena, V.C., Korenevsky, A.A., DiDonato, L.N., Sullivan, S.A., Konishi, H., Hu, H., Leang,C., Butler, J.E., Kim, B., & Lovley, D.R. (2007). Importance of c-Type cytochromes for U(VI) reduction by *Geobacter sulfurreducens. BMC Microbiology*, 7 (16).

74. Liu, M.X., Dong, F.Q., Yan, X.Y., Zeng, W.M., Hou, L.Y., & Pang, X.F. (2010). Biosorption of uranium by *Saccharomyces cerevisiae* and surface interactions under culture conditions. *Bioresource Technology*, 101 (22), pp. 8573-8580.

75. Sakamoto, F., Ohnuki, T., Kozai, N., Fujii, T., Lefuji, H., & Fancis, A.J. (2005). Effect of Uranium (VI) on the Growth of Yeast and Influence of Metabolism of Yeast on Adsorption of U(VI). *Journal of Nuclear and Radiochemical Sciences*, 6 (1), pp. 99-101.

76. Ranville, J.F. and Stucker, V (2009). *Ion concentrations of Well B1 at Old Rifle*. Personal communication.

77. Guillaumont, R., Fanghanel, T., Neck, V., Fuger, J., Palmer, D.A., Grenthe, I., & Rand, M.H. (2003). *Chemical thermodynamics 5, Update on the chemical thermodynamics of uranium, neptunium, plutonium, americium and technetium.* Amsterdam: Elsevier.

78. National Institute of Standards and Technology (NIST) (2004). *Critically selected stability constant of metal complex database* (Ver. 8.0). Gaithersburg, MD: U.S. Department of Commerce.

79. Turner, D.R. & Sassman, S.A. (1996). Approaches to sorption modeling for high-level waste performance assessment. *Journal of Contaminate Hydrology*, 21 (1-4), pp. 311-332.

80. Stumm, W. & Morgan, J.J. (1996). *Aquatic chemistry*. Hoboken, NJ: John Wiley & Sons.

81. Snoeyink, V.L. & Jenkins, D.J. (1980). *Water chemistry.* Hoboken, NJ: John Wiley & Sons.

82. Kohler, M., Curtis, G.P., Meece, D.E., & Davis, J.A. (2004). Methods for estimating adsorbed uranium(VI) and distribution coefficients of contaminated sediments. *Environmental Science and Technology*, 38 (1), pp. 240-247

83. Yabusaki, S.B. (2009*). Conversation about sorption density*. Personal communication.

84. Harris, D.C. (2007) *Quantitative chemical analysis* (7th ed). New York, NY: WH Freeman.

85. Grenthe, I. & Plyasunov, A. (1997). On the use of semiempirical electrolyte theories for the modeling of solution chemical data. *Pure and Applied Chemistry*, 69 (5), pp. 951-958.

86. Eaton, A., Clesceri, L.S., Rice, E.W., & Greenberg, A.E. (2005) *Standard methods for the examination of water and wastewater* (21st ed). Baltimore, MD: American Public Health Association.

87. Lovley, D.R. & Phillips, E.P. (1988). Novel mode of microbial energy-metabolism - organic-carbon oxidation coupled to dissimilatory reduction of iron or manganese. *Applied and Environmental Microbiology*, 54 (6), pp. 1472-1480.

88. Tully, J.G., Whitcomb, R.F., Rose, D.L., Bove, J.M., Carle, P., Somerson, N.L., Willamson, D.L., & Eden-Green, S. (1994). Acholeplasma brassicae sp. nov. and Acholeplasma palmae sp. nov., Two Non-Sterol-Requiring Mollicutes from Plant Surfaces. *International Journal of Systematic Bacteriology*, 44 (4).

89. Barlett, M. (2009). *Average Geobacter uraniireducens properties and rising procedures*, Personal communication.

90. Martins, M., Faleiro, M.L., da Costa, A.M.R., Chaves, S., Tenreiro, R., Matos, A.P., & Costa, M.C. (2010). Mechanism of uranium (VI) removal by two anaerobic bacterial communities. *Journal of Hazardous Materials*, 184 (1-3), pp. 89-96.

91. Ohnuki, T., Yoshida, T., Ozaki, T., Samadfam, M., Kozai, N., Yubta, K., Mitsugashira, T., Kasama, T., & Francis, A.J. (2005). Interactions of uranium with bacteria and kaolinite clay. *Chemical Geology*, 220 (3-4), pp. 237-243.

92. Ohnuki, T., Kozai, N. Sakamoto, F., Ozaki, T., Nankawa, T., Suzuki, Y., & Francis, A.J. (2010). Association of Actinides with Microorganisms and Clay: Implications for Radionuclide Migration from Waste-Repository Sites. *Geomicrobiology Journal*, 27 (3), pp. 225-230.

93. Esteve-Nunez, A., Sosnik, J., Visconti, P., & Lovley, D.R. (2008). Fluorescent properties of c-type cytochromes reveal their potential role as an extracytoplasmic electron sink in Geobacter sulfurreducens. *Environmental Microbiology*, 10 (2), pp. 497-505.

94.Turner, D.L., Salgueiro, C.A., Catarino, T., Legall, J., & Xavier, A.V. (1996). NMR studies of cooperativity in the tetrahaem cytochrome c3 from Desulfovibrio vulgaris. *European Journal of Biochemistry*, **241** (3), pp. 723-731.

95.Esteve-Nunez, A., Rothermich, M., Sharma, M., & Lovley, D.R. (2005). Growth of Geobacter sulfurreducens under nutrient-limiting conditions in continuous culture. *Environental Microbiology*, **7** (5), pp. 641-648.

96. Bargar, J.R., Reitmeyer, R. & Davis, J.A (1999). Spectroscopic confirmation of uranium(VI)-carbonato adsorption complexes on hematite. *Environmental Science & Technology*, 33 (14), pp. 2481-2484.

Appendices

Appendix A

Supporting data for Chapter 3

Analytical Error Only					
Species	TrueValue	Mean	StdDev	Skewness	Kurtosis
Ca+2	-2.312	-2.313	0.016	-0.2	0.02
Na+	-2.065	-2.065	0.007	0.024	0.013
Mg+2	-2.381	-2.382	0.014	-0.262	0.212
SO4-2	-2.233	-2.234	0.015	-0.133	-0.008
CO3-2	-4.924	-4.925	0.051	-0.001	-0.093
Cl-	-2.273	-2.273	0.004	-0.039	-0.001
NO3-	-3.717	-3.717	0.013	-0.001	0.062
UO2+2	-15.445	-15.442	0.152	0.011	-0.084
K+	-3.522	-3.522	0.006	-0.012	0.044
Sr+2	-4.58	-4.582	0.02	-0.456	0.331
H+	-7.18	-7.18	0.02	0.016	0.006
H2O	1	1	0	0	0
(UO2)2(OH)2+2	-20.665	-20.658	0.294	-0.001	-0.086
(UO2)2CO3(OH)3-	-13.335	-13.329	0.89	-0.006	-0.01
(UO2)2(OH)+3	-25.409	-25.417	1.041	0	0.101
(UO2)3(CO3)6-6	-21.878	-21.868	1.026	-0.02	-0.025
(UO2)3(OH)4+2	-26.545	-26.53	0.524	0.011	-0.072
(UO2)3(OH)5+	-22.358	-22.352	0.447	-0.008	-0.108
(UO2)3(OH)7-	-22.82	-22.813	0.903	-0.012	0.082
(UO2)4(OH)7+	-28.308	-28.306	1.156	0.008	-0.089
Ca(NO3)2	-14.762	-14.763	0.104	0.029	-0.046
Ca2UO2(CO3)3(aq)	-6.203	-6.204	0.02	-0.312	0.135
CaCl+	-4.529	-4.53	0.015	-0.182	-0.015
CaCO3(aq)	-4.703	-4.705	0.085	0.025	-0.016
CaHCO3+	-3.574	-3.576	0.102	-0.042	-0.022
CaNO3+	-5.873	-5.873	0.201	-0.055	0.03
CaOH+	-7.173	-7.173	0.102	0.011	-0.043
CaSO4(aq)	-2.872	-2.874	0.051	-0.121	-0.013
CaUO2(CO3)3-2	-6.723	-6.725	0.061	-0.165	0.077
H2CO3*(aq)	-3.119	-3.119	0.048	0.03	-0.007
HCO3-	-2.119	-2.119	0.044	0.016	-0.103
HSO4-	-7.767	-7.767	0.026	-0.063	-0.005
KCl(aq)	-6.267	-6.266	0.1	0.011	-0.072
KNO3(aq)	-7.601	-7.601	0.082	-0.003	-0.09
KOH(aq)	-9.271	-9.27	0.102	0.011	-0.006
KSO4-	-5.248	-5.249	0.017	-0.036	0.036
Mg2CO3+2	-6.783	-6.786	0.114	0.006	-0.053
MgCl+	-4.398	-4.398	0.099	-0.007	0.048
MgCO3(aq)	-5.072	-5.074	0.086	0.021	0.01
MgHCO3+	-3.833	-3.835	0.072	-0.027	-0.023
MgOH+	-5.962	-5.963	0.038	-0.063	0.057
MgSO4(aq)	-3.041	-3.042	0.055	-0.082	0.078
NaCl(aq)	-4.81	-4.81	0.008	0.008	0.086
NaCO3-	-6.063	-6.064	0.112	0.037	-0.061
NaHCO3(aq)	-4.656	-4.657	0.046	0.009	-0.109
NaNO3(aq)	-6.504	-6.504	0.014	0.014	0.039
NaOH(aq)	-7.954	-7.954	0.037	0.001	0.046
NaSO4-	-3.852	-3.852	0.087	0.024	-0.002
SrCl+	-6.977	-6.978	0.054	-0.043	0.007
SrCO3(aq)	-7.381	-7.384	0.051	-0.052	-0.07
SrHCO3+	-5.832	-5.835	0.054	-0.019	-0.018
SrNO3+	-8.041	-8.04	0.201	-0.015	0.022
SrOH+	-9.921	-9.923	0.105	0.047	-0.052
SrSO4(aq)	-5.2	-5.203	0.082	-0.126	0.02
UO2(CO3)2-2	-9.37	-9.37	0.11	-0.025	-0.02
UO2(CO3)3-4	-8.377	-8.377	0.06	0.011	-0.027
UO2(OH)2	-11.75	-11.748	0.158	0.003	-0.103
UO2(OH)3-	-11.67	-11.666	0.444	0.037	-0.031
UO2(OH)4-2	-15.468	-15.472	0.694	0.006	0.028
UO2(SO4)2-2	-16.458	-16.456	0.168	0.007	-0.109
UO2Cl+	-17.891	-17.888	0.155	0.001	-0.08
UO2Cl2(aq)	-21.607	-21.598	0.428	0.014	-0.031
UO2CO3(aq)	-11.116	-11.114	0.112	-0.001	-0.097
UO2NO3+	-19.205	-19.202	0.215	0.026	-0.03
UO2OH+	-12.858	-12.858	0.282	-0.008	-0.032
UO2(SO4)3-4	-19.123	-19.124	0.406	0.044	0.016
Mg2UO2(CO3)3(aq)	-8.681	-8.683	0.207	0.012	0.005
MgUO2(CO3)3-2	-7.862	-7.863	0.064	-0.042	-0.027
SrUO2(CO3)3-2	-9.311	-9.313	0.065	-0.002	0.026
UO2SO4(aq)	-15.215	-15.212	0.155	-0.005	-0.071
OH-	-5.817	-5.817	0.02	-0.023	0.022

Time Error Only					
Species	TrueValue	Mean	StdDev	Skewness	Kurtosis
Ca+2	-2.439	-2.439	0.104	-0.012	-0.039
Na+	-2.065	-2.066	0.007	0.02	0.013
Mg+2	-2.386	-2.387	0.015	-0.301	0.28
SO4-2	-2.219	-2.221	0.025	-0.121	0.036
CO3-2	-5.108	-5.112	0.161	-0.064	-0.031
Cl-	-2.273	-2.273	0.004	-0.035	0.007
NO3-	-3.716	-3.716	0.013	0	0.062
UO2+2	-14.873	-14.864	0.501	0.044	-0.016
K+	-3.522	-3.522	0.007	-0.013	0.051
Sr+2	-4.585	-4.586	0.022	-0.445	0.301
H+	-7.04	-7.039	0.121	0.016	0.006
H2O	1	1	0	0	0
(UO2)2(OH)2+2	-19.789	-19.773	0.829	0.03	-0.008
(UO2)2CO3(OH)3-	-12.765	-12.754	1.064	0.021	-0.043
(UO2)2(OH)+3	-24.407	-24.403	1.344	0.048	0.058
(UO2)3(CO3)6-6	-21.27	-21.254	1.209	-0.035	0.031
(UO2)3(OH)4+2	-25.364	-25.336	1.201	0.014	-0.048
(UO2)3(OH)5+	-21.309	-21.291	1.107	0.014	-0.005
(UO2)3(OH)7-	-22.046	-22.03	1.271	-0.017	0.002
(UO2)4(OH)7+	-26.954	-26.937	1.759	0.012	-0.03
Ca(NO3)2	-14.874	-14.875	0.138	-0.023	-0.066
Ca2UO2(CO3)3(aq)	-6.384	-6.388	0.088	-0.064	0.029
CaCl+	-4.646	-4.647	0.098	-0.053	-0.044
CaCO3(aq)	-4.997	-5.001	0.196	-0.023	0.01
CaHCO3+	-3.728	-3.731	0.155	-0.05	0.022
CaNO3+	-5.99	-5.99	0.223	-0.058	-0.014
CaOH+	-7.431	-7.431	0.184	0.007	-0.051
CaSO4(aq)	-2.967	-2.97	0.095	-0.132	0.018
CaUO2(CO3)3-2	-6.796	-6.8	0.113	-0.111	0.095
H2CO3*(aq)	-3.009	-3.012	0.136	-0.021	0.07
HCO3-	-2.154	-2.157	0.086	0.004	-0.12
HSO4-	-7.604	-7.605	0.124	0.004	-0.001
KCl(aq)	-6.262	-6.262	0.1	0.01	-0.075
KNO3(aq)	-7.596	-7.596	0.082	-0.003	-0.088
KOH(aq)	-9.407	-9.408	0.157	-0.033	-0.031
KSO4-	-5.226	-5.229	0.028	-0.169	0.065
Mg2CO3+2	-6.959	-6.965	0.186	-0.038	-0.053
MgCl+	-4.393	-4.394	0.1	-0.006	0.044
MgCO3(aq)	-5.243	-5.249	0.171	-0.059	-0.056
MgHCO3+	-3.864	-3.869	0.1	-0.025	-0.082
MgOH+	-6.097	-6.1	0.124	-0.028	0.014
MgSO4(aq)	-3.014	-3.017	0.059	-0.088	0.083
NaCl(aq)	-4.806	-4.806	0.009	-0.024	0.089
NaCO3-	-6.238	-6.243	0.188	-0.008	-0.039
NaHCO3(aq)	-4.687	-4.69	0.085	-0.007	-0.131
NaNO3(aq)	-6.499	-6.5	0.015	-0.012	0.095
NaOH(aq)	-8.09	-8.091	0.125	-0.008	0.041
NaSO4-	-3.829	-3.831	0.09	0.023	0.005
SrCl+	-6.972	-6.974	0.055	-0.048	0.001
SrCO3(aq)	-7.552	-7.559	0.157	-0.085	-0.015
SrHCO3+	-5.863	-5.869	0.088	-0.02	-0.087
SrNO3+	-8.036	-8.036	0.201	-0.015	0.022
SrOH+	-10.056	-10.06	0.158	-0.019	-0.043
SrSO4(aq)	-5.173	-5.178	0.083	-0.154	0.048
UO2(CO3)2-2	-9.149	-9.149	0.25	-0.02	0.03
UO2(CO3)3-4	-8.358	-8.359	0.172	0.038	0.01
UO2(OH)2	-11.445	-11.44	0.353	0.001	-0.011
UO2(OH)3-	-11.505	-11.499	0.523	0.034	0.027
UO2(OH)4-2	-15.448	-15.45	0.751	0.011	-0.005
UO2(SO4)2-2	-15.841	-15.836	0.519	0.028	-0.011
UO2Cl+	-17.311	-17.302	0.505	0.039	-0.011
UO2Cl2(aq)	-21.021	-21.008	0.643	0.023	-0.022
UO2CO3(aq)	-10.711	-10.707	0.363	0.012	0.01
UO2NO3+	-18.624	-18.615	0.527	0.055	0.018
UO2OH+	-12.418	-12.414	0.479	0.003	0.011
UO2(SO4)3-4	-18.511	-18.507	0.637	0.046	0.022
Mg2UO2(CO3)3(aq)	-8.618	-8.625	0.275	-0.02	-0.037
MgUO2(CO3)3-2	-7.813	-7.817	0.186	-0.04	-0.002
SrUO2(CO3)3-2	-9.262	-9.267	0.187	-0.025	0.031
UO2SO4(aq)	-14.612	-14.605	0.511	0.033	-0.005
OH-	-5.957	-5.958	0.121	-0.017	0.009

Space Error Only					
Species	TrueValue	Mean	StdDev	Skewness	Kurtosis
Ca+2	-2.436	-2.439	0.107	-0.035	-0.043
Na+	-2.064	-2.064	0.007	-0.059	0.109
Mg+2	-2.368	-2.372	0.027	-0.772	1.035
SO4-2	-2.343	-2.341	0.173	0.036	0.003
CO3-2	-5.05	-5.052	0.214	-0.071	-0.017
Cl-	-2.273	-2.273	0.004	-0.036	0.013
NO3-	-3.716	-3.716	0.013	0	0.06
UO2+2	-15.278	-15.251	0.723	0.042	-0.012
K+	-3.52	-3.521	0.007	-0.084	0.07
Sr+2	-4.566	-4.571	0.031	-0.818	1.019
H+	-7.13	-7.129	0.161	0.016	0.006
H2O	1	1	0	0	0
(UO2)2(OH)2+2	-20.402	-20.355	1.235	0.029	-0.005
(UO2)2CO3(OH)3-	-13.21	-13.172	1.328	0.019	-0.04
(UO2)2(OH)+3	-25.126	-25.087	1.663	0.042	0.051
(UO2)3(CO3)6-6	-22.134	-22.056	1.603	-0.045	0.039
(UO2)3(OH)4+2	-26.187	-26.115	1.784	0.016	-0.033
(UO2)3(OH)5+	-22.031	-21.972	1.689	0.014	-0.007
(UO2)3(OH)7-	-22.583	-22.527	1.757	-0.008	-0.017
(UO2)4(OH)7+	-27.886	-27.814	2.433	0.003	-0.037
Ca(NO3)2	-14.856	-14.864	0.144	-0.061	-0.079
Ca2UO2(CO3)3(aq)	-6.547	-6.552	0.328	-0.011	0.017
CaCl+	-4.633	-4.64	0.104	-0.12	-0.012
CaCO3(aq)	-4.915	-4.927	0.24	-0.038	0.001
CaHCO3+	-3.736	-3.746	0.173	-0.062	0.008
CaNO3+	-5.977	-5.983	0.226	-0.063	-0.013
CaOH+	-7.327	-7.335	0.216	-0.002	-0.016
CaSO4(aq)	-3.067	-3.076	0.155	-0.199	0.081
CaUO2(CO3)3-2	-6.982	-6.978	0.338	-0.019	0.06
H2CO3*(aq)	-3.116	-3.12	0.184	-0.029	0.068
HCO3-	-2.176	-2.179	0.116	0.006	-0.116
HSO4-	-7.807	-7.807	0.23	-0.013	-0.058
KCl(aq)	-6.256	-6.257	0.1	0.005	-0.076
KNO3(aq)	-7.589	-7.591	0.083	0.002	-0.077
KOH(aq)	-9.31	-9.313	0.189	-0.038	-0.021
KSO4-	-5.337	-5.34	0.16	-0.066	-0.041
Mg2CO3+2	-6.846	-6.862	0.236	-0.072	-0.062
MgCl+	-4.366	-4.372	0.105	-0.02	0.034
MgCO3(aq)	-5.147	-5.16	0.22	-0.076	-0.065
MgHCO3+	-3.858	-3.869	0.128	-0.034	-0.126
MgOH+	-5.98	-5.988	0.166	-0.038	-0.003
MgSO4(aq)	-3.1	-3.108	0.141	-0.248	0.073
NaCl(aq)	-4.799	-4.801	0.012	-0.375	0.512
NaCO3-	-6.168	-6.174	0.234	-0.029	-0.034
NaHCO3(aq)	-4.701	-4.707	0.115	-0.006	-0.136
NaNO3(aq)	-6.492	-6.495	0.017	-0.119	0.21
NaOH(aq)	-7.993	-7.996	0.164	-0.011	0.029
NaSO4-	-3.941	-3.943	0.183	-0.044	-0.047
SrCl+	-6.944	-6.951	0.064	-0.222	0.162
SrCO3(aq)	-7.455	-7.468	0.209	-0.096	-0.033
SrHCO3+	-5.856	-5.868	0.118	-0.052	-0.117
SrNO3+	-8.007	-8.013	0.205	-0.023	0.026
SrOH+	-9.937	-9.947	0.193	-0.038	-0.019
SrSO4(aq)	-5.258	-5.267	0.152	-0.278	0.03
UO2(CO3)2-2	-9.417	-9.401	0.43	-0.015	0.004
UO2(CO3)3-4	-8.588	-8.567	0.376	0.019	0.07
UO2(OH)2	-11.654	-11.636	0.542	0.006	0.002
UO2(OH)3-	-11.624	-11.605	0.654	0.022	0.017
UO2(OH)4-2	-15.482	-15.47	0.849	0.014	-0.037
UO2(SO4)2-2	-16.472	-16.448	0.828	0.034	-0.019
UO2Cl+	-17.705	-17.682	0.726	0.039	-0.007
UO2Cl2(aq)	-21.411	-21.383	0.827	0.018	-0.042
UO2CO3(aq)	-11.037	-11.019	0.556	0.011	0.018
UO2NO3+	-19.019	-18.994	0.741	0.052	0.025
UO2OH+	-12.722	-12.703	0.662	0.014	0.001
UO2(SO4)3-4	-19.286	-19.255	1.003	0.052	-0.023
Mg2UO2(CO3)3(aq)	-8.751	-8.758	0.418	-0.021	-0.004
MgUO2(CO3)3-2	-7.984	-7.98	0.368	-0.029	0.062
SrUO2(CO3)3-2	-9.432	-9.428	0.368	-0.026	0.071
UO2SO4(aq)	-15.119	-15.097	0.759	0.035	-0.008
OH-	-5.867	-5.868	0.161	-0.017	0.008

Analytical Error with Adsorption Reactions					
Species	TrueValue	Mean	StdDev	Skewness	Kurtosis
Ca+2	-2.312	-2.313	0.016	-0.217	0.093
Na+	-2.065	-2.065	0.007	0.021	0.07
Mg+2	-2.381	-2.382	0.014	-0.263	0.214
SO4-2	-2.233	-2.234	0.015	-0.144	0.073
CO3-2	-4.924	-4.926	0.05	0.027	-0.022
Cl-	-2.273	-2.273	0.004	-0.013	0.034
NO3-	-3.717	-3.717	0.013	0.032	-0.024
UO2+2	-14.942	-14.948	0.091	-0.123	0.065
K+	-3.522	-3.522	0.007	-0.053	-0.038
Sr+2	-4.58	-4.582	0.02	-0.476	0.484
SSOH	-9.659	-9.653	0.13	0.077	0.068
SOH	-4.516	-4.516	0.006	-0.12	-0.144
WOH	-1.485	-1.485	0	-0.617	0.7
H+	-7.18	-7.18	0.02	-0.011	0.005
H2O	1	1	0	0	0
(UO2)2(OH)2+2	-19.659	-19.673	0.172	-0.12	0.099
(UO2)2CO3(OH)3-	-12.33	-12.348	0.857	0.031	-0.034
(UO2)2(OH)+3	-24.404	-24.421	1.026	-0.015	-0.019
(UO2)3(CO3)6-6	-20.371	-20.395	1.017	-0.011	0.112
(UO2)3(OH)4+2	-25.036	-25.056	0.387	0.032	-0.024
(UO2)3(OH)5+	-20.85	-20.871	0.272	-0.081	-0.005
(UO2)3(OH)7-	-21.312	-21.314	0.834	-0.047	0.027
(UO2)4(OH)7+	-26.297	-26.316	1.046	-0.001	0.049
Ca(NO3)2	-14.762	-14.764	0.103	-0.013	0.007
Ca2UO2(CO3)3(aq)	-5.701	-5.715	0.085	-0.44	0.16
CaCl+	-4.529	-4.53	0.015	-0.19	0.069
CaCO3(aq)	-4.704	-4.708	0.085	-0.004	-0.024
CaHCO3+	-3.575	-3.577	0.103	-0.062	-0.042
CaNO3+	-5.873	-5.878	0.199	-0.061	0.037
CaOH+	-7.173	-7.175	0.103	0	-0.044
CaSO4(aq)	-2.872	-2.874	0.051	-0.078	0.017
CaUO2(CO3)3-2	-6.222	-6.234	0.098	-0.26	0.093
H2CO3*(aq)	-3.119	-3.119	0.048	0.031	0.093
HCO3-	-2.119	-2.12	0.043	0.021	0.074
HSO4-	-7.766	-7.767	0.026	-0.046	0.057
KCl(aq)	-6.267	-6.265	0.1	0.004	0.001
KNO3(aq)	-7.601	-7.602	0.081	0.016	-0.045
KOH(aq)	-9.271	-9.27	0.103	0.003	-0.028
KSO4-	-5.248	-5.249	0.017	-0.063	0.034
Mg2CO3+2	-6.784	-6.788	0.114	0.036	-0.026
MgCl+	-4.398	-4.399	0.099	-0.009	-0.061
MgCO3(aq)	-5.073	-5.075	0.085	0.02	-0.071
MgHCO3+	-3.834	-3.836	0.072	-0.039	0.001
MgOH+	-5.962	-5.962	0.038	-0.041	-0.017
MgSO4(aq)	-3.041	-3.043	0.055	-0.097	0.088
NaCl(aq)	-4.81	-4.81	0.008	0.016	0.039
NaCO3-	-6.063	-6.065	0.111	0.016	0.018
NaHCO3(aq)	-4.656	-4.657	0.045	-0.002	0.059
NaNO3(aq)	-6.504	-6.504	0.014	-0.027	0.026
NaOH(aq)	-7.954	-7.954	0.036	-0.003	0.009
NaSO4-	-3.852	-3.853	0.089	-0.047	0.053
SrCl+	-6.977	-6.979	0.053	0.018	-0.051
SrCO3(aq)	-7.382	-7.385	0.05	-0.03	-0.026
SrHCO3+	-5.833	-5.835	0.053	-0.045	0.016
SrNO3+	-8.041	-8.042	0.202	0.039	-0.013
SrOH+	-9.921	-9.925	0.105	-0.037	-0.023
SrSO4(aq)	-5.2	-5.203	0.081	-0.138	0.014
UO2(CO3)2-2	-8.868	-8.877	0.105	-0.042	0.07
UO2(CO3)3-4	-7.875	-7.887	0.098	-0.197	0.059
UO2(OH)2	-11.247	-11.255	0.107	-0.046	-0.02
UO2(OH)3-	-11.167	-11.173	0.43	-0.006	0.09
UO2(OH)4-2	-14.965	-14.969	0.689	-0.03	-0.002
UO2(SO4)2-2	-15.955	-15.964	0.117	-0.113	0.042
UO2Cl+	-17.389	-17.395	0.094	-0.114	0.093
UO2Cl2(aq)	-21.104	-21.112	0.414	-0.003	0.023
UO2CO3(aq)	-10.613	-10.621	0.065	-0.047	-0.005
UO2NO3+	-18.702	-18.711	0.176	0	-0.05
UO2OH+	-12.355	-12.365	0.255	0.019	0.05
UO2(SO4)3-4	-18.62	-18.627	0.396	-0.01	0.001
Mg2UO2(CO3)3(aq)	-8.179	-8.189	0.218	0.007	-0.067
MgUO2(CO3)3-2	-7.36	-7.372	0.095	-0.198	0.048
SrUO2(CO3)3-2	-8.809	-8.822	0.095	-0.219	0.094
UO2SO4(aq)	-14.712	-14.719	0.094	-0.127	0.084
OH-	-5.817	-5.817	0.02	0.009	-0.027
SSOUO2+	-5.484	-5.484	0	-0.938	1.715
SOUO2+	-5.671	-5.679	0.091	-0.493	0.42
WOUO2+	-6.85	-6.857	0.127	-0.078	0.004
SSOUOOH	-9.723	-9.724	0.142	-0.023	-0.042
SOUOOH	-6.733	-6.74	0.124	-0.005	-0.029
WOUOOH	-6.592	-6.599	0.126	-0.102	-0.034

Temporal Error with Adsorption Reactions					
Species	TrueValue	Mean	StdDev	Skewness	Kurtosis
Ca+2	-2.439	-2.44	0.103	0.02	-0.061
Na+	-2.065	-2.065	0.007	0.017	0.074
Mg+2	-2.386	-2.386	0.015	-0.29	0.209
SO4-2	-2.219	-2.221	0.025	-0.125	0.068
CO3-2	-5.108	-5.114	0.16	-0.003	-0.042
Cl-	-2.273	-2.273	0.004	-0.014	0.045
NO3-	-3.716	-3.717	0.013	0.033	-0.027
UO2+2	-14.605	-14.642	0.268	-0.333	0.355
K+	-3.522	-3.522	0.007	-0.054	-0.036
Sr+2	-4.585	-4.586	0.022	-0.472	0.449
SSOH	-9.864	-9.826	0.219	0.281	0.325
SOH	-4.533	-4.533	0.018	-0.67	0.711
WOH	-1.485	-1.485	0	-1.106	2.794
H+	-7.04	-7.037	0.121	-0.011	0.005
H2O	1	1	0	0	0
(UO2)2(OH)2+2	-19.253	-19.332	0.391	-0.369	0.421
(UO2)2CO3(OH)3-	-12.23	-12.322	0.912	-0.002	-0.011
(UO2)2(OH)+3	-23.871	-23.95	1.107	-0.025	-0.038
(UO2)3(CO3)6-6	-20.467	-20.605	1.19	-0.077	0.035
(UO2)3(OH)4+2	-24.561	-24.681	0.619	-0.229	0.193
(UO2)3(OH)5+	-20.505	-20.63	0.542	-0.281	0.229
(UO2)3(OH)7-	-21.243	-21.353	0.989	-0.072	0.057
(UO2)4(OH)7+	-25.883	-26.041	1.218	-0.079	0.027
Ca(NO3)2	-14.874	-14.876	0.138	-0.084	-0.013
Ca2UO2(CO3)3(aq)	-6.117	-6.176	0.346	-0.447	0.042
CaCl+	-4.646	-4.648	0.097	-0.019	-0.079
CaCO3(aq)	-4.997	-5.006	0.195	0.003	-0.095
CaHCO3+	-3.728	-3.733	0.156	-0.058	0.004
CaNO3+	-5.99	-5.996	0.221	-0.061	0.078
CaOH+	-7.431	-7.435	0.185	0.009	-0.054
CaSO4(aq)	-2.967	-2.971	0.096	-0.111	-0.001
CaUO2(CO3)3-2	-6.528	-6.585	0.325	-0.429	0.057
H2CO3*(aq)	-3.009	-3.011	0.135	-0.003	-0.038
HCO3-	-2.154	-2.158	0.084	0.015	0.038
HSO4-	-7.604	-7.604	0.124	-0.032	0.008
KCl(aq)	-6.262	-6.261	0.1	0.003	-0.005
KNO3(aq)	-7.596	-7.597	0.081	0.015	-0.05
KOH(aq)	-9.407	-9.409	0.157	0.003	0.025
KSO4-	-5.226	-5.229	0.028	-0.177	0.104
Mg2CO3+2	-6.959	-6.968	0.186	0.013	-0.033
MgCl+	-4.393	-4.395	0.099	-0.009	-0.06
MgCO3(aq)	-5.243	-5.251	0.17	0.008	-0.057
MgHCO3+	-3.864	-3.87	0.099	-0.053	-0.009
MgOH+	-6.097	-6.1	0.124	0.001	-0.002
MgSO4(aq)	-3.014	-3.018	0.059	-0.114	0.037
NaCl(aq)	-4.806	-4.806	0.008	-0.021	0.025
NaCO3-	-6.238	-6.245	0.186	-0.003	-0.024
NaHCO3(aq)	-4.687	-4.691	0.084	-0.004	0.024
NaNO3(aq)	-6.499	-6.5	0.015	-0.034	0.02
NaOH(aq)	-8.09	-8.093	0.124	0.003	-0.009
NaSO4-	-3.829	-3.832	0.091	-0.026	0.018
SrCl+	-6.972	-6.975	0.054	0.013	-0.058
SrCO3(aq)	-7.553	-7.561	0.156	-0.011	-0.04
SrHCO3+	-5.864	-5.869	0.086	-0.041	0.023
SrNO3+	-8.036	-8.038	0.203	0.039	-0.011
SrOH+	-10.056	-10.063	0.158	-0.013	-0.097
SrSO4(aq)	-5.173	-5.178	0.083	-0.154	0.037
UO2(CO3)2-2	-8.882	-8.931	0.226	-0.221	0.166
UO2(CO3)3-4	-8.091	-8.145	0.328	-0.357	-0.009
UO2(OH)2	-11.178	-11.22	0.194	-0.196	0.153
UO2(OH)3-	-11.238	-11.281	0.484	-0.036	0.1
UO2(OH)4-2	-15.18	-15.223	0.759	-0.041	0.007
UO2(SO4)2-2	-15.573	-15.615	0.287	-0.342	0.314
UO2Cl+	-17.043	-17.08	0.27	-0.34	0.355
UO2Cl2(aq)	-20.753	-20.792	0.486	-0.059	0.069
UO2CO3(aq)	-10.443	-10.487	0.184	-0.22	0.269
UO2NO3+	-18.357	-18.396	0.305	-0.202	0.184
UO2OH+	-12.15	-12.193	0.309	-0.09	0.094
UO2(SO4)3-4	-18.243	-18.282	0.477	-0.096	0.096
Mg2UO2(CO3)3(aq)	-8.35	-8.407	0.375	-0.203	-0.051
MgUO2(CO3)3-2	-7.545	-7.602	0.322	-0.349	0.01
SrUO2(CO3)3-2	-8.994	-9.052	0.322	-0.356	0.033
UO2SO4(aq)	-14.344	-14.383	0.275	-0.356	0.364
OH-	-5.957	-5.96	0.121	0.011	0
SSOUO2+	-5.484	-5.484	0	-2.253	14.136
SOUO2+	-5.483	-5.523	0.171	-0.657	0.892
WOUO2+	-6.645	-6.684	0.217	-0.311	0.303
SSOUOOH	-9.859	-9.862	0.184	-0.042	-0.058
SOUOOH	-6.681	-6.722	0.195	-0.174	0.082
WOUOOH	-6.522	-6.565	0.205	-0.203	0.128

Space Error with Adsorption Reactions					
Species	TrueValue	Mean	StdDev	Skewness	Kurtosis
Ca+2	-2.436	-2.44	0.106	0.004	-0.114
Na+	-2.064	-2.064	0.007	-0.062	0.165
Mg+2	-2.368	-2.372	0.027	-0.813	1.18
SO4-2	-2.343	-2.345	0.175	0.036	0.042
CO3-2	-5.05	-5.056	0.212	-0.011	-0.041
Cl-	-2.273	-2.273	0.004	-0.02	0.039
NO3-	-3.716	-3.717	0.013	0.031	-0.024
UO2+2	-14.768	-15.207	1.331	-1.66	2.184
K+	-3.52	-3.521	0.007	-0.102	0.014
Sr+2	-4.566	-4.57	0.031	-0.79	0.951
SSOH	-9.801	-9.375	1.265	1.678	2.081
SOH	-4.527	-4.55	0.088	-3.236	16.269
WOH	-1.485	-1.485	0	-10.518	255.787
H+	-7.13	-7.127	0.161	-0.011	0.005
H2O	1	1	0	0	0
(UO2)2(OH)2+2	-19.383	-20.271	2.618	-1.778	2.453
(UO2)2CO3(OH)3-	-12.191	-13.098	2.728	-1.587	2.197
(UO2)2(OH)+3	-24.107	-24.991	2.824	-1.397	1.748
(UO2)3(CO3)6-6	-20.606	-21.95	4.078	-1.663	2.352
(UO2)3(OH)4+2	-24.658	-25.995	3.928	-1.787	2.483
(UO2)3(OH)5+	-20.503	-21.847	3.917	-1.816	2.556
(UO2)3(OH)7-	-21.055	-22.388	4.014	-1.715	2.417
(UO2)4(OH)7+	-25.848	-27.632	5.313	-1.731	2.399
Ca(NO3)2	-14.856	-14.865	0.144	-0.092	-0.07
Ca2UO2(CO3)3(aq)	-6.038	-6.519	1.353	-1.739	2.573
CaCl+	-4.634	-4.641	0.104	-0.084	-0.102
CaCO3(aq)	-4.915	-4.932	0.239	-0.009	-0.075
CaHCO3+	-3.736	-3.749	0.175	-0.068	0.021
CaNO3+	-5.977	-5.988	0.224	-0.066	0.053
CaOH+	-7.328	-7.338	0.216	0.004	-0.039
CaSO4(aq)	-3.068	-3.079	0.156	-0.196	0.089
CaUO2(CO3)3-2	-6.473	-6.944	1.348	-1.749	2.577
H2CO3*(aq)	-3.116	-3.119	0.184	-0.009	-0.041
HCO3-	-2.176	-2.181	0.114	0.017	0.049
HSO4-	-7.807	-7.81	0.231	-0.036	-0.013
KCl(aq)	-6.256	-6.256	0.1	0.003	0.002
KNO3(aq)	-7.589	-7.592	0.081	0.016	-0.057
KOH(aq)	-9.31	-9.314	0.19	0.003	0.021
KSO4-	-5.337	-5.343	0.162	-0.067	-0.004
Mg2CO3+2	-6.846	-6.865	0.236	-0.018	-0.018
MgCl+	-4.366	-4.372	0.105	-0.033	-0.042
MgCO3(aq)	-5.147	-5.162	0.22	-0.01	-0.05
MgHCO3+	-3.858	-3.871	0.128	-0.063	-0.008
MgOH+	-5.98	-5.989	0.167	-0.001	0.006
MgSO4(aq)	-3.1	-3.112	0.142	-0.26	0.068
NaCl(aq)	-4.799	-4.801	0.011	-0.404	0.71
NaCO3-	-6.168	-6.178	0.231	-0.009	-0.029
NaHCO3(aq)	-4.702	-4.709	0.113	0.001	0.034
NaNO3(aq)	-6.492	-6.495	0.017	-0.14	0.121
NaOH(aq)	-7.993	-7.998	0.163	0.006	-0.006
NaSO4-	-3.941	-3.947	0.184	-0.039	-0.078
SrCl+	-6.944	-6.951	0.064	-0.184	0.178
SrCO3(aq)	-7.455	-7.471	0.208	-0.024	-0.026
SrHCO3+	-5.856	-5.868	0.117	-0.058	0.03
SrNO3+	-8.007	-8.014	0.206	0.021	0.006
SrOH+	-9.938	-9.95	0.194	-0.006	-0.083
SrSO4(aq)	-5.258	-5.27	0.154	-0.321	0.051
UO2(CO3)2-2	-8.908	-9.364	1.313	-1.822	2.661
UO2(CO3)3-4	-8.079	-8.535	1.354	-1.729	2.53
UO2(OH)2	-11.145	-11.595	1.309	-1.816	2.578
UO2(OH)3-	-11.115	-11.566	1.393	-1.561	2.156
UO2(OH)4-2	-14.973	-15.423	1.521	-1.201	1.536
UO2(SO4)2-2	-15.962	-16.413	1.38	-1.48	1.824
UO2Cl+	-17.196	-17.637	1.331	-1.658	2.177
UO2Cl2(aq)	-20.901	-21.345	1.389	-1.452	1.839
UO2CO3(aq)	-10.527	-10.977	1.305	-1.808	2.554
UO2NO3+	-18.509	-18.953	1.334	-1.631	2.124
UO2OH+	-12.213	-12.66	1.329	-1.699	2.323
UO2(SO4)3-4	-18.776	-19.22	1.494	-1.17	1.343
Mg2UO2(CO3)3(aq)	-8.242	-8.72	1.365	-1.689	2.425
MgUO2(CO3)3-2	-7.475	-7.946	1.349	-1.743	2.551
SrUO2(CO3)3-2	-8.923	-9.394	1.35	-1.745	2.555
UO2SO4(aq)	-14.61	-15.056	1.345	-1.607	2.065
OH-	-5.867	-5.87	0.161	0.011	0.001
SSOUO2+	-5.484	-5.501	0.066	-5.127	31.3
SOUO2+	-5.54	-6.007	1.262	-1.929	2.805
WOUO2+	-6.707	-7.152	1.314	-1.766	2.434
SSOUOOH	-9.763	-9.787	0.223	-0.166	0.163
SOUOOH	-6.642	-7.114	1.266	-1.934	2.851
WOUOOH	-6.489	-6.939	1.311	-1.81	2.563

Analytical Error with Adsorption Reactions and Low Uranium Concentration					
Species	TrueValue	Mean	StdDev	Skewness	Kurtosis
Ca+2	-2.312	-2.313	0.016	-0.217	0.094
Na+	-2.065	-2.065	0.007	0.021	0.07
Mg+2	-2.381	-2.382	0.014	-0.263	0.214
SO4-2	-2.233	-2.234	0.015	-0.144	0.073
CO3-2	-4.924	-4.926	0.05	0.027	-0.022
Cl-	-2.273	-2.273	0.004	-0.013	0.034
NO3-	-3.717	-3.717	0.013	0.032	-0.024
UO2+2	-16.333	-16.351	0.134	-0.281	0.215
K+	-3.522	-3.522	0.007	-0.053	-0.038
Sr+2	-4.58	-4.582	0.02	-0.476	0.484
SSOH	-8.268	-8.251	0.162	0.18	0.138
SOH	-4.485	-4.485	0	-0.501	0.314
WOH	-1.485	-1.485	0	0	0
H+	-7.18	-7.18	0.02	-0.011	0.005
H2O	1	1	0	0	0
(UO2)2(OH)2+2	-22.441	-22.478	0.262	-0.305	0.262
(UO2)2CO3(OH)3-	-15.112	-15.154	0.878	0.012	-0.026
(UO2)2(OH)+3	-27.186	-27.227	1.047	-0.013	-0.04
(UO2)3(CO3)6-6	-24.543	-24.601	1.07	-0.035	0.058
(UO2)3(OH)4+2	-29.21	-29.265	0.487	-0.146	0.098
(UO2)3(OH)5+	-25.024	-25.08	0.402	-0.286	0.203
(UO2)3(OH)7-	-25.486	-25.523	0.889	-0.062	0.048
(UO2)4(OH)7+	-31.862	-31.928	1.117	-0.048	0.025
Ca(NO3)2	-14.762	-14.763	0.103	-0.013	0.007
Ca2UO2(CO3)3(aq)	-7.091	-7.116	0.138	-0.433	0.475
CaCl+	-4.529	-4.53	0.015	-0.19	0.07
CaCO3(aq)	-4.703	-4.707	0.085	-0.004	-0.024
CaHCO3+	-3.574	-3.577	0.103	-0.062	-0.042
CaNO3+	-5.873	-5.878	0.199	-0.061	0.037
CaOH+	-7.173	-7.174	0.103	0	-0.044
CaSO4(aq)	-2.872	-2.873	0.051	-0.078	0.017
CaUO2(CO3)3-2	-7.611	-7.635	0.146	-0.339	0.344
H2CO3*(aq)	-3.119	-3.119	0.048	0.031	0.093
HCO3-	-2.119	-2.12	0.043	0.021	0.074
HSO4-	-7.767	-7.767	0.026	-0.046	0.057
KCl(aq)	-6.267	-6.265	0.1	0.004	0.001
KNO3(aq)	-7.601	-7.602	0.081	0.016	-0.045
KOH(aq)	-9.271	-9.27	0.103	0.003	-0.028
KSO4-	-5.248	-5.249	0.017	-0.063	0.034
Mg2CO3+2	-6.783	-6.787	0.114	0.036	-0.026
MgCl+	-4.398	-4.399	0.099	-0.009	-0.061
MgCO3(aq)	-5.072	-5.074	0.085	0.02	-0.071
MgHCO3+	-3.833	-3.836	0.072	-0.039	0.001
MgOH+	-5.962	-5.962	0.038	-0.041	-0.017
MgSO4(aq)	-3.041	-3.043	0.055	-0.097	0.088
NaCl(aq)	-4.81	-4.81	0.008	0.016	0.039
NaCO3-	-6.063	-6.065	0.111	0.016	0.018
NaHCO3(aq)	-4.656	-4.657	0.045	-0.003	0.058
NaNO3(aq)	-6.504	-6.504	0.014	-0.027	0.026
NaOH(aq)	-7.954	-7.954	0.036	-0.003	0.009
NaSO4-	-3.852	-3.853	0.089	-0.047	0.053
SrCl+	-6.977	-6.979	0.053	0.018	-0.051
SrCO3(aq)	-7.381	-7.384	0.05	-0.03	-0.027
SrHCO3+	-5.832	-5.835	0.053	-0.045	0.016
SrNO3+	-8.041	-8.042	0.202	0.039	-0.013
SrOH+	-9.921	-9.925	0.105	-0.038	-0.023
SrSO4(aq)	-5.2	-5.203	0.081	-0.138	0.014
UO2(CO3)2-2	-10.258	-10.28	0.148	-0.207	0.237
UO2(CO3)3-4	-9.265	-9.289	0.146	-0.338	0.349
UO2(OH)2	-12.639	-12.658	0.146	-0.214	0.175
UO2(OH)3-	-12.559	-12.576	0.442	-0.011	0.09
UO2(OH)4-2	-16.357	-16.372	0.696	-0.027	0.003
UO2(SO4)2-2	-17.346	-17.367	0.152	-0.226	0.106
UO2Cl+	-18.78	-18.798	0.136	-0.26	0.207
UO2Cl2(aq)	-22.495	-22.515	0.425	-0.001	0.001
UO2CO3(aq)	-12.004	-12.024	0.12	-0.406	0.537
UO2NO3+	-20.094	-20.114	0.199	-0.055	-0.028
UO2OH+	-13.747	-13.768	0.273	-0.022	0.042
UO2(SO4)3-4	-20.011	-20.03	0.409	-0.028	0.035
Mg2UO2(CO3)3(aq)	-9.569	-9.591	0.243	-0.055	-0.022
MgUO2(CO3)3-2	-8.751	-8.774	0.143	-0.355	0.436
SrUO2(CO3)3-2	-10.2	-10.224	0.144	-0.35	0.386
UO2SO4(aq)	-16.103	-16.122	0.137	-0.266	0.168
OH-	-5.817	-5.817	0.02	0.009	-0.027
SSOUO2+	-5.485	-5.485	0	-1.62	5.537
SOUO2+	-7.032	-7.051	0.136	-0.389	0.232
WOUO2+	-8.241	-8.259	0.162	-0.18	0.045
SSOUOOH	-9.724	-9.725	0.142	-0.024	-0.043
SOUOOH	-8.094	-8.112	0.161	-0.135	0.05
WOUOOH	-7.983	-8.002	0.161	-0.189	0.077

Temporal Error with Adsorption Reactions and Low Uranium Concentration					
Species	TrueValue	Mean	StdDev	Skewness	Kurtosis
Ca+2	-2.439	-2.44	0.103	0.02	-0.061
Na+	-2.065	-2.065	0.007	0.017	0.074
Mg+2	-2.386	-2.386	0.015	-0.29	0.209
SO4-2	-2.219	-2.221	0.025	-0.125	0.068
CO3-2	-5.108	-5.114	0.16	-0.003	-0.042
Cl-	-2.273	-2.273	0.004	-0.014	0.045
NO3-	-3.716	-3.717	0.013	0.033	-0.027
UO2+2	-15.999	-16.539	1.16	-0.42	-1.319
K+	-3.522	-3.522	0.007	-0.054	-0.036
Sr+2	-4.585	-4.586	0.022	-0.472	0.449
SSOH	-8.471	-7.948	1.123	0.403	-1.401
SOH	-4.486	-4.488	0.005	-1.702	3.318
WOH	-1.485	-1.485	0	-2.092	7.367
H+	-7.04	-7.037	0.121	-0.011	0.005
H2O	1	1	0	0	0
(UO2)2(OH)2+2	-22.04	-23.126	2.3	-0.452	-1.345
(UO2)2CO3(OH)3-	-15.016	-16.115	2.449	-0.398	-1
(UO2)2(OH)+3	-26.658	-27.744	2.525	-0.331	-0.949
(UO2)3(CO3)6-6	-24.646	-26.294	3.646	-0.435	-1.061
(UO2)3(OH)4+2	-28.741	-30.371	3.46	-0.456	-1.324
(UO2)3(OH)5+	-24.685	-26.321	3.452	-0.465	-1.332
(UO2)3(OH)7-	-25.423	-27.043	3.559	-0.432	-1.168
(UO2)4(OH)7+	-31.456	-33.628	4.703	-0.444	-1.209
Ca(NO3)2	-14.874	-14.876	0.138	-0.084	-0.013
Ca2UO2(CO3)3(aq)	-7.509	-8.072	1.203	-0.48	-1.063
CaCl+	-4.646	-4.648	0.097	-0.019	-0.079
CaCO3(aq)	-4.996	-5.006	0.195	0.004	-0.095
CaHCO3+	-3.727	-3.733	0.156	-0.058	0.003
CaNO3+	-5.99	-5.996	0.221	-0.061	0.078
CaOH+	-7.431	-7.435	0.185	0.009	-0.054
CaSO4(aq)	-2.967	-2.971	0.096	-0.111	-0.001
CaUO2(CO3)3-2	-7.921	-8.482	1.196	-0.485	-1.091
H2CO3*(aq)	-3.009	-3.011	0.135	-0.003	-0.038
HCO3-	-2.154	-2.158	0.084	0.015	0.038
HSO4-	-7.604	-7.604	0.124	-0.032	0.008
KCl(aq)	-6.262	-6.261	0.1	0.003	-0.005
KNO3(aq)	-7.596	-7.597	0.081	0.015	-0.05
KOH(aq)	-9.407	-9.409	0.157	0.003	0.025
KSO4-	-5.226	-5.229	0.028	-0.177	0.104
Mg2CO3+2	-6.959	-6.968	0.186	0.013	-0.033
MgCl+	-4.393	-4.395	0.099	-0.009	-0.06
MgCO3(aq)	-5.243	-5.251	0.17	0.008	-0.058
MgHCO3+	-3.864	-3.87	0.099	-0.053	-0.009
MgOH+	-6.097	-6.1	0.124	0.001	-0.002
MgSO4(aq)	-3.014	-3.018	0.059	-0.114	0.037
NaCl(aq)	-4.806	-4.806	0.008	-0.021	0.025
NaCO3-	-6.238	-6.245	0.186	-0.003	-0.025
NaHCO3(aq)	-4.687	-4.691	0.084	-0.005	0.023
NaNO3(aq)	-6.499	-6.5	0.015	-0.034	0.02
NaOH(aq)	-8.09	-8.093	0.124	0.003	-0.009
NaSO4-	-3.829	-3.832	0.091	-0.026	0.018
SrCl+	-6.972	-6.975	0.054	0.013	-0.058
SrCO3(aq)	-7.552	-7.561	0.156	-0.011	-0.04
SrHCO3+	-5.863	-5.869	0.086	-0.041	0.023
SrNO3+	-8.036	-8.038	0.203	0.039	-0.011
SrOH+	-10.056	-10.063	0.158	-0.013	-0.097
SrSO4(aq)	-5.173	-5.178	0.083	-0.154	0.037
UO2(CO3)2-2	-10.275	-10.828	1.165	-0.477	-1.24
UO2(CO3)3-4	-9.483	-10.041	1.197	-0.481	-1.098
UO2(OH)2	-12.571	-13.117	1.154	-0.468	-1.306
UO2(OH)3-	-12.631	-13.178	1.241	-0.398	-0.946
UO2(OH)4-2	-16.574	-17.119	1.375	-0.303	-0.603
UO2(SO4)2-2	-16.966	-17.512	1.163	-0.416	-1.304
UO2Cl+	-18.436	-18.977	1.161	-0.419	-1.319
UO2Cl2(aq)	-22.146	-22.689	1.224	-0.346	-1.051
UO2CO3(aq)	-11.836	-12.383	1.151	-0.462	-1.331
UO2NO3+	-19.75	-20.293	1.166	-0.412	-1.285
UO2OH+	-13.544	-14.089	1.172	-0.427	-1.237
UO2(SO4)3-4	-19.636	-20.179	1.226	-0.365	-1.044
Mg2UO2(CO3)3(aq)	-9.743	-10.303	1.211	-0.466	-1.06
MgUO2(CO3)3-2	-8.938	-9.498	1.194	-0.481	-1.109
SrUO2(CO3)3-2	-10.387	-10.948	1.195	-0.482	-1.109
UO2SO4(aq)	-15.737	-16.28	1.162	-0.418	-1.317
OH-	-5.957	-5.96	0.121	0.011	0
SSOUO2+	-5.485	-5.504	0.036	-2.251	5.304
SOUO2+	-6.83	-7.375	1.147	-0.469	-1.327
WOUO2+	-8.038	-8.581	1.155	-0.45	-1.324
SSOUOOH	-9.859	-9.882	0.188	-0.054	-0.083
SOUOOH	-8.027	-8.574	1.155	-0.468	-1.3
WOUOOH	-7.915	-8.461	1.157	-0.466	-1.298

Space Error with Adsorption Reactions and Low Uranium Concentration					
Species	TrueValue	Mean	StdDev	Skewness	Kurtosis
Ca+2	-2.436	-2.44	0.106	0.003	-0.113
Na+	-2.064	-2.064	0.007	-0.062	0.165
Mg+2	-2.368	-2.372	0.027	-0.813	1.181
SO4-2	-2.343	-2.345	0.175	0.036	0.042
CO3-2	-5.05	-5.056	0.212	-0.011	-0.042
Cl-	-2.273	-2.273	0.004	-0.02	0.039
NO3-	-3.716	-3.717	0.013	0.031	-0.024
UO2+2	-16.139	-16.92	1.886	-0.054	-1.651
K+	-3.52	-3.521	0.007	-0.102	0.014
Sr+2	-4.566	-4.57	0.031	-0.79	0.952
SSOH	-8.432	-7.763	1.735	-0.009	-1.735
SOH	-4.486	-4.5	0.033	-4.47	33.115
WOH	-1.485	-1.485	0	-11.13	316
H+	-7.13	-7.127	0.161	-0.011	0.005
H2O	1	1	0	0	0
(UO2)2(OH)2+2	-22.124	-23.697	3.747	-0.071	-1.688
(UO2)2CO3(OH)3-	-14.932	-16.523	3.839	-0.089	-1.514
(UO2)2(OH)+3	-26.847	-28.416	3.9	-0.051	-1.46
(UO2)3(CO3)6-6	-24.716	-27.087	5.764	-0.107	-1.534
(UO2)3(OH)4+2	-28.769	-31.133	5.625	-0.078	-1.682
(UO2)3(OH)5+	-24.613	-26.985	5.621	-0.083	-1.686
(UO2)3(OH)7-	-25.166	-27.526	5.697	-0.087	-1.598
(UO2)4(OH)7+	-31.329	-34.484	7.553	-0.085	-1.627
Ca(NO3)2	-14.855	-14.864	0.144	-0.092	-0.069
Ca2UO2(CO3)3(aq)	-7.407	-8.231	1.924	-0.139	-1.512
CaCl+	-4.633	-4.64	0.104	-0.085	-0.101
CaCO3(aq)	-4.915	-4.932	0.239	-0.009	-0.077
CaHCO3+	-3.736	-3.748	0.175	-0.068	0.02
CaNO3+	-5.977	-5.988	0.224	-0.066	0.053
CaOH+	-7.327	-7.338	0.216	0.004	-0.039
CaSO4(aq)	-3.067	-3.079	0.156	-0.195	0.089
CaUO2(CO3)3-2	-7.842	-8.656	1.919	-0.138	-1.524
H2CO3*(aq)	-3.116	-3.119	0.184	-0.008	-0.041
HCO3-	-2.175	-2.181	0.114	0.017	0.047
HSO4-	-7.807	-7.81	0.231	-0.036	-0.013
KCl(aq)	-6.256	-6.256	0.1	0.003	0.002
KNO3(aq)	-7.589	-7.592	0.081	0.016	-0.057
KOH(aq)	-9.31	-9.314	0.19	0.003	0.021
KSO4-	-5.337	-5.343	0.162	-0.067	-0.004
Mg2CO3+2	-6.846	-6.865	0.236	-0.018	-0.018
MgCl+	-4.366	-4.372	0.105	-0.033	-0.042
MgCO3(aq)	-5.147	-5.162	0.22	-0.01	-0.051
MgHCO3+	-3.858	-3.87	0.128	-0.064	-0.008
MgOH+	-5.98	-5.989	0.167	-0.001	0.006
MgSO4(aq)	-3.1	-3.112	0.143	-0.26	0.068
NaCl(aq)	-4.799	-4.801	0.011	-0.404	0.709
NaCO3-	-6.168	-6.177	0.231	-0.009	-0.03
NaHCO3(aq)	-4.701	-4.708	0.113	0	0.033
NaNO3(aq)	-6.492	-6.495	0.017	-0.14	0.121
NaOH(aq)	-7.993	-7.998	0.163	0.006	-0.006
NaSO4-	-3.941	-3.947	0.184	-0.039	-0.078
SrCl+	-6.944	-6.951	0.064	-0.184	0.178
SrCO3(aq)	-7.455	-7.471	0.208	-0.025	-0.027
SrHCO3+	-5.856	-5.868	0.117	-0.058	0.029
SrNO3+	-8.007	-8.014	0.206	0.021	0.006
SrOH+	-9.938	-9.95	0.194	-0.006	-0.083
SrSO4(aq)	-5.258	-5.27	0.154	-0.321	0.051
UO2(CO3)2-2	-10.278	-11.076	1.887	-0.109	-1.631
UO2(CO3)3-4	-9.449	-10.247	1.923	-0.137	-1.518
UO2(OH)2	-12.515	-13.308	1.877	-0.089	-1.673
UO2(OH)3-	-12.485	-13.279	1.938	-0.098	-1.468
UO2(OH)4-2	-16.343	-17.136	2.037	-0.094	-1.187
UO2(SO4)2-2	-17.333	-18.126	1.918	-0.047	-1.547
UO2Cl+	-18.566	-19.35	1.886	-0.053	-1.651
UO2Cl2(aq)	-22.271	-23.058	1.926	-0.046	-1.511
UO2CO3(aq)	-11.897	-12.69	1.874	-0.082	-1.683
UO2NO3+	-19.879	-20.666	1.888	-0.055	-1.636
UO2OH+	-13.583	-14.373	1.886	-0.072	-1.634
UO2(SO4)3-4	-20.146	-20.933	2.004	-0.041	-1.308
Mg2UO2(CO3)3(aq)	-9.612	-10.432	1.929	-0.135	-1.5
MgUO2(CO3)3-2	-8.845	-9.658	1.919	-0.136	-1.529
SrUO2(CO3)3-2	-10.292	-11.106	1.919	-0.136	-1.53
UO2SO4(aq)	-15.98	-16.769	1.895	-0.051	-1.626
OH-	-5.867	-5.87	0.161	0.011	0.001
SSOUO2+	-5.485	-5.602	0.18	-1.749	2.851
SOUO2+	-6.869	-7.671	1.855	-0.092	-1.699
WOUO2+	-8.078	-8.865	1.877	-0.072	-1.679
SSOUOOH	-9.764	-9.887	0.279	-0.493	0.401
SOUOOH	-7.971	-8.777	1.861	-0.103	-1.682
WOUOOH	-7.86	-8.652	1.879	-0.089	-1.67

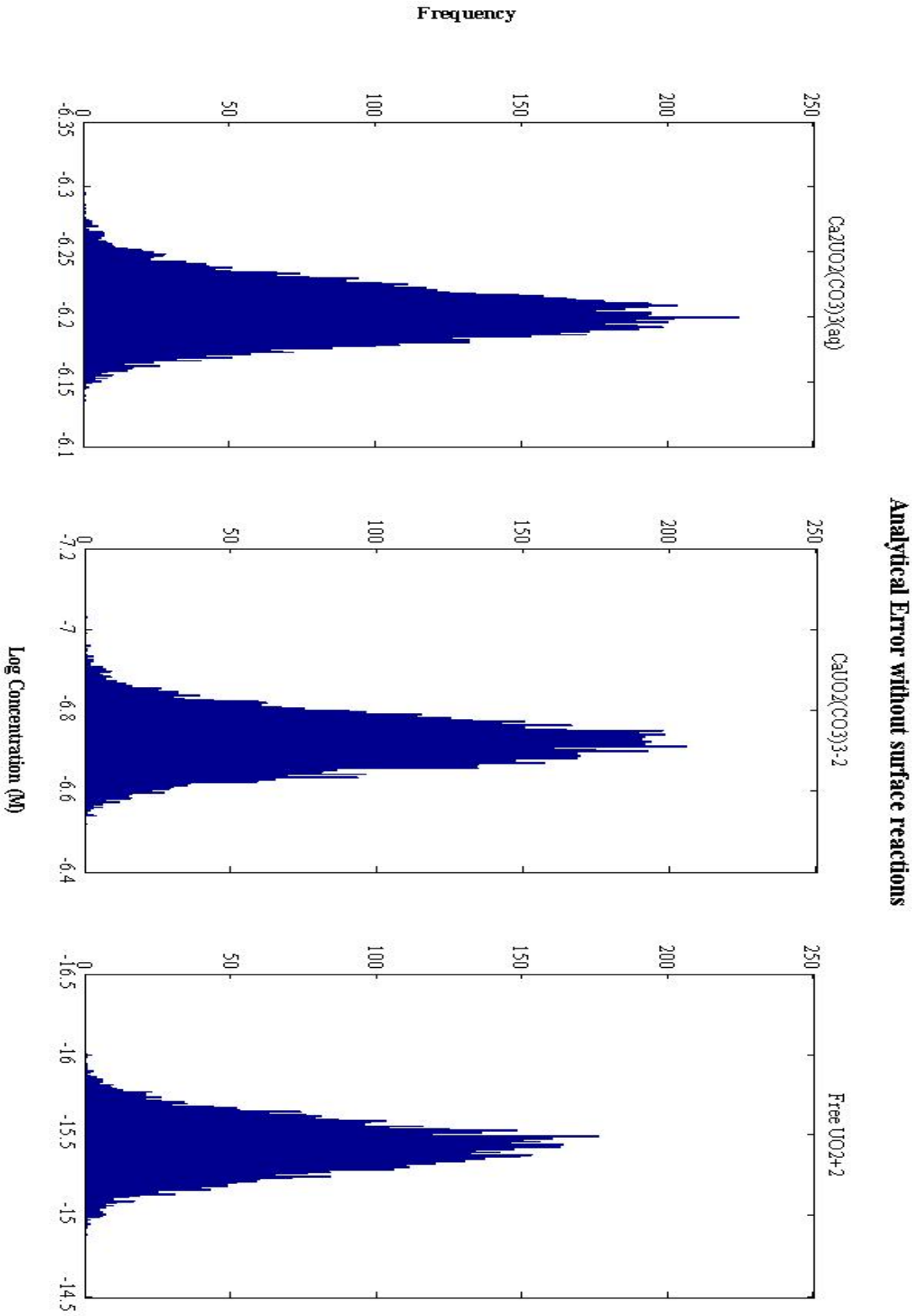
Analytical Error without surface reactions
Frequency
Log Concentration (M)
Ca2UO2(CO3)3(aq)
CaUO2(CO3)3-2
Free UO2+2
0
50
100
150
200
250
-6.35
-6.3
-6.25
-6.2
-6.15
-6.1
-7.2
-7
-6.8
-6.6
-6.4
-16.5
-16
-15.5
-15
-14.5

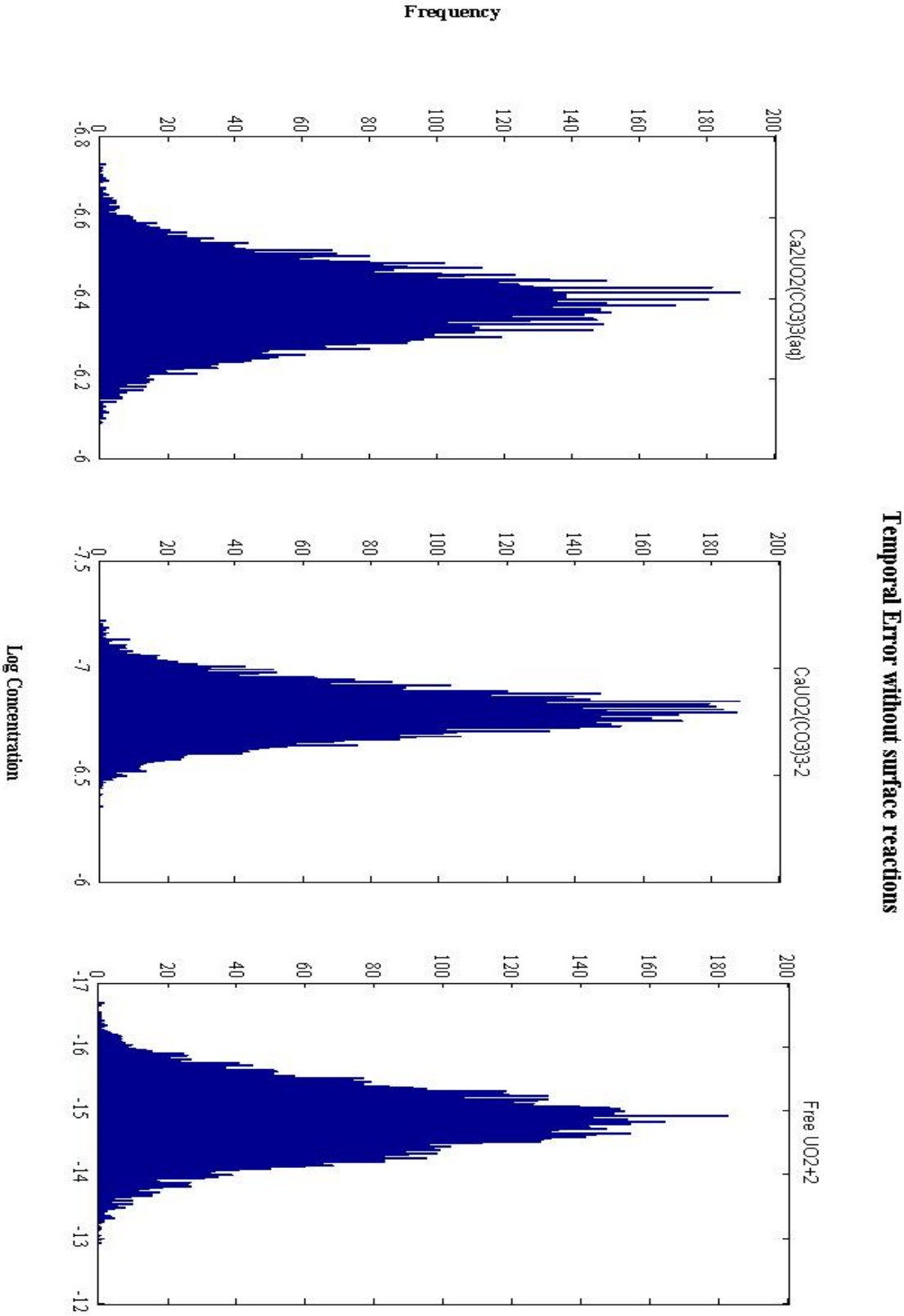
Temporal Error without surface reactions
Frequency
Log Concentration
Ca2UO2(CO3)3(aq)
CaUO2(CO3)3-2
Free UO2+2
0
20
40
60
80
100
120
140
160
180
200
-6.8
-6.6
-6.4
-6.2
-6
-7.5
-7
-6.5
-6
-17
-16
-15
-14
-13
-12

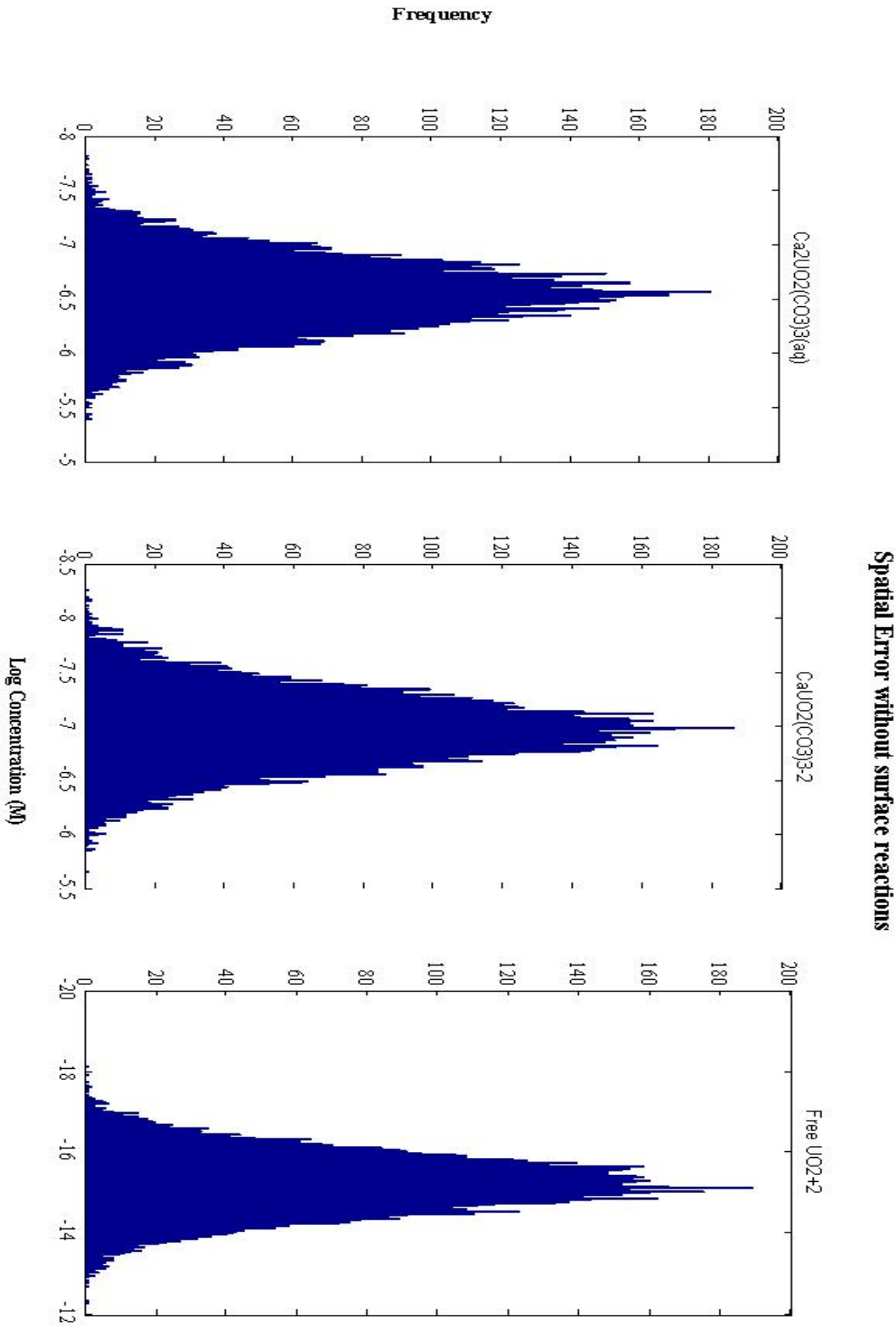
Spatial Error without surface reactions
Frequency
Log Concentration (M)
Ca2UO2(CO3)3(aq)
CaUO2(CO3)3-2
Free UO2+2

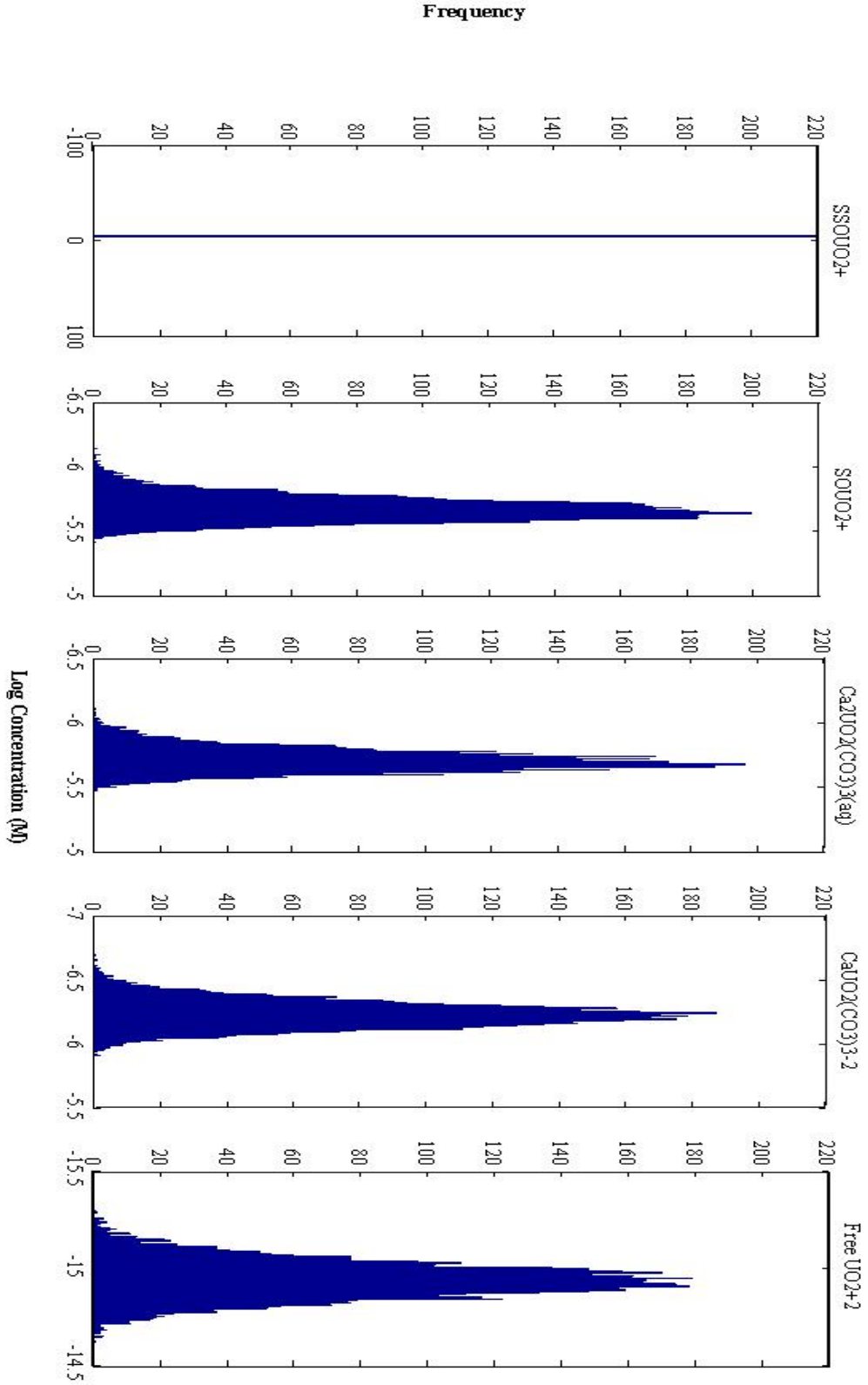
Analytical Error with surface reactions
Frequency
Log Concentration (M)
SSOUO2+
SOUO2+
Ca2UO2(CO3)3(aq)
CaUO2(CO3)3-2
Free UO2+2

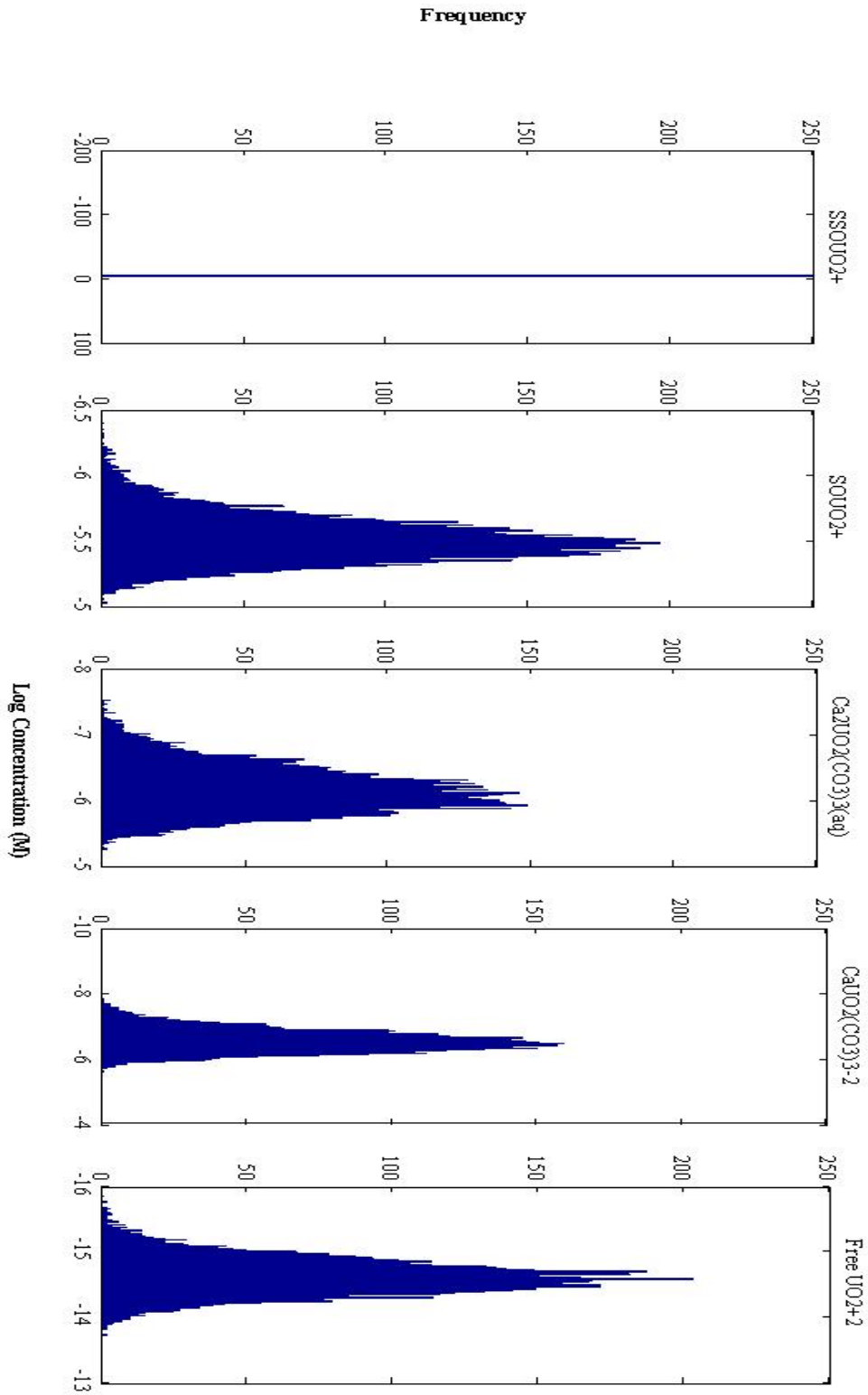
Temporal Error with surface reactions
Frequency
Log Concentration (M)
SSOUO2+
SOUO2+
Ca2UO2(CO3)3(aq)
CaUO2(CO3)3-2
Free UO2+2

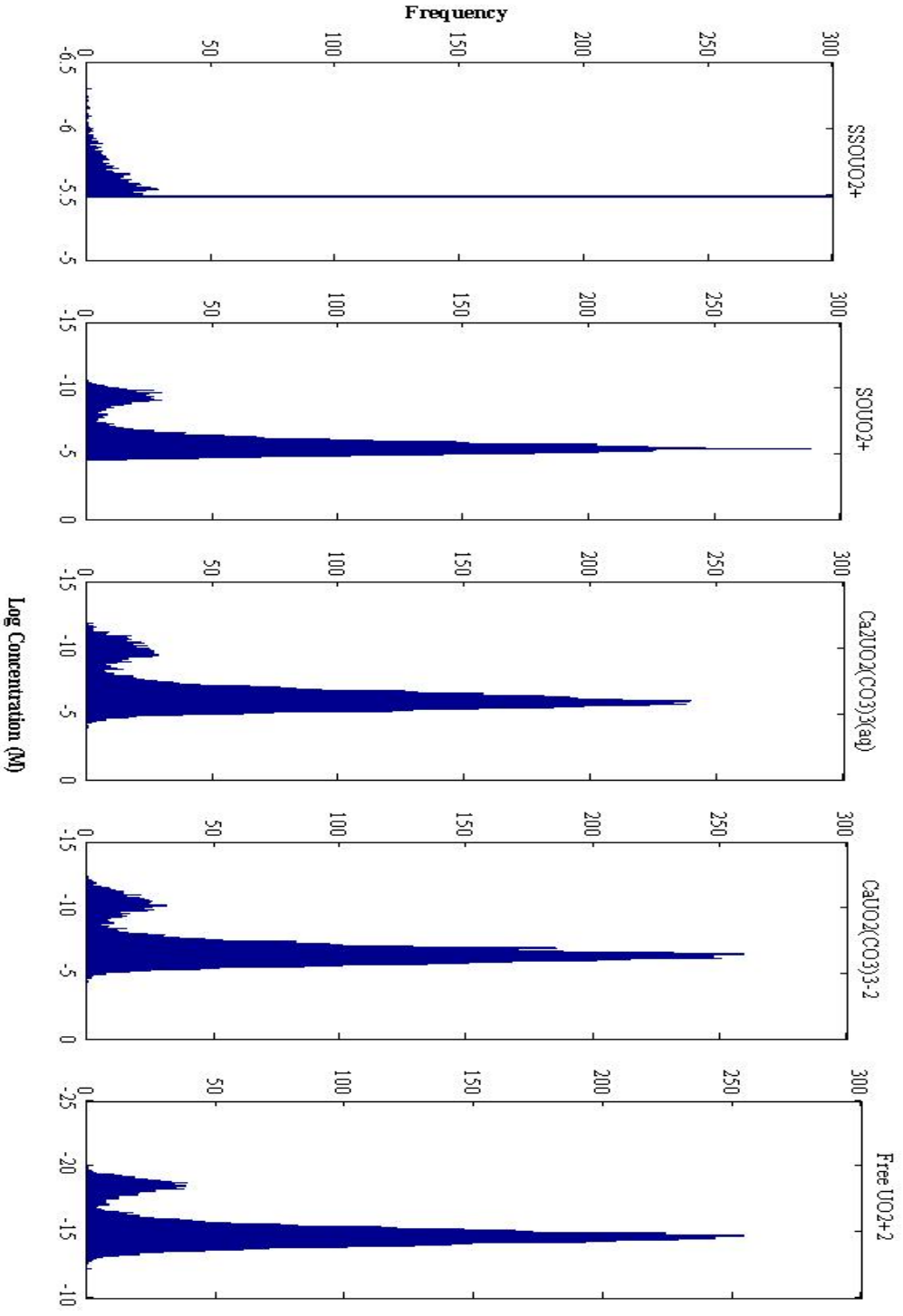
Spatial Error with surface reactions
Frequency
Log Concentration (M)
SSOUO2+
SOUO2+
Ca2UO2(CO3)3(aq)
CaUO2(CO3)3-2
Free UO2+2

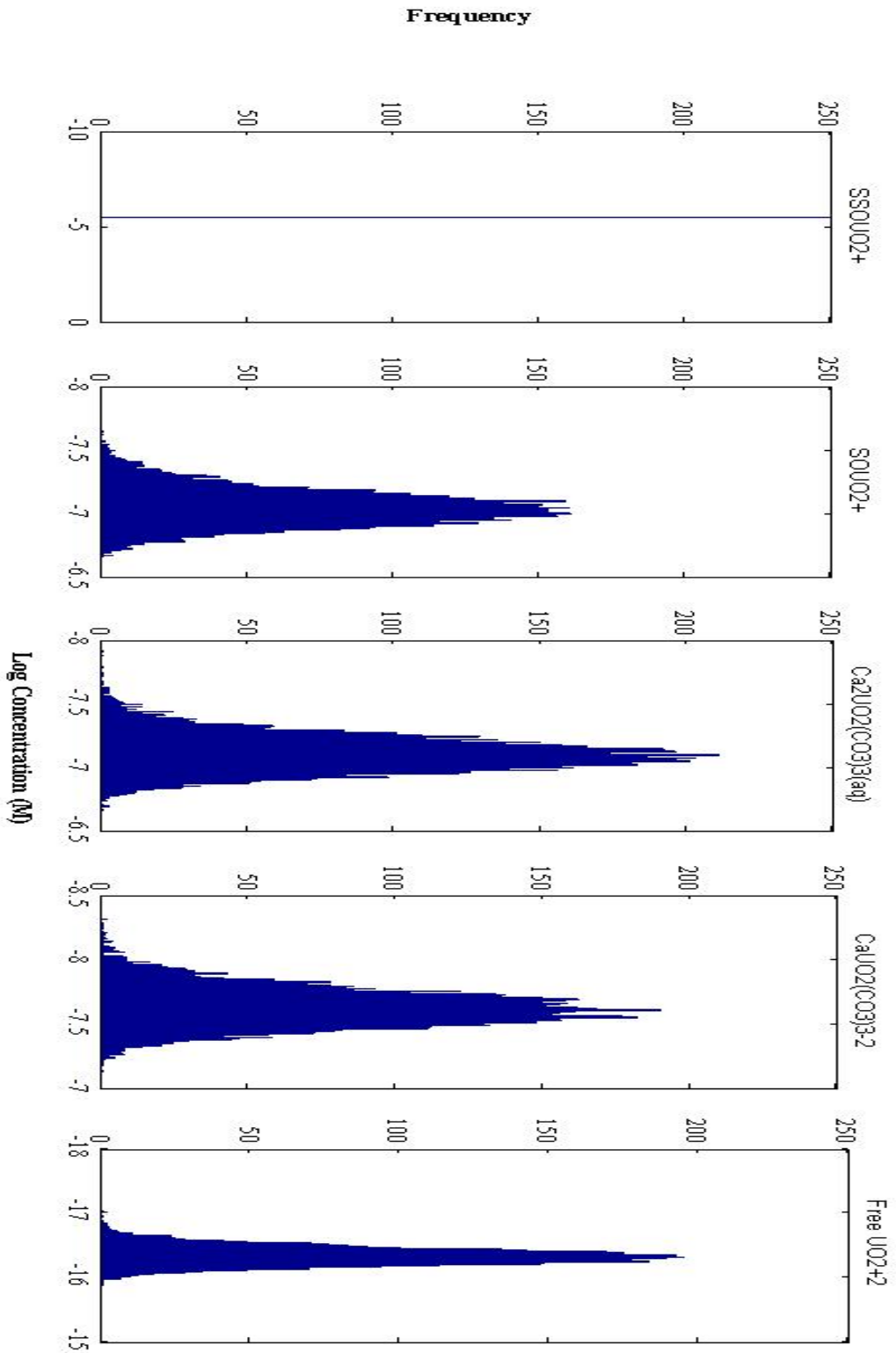
Analytical Error with surface reactions and low concentration of uranium
Frequency
SSOUO2+
SOUO2+
Ca2UO2(CO3)3(aq)
CaUO2(CO3)3-2
Free UO2+2
Log Concentration (M)

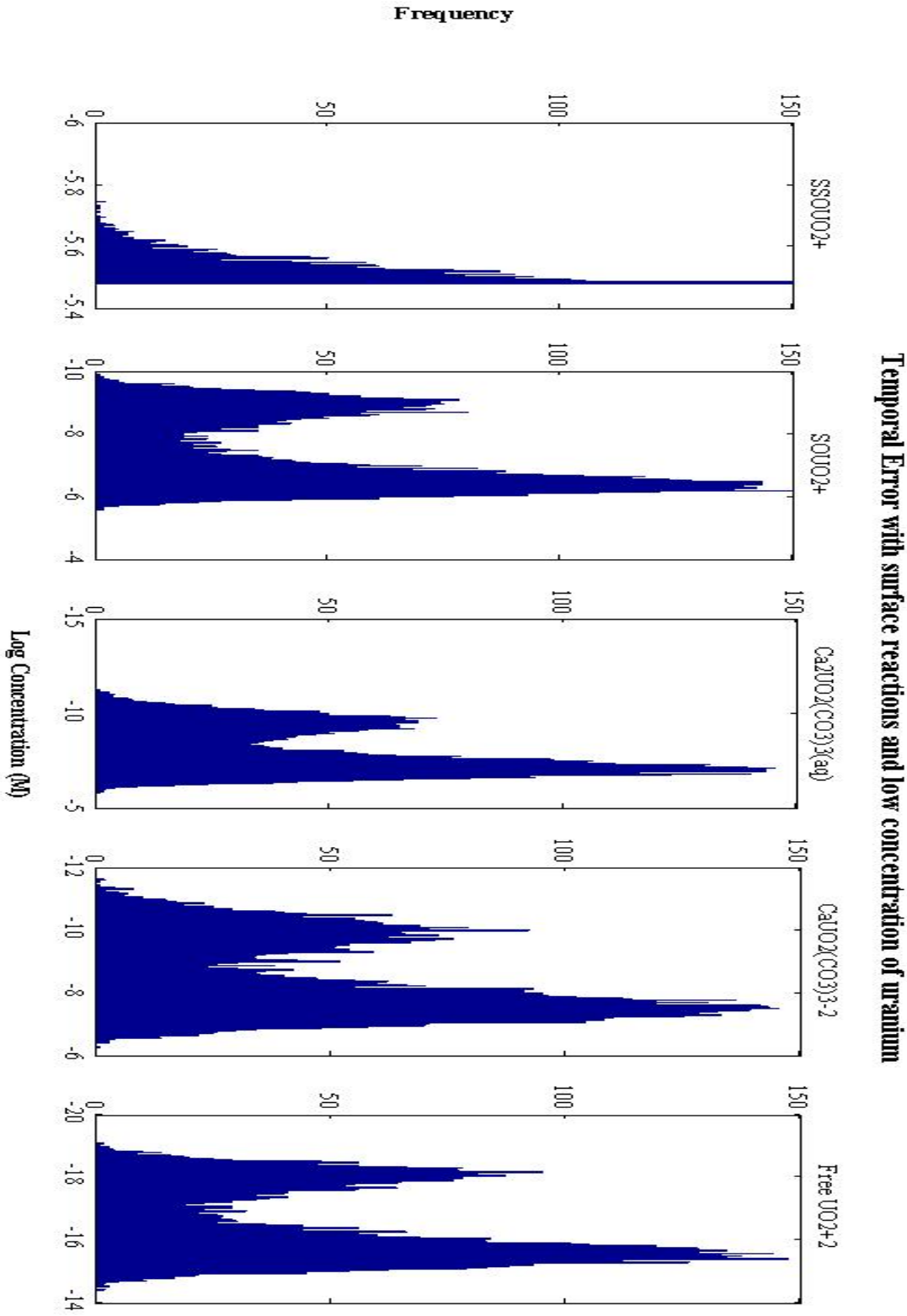
Temporal Error with surface reactions and low concentration of uranium
Frequency
Log Concentration (M)
SSOUO2+
SOUO2+
Ca2UO2(CO3)3(aq)
CaUO2(CO3)3-2
Free UO2+2

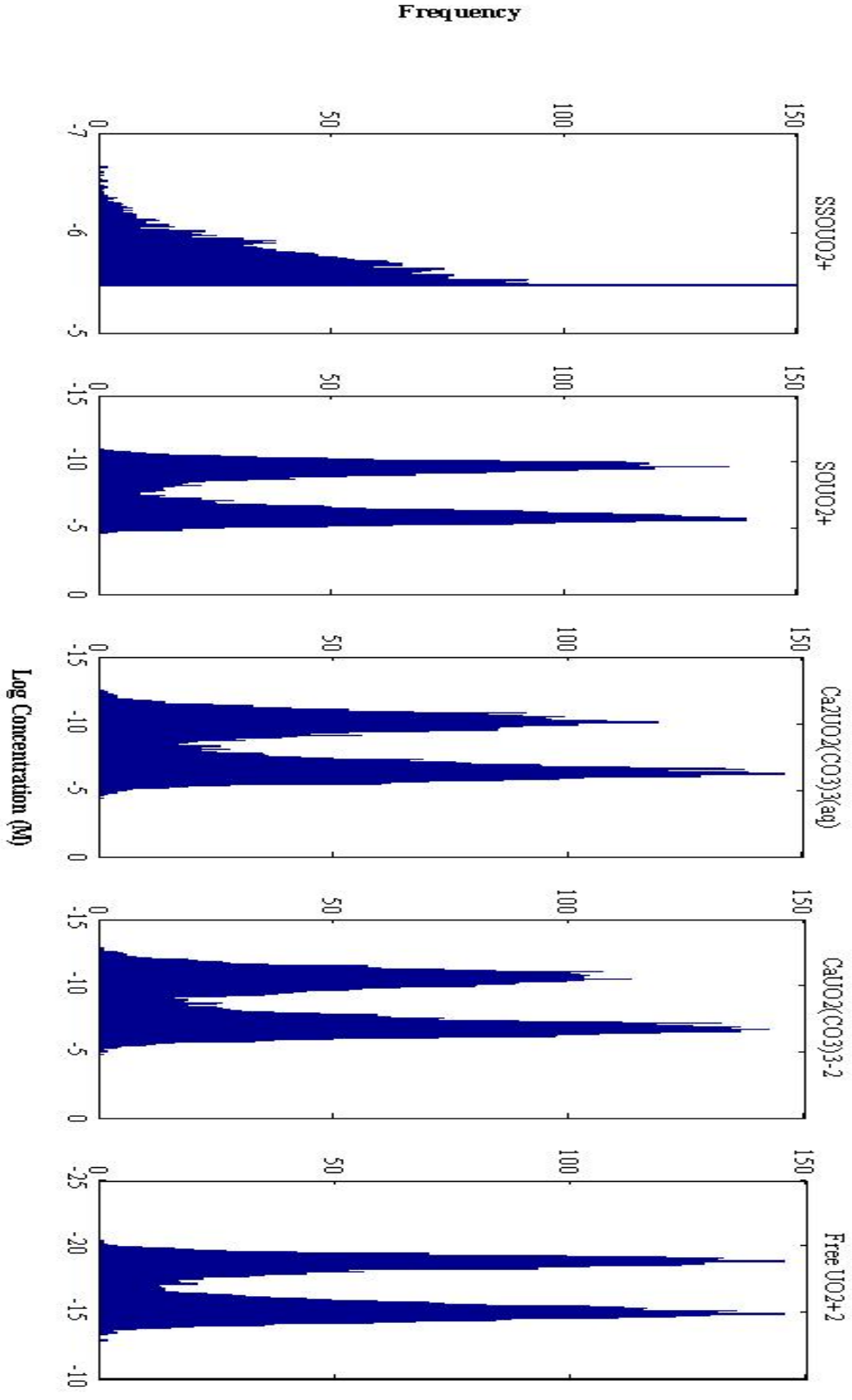
Spatial Error with surface reactions and low concentration of uranium
Frequency
Log Concentration (M)
SSOUO2+
SOUO2+
Ca2UO2(CO3)3(aq)
CaUO2(CO3)3-2
Free UO2+2

Appendix B

Supporting data for Chapter 4

Biosorption:

Removal of U(VI) in the absence of acetate

Lucie N'Guessan and Derek Lovley

University of Massachusetts, Amherst

The Role of Biosorption in the Continued Removal of Uranium from Groundwater in the Absence of Acetate

Selected Organisms

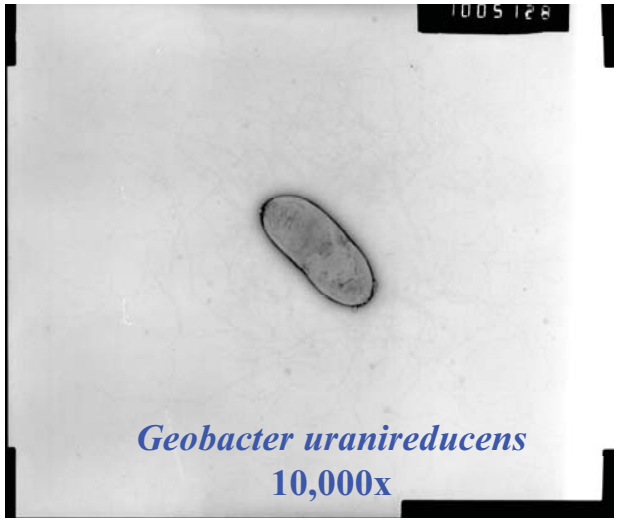

- *Geobacteraceae*
- Dissimilatory metal reducing bacteria
- Iron reduction
- Uranium reduction
- Predominant in the first phase of biostimulation

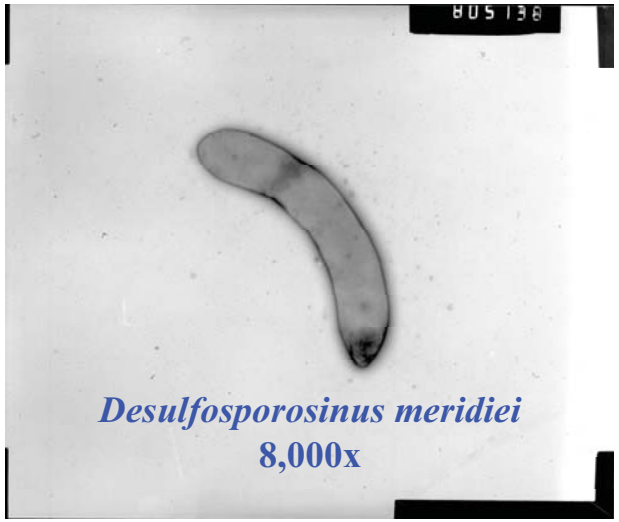

- *Firmicutes: Clostridia*
- Sulfate reduction
- Uranium reduction
- Predominant in the second phase of biostimulation

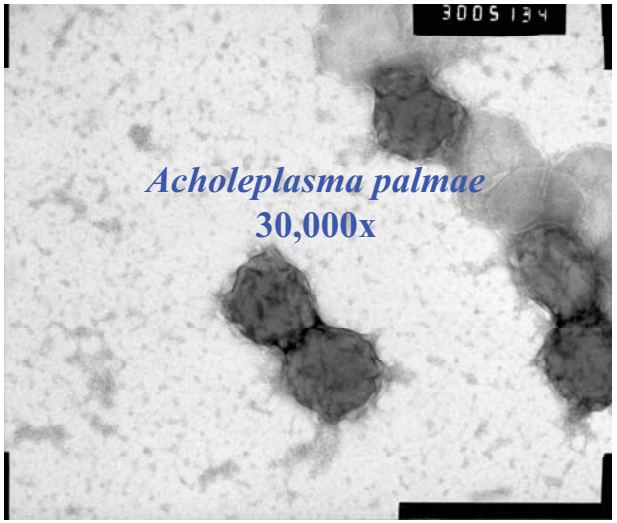

- *Firmicutes: Mollicutes*
- Uranium removal?
- Predominant in the third phase of biostimulation

Biosorption: *G. uranireducens*

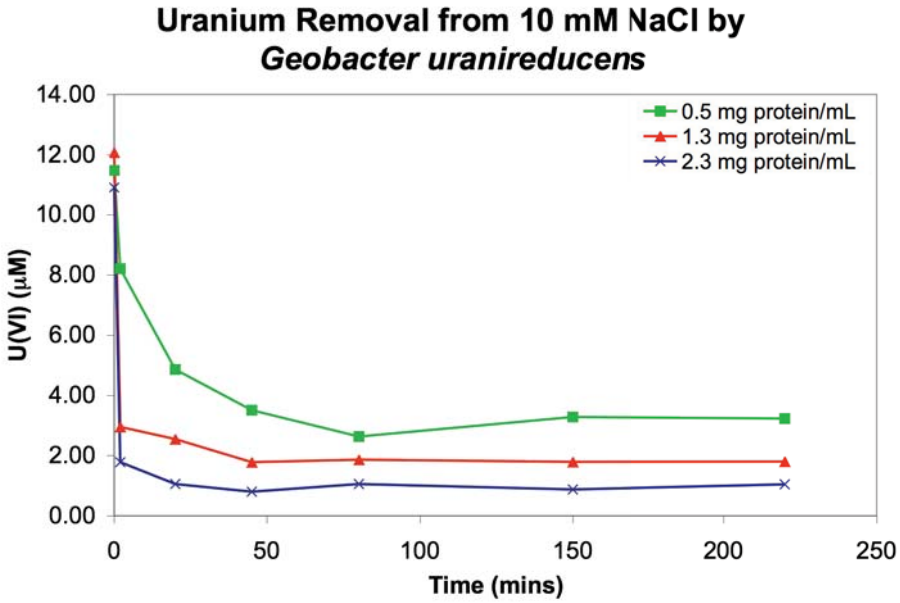

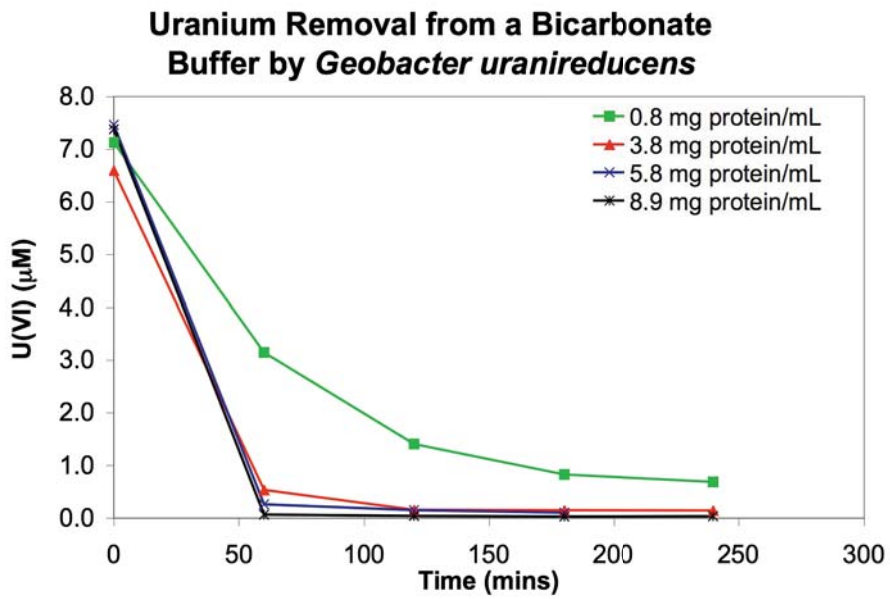

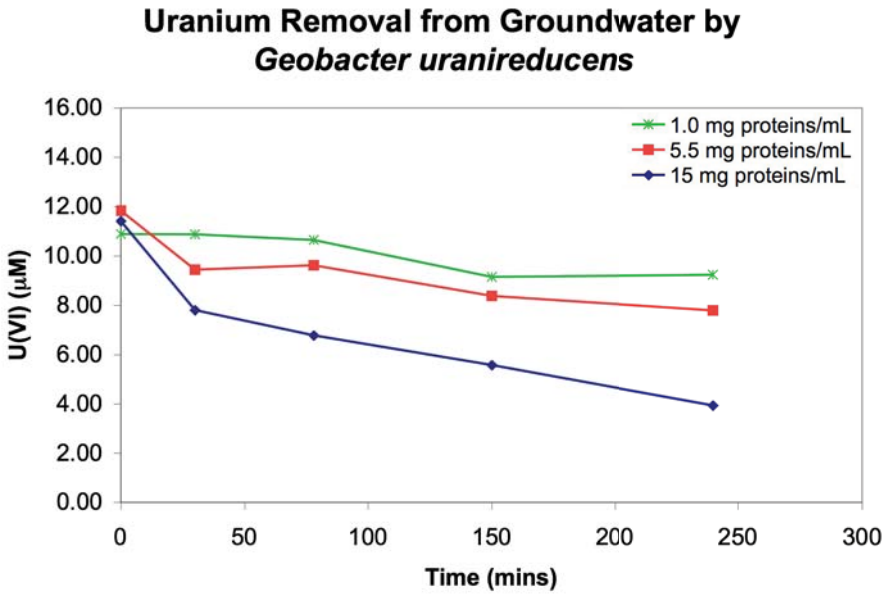

Biosorption: *D. meridiei*

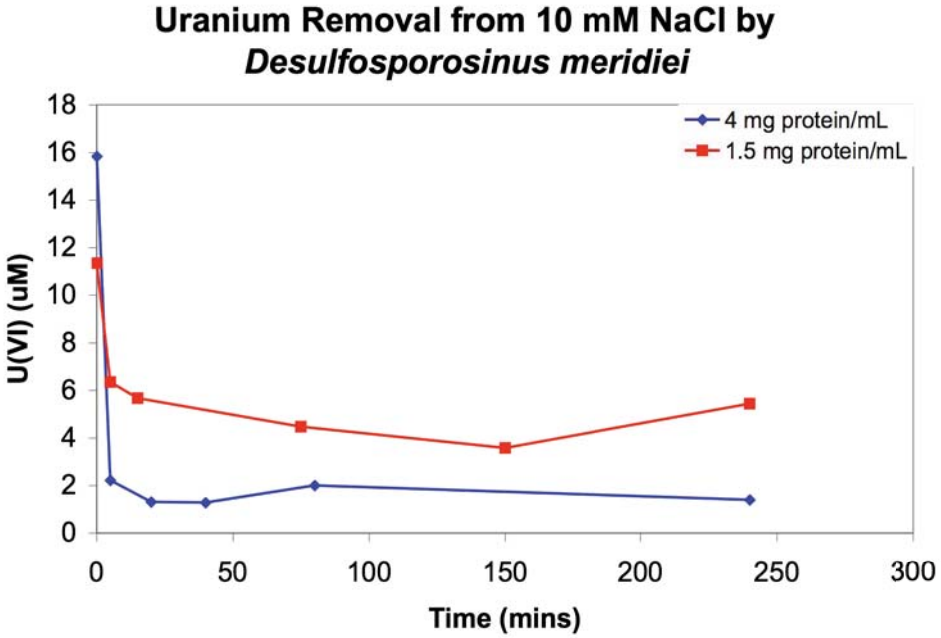

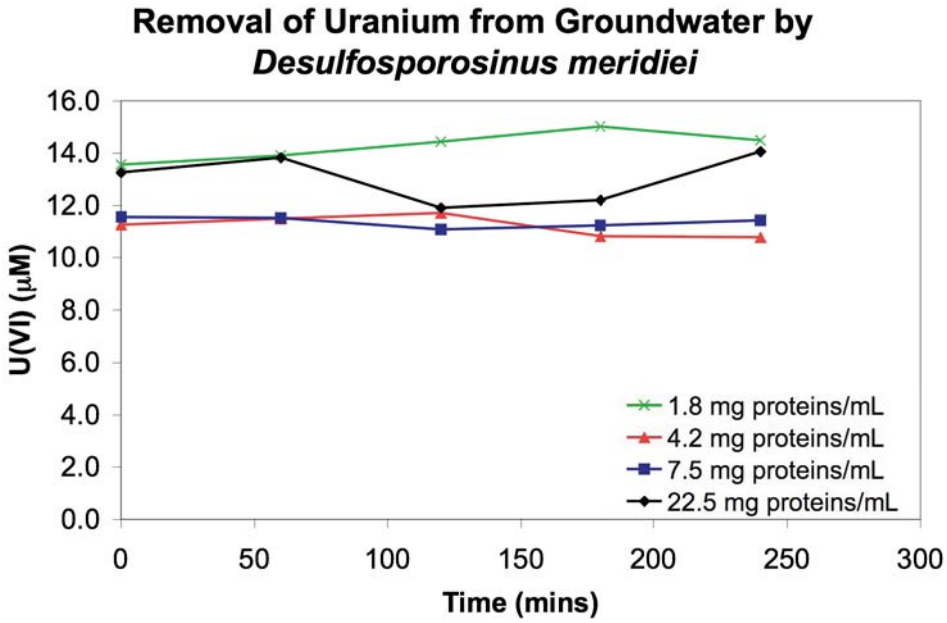

Biosorption: *A. palmae*

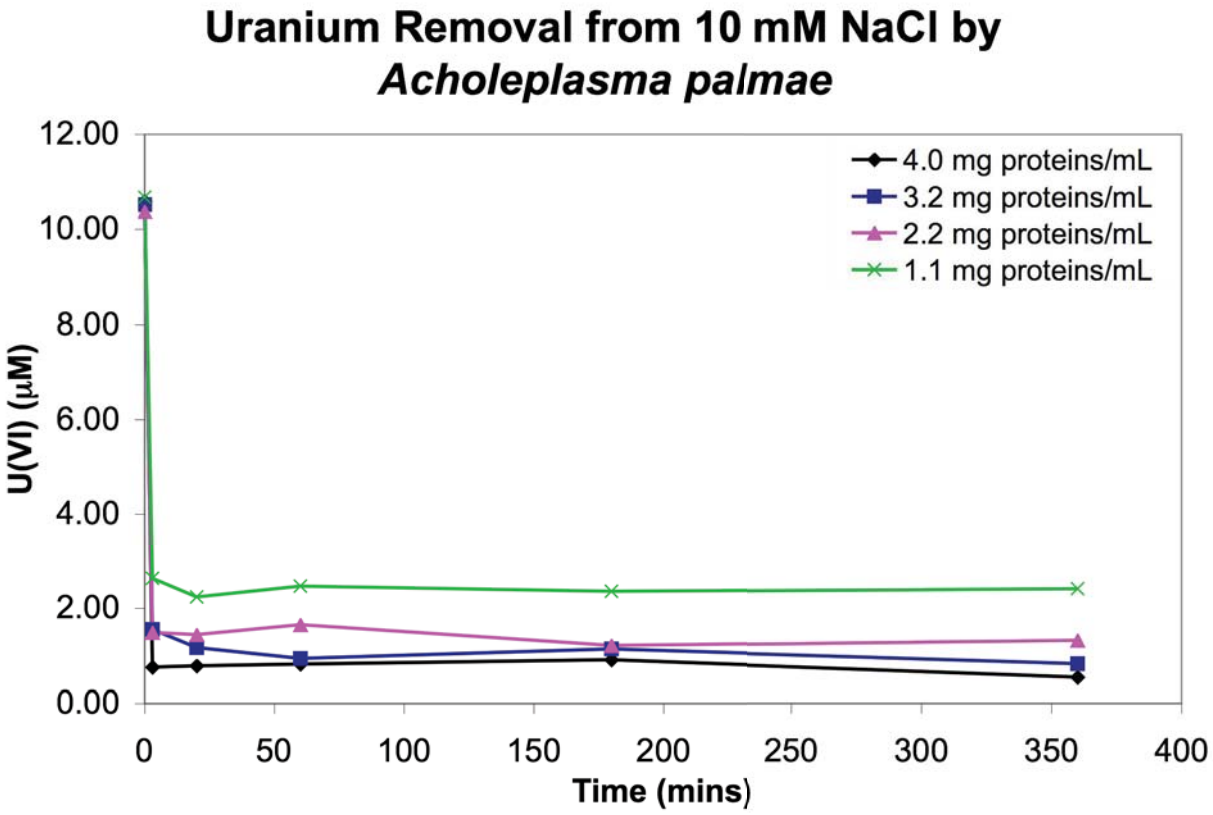

Uranium-Biosorption Isotherm for *G. uranireducens*, *D. meridiei*, and *A. palmae*

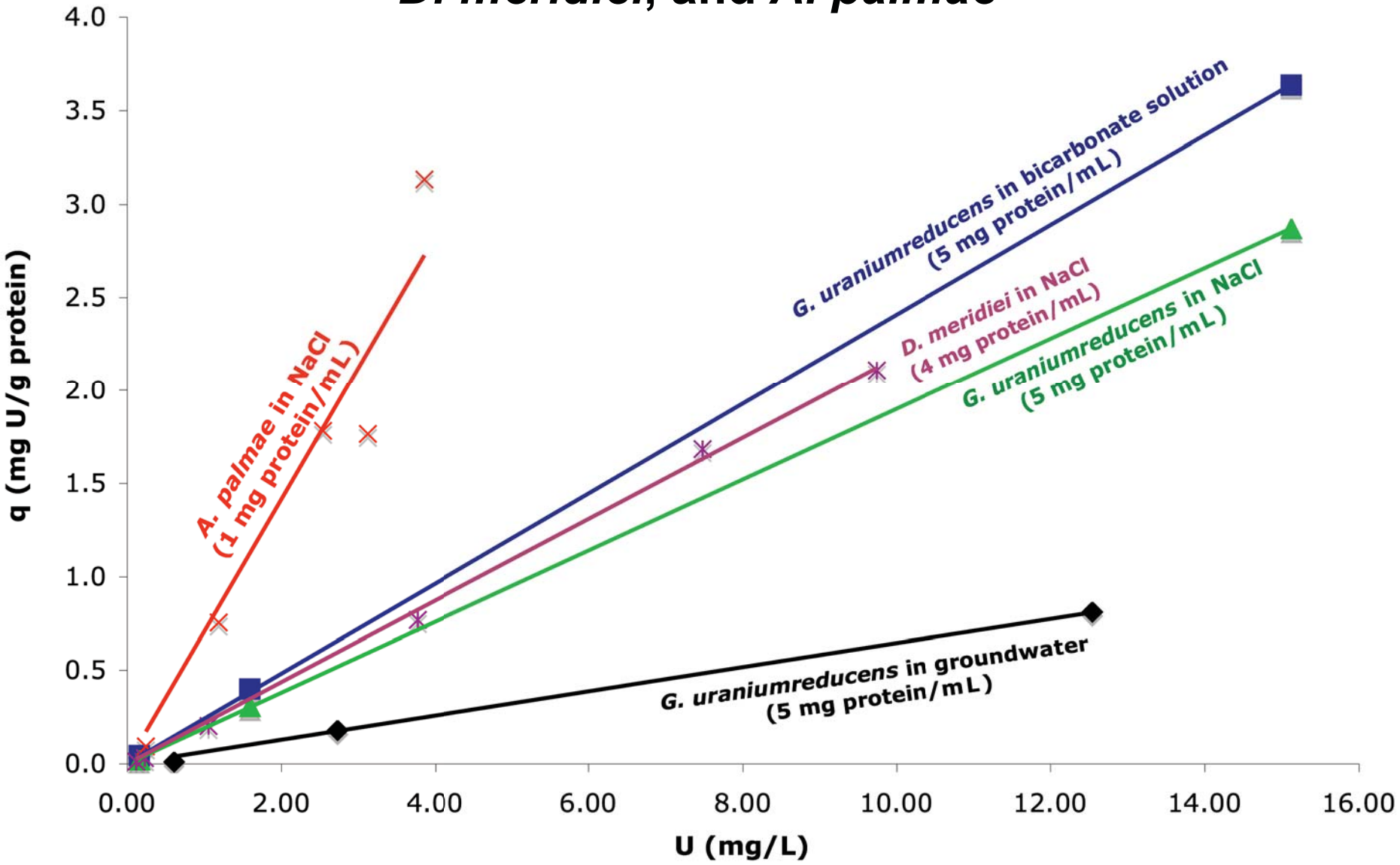

Work In-Progress and Future Work

- Biosorption experiments
  - *D. meridiei, A. palmae sorption isotherms*
  - Elucidation of uranium sorption mechanisms
  - Competitive sorption
  - Influence of environmental conditions on sorption capacities

- Specific experiments
  - Uranium sorption by *Geobacter sp.*
  - Reduction of sorbed uranium by *Geobacter* sp.
  - Uranium sorption capacity of *Geobacter* sp. upon loss of extracellular proteins and/or exopolysaccharide

large CO2	Min	Sec	Min	Vol (ml)	Flow rate (ml/min)
10	21	32.12	21.53533	1580	73.36779866
10	21	32.59	21.54317	1580	73.34112131
10	23	11.69	23.19483	1600	68.98087936
30	9	5.34	9.089	1580	173.8365057
30	9	1.5	9.025	1580	175.0692521
30	8	57.34	8.955667	1580	176.4246101
60	4	52.2	4.87	1580	324.4353183
60	4	42.72	4.712	1580	335.3140917
60	4	39.29	4.654833	1580	339.4321315

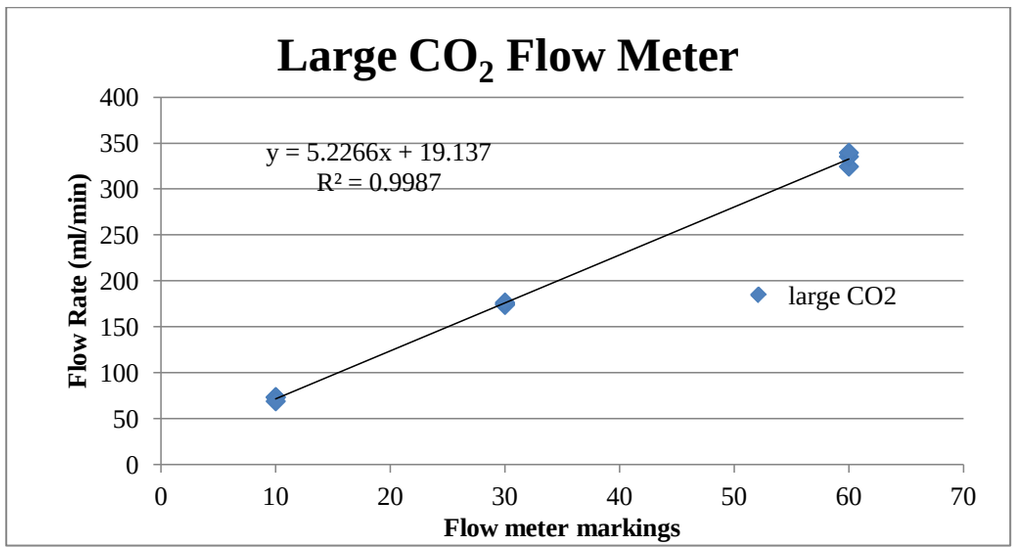

N2	Min	Sec	Min		
10	3	10.93	3.182167	1580	496.5170481
10	3	25.16	3.419333	1580	462.0783779
10	3	31.68	3.528	1580	447.845805
30	0	49.87	0.831167	1600	1925.005013
30	0	49.22	0.820333	1600	1950.426656
30	0	49.22	0.820333	1600	1950.426656
60	0	23.68	0.394667	1600	4054.054054
60	0	23.5	0.391667	1600	4085.106383
60	0	23.31	0.3885	1600	4118.404118
90	0	16.03	0.267167	1630	6101.060512
90	0	15.32	0.255333	1600	6266.318538

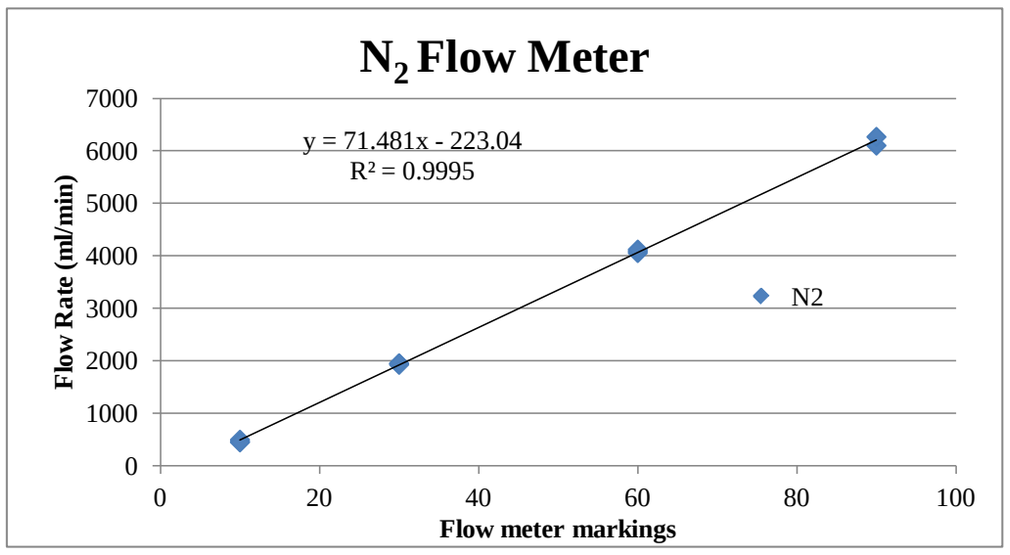

Small CO2	Min	Sec	Min		
4	9	34.66	9.577667	14	1.461733895
4	10	6	10.1	14	1.386138614
4	10	21.34	10.35567	14	1.351916825
30	4	15.69	4.2615	14	3.285228206
30	4	12.12	4.202	14	3.331746787
57	2	21.16	2.352667	14	5.950694248
57	2	26.12	2.435333	14	5.748699699
57	2	23	2.383333	14	5.874125874

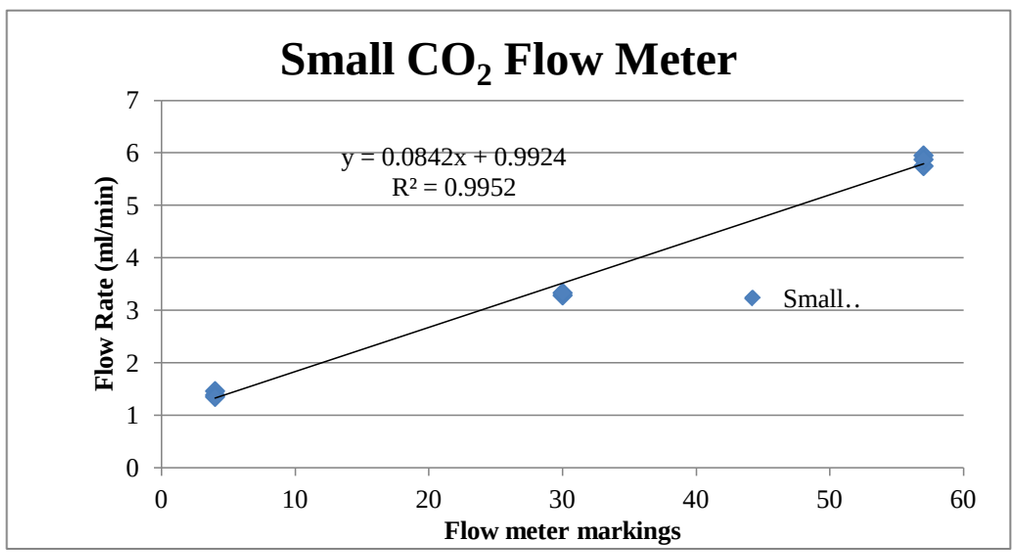

G. uraniireducens at 2% P_{CO2}

bacteria Concentration (mg/ml)	Uptake (%)	uptake (mg/l)	Wt adsorbed/wt bacteria (mg/g)	Ce(mg/L)	Wt adsorbed/wt bacteria (umoles U/kg)	Ce (umol/l)
35	59%	0.180	0.005082	0.125	21.354	0.526
39	48%	0.148	0.003746	0.160	15.738	0.674
38	56%	0.177	0.004707	0.141	19.777	0.593
25	36%	0.140	0.006	0.246	23.173	1.034
25	43%	0.171	0.007	0.223	28.985	0.937
25	42%	0.164	0.007	0.229	27.799	0.962
200	99%	0.366	0.002	0.001	7.689	0.004
200	99%	0.320	0.002	0.001	6.723	0.004
200	85%	0.346	0.002	0.06	7.269	0.252
5	11%	0.044	0.009	0.353	36.975	1.483
5	11%	0.048	0.010	0.382	40.336	1.605
14	27%	0.042	0.003	0.116274246	12.741	0.489
14	9%	0.014	0.001	0.148589045	4.339	0.624
14	9%	0.015	0.001	0.146463066	4.362	0.615
15	25%	0.065	0.004	0.194172414	18.103	0.816
15	21%	0.051	0.003	0.195968309	14.393	0.823
15	32%	0.112	0.007	0.243678919	31.458	1.024
15	19%	0.068	0.005	0.290499688	19.023	1.221
15	37%	0.136	0.009	0.233242224	38.036	0.980

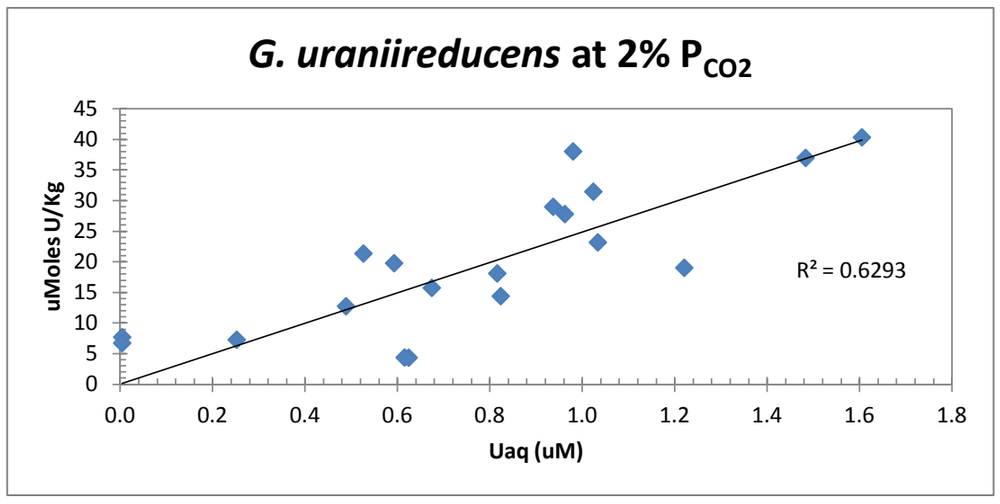

Regression Statistics	
Multiple R	0.95418173
R Square	0.910462774
Adjusted R Square	0.854907219
Standard Error	7.027882372
Observations	19

ANOVA

	df	*SS*	*MS*	*F*	*Significance F*
Regression	1	9040.241493	9040.241493	183.0337022	1.57383E-10
Residual	18	889.0403514	49.39113063		
Total	19	9929.281845			

	Coefficients	*Standard Error*	*t Stat*	*P-value*	*Lower 95%*	*Upper 95%*
Intercept	0	#N/A	#N/A	#N/A	#N/A	#N/A
X Variable 1	24.84631054	1.836523022	13.52899487	7.15425E-11	20.98791885	28.70470223

RESIDUAL OUTPUT

Observation	*Predicted Y*	*Residuals*
1	13.07789422	8.275886558
2	16.75165793	-1.013349318
3	14.72622467	5.050736089
4	25.68148064	-2.508926216
5	23.2803666	5.704813104
6	23.90674418	3.89257525
7	0.104396263	7.584679367
8	0.104396263	6.618292813
9	6.263775766	1.005131797
10	36.85188076	0.122909157
11	39.87937238	0.456762074
12	12.13859674	0.601942636
13	15.51214099	-11.1735132
14	15.29019675	-10.92798366
15	20.27087431	-2.167529104
16	20.45835906	-6.065392114
17	25.43916846	6.018431259
18	30.32708171	-11.30444586
19	24.34961645	13.68680287

PROBABILITY OUTPUT

Percentile	*Y*
2.631578947	4.338627791
7.894736842	4.362213085
13.15789474	6.722689076
18.42105263	7.268907563
23.68421053	7.68907563
28.94736842	12.74053938
34.21052632	14.39296695
39.47368421	15.73830861
44.73684211	18.10334521
50	19.02263585
55.26315789	19.77696075
60.52631579	21.35378078
65.78947368	23.17255443
71.05263158	27.79931943
76.31578947	28.9851797
81.57894737	31.45759972
86.84210526	36.97478992
92.10526316	38.03641933
97.36842105	40.33613445

G. uraniireducens at atmospheric P_{CO2}

bacteria Concentration (mg/ml)	uptake	Adsorbed (mg/L)	Wt adsorbed/wt bacteria (mg/g)	Ce(mg/L)	Wt adsorbed/wt bacteria (umoles U/kg)	Ce (umol/l)
36.510	98%	0.303	0.008	0.003	34.813	0.015
8.000	92%	0.241	0.030	0.021	126.576	0.088
8.000	91%	0.223	0.028	0.021	117.122	0.088
8.000	93%	0.248	0.031	0.018	130.252	0.076
15.000	99%	15.925	1.062	0.085	4460.784	0.357
15.000	100%	14.446	0.963	0.064	4046.499	0.269
15.000	100%	15.219	1.015	0.071	4263.025	0.298
15.000	99%	4.614	0.308	0.039	1292.437	0.164
15.000	99%	4.723	0.315	0.033	1322.969	0.139
15.000	99%	4.673	0.312	0.032	1308.824	0.134
11.500	98%	3.070	0.267	0.066	1121.829	0.277
11.500	99%	3.141	0.273	0.042	1147.726	0.177
11.500	98%	3.523	0.306	0.058	1287.358	0.246
14.000	100%	2.743	0.196	0.060	823.280	0.251
14.000	99%	2.502	0.179	0.055	750.993	0.232
14.000	99%	2.380	0.170	0.055	714.412	0.232
14.000	99%	5.184	0.370	0.053	1555.786	0.221
14.000	98%	5.185	0.370	0.058	1556.102	0.245
14.000	99%	5.415	0.387	0.059	1625.070	0.248

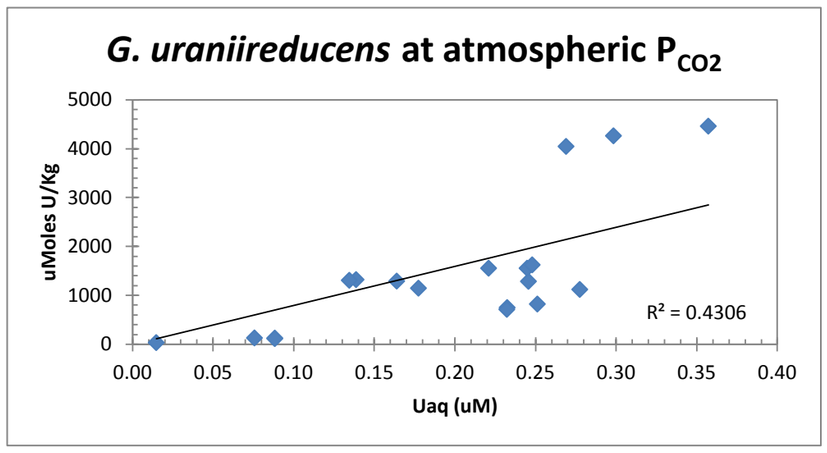

SUMMARY OUTPUT

Regression Statistics	
Multiple R	0.878291427
R Square	0.771395832
Adjusted R Square	0.715840276
Standard Error	963.5001286
Observations	19

ANOVA

	df	*SS*	*MS*	*F*	*Significance F*
Regression	1	56385729.24	56385729.24	60.738722	5.20135E-07
Residual	18	16709984.96	928332.4978		
Total	19	73095714.2			

	Coefficients	*Standard Error*	*t Stat*	*P-value*	*Lower 95%*	*Upper 95%*
Intercept	0	#N/A	#N/A	#N/A	#N/A	#N/A
X Variable 1	7985.044175	1024.576757	7.793505098	3.549E-07	5832.488289	10137.6

RESIDUAL OUTPUT

Observation	*Predicted Y*	*Residuals*
1	117.2739979	-82.46086233
2	704.5627213	-577.9870911
3	704.5627213	-587.4408726
4	603.910904	-473.6588032
5	2851.801491	1608.982823
6	2147.23877	1899.25983
7	2382.09301	1880.9322
8	1308.473625	-16.03665055
9	1107.169991	215.799197
10	1073.619385	235.2041445
11	2215.145196	-1093.316186
12	1416.154966	-268.4290175
13	1960.979227	-673.6210682
14	2005.0664	-1181.786553
15	1855.52464	-1104.531952
16	1853.923857	-1139.512317
17	1763.65201	-207.8663796
18	1954.240923	-398.1388643
19	1979.511239	-354.4407772
20	2088.192512	-48.27913949
21	3250.87527	-1340.021505

PROBABILITY OUTPUT

Percentile	*Y*
2.6315789	34.81313557
7.8947368	117.1218487
13.157895	126.5756303
18.421053	130.2521008
23.684211	714.4115396
28.947368	750.9926883
34.210526	823.2798469
39.473684	1121.82901
44.736842	1147.725948
50	1287.358159
55.263158	1292.436975
60.526316	1308.823529
65.789474	1322.969188
71.052632	1555.78563
76.315789	1556.102059
81.578947	1625.070462
86.842105	4046.498599
92.105263	4263.02521
97.368421	4460.784314

G. uraniireducens at atmospheric P_{CO2}

bacteria Concentration (mg/ml)	uptake	Adsorbed (mg/L)	Wt adsorbed/wt bacteria (mg/g)	Ce(mg/L)	Wt adsorbed/wt bacteria (umoles U/kg)	Ce (umol/l)
36.510	98%	0.303	0.008	0.003	34.813	0.015
8.000	92%	0.241	0.030	0.021	126.576	0.088
8.000	91%	0.223	0.028	0.021	117.122	0.088
8.000	93%	0.248	0.031	0.018	130.252	0.076
15.000	99%	15.925	1.062	0.085		
15.000	100%	14.446	0.963	0.064		
15.000	100%	15.219	1.015	0.071		
15.000	99%	4.614	0.308	0.039	1292.437	0.164
15.000	99%	4.723	0.315	0.033	1322.969	0.139
15.000	99%	4.673	0.312	0.032	1308.824	0.134
11.500	98%	3.070	0.267	0.066	1121.829	0.277
11.500	99%	3.141	0.273	0.042	1147.726	0.177
11.500	98%	3.523	0.306	0.058	1287.358	0.246
14.000	100%	2.743	0.196	0.060	823.280	0.251
14.000	99%	2.502	0.179	0.055	750.993	0.232
14.000	99%	2.380	0.170	0.055	714.412	0.232
14.000	99%	5.184	0.370	0.053	1555.786	0.221
14.000	98%	5.185	0.370	0.058	1556.102	0.245
14.000	99%	5.415	0.387	0.059	1625.070	0.248

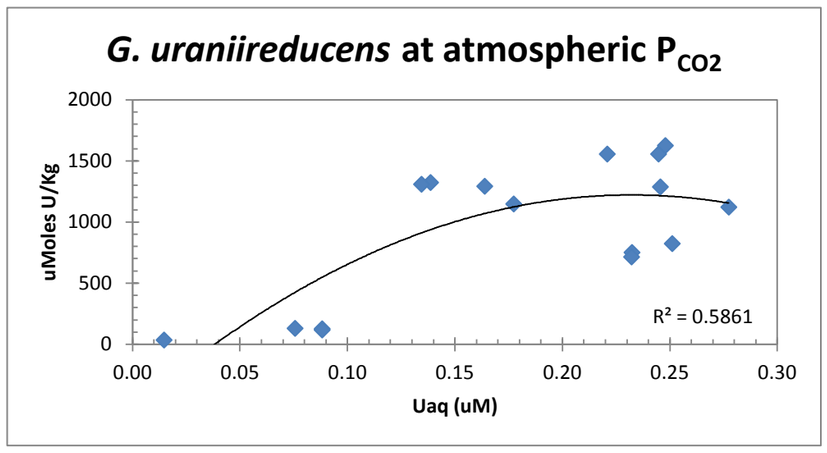

SUMMARY OUTPUT

Regression Statistics	
Multiple R	0.878291427
R Square	0.771395832
Adjusted R Square	0.715840276
Standard Error	963.5001286
Observations	19

ANOVA

	df	*SS*	*MS*	*F*	*Significance F*
Regression	1	56385729.24	56385729.24	60.738722	5.20135E-07
Residual	18	16709984.96	928332.4978		
Total	19	73095714.2			

	Coefficients	*Standard Error*	*t Stat*	*P-value*	*Lower 95%*	*Upper 95%*
Intercept	0	#N/A	#N/A	#N/A	#N/A	#N/A
X Variable 1	7985.044175	1024.576757	7.793505098	3.549E-07	5832.488289	10137.6

RESIDUAL OUTPUT

Observation	*Predicted Y*	*Residuals*
1	117.2739979	-82.46086233
2	704.5627213	-577.9870911
3	704.5627213	-587.4408726
4	603.910904	-473.6588032
5	2851.801491	1608.982823
6	2147.23877	1899.25983
7	2382.09301	1880.9322
8	1308.473625	-16.03665055
9	1107.169991	215.799197
10	1073.619385	235.2041445
11	2215.145196	-1093.316186
12	1416.154966	-268.4290175
13	1960.979227	-673.6210682
14	2005.0664	-1181.786553
15	1855.52464	-1104.531952
16	1853.923857	-1139.512317
17	1763.65201	-207.8663796
18	1954.240923	-398.1388643
19	1979.511239	-354.4407772
20	2088.192512	-48.27913949
21	3250.87527	-1340.021505

PROBABILITY OUTPUT

Percentile	*Y*
2.6315789	34.81313557
7.8947368	117.1218487
13.157895	126.5756303
18.421053	130.2521008
23.684211	714.4115396
28.947368	750.9926883
34.210526	823.2798469
39.473684	1121.82901
44.736842	1147.725948
50	1287.358159
55.263158	1292.436975
60.526316	1308.823529
65.789474	1322.969188
71.052632	1555.78563
76.315789	1556.102059
81.578947	1625.070462
86.842105	4046.498599
92.105263	4263.02521
97.368421	4460.784314

A. palmae at atmospheric P_{CO2}

Target U (uM)	Measured U (uM)	Loss to container sorption	bacteria Concentration (mg/ml)	Adsorbed (mg/L)	Wt adsorbed/wt bacteria (mg/g)	Ce(mg/L)	Wt adsorbed/wt bacteria umoles (U/kg)	Ce (umol/l)
1.4	0.770	45%	8.5	0.178	0.021	0.005	87.964	0.023
1.4	0.754	46%	8.5	0.175	0.021	0.004	86.582	0.018
1.4	0.762	46%	8.5	0.174	0.021	0.007	86.215	0.029
75	51.173	32%	8.5	11.617	1.367	0.563	5742.224	2.364
75	55.543	26%	8.5	12.278	1.444	0.942	6069.026	3.956
75	52.089	31%	8.5	11.619	1.367	0.778	5743.547	3.269
14	5.016	64%	8.5	1.152	0.136	0.042	569.494	0.175
14	5.273	62%	8.5	1.182	0.139	0.073	584.349	0.306
14	4.763	66%	8.5	1.065	0.125	0.069	526.256	0.289
45	21.486	52%	8.5	4.889	0.575	0.225	2416.719	0.943
45	21.072	53%	8.5	4.796	0.564	0.219	2370.789	0.921
45	22.192	51%	8.5	5.079	0.598	0.203	2510.551	0.852
45	13.178	71%	8.5	3.071	0.361	0.066	1517.830	0.277
45	13.376	70%	8.5	3.164	0.372	0.019	1564.111	0.081
45	15.050	67%	8.5	3.549	0.418	0.032	1754.557	0.136

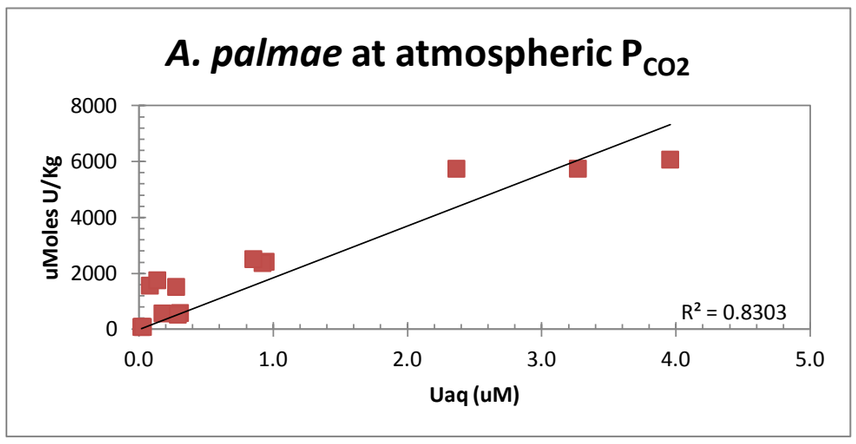

SUMMARY OUTPUT

Regression Statistics	
Multiple R	0.95803042
R Square	0.91782229
Adjusted R Square	0.84639372
Standard Error	871.366311
Observations	15

ANOVA

	df	*SS*	*MS*	*F*	*Significance F*
Regression	1	118722802	118722802	156.362501	1.27323E-08
Residual	14	10629909.47	759279.2475		
Total	15	129352711.4			

	Coefficients	*Standard Error*	*t Stat*	*P-value*	*Lower 95%*	*Upper 95%*
Intercept	0	#N/A	#N/A	#N/A	#N/A	#N/A
X Variable 1	1849.55744	147.9113563	12.50449922	5.5033E-09	1532.319133	2166.795747

RESIDUAL OUTPUT

Observation	*Predicted Y*	*Residuals*
1	41.9542264	46.00986458
2	33.7373576	52.84511322
3	54.4797752	31.73544764
4	4373.10488	1369.119144
5	7317.7336	-1248.707353
6	6046.16714	-302.6199038
7	324.015886	245.4785482
8	565.097305	19.25200768
9	535.443615	-9.187885895
10	1745.052	671.6670262
11	1702.92126	667.8681494
12	1575.68694	934.8641997
13	512.126602	1005.703275
14	150.289753	1413.821092
15	252.40584	1502.150878

PROBABILITY OUTPUT

Percentile	*Y*
3.33333333	86.21522281
10	86.58247084
16.6666667	87.96409095
23.3333333	526.2557291
30	569.494434
36.6666667	584.3493129
43.3333333	1517.829876
50	1564.110845
56.6666667	1754.556718
63.3333333	2370.789412
70	2416.719031
76.6666667	2510.551142
83.3333333	5742.224024
90	5743.547232
96.6666667	6069.026248

A. palmae at 2% P_{CO2}

Sample	bacteria Concentration (mg/ml)	Adsorbed (mg/L)	Wt adsorbed/wt bacteria (mg/g)	Ce(mg/L)	K(l/g)	K (L/Kg)	Date
1	25	0.107	0.004	0.282	0.015	15.18	10/4/2010
2	30	0.072	0.002	0.306	0.008	7.83	2/28/2011

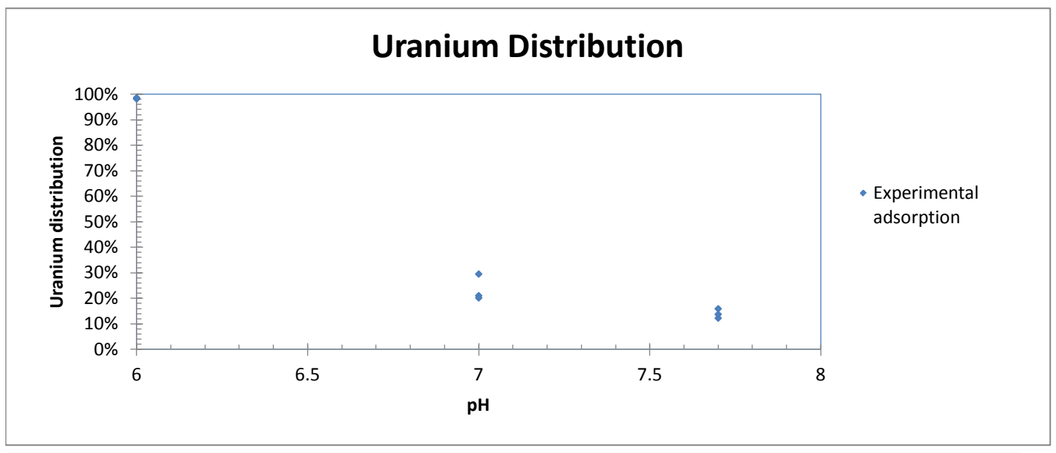

pH	Initial U (mg/L)	final U (mg/L)	% U sorbed
5	0.169	0.007	96%
5	0.180	0.006	97%
5	0.180	0.006	97%
6	0.274	0.005	98%
6	0.242	0.004	98%
6	0.287	0.004	99%
7.7	0.377	0.317	16%
7.7	0.376	0.330	12%
7.7	0.386	0.333	14%
7	0.361	0.254	30%
7	0.358	0.283	21%
7	0.361	0.288	20%

20 mg/ml bacterial concentration of pH tests

Summary uranium distribution

pH	VisualMINTEQ results Ca	Visual Minteq Results Non-Ca-UO2-CO3	Experimental U-bacteria (average)
6	36.10%	58.87%	98.38%
7	99.42%	0.58%	23.58%
7.5	88.55%	11.45%	13.96%

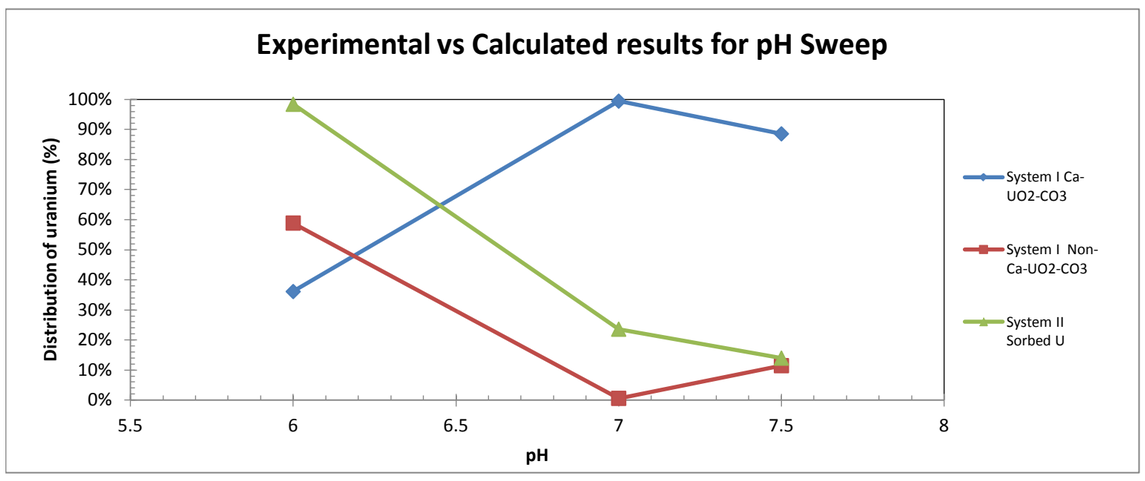

Species	Uranium distribution at different pH values simulated from VisualMINTEQ				
	pH 6	pH 6.5	pH 7	pH 7.5	pH 8
(UO2)2(OH)2+2	0.02%	0.00%	0.00%	0.00%	0%
(UO2)2CO3(OH)3-	8.56%	0.02%	0.00%	0.00%	0%
(UO2)2OH+3	0.00%	0.00%	0.00%	0.00%	0%
(UO2)3(CO3)6-6	0.00%	0.00%	0.00%	0.00%	0%
(UO2)3(OH)4+2	0.00%	0.00%	0.00%	0.00%	0%
(UO2)3(OH)5+	0.01%	0.00%	0.00%	0.00%	0%
(UO2)3(OH)7-	0.00%	0.00%	0.00%	0.00%	0%
(UO2)4(OH)7+	0.00%	0.00%	0.00%	0.00%	0%
Ca+2	0.00%	0.00%	0.00%	0.00%	0%
Ca2UO2(CO3)3 (aq)	28.51%	76.27%	77.90%	24.07%	1%
CaCl+	0.00%	0.00%	0.00%	0.00%	0%
CaCO3 (aq)	0.00%	0.00%	0.00%	0.00%	0%
CaHCO3+	0.00%	0.00%	0.00%	0.00%	0%
CaOH+	0.00%	0.00%	0.00%	0.00%	0%
CaSO4 (aq)	0.00%	0.00%	0.00%	0.00%	0%
CaUO2(CO3)3-2	7.58%	20.47%	21.52%	64.48%	31%
Cl-1	0.00%	0.00%	0.00%	0.00%	0%
CO3-2	0.00%	0.00%	0.00%	0.00%	0%
H+1	0.00%	0.00%	0.00%	0.00%	0%
H2CO3* (aq)	0.00%	0.00%	0.00%	0.00%	0%
HCO3-	0.00%	0.00%	0.00%	0.00%	0%
HSO4-	0.00%	0.00%	0.00%	0.00%	0%
Na+1	0.00%	0.00%	0.00%	0.00%	0%
NaCl (aq)	0.00%	0.00%	0.00%	0.00%	0%
NaCO3-	0.00%	0.00%	0.00%	0.00%	0%
NaHCO3 (aq)	0.00%	0.00%	0.00%	0.00%	0%
NaOH (aq)	0.00%	0.00%	0.00%	0.00%	0%
NaSO4-	0.00%	0.00%	0.00%	0.00%	0%
OH-	0.00%	0.00%	0.00%	0.00%	0%
SO4-2	0.00%	0.00%	0.00%	0.00%	0%
UO2(CO3)2-2	6.09%	1.65%	0.18%	0.52%	0%
UO2(CO3)3-4	0.13%	0.35%	0.39%	10.92%	67%
UO2(OH)2 (aq)	0.25%	0.01%	0.00%	0.00%	0%
UO2(OH)3-	0.00%	0.00%	0.00%	0.00%	0%
UO2(OH)4-2	0.00%	0.00%	0.00%	0.00%	0%
UO2(SO4)2-2	0.09%	0.00%	0.00%	0.00%	0%
UO2(SO4)3-4	0.00%	0.00%	0.00%	0.00%	0%
UO2+2	0.74%	0.00%	0.00%	0.00%	0%
UO2Cl+	0.01%	0.00%	0.00%	0.00%	0%
UO2Cl2 (aq)	0.00%	0.00%	0.00%	0.00%	0%
UO2CO3 (aq)	44.10%	1.20%	0.01%	0.00%	0%
UO2OH+	2.43%	0.02%	0.00%	0.00%	0%
UO2SO4 (aq)	1.48%	0.00%	0.00%	0.00%	0%

Cryo-EM images of *G. uraniireducens* exposed to atmospheric P_{CO2}

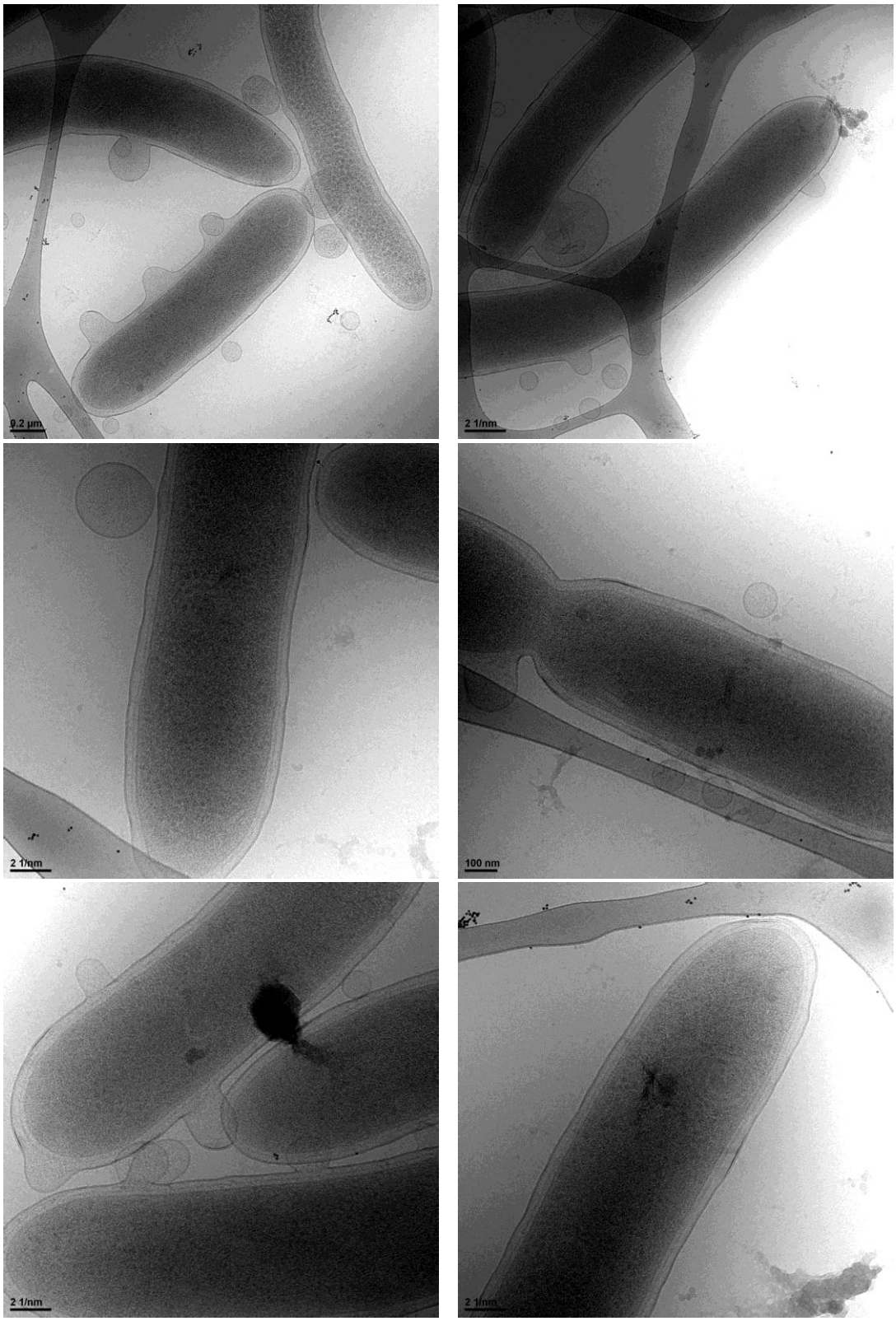

Cryo-EM images of *G. uraniireducens* exposed to atmospheric P_{CO2}

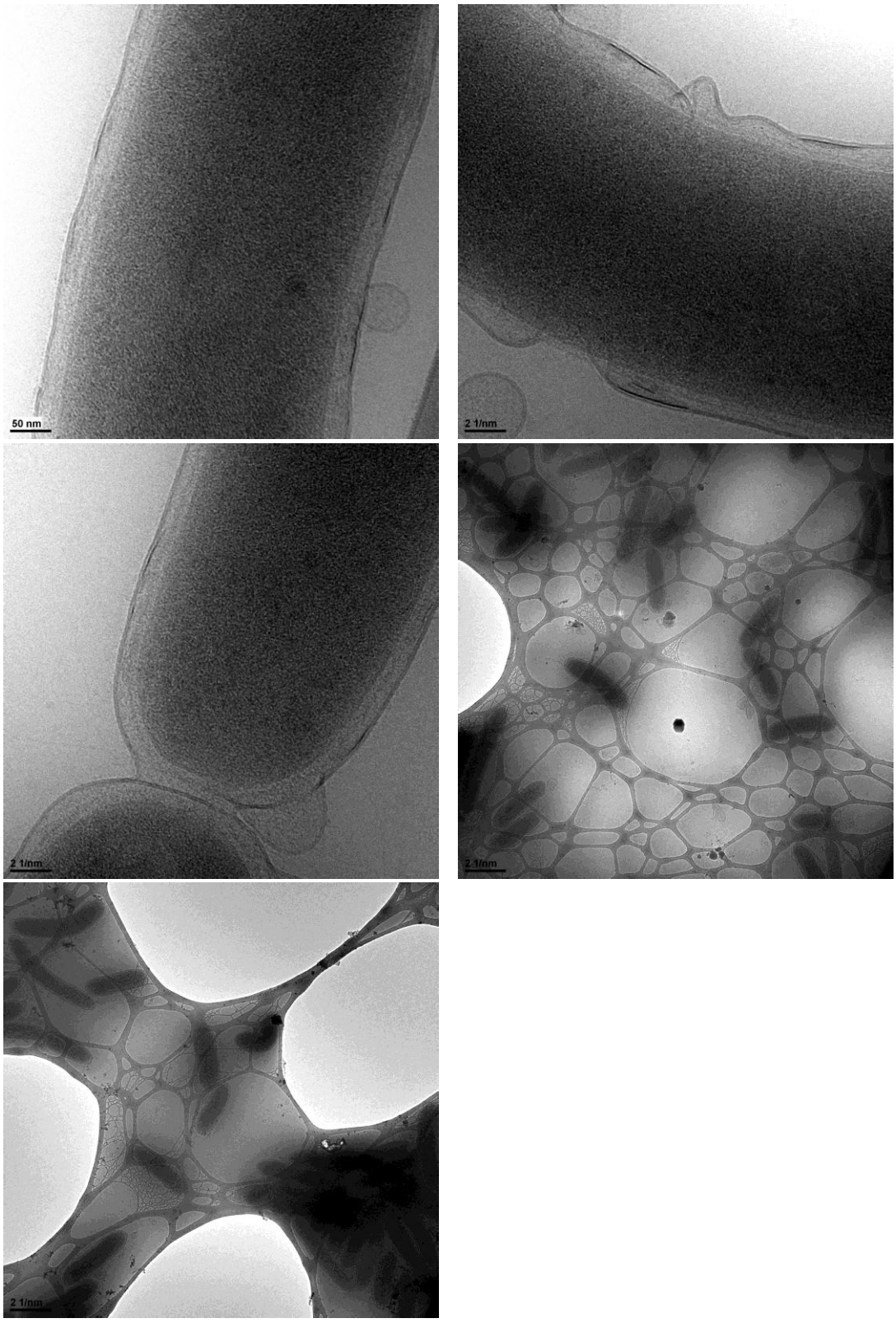

Cryo-EM images of *G. uraniireducens* exposed to 2% P_{CO2}

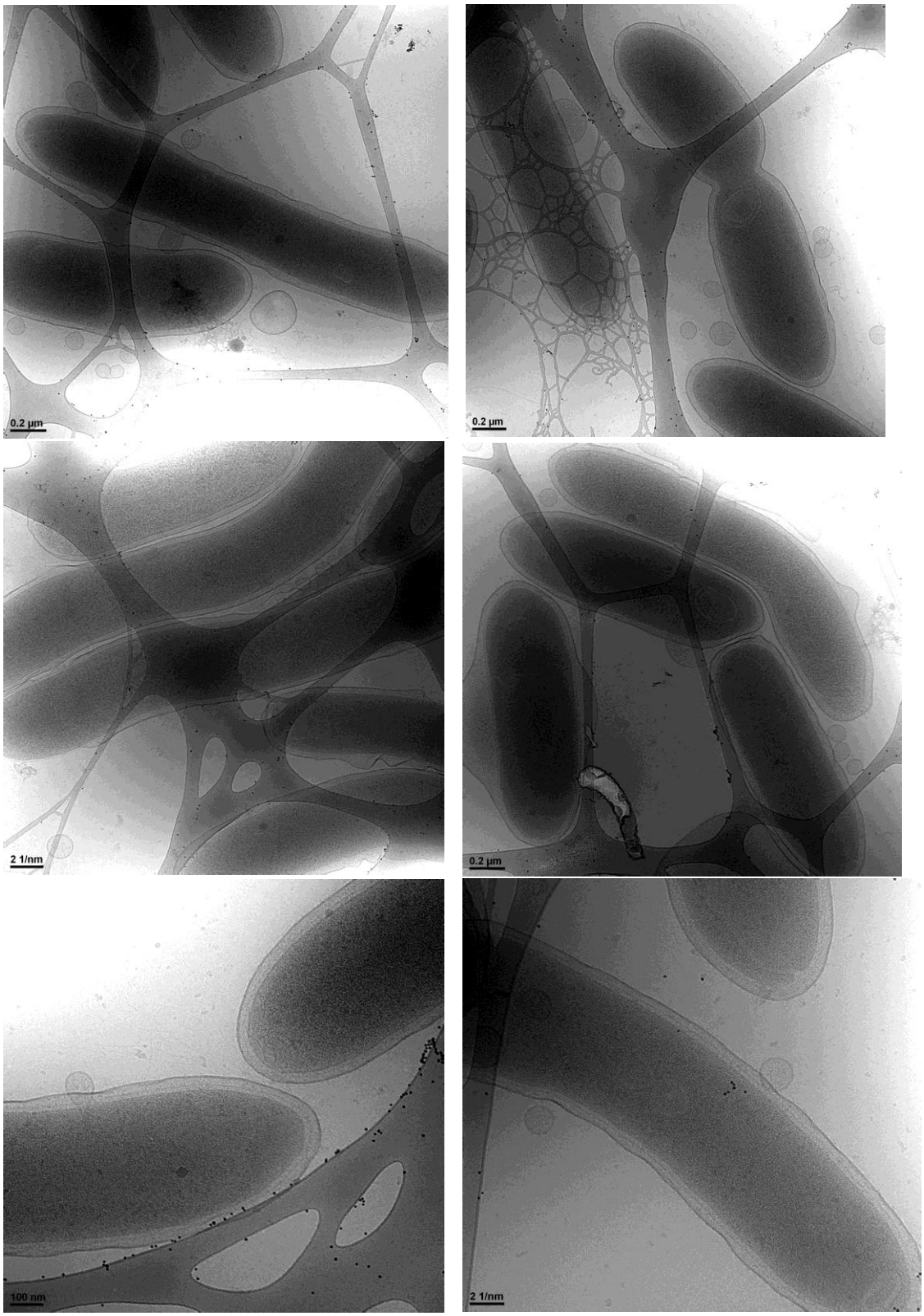

Cryo-EM images of *G. uraniireducens* exposed to 2% P_{CO2}

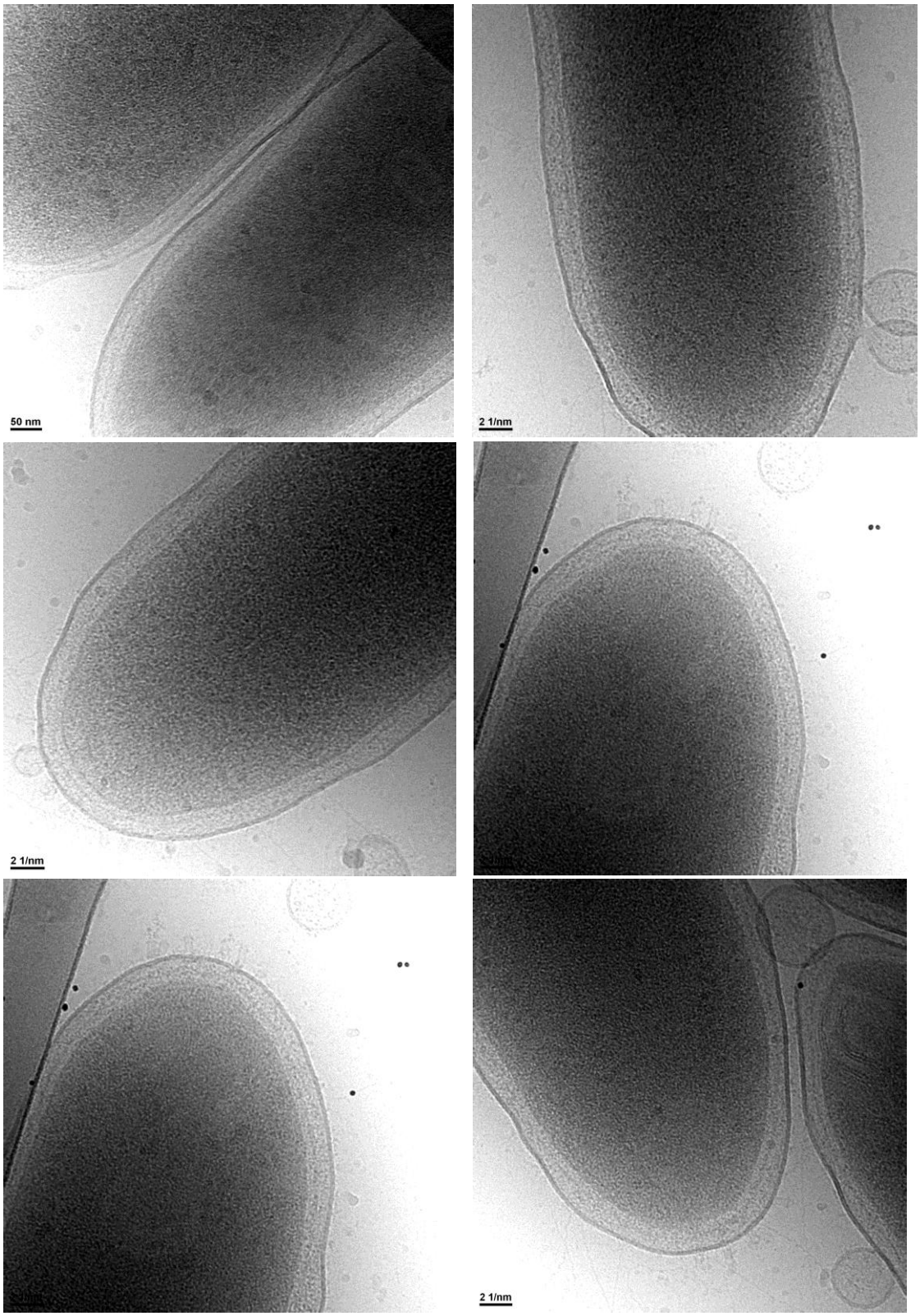

Cryo-EM images of *G. uraniireducens* exposed to 2% P_{CO2}

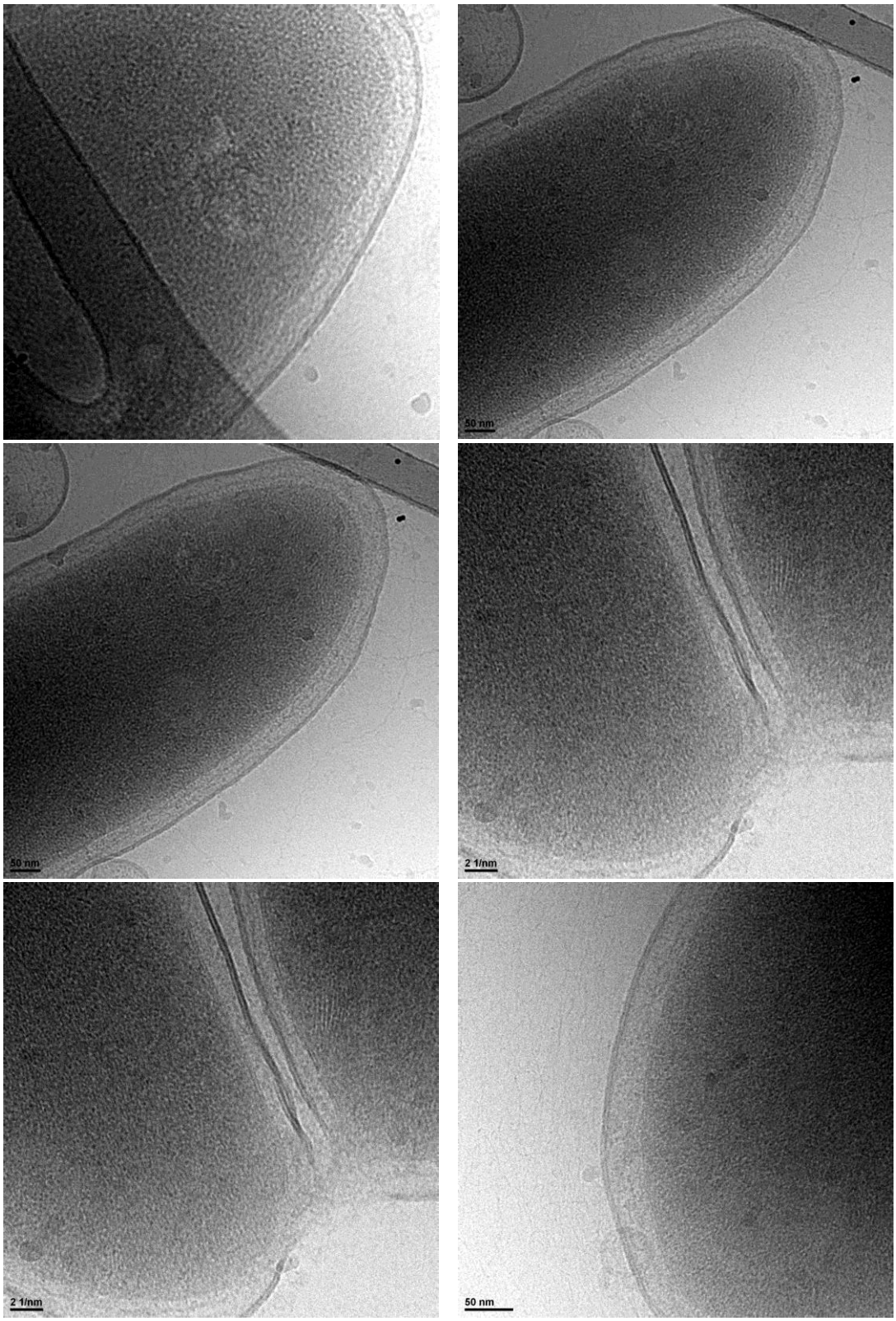

Cryo-EM images of *G. uraniireducens* exposed to 2% P_{CO2}

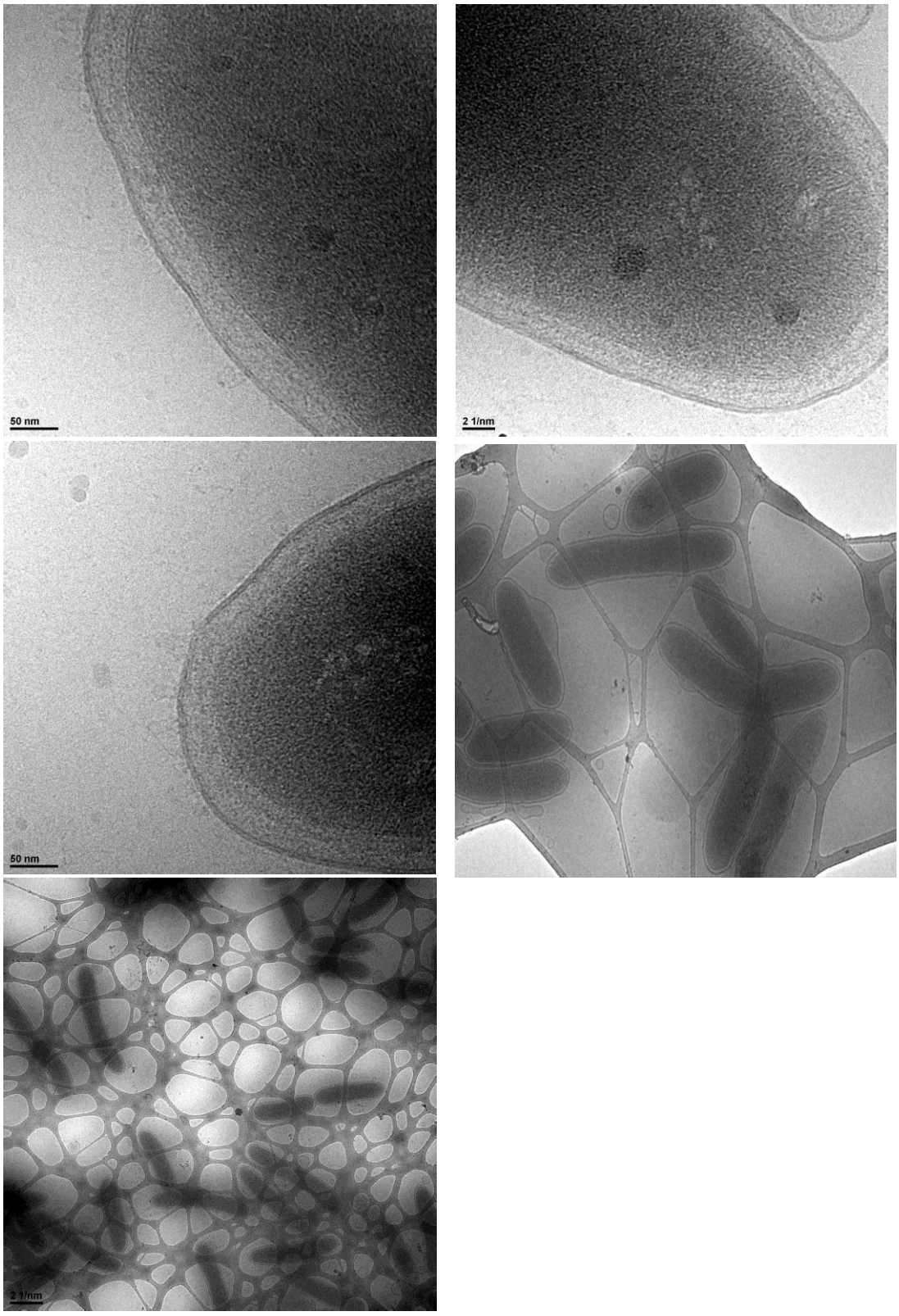

Cryo-EM images of *A. palmae* 2% P_{CO2}

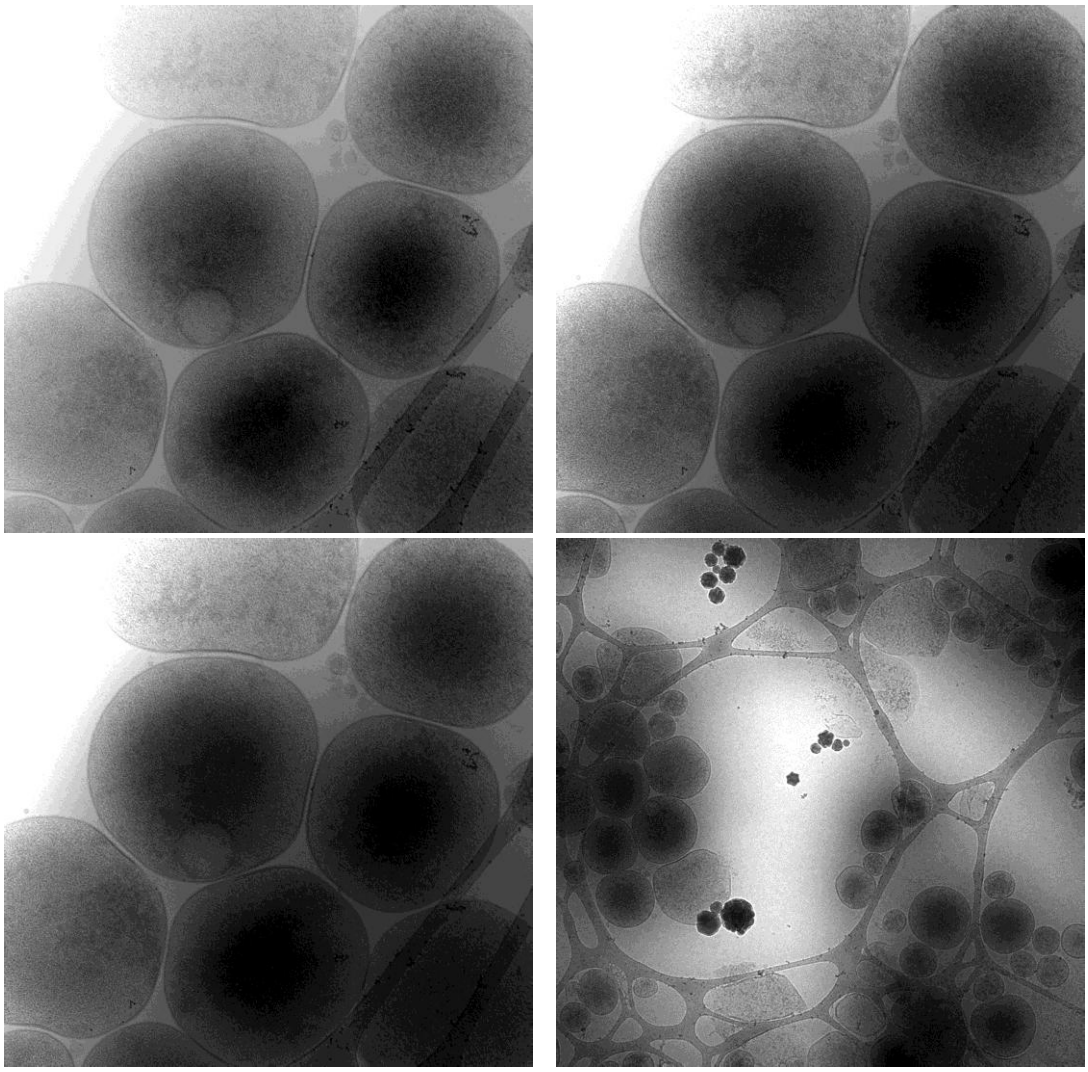

Component	mM
H+	-4.75
CO32-	3.3
UO2+2	0.0014
Ca+2	7
SO4-2	8.5
Na+1	5
Cl-1	1E-10
pH	6.95
Temperature	25 C
Ionic Strength	0.0266
Charge imbalance	4.3

Mineral	log IAP	Sat. Index	Stoichiometry					
Anhydrite	-5.051	-0.691	1	Ca+2	1	SO4-2		
Aragonite	-8.533	-0.197	1	Ca+2	1	CO3-2		
CaCO3xH2O	-8.533	-1.389	1	Ca+2	1	CO3-2	1	H2O
Calcite	-8.533	-0.053	1	Ca+2	1	CO3-2		
Gummite	0.276	-7.396	-2	H+1	1	UO2+2	1	H2O
Gypsum	-5.051	-0.441	1	Ca+2	1	SO4-2	2	H2O
Halite	-15.449	-16.999	1	Na+1	1	Cl-1		
Lime	11.315	-21.385	-2	H+1	1	Ca+2	1	H2O
Mirabilite	-7.222	-6.108	2	Na+1	1	SO4-2	10	H2O
Natron	-10.704	-9.393	2	Na+1	1	CO3-2	10	H2O
Portlandite	11.315	-11.389	1	Ca+2	2	H2O	-2	H+1
Rutherfordine	-19.572	-4.812	1	UO2+2	1	CO3-2		
Schoepite	0.276	-5.114	1	UO2+2	3	H2O	-2	H+1
Thenardite	-7.222	-7.544	2	Na+1	1	SO4-2		
Thermonatrite	-10.704	-11.341	2	Na+1	1	CO3-2	1	H2O
UO2(OH)2 (beta)	0.276	-5.335	-2	H+1	1	UO2+2	2	H2O
UO3	0.276	-7.424	-2	H+1	1	UO2+2	1	H2O
Vaterite	-8.533	-0.62	1	Ca+2	1	CO3-2		

Sweep of critical component with highest concentration tested to check for precipiation. Component swept highlighted.

Component	mM
H+	-4.75
CO32-	0.07
UO2+2	0.0014
Ca+2	7
SO4-2	8.5
Na+1	5
Cl-1	1E-10
pH	6.95
Temperature	25 C
Ionic Strength	0.0249
Charge imbalance	7.05

Mineral	log IAP	Sat. Index	Stoichiometry					
Anhydrite	-5.037	-0.677	1	Ca+2	1	SO4-2		
Aragonite	-10.242	-1.906	1	Ca+2	1	CO3-2		
CaCO3xH2O	-10.242	-3.098	1	Ca+2	1	CO3-2	1	H2O
Calcite	-10.242	-1.762	1	Ca+2	1	CO3-2		
Gummite	4.564	-3.108	-2	H+1	1	UO2+2	1	H2O
Gypsum	-5.037	-0.427	1	Ca+2	1	SO4-2	2	H2O
Halite	-15.446	-16.996	1	Na+1	1	Cl-1		
Lime	11.327	-21.372	-2	H+1	1	Ca+2	1	H2O
Mirabilite	-7.216	-6.102	2	Na+1	1	SO4-2	10	H2O
Natron	-12.421	-11.11	2	Na+1	1	CO3-2	10	H2O
Portlandite	11.327	-11.377	1	Ca+2	2	H2O	-2	H+1
Rutherfordine	-17.006	-2.246	1	UO2+2	1	CO3-2		
Schoepite	4.564	-0.826	1	UO2+2	3	H2O	-2	H+1
Thenardite	-7.216	-7.538	2	Na+1	1	SO4-2		
Thermonatrite	-12.421	-13.058	2	Na+1	1	CO3-2	1	H2O
UO2(OH)2 (beta)	4.564	-1.048	-2	H+1	1	UO2+2	2	H2O
UO3	4.564	-3.136	-2	H+1	1	UO2+2	1	H2O
Vaterite	-10.242	-2.329	1	Ca+2	1	CO3-2		

Component	mM
H+	-4.75
CO32-	3.3
UO2+2	0.0014
Ca+2	6.55
SO4-2	10
Na+1	10
Cl-1	1E-10
pH	6.95
Temperature	25 C
Ionic Strength	0.0308
Charge imbalance	0.06

Mineral	log IAP	Sat. Index	Stoichiometry					
Anhydrite	-5.044	-0.684	1	Ca+2	1	SO4-2		
Aragonite	-8.593	-0.257	1	Ca+2	1	CO3-2		
CaCO3xH2O	-8.593	-1.449	1	Ca+2	1	CO3-2	1	H2O
Calcite	-8.593	-0.113	1	Ca+2	1	CO3-2		
Gummite	0.381	-7.291	-2	H+1	1	UO2+2	1	H2O
Gypsum	-5.044	-0.434	1	Ca+2	1	SO4-2	2	H2O
Halite	-15.158	-16.708	1	Na+1	1	Cl-1		
Lime	11.255	-21.444	-2	H+1	1	Ca+2	1	H2O
Mirabilite	-6.565	-5.451	2	Na+1	1	SO4-2	10	H2O
Natron	-10.113	-8.802	2	Na+1	1	CO3-2	10	H2O
Portlandite	11.255	-11.449	1	Ca+2	2	H2O	-2	H+1
Rutherfordine	-19.467	-4.707	1	UO2+2	1	CO3-2		
Schoepite	0.381	-5.009	1	UO2+2	3	H2O	-2	H+1
Thenardite	-6.565	-6.886	2	Na+1	1	SO4-2		
Thermonatrite	-10.113	-10.75	2	Na+1	1	CO3-2	1	H2O
UO2(OH)2 (beta)	0.381	-5.231	-2	H+1	1	UO2+2	2	H2O
UO3	0.381	-7.319	-2	H+1	1	UO2+2	1	H2O
Vaterite	-8.593	-0.68	1	Ca+2	1	CO3-2		

Sweep of critical component with highest concentration tested to check for precipiation. Component swept highlighted.

Component	mM
H+	-4.75
CO32-	0.07
UO2+2	0.0014
Ca+2	6.55
SO4-2	10
Na+1	10
Cl-1	1E-10
pH	6.95
Temperature	25 C
Ionic Strength	0.0292
Charge imbalance	8.9

Mineral	log IAP	Sat. Index	Stoichiometry					
Anhydrite	-5.031	-0.671	1	Ca+2	1	SO4-2		
Aragonite	-10.303	-1.967	1	Ca+2	1	CO3-2		
CaCO3xH2O	-10.303	-3.159	1	Ca+2	1	CO3-2	1	H2O
Calcite	-10.303	-1.823	1	Ca+2	1	CO3-2		
Gummite	4.569	-3.103	-2	H+1	1	UO2+2	1	H2O
Gypsum	-5.031	-0.421	1	Ca+2	1	SO4-2	2	H2O
Halite	-15.155	-16.705	1	Na+1	1	Cl-1		
Lime	11.266	-21.433	-2	H+1	1	Ca+2	1	H2O
Mirabilite	-6.558	-5.444	2	Na+1	1	SO4-2	10	H2O
Natron	-11.831	-10.52	2	Na+1	1	CO3-2	10	H2O
Portlandite	11.266	-11.438	1	Ca+2	2	H2O	-2	H+1
Rutherfordine	-17	-2.24	1	UO2+2	1	CO3-2		
Schoepite	4.569	-0.821	1	UO2+2	3	H2O	-2	H+1
Thenardite	-6.558	-6.88	2	Na+1	1	SO4-2		
Thermonatrite	-11.831	-12.468	2	Na+1	1	CO3-2	1	H2O
UO2(OH)2 (beta)	4.569	-1.042	-2	H+1	1	UO2+2	2	H2O
UO3	4.569	-3.131	-2	H+1	1	UO2+2	1	H2O
Vaterite	-10.303	-2.39	1	Ca+2	1	CO3-2		

Component	mM
H+	-4.75
CO32-	3.3
UO2+2	0.02
Ca+2	6.55
SO4-2	8.5
Na+1	10
Cl-1	1E-10
pH	6.95
Temperature	25 C
Ionic Strength	0.0286
Charge imbalance	7.68

Mineral	log IAP	Sat. Index	Stoichiometry					
Anhydrite	-5.09	-0.73	1	Ca+2	1	SO4-2		
Aragonite	-8.569	-0.233	1	Ca+2	1	CO3-2		
CaCO3xH2O	-8.569	-1.425	1	Ca+2	1	CO3-2	1	H2O
Calcite	-8.569	-0.089	1	Ca+2	1	CO3-2		
Gummite	1.494	-6.178	-2	H+1	1	UO2+2	1	H2O
Gypsum	-5.09	-0.48	1	Ca+2	1	SO4-2	2	H2O
Halite	-15.153	-16.703	1	Na+1	1	Cl-1		
Lime	11.279	-21.42	-2	H+1	1	Ca+2	1	H2O
Mirabilite	-6.627	-5.513	2	Na+1	1	SO4-2	10	H2O
Natron	-10.106	-8.795	2	Na+1	1	CO3-2	10	H2O
Portlandite	11.279	-11.425	1	Ca+2	2	H2O	-2	H+1
Rutherfordine	-18.354	-3.594	1	UO2+2	1	CO3-2		
Schoepite	1.494	-3.896	1	UO2+2	3	H2O	-2	H+1
Thenardite	-6.627	-6.949	2	Na+1	1	SO4-2		
Thermonatrite	-10.106	-10.743	2	Na+1	1	CO3-2	1	H2O
UO2(OH)2 (beta)	1.494	-4.117	-2	H+1	1	UO2+2	2	H2O
UO3	1.494	-6.206	-2	H+1	1	UO2+2	1	H2O
Vaterite	-8.569	-0.656	1	Ca+2	1	CO3-2		

Sweep of critical component with highest concentration tested to check for precipiation. Component swept highlighted.

Component	mM
H+	-4.75
CO32-	0.07
UO2+2	0.02
Ca+2	6.55
SO4-2	8.5
Na+1	5
Cl-1	1E-10
pH	6.95
Temperature	25 C
Ionic Strength	0.0244
Charge imbalance	3.8

Mineral	log IAP	Sat. Index	Stoichiometry					
Anhydrite	-5.058	-0.698	1	Ca+2	1	SO4-2		
Aragonite	-10.272	-1.936	1	Ca+2	1	CO3-2		
CaCO3xH2O	-10.272	-3.128	1	Ca+2	1	CO3-2	1	H2O
Calcite	-10.272	-1.792	1	Ca+2	1	CO3-2		
Gummite	5.185	-2.487	-2	H+1	1	UO2+2	1	H2O
Gypsum	-5.058	-0.448	1	Ca+2	1	SO4-2	2	H2O
Halite	-15.444	-16.994	1	Na+1	1	Cl-1		
Lime	11.297	-21.402	-2	H+1	1	Ca+2	1	H2O
Mirabilite	-7.206	-6.092	2	Na+1	1	SO4-2	10	H2O
Natron	-12.421	-11.11	2	Na+1	1	CO3-2	10	H2O
Portlandite	11.297	-11.407	1	Ca+2	2	H2O	-2	H+1
Rutherfordine	-16.384	-1.624	1	UO2+2	1	CO3-2		
Schoepite	5.185	-0.205	1	UO2+2	3	H2O	-2	H+1
Thenardite	-7.206	-7.528	2	Na+1	1	SO4-2		
Thermonatrite	-12.421	-13.058	2	Na+1	1	CO3-2	1	H2O
UO2(OH)2 (beta)	5.185	-0.426	-2	H+1	1	UO2+2	2	H2O
UO3	5.185	-2.515	-2	H+1	1	UO2+2	1	H2O
Vaterite	-10.272	-2.359	1	Ca+2	1	CO3-2		

Freeze Dried Sample

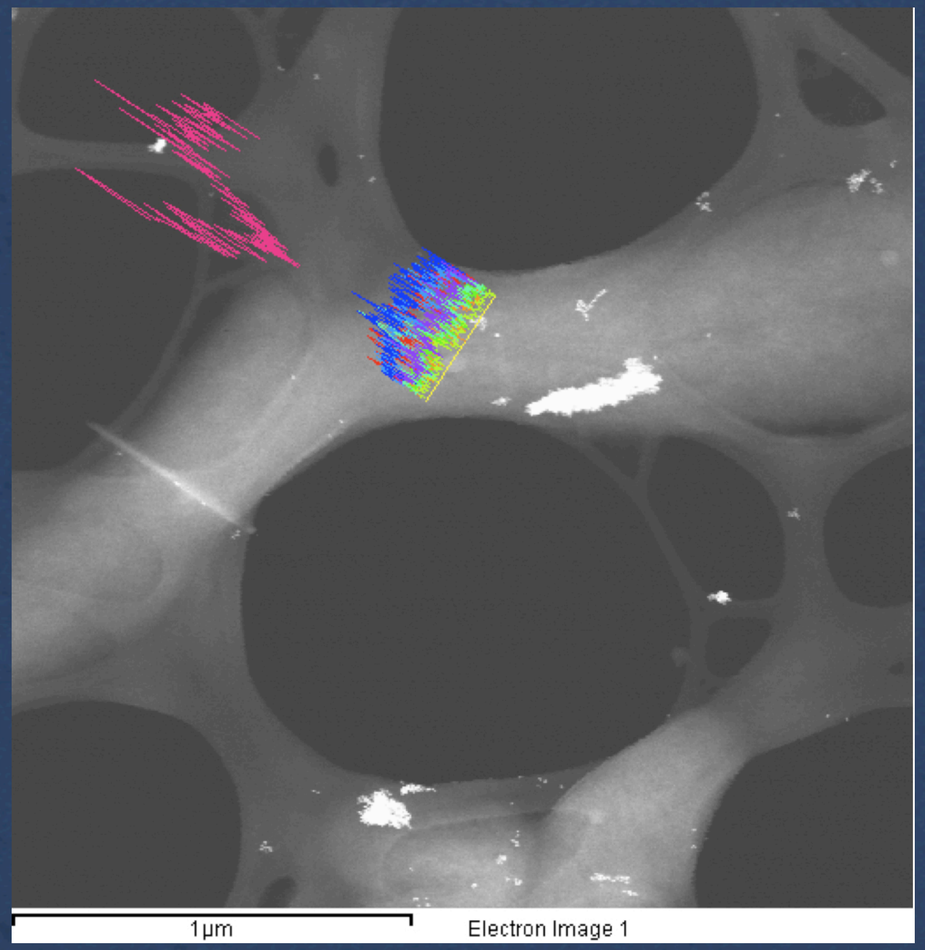

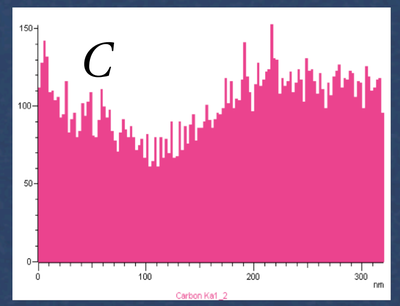

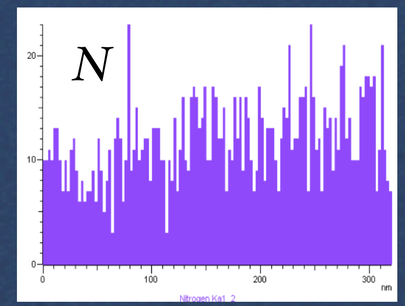

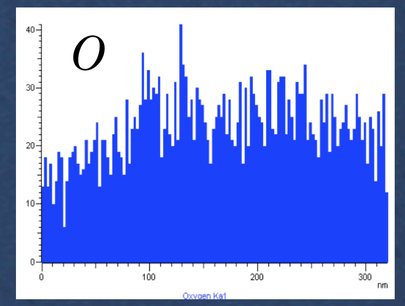

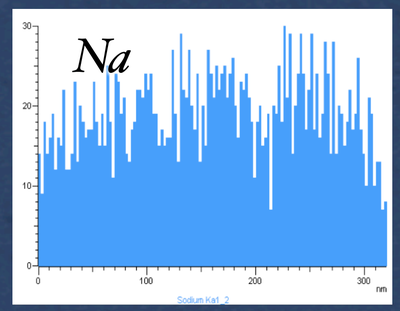

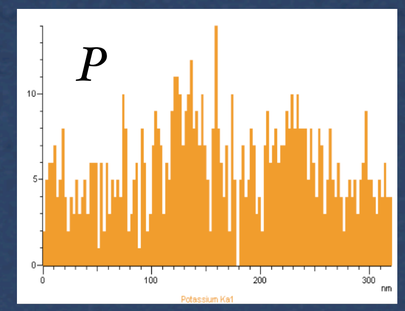

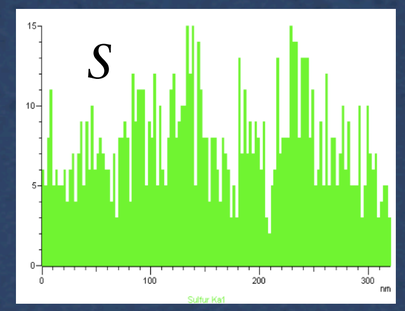

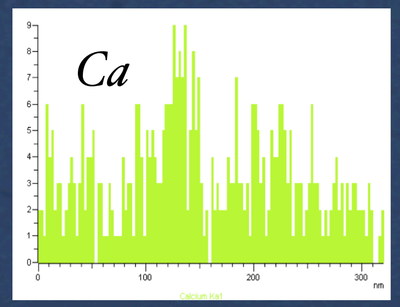

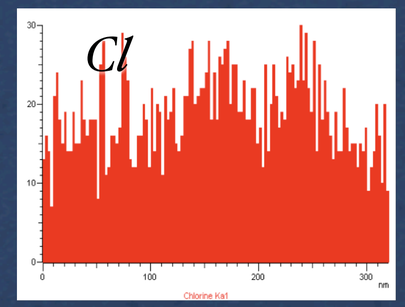

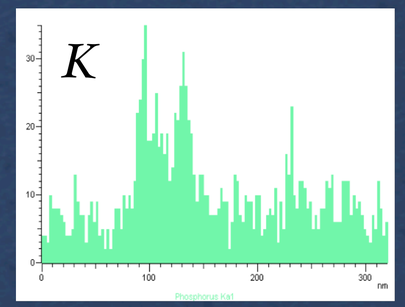

Freeze Dried Sample

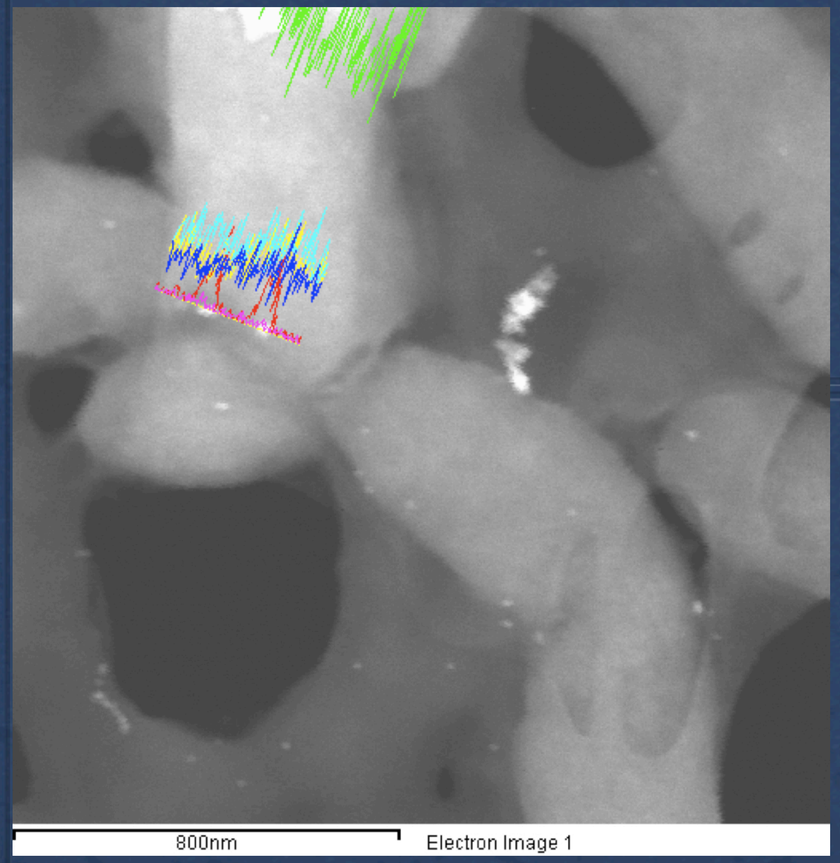

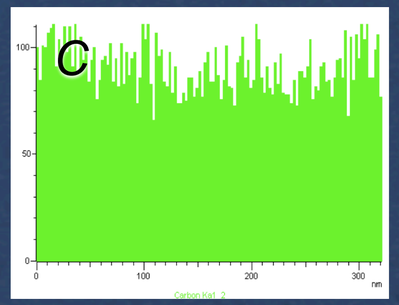

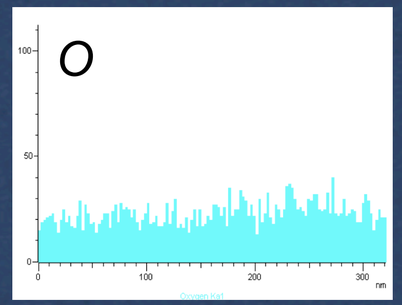

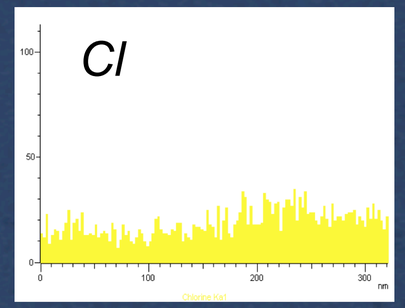

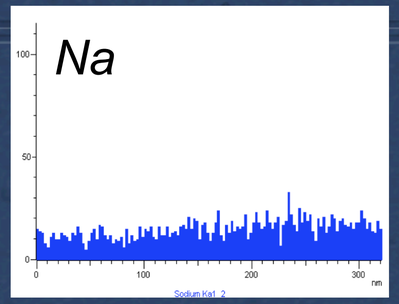

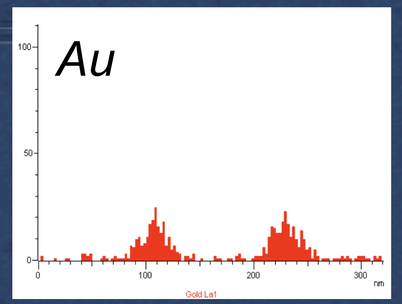

Linescan through
10 nm Au on cell

Air Dried Sample

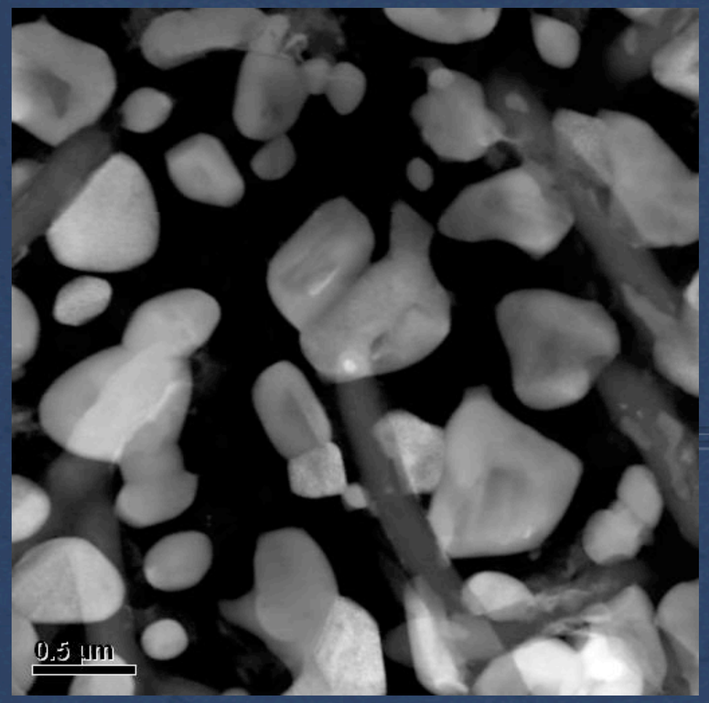

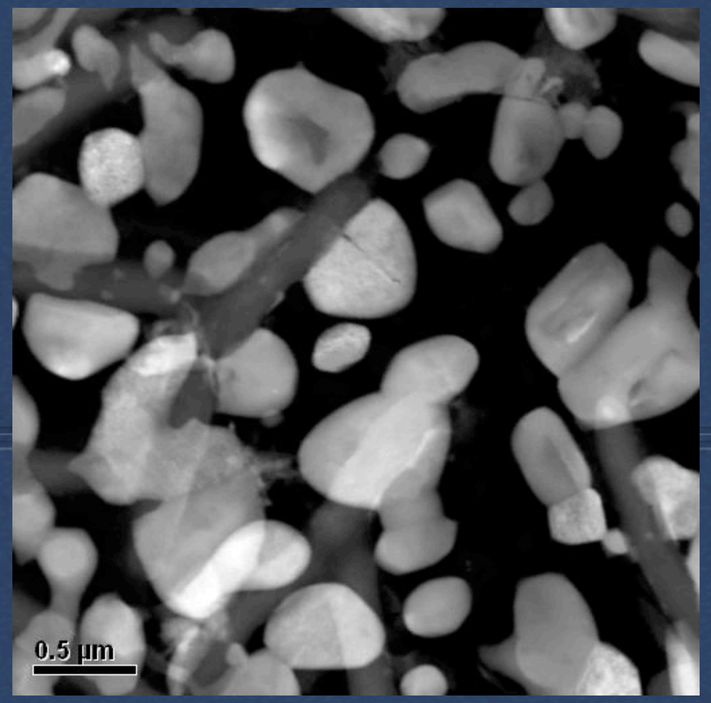

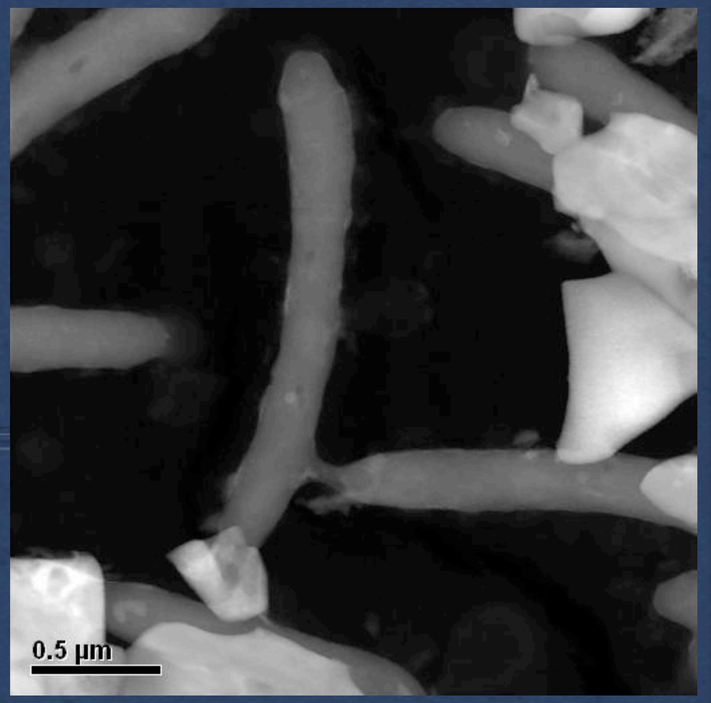

Many salt crystals

Air Dried Sample

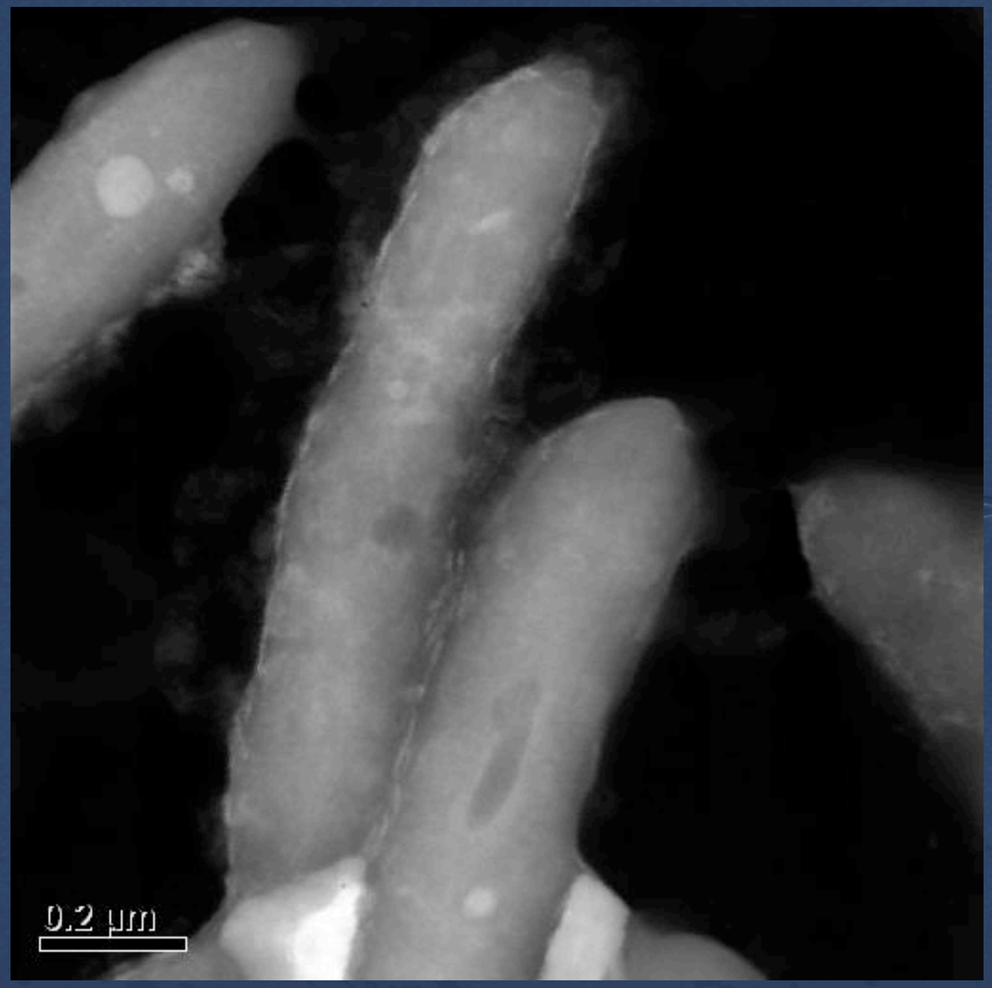

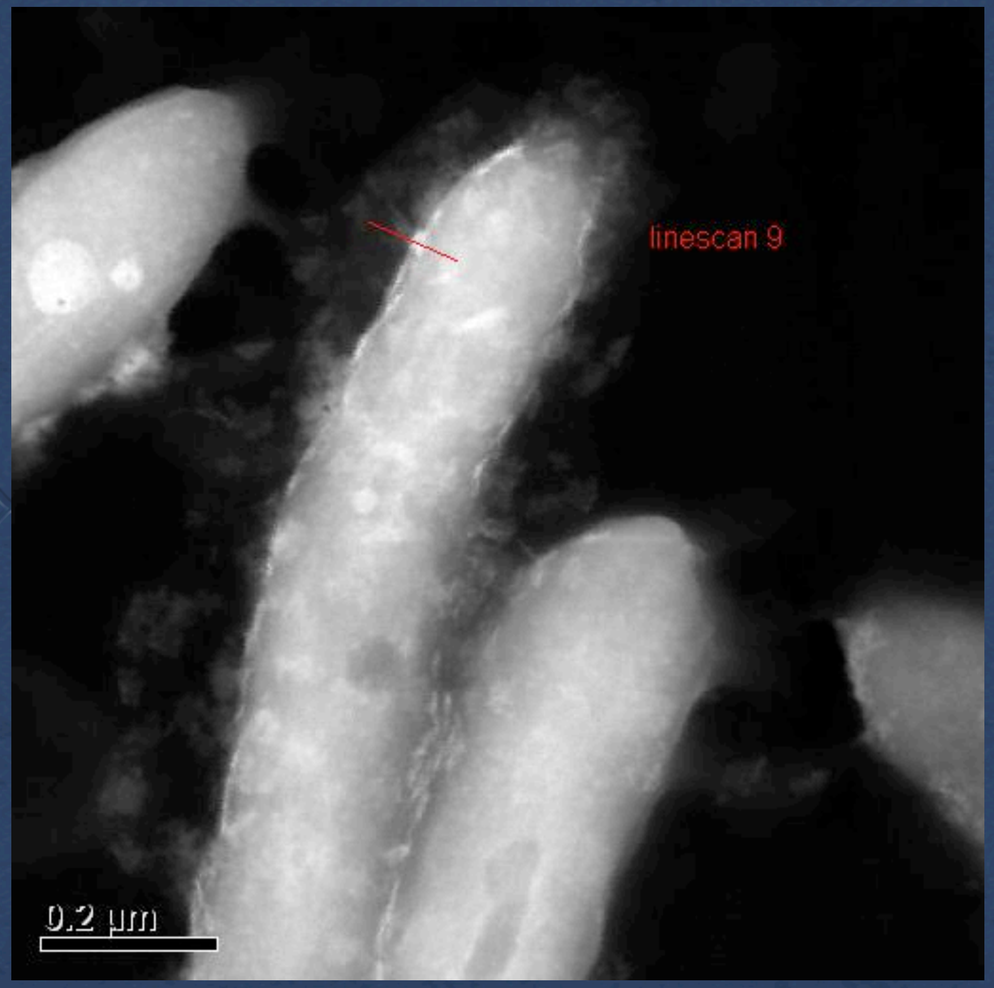

Air Dried Sample

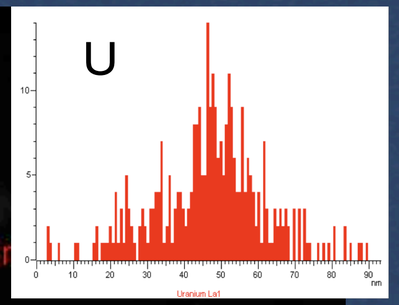

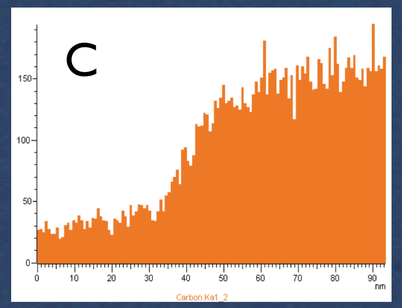

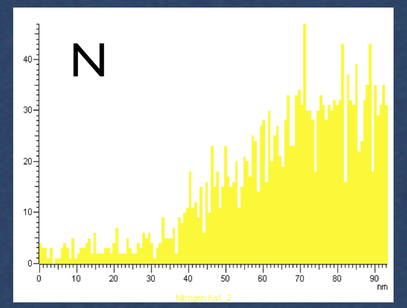

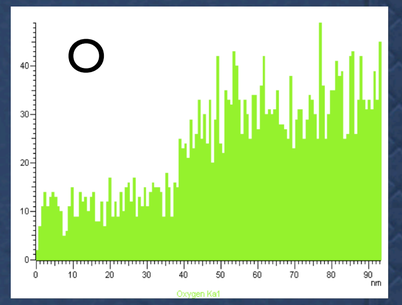

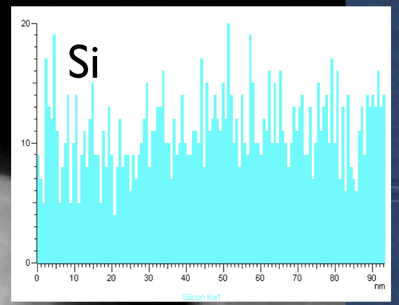

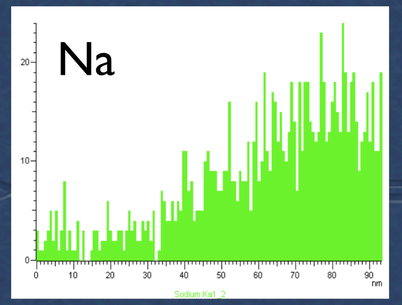

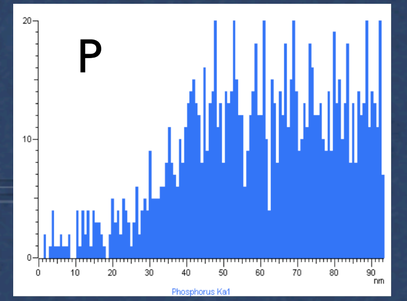

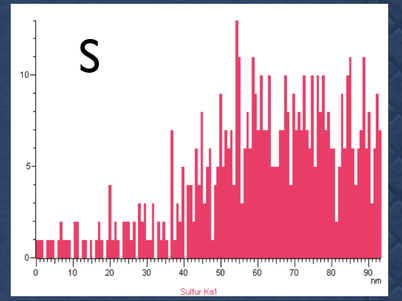

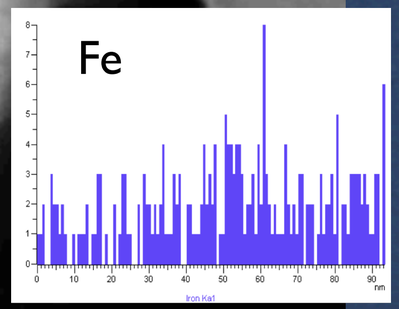

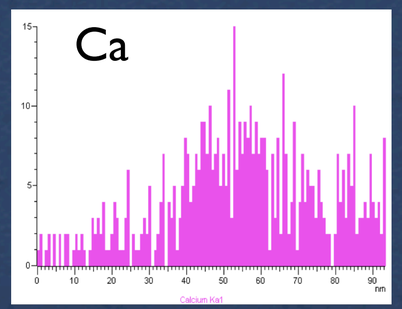

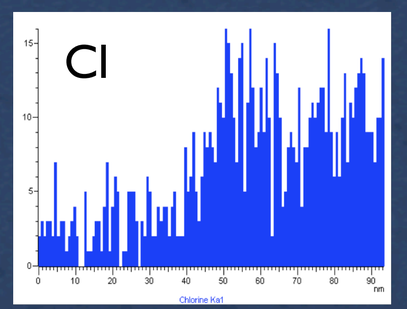

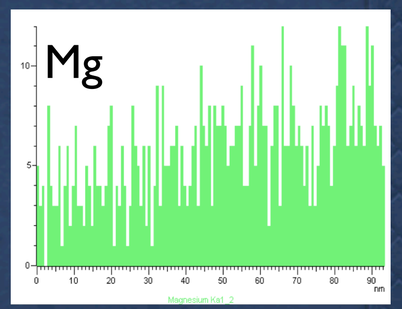

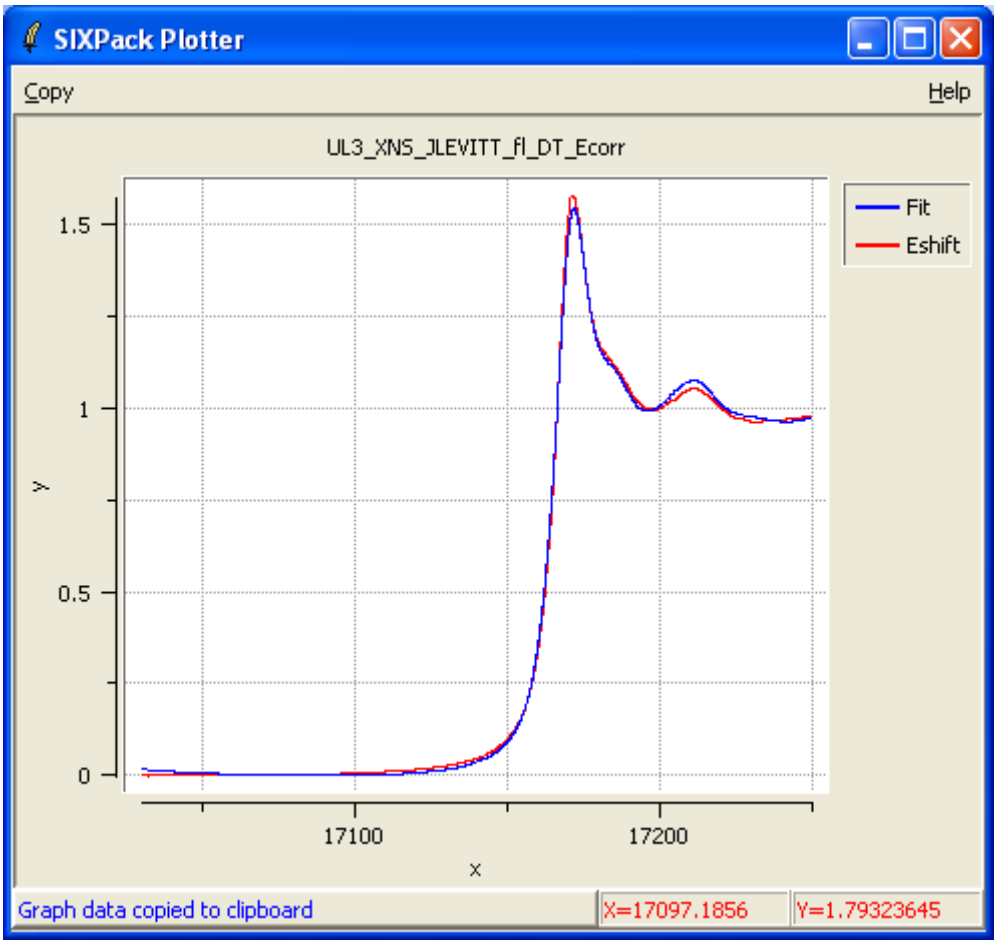

Eshift	Data	Energy	Fit
17030.0	-0.000557853922124	17030.0	0.0155305100504
17030.05	-0.00053549802822	17030.05	0.0154697788465
17030.1	-0.00049053280844	17030.1	0.0154083435762
17030.15	-0.000430004493327	17030.15	0.0153486606608
17030.2	-0.000361006038244	17030.2	0.0152931865222
17030.25	-0.000290738204625	17030.25	0.0152443775819
17030.3	-0.000226378682421	17030.3	0.0152046902616
17030.35	-0.000175089641456	17030.35	0.0151765809828
17030.4	-0.000144118255631	17030.4	0.0151625061672

17030.45	-0.000140312771763	17030.45	0.0151649222365
17030.5	-0.00016482076765	17030.5	0.0151862856122
17030.55	-0.000210568301863	17030.55	0.0152279274952
17030.6	-0.00027022948746	17030.6	0.0152866782024
17030.65	-0.000336381575901	17030.65	0.0153582428304
17030.7	-0.000401623352011	17030.7	0.0154383264752
17030.75	-0.000458564328723	17030.75	0.0155226342333
17030.8	-0.000499749638546	17030.8	0.0156068712008
17030.85	-0.000518032313884	17030.85	0.0156867424741
17030.9	-0.000511930931346	17030.9	0.0157579531493
17030.95	-0.000488813686925	17030.95	0.0158162083229
17031.0	-0.000456481635184	17031.0	0.0158572130911
17031.05	-0.000422818132276	17031.05	0.0158777608906
17031.1	-0.000395688364345	17031.1	0.0158789985201
17031.15	-0.000382947895991	17031.15	0.0158631611188
17031.2	-0.000392508921414	17031.2	0.0158324838258
17031.25	-0.000431998081022	17031.25	0.0157892017802
17031.3	-0.000501677695611	17031.3	0.0157355501212
17031.35	-0.00058937130065	17031.35	0.015673763988
17031.4	-0.00068204263234	17031.4	0.0156060785197
17031.45	-0.000766573462908	17031.45	0.0155347288555
17031.5	-0.000829866004543	17031.5	0.0154619501345
17031.55	-0.000858822673619	17031.55	0.0153896698642

17031.6	-0.000840324630513	17031.6	0.0153185850257
17031.65	-0.000761431670399	17031.65	0.0152490849685
17031.7	-0.00062068637785	17031.7	0.0151815590419
17031.75	-0.000438368764847	17031.75	0.0151163965955
17031.8	-0.000237012640239	17031.8	0.0150539869786
17031.85	-3.9191457681e-005	17031.85	0.0149947195407
17031.9	0.000132533951924	17031.9	0.0149389836312
17031.95	0.000255591911476	17031.95	0.0148871685996
17032.0	0.000307441505815	17032.0	0.0148396637953
17032.05	0.00026554652871	17032.05	0.0147964252441
17032.1	0.000122565109451	17032.1	0.0147556756778
17032.15	-9.78860346234e-005	17032.15	0.0147152045042
17032.2	-0.000368165898831	17032.2	0.0146728011313
17032.25	-0.000660690246395	17032.25	0.0146262549672
17032.3	-0.000947866600982	17032.3	0.01457335542
17032.35	-0.00120207864788	17032.35	0.0145118918975
17032.4	-0.00139581366546	17032.4	0.0144396538077
17032.45	-0.0015012624717	17032.45	0.0143544305588
17032.5	-0.0015040436004	17032.5	0.0142540115588
17032.55	-0.0014202203865	17032.55	0.0141374484583
17032.6	-0.00127117621599	17032.6	0.0140088418792
17032.65	-0.00107804986552	17032.65	0.0138735546861
17032.7	-0.000862039993187	17032.7	0.0137369497435

17032.75	-0.000644352126428	17032.75	0.0136043899162
17032.8	-0.000446104433773	17032.8	0.0134812380686
17032.85	-0.000288705548422	17032.85	0.0133728570654
17032.9	-0.000185617768854	17032.9	0.0132846097712
17032.95	-0.000130987047515	17032.95	0.0132218590504
17033.0	-0.000114940147681	17033.0	0.0131899677678
17033.05	-0.000127844815822	17033.05	0.0131923335175
17033.1	-0.000160005774599	17033.1	0.0132244928118
17033.15	-0.000201735044879	17033.15	0.0132800168927
17033.2	-0.000243378478529	17033.2	0.0133524770021
17033.25	-0.000275154698188	17033.25	0.0134354443821
17033.3	-0.000289799339612	17033.3	0.0135224902744
17033.35	-0.000286602931007	17033.35	0.0136071859211
17033.4	-0.000266456949615	17033.4	0.0136831025642
17033.45	-0.000230140510889	17033.45	0.0137438114455
17033.5	-0.00017846554869	17033.5	0.013782883807
17033.55	-0.000112228155892	17033.55	0.013795549118
17033.6	-3.22549709175e-005	17033.6	0.0137836697575
17033.65	6.07262426776e-005	17033.65	0.0137507663318
17033.7	0.00016462207615	17033.7	0.0137003594473
17033.75	0.0002733990531	17033.75	0.0136359697102
17033.8	0.000379827048987	17033.8	0.0135611177271
17033.85	0.000476768503578	17033.85	0.0134793241041

17033.9	0.000557065332118	17033.9	0.0133941094476
17033.95	0.000613544147391	17033.95	0.0133089943639
17034.0	0.000639113296495	17034.0	0.0132274994595
17034.05	0.000626386882513	17034.05	0.0131522156381
17034.1	0.000571424481219	17034.1	0.0130820149935
17034.15	0.000480934325084	17034.15	0.0130148399169
17034.2	0.000365322424205	17034.2	0.0129486327995
17034.25	0.000234694567404	17034.25	0.0128813360326
17034.3	9.92377486233e-005	17034.3	0.0128108920074
17034.35	-3.08638623683e-005	17034.35	0.0127352431152
17034.4	-0.000145496004223	17034.4	0.0126523317471
17034.45	-0.000234274694082	17034.45	0.0125601002944
17034.5	-0.000289563005232	17034.5	0.0124564911483
17034.55	-0.000312825036949	17034.55	0.0123405070408
17034.6	-0.000309109595756	17034.6	0.0122153920663
17034.65	-0.000283169691414	17034.65	0.0120854506597
17034.7	-0.000239844516719	17034.7	0.0119549872564
17034.75	-0.000183953271227	17034.75	0.0118283062912
17034.8	-0.000120308944418	17034.8	0.0117097121994
17034.85	-5.37678205407e-005	17034.85	0.011603509416
17034.9	1.11946259612e-005	17034.9	0.0115140023761
17034.95	7.15076156675e-005	17034.95	0.0114454955148
17035.0	0.000124760713354	17035.0	0.0114022932672

17035.05	0.000168489213208	17035.05	0.0113874285826
17035.1	0.000200247640401	17035.1	0.0113988484667
17035.15	0.000217575772756	17035.15	0.0114332284395
17035.2	0.000218053146495	17035.2	0.0114872440212
17035.25	0.000199118935884	17035.25	0.0115575707316
17035.3	0.00015928774295	17035.3	0.0116408840909
17035.35	0.000101337430277	17035.35	0.0117338596189
17035.4	3.02844808081e-005	17035.4	0.0118331728356
17035.45	-4.90293973745e-005	17035.45	0.0119354992612
17035.5	-0.000131708994105	17035.5	0.0120375144155
17035.55	-0.000212864766451	17035.55	0.0121363093493
17035.6	-0.00028763800463	17035.6	0.0122306372362
17035.65	-0.000351043928077	17035.65	0.0123196667805
17035.7	-0.000398992287463	17035.7	0.0124025666865
17035.75	-0.000431220085239	17035.75	0.0124785056585
17035.8	-0.000449699537324	17035.8	0.0125466524008
17035.85	-0.000456236582974	17035.85	0.0126061756176
17035.9	-0.000452692761363	17035.9	0.0126562440134
17035.95	-0.000440914503159	17035.95	0.0126960262924
17036.0	-0.000422753073137	17036.0	0.0127246911589
17036.05	-0.000400055561576	17036.05	0.0127417904447
17036.1	-0.000374688890583	17036.1	0.0127484084913
17036.15	-0.000348614298199	17036.15	0.0127460127678

17036.2	-0.000323857018756	17036.2	0.0127360707433
17036.25	-0.000302438692087	17036.25	0.0127200498867
17036.3	-0.000286380050952	17036.3	0.0126994176672
17036.35	-0.000277710593168	17036.35	0.0126756415537
17036.4	-0.000278425663402	17036.4	0.0126501890152
17036.45	-0.000290646678998	17036.45	0.0126245275209
17036.5	-0.000315751384137	17036.5	0.0126001245398
17036.55	-0.000351208396682	17036.55	0.0125780284273
17036.6	-0.000391557310837	17036.6	0.0125576110849
17036.65	-0.000431510539823	17036.65	0.0125378253006
17036.7	-0.00046571575892	17036.7	0.0125176238623
17036.75	-0.000488823888205	17036.75	0.0124959595578
17036.8	-0.000495537606538	17036.8	0.0124717851752
17036.85	-0.000480351708341	17036.85	0.0124440535023
17036.9	-0.000438925937373	17036.9	0.012411717327
17036.95	-0.000373633473388	17036.95	0.0123737294374
17037.0	-0.000292375233255	17037.0	0.0123290426212
17037.05	-0.000202769125896	17037.05	0.0122770508925
17037.1	-0.000112553759382	17037.1	0.0122189131696
17037.15	-2.94500687771e-005	17037.15	0.0121562295968
17037.2	3.88710179806e-005	17037.2	0.0120906003183
17037.25	8.45226675274e-005	17037.25	0.0120236254786
17037.3	0.000100747883656	17037.3	0.011956905222

17037.35	8.83699203447e-005	17037.35	0.0118920396928
17037.4	5.53678328746e-005	17037.4	0.0118306290353
17037.45	9.45457946706e-006	17037.45	0.0117742733939
17037.5	-4.15107649649e-005	17037.5	0.0117245729128
17037.55	-8.96961639728e-005	17037.55	0.0116824959828
17037.6	-0.000127307543942	17037.6	0.01164648398
17037.65	-0.000146373108801	17037.65	0.0116143465267
17037.7	-0.00013981850726	17037.7	0.0115838932456
17037.75	-0.000107317234865	17037.75	0.0115529337589
17037.8	-5.55014721219e-005	17037.8	0.0115192776892
17037.85	9.1802030824e-006	17037.85	0.011480734659
17037.9	8.01448428462e-005	17037.9	0.0114351142906
17037.95	0.000150840012179	17037.95	0.0113802262065
17038.0	0.000214725594417	17038.0	0.0113138800291
17038.05	0.000265182093057	17038.05	0.0112345118155
17038.1	0.00029598366227	17038.1	0.0111430633606
17038.15	0.000304268144056	17038.15	0.0110411028938
17038.2	0.000290955379095	17038.2	0.0109301986447
17038.25	0.000256910696227	17038.25	0.0108119188426
17038.3	0.000203068761322	17038.3	0.0106878317171
17038.35	0.000130340849896	17038.35	0.0105595054976
17038.4	3.966246185e-005	17038.4	0.0104285084136
17038.45	-6.81041864373e-005	17038.45	0.0102964086946

17038.5	-0.000191762503454	17038.5	0.01016477457
17038.55	-0.000326547274524	17038.55	0.01003548771
17038.6	-0.000463140610534	17038.6	0.00991168354743
17038.65	-0.000592194519381	17038.65	0.0097968109559
17038.7	-0.000704294876536	17038.7	0.00969431880899
17038.75	-0.000790034413433	17038.75	0.00960765598025
17038.8	-0.000840044570163	17038.8	0.00954027134325
17038.85	-0.000844795441355	17038.85	0.00949561377157
17038.9	-0.000795503188589	17038.9	0.00947713213877
17038.95	-0.000692964381272	17038.95	0.00948827531843
17039.0	-0.000551244464631	17039.0	0.00953249218411
17039.05	-0.000384703226831	17039.05	0.00961145405427
17039.1	-0.000207871751223	17039.1	0.00971972202689
17039.15	-3.52435794149e-005	17039.15	0.00985007964487
17039.2	0.000118708875209	17039.2	0.00999531045105
17039.25	0.000239391309766	17039.25	0.0101481979883
17039.3	0.000312785246693	17039.3	0.0103015257996
17039.35	0.000334136245647	17039.35	0.0104480774276
17039.4	0.000312597225576	17039.4	0.0105806364154
17039.45	0.00025787073841	17039.45	0.0106919863058
17039.5	0.000179807763163	17039.5	0.0107749106417
17039.55	8.82216111224e-005	17039.55	0.0108242698213
17039.6	-7.0721626037e-006	17039.6	0.0108432316647

17039.65	-9.62293248742e-005	17039.65	0.0108370408474
17039.7	-0.000169559788961	17039.7	0.0108109420448
17039.75	-0.000221362750811	17039.75	0.0107701799324
17039.8	-0.000252675296084	17039.8	0.0107199991857
17039.85	-0.000265000188193	17039.85	0.01066564448
17039.9	-0.000259884859898	17039.9	0.0106123604909
17039.95	-0.00023886465223	17039.95	0.0105653918939
17040.0	-0.0002034786038	17040.0	0.0105299833644
17040.05	-0.000155263054841	17040.05	0.0105095939473
17040.1	-9.57653521963e-005	17040.1	0.0105005401656
17040.15	-2.69951338599e-005	17040.15	0.0104973529118
17040.2	4.81949275962e-005	17040.2	0.0104945630783
17040.25	0.000126874984215	17040.25	0.0104867015577
17040.3	0.000206112239136	17040.3	0.0104682992422
17040.35	0.000282974685648	17040.35	0.0104338870245
17040.4	0.000354530105343	17040.4	0.0103779957969
17040.45	0.000417846336452	17040.45	0.0102951564519
17040.5	0.000470002634987	17040.5	0.010179899882
17040.55	0.000509520406433	17040.55	0.0100291380817
17040.6	0.000537754114235	17040.6	0.00984930745409
17040.65	0.000556388245355	17040.65	0.00964922550428
17040.7	0.000567107342576	17040.7	0.00943770973746
17040.75	0.00057159574008	17040.75	0.00922357765875

17040.8	0.000571538550646	17040.8	0.00901564677331
17040.85	0.000568617981261	17040.85	0.00882273458628
17040.9	0.000564515762415	17040.9	0.00865365860279
17040.95	0.000559442284322	17040.95	0.00851723632802
17041.0	0.000550610035148	17041.0	0.00842228526711
17041.05	0.000534841862325	17041.05	0.00837479284805
17041.1	0.000508965915213	17041.1	0.00836942619022
17041.15	0.000469810273477	17041.15	0.00839802233586
17041.2	0.000414197990842	17041.2	0.0084524183272
17041.25	0.000338972294516	17041.25	0.00852445120646
17041.3	0.000240925717384	17041.3	0.00860595801588
17041.35	0.000120303280277	17041.35	0.00868877579769
17041.4	-1.50931506505e-005	17041.4	0.00876474159412
17041.45	-0.000156259300415	17041.45	0.0088256924474
17041.5	-0.000294235123862	17041.5	0.00886346539976
17041.55	-0.000420051414347	17041.55	0.00887211389966
17041.6	-0.000524731193867	17041.6	0.00885455702045
17041.65	-0.000599337731335	17041.65	0.0088159302417
17041.7	-0.000634809802916	17041.7	0.008761369043
17041.75	-0.000626322529548	17041.75	0.00869600890393
17041.8	-0.000578997643971	17041.8	0.00862498530406
17041.85	-0.000499857311757	17041.85	0.00855343372296
17041.9	-0.000395821765341	17041.9	0.00848648964022

17041.95 -0.000273837678232 17041.95 0.00842928853541

17042.0 -0.00014084903028 17042.0 0.00838696588812

17042.05 -3.78413483188e-006 17042.05 0.00836337597013

17042.1 0.000130370384104 17042.1 0.00835724822214

17042.15 0.000255780550993 17042.15 0.00836603087705

17042.2 0.000369614092114 17042.2 0.00838717216774

17042.25 0.000469771931463 17042.25 0.00841812032714

17042.3 0.000554103298262 17042.3 0.00845632358814

17042.35 0.000620473346204 17042.35 0.00849923018364

17042.4 0.000666736632121 17042.4 0.00854428834655

17042.45 0.000690774175831 17042.45 0.00858894630977

17042.5 0.000690379368418 17042.5 0.00863065230619

17042.55 0.000664688027396 17042.55 0.00866730451396

17042.6 0.000616578858462 17042.6 0.00869860089211

17042.65 0.000549990641322 17042.65 0.00872468934491

17042.7 0.000468781211584 17042.7 0.00874571777665

17042.75 0.000376830909918 17042.75 0.00876183409158

17042.8 0.00027801444078 17042.8 0.00877318619398

17042.85 0.00017620654842 17042.85 0.00877992198813

17042.9 7.52871251358e-005 17042.9 0.00878218937829

17042.95 -2.09290298145e-005 17042.95 0.00878013626873

17043.0 -0.00010882849713 17043.0 0.00877391056373

17043.05 -0.00018486817256 17043.05 0.00876346922287

17043.1	-0.000245497894891	17043.1	0.008748005427
17043.15	-0.000287174187474	17043.15	0.00872652141228
17043.2	-0.00030633430429	17043.2	0.00869801941485
17043.25	-0.000299485892223	17043.25	0.00866150167088
17043.3	-0.000262886053033	17043.3	0.00861597041653
17043.35	-0.000195328121452	17043.35	0.00856042788795
17043.4	-0.000104006738116	17043.4	0.0084938763213
17043.45	5.74818208567e-007	17043.45	0.00841531795274
17043.5	0.000108184513623	17043.5	0.00832375501842
17043.55	0.000208517538252	17043.55	0.00821896920601
17043.6	0.000291262224361	17043.6	0.00810386000921
17043.65	0.00034620711162	17043.65	0.00798210637319
17043.7	0.000362761217346	17043.7	0.00785738724317
17043.75	0.000333746229237	17043.75	0.00773338156435
17043.8	0.00026411597034	17043.8	0.00761376828191
17043.85	0.000164207777171	17043.85	0.00750222634106
17043.9	4.3918986864e-005	17043.9	0.00740243468699
17043.95	-8.67241800216e-005	17043.95	0.0073180722649
17044.0	-0.000217714011394	17044.0	0.00725281801999
17044.05	-0.000339097644786	17044.05	0.00720896126988
17044.1	-0.000440690865368	17044.1	0.00718323282191
17044.15	-0.000514104909036	17044.15	0.00717097385582
17044.2	-0.000558071909476	17044.2	0.00716752555138

17044.25	-0.000575063439346	17044.25	0.00716822908836
17044.3	-0.000567257656559	17044.3	0.00716842564649
17044.35	-0.000536927712852	17044.35	0.00716345640555
17044.4	-0.000486316264058	17044.4	0.00714866254529
17044.45	-0.000417692955789	17044.45	0.00711938524547
17044.5	-0.000333251674429	17044.5	0.00707096568584
17044.55	-0.000235707312585	17044.55	0.00700043803289
17044.6	-0.000130001148648	17044.6	0.00691160839998
17044.65	-2.23744407093e-005	17044.65	0.00680997588718
17044.7	8.10268905162e-005	17044.7	0.00670103959458
17044.75	0.000174029818481	17044.75	0.00659029862226
17044.8	0.00025045054295	17044.8	0.0064832520703
17044.85	0.000304175464261	17044.85	0.00638539903879
17044.9	0.000328825988703	17044.9	0.00630223862779
17044.95	0.000319753973822	17044.95	0.0062392699374
17045.0	0.000280323460321	17045.0	0.0062019920677
17045.05	0.000219081579178	17045.05	0.00619417665596
17045.1	0.000144217582993	17045.1	0.0062126854882
17045.15	6.40439864172e-005	17045.15	0.00625265288766
17045.2	-1.31475539244e-005	17045.2	0.00630921317756
17045.25	-7.91052113052e-005	17045.25	0.00637750068112
17045.3	-0.000125399515897	17045.3	0.00645264972156
17045.35	-0.000144662341758	17045.35	0.00652979462211

17045.4	-0.000135107708321	17045.4	0.006604069706
17045.45	-9.91327247683e-005	17045.45	0.00667060929643
17045.5	-3.88856053994e-005	17045.5	0.00672454771665
17045.55	4.33850590167e-005	17045.55	0.00676188010499
17045.6	0.000145464927014	17045.6	0.00678204486028
17045.65	0.000265103036394	17045.65	0.00678534119648
17045.7	0.000400159409369	17045.7	0.00677206832752
17045.75	0.000547885889007	17045.75	0.00674252546737
17045.8	0.00070203344255	17045.8	0.00669701182997
17045.85	0.000853470620965	17045.85	0.00663582662928
17045.9	0.000993212498591	17045.9	0.00655926907923
17045.95	0.00111221521674	17045.95	0.00646763839378
17046.0	0.00120142915405	17046.0	0.00636123378689
17046.05	0.00125188667298	17046.05	0.00624101613861
17046.1	0.00125430091747	17046.1	0.00611059299342
17046.15	0.00120108223422	17046.15	0.00597423356191
17046.2	0.00109543795418	17046.2	0.00583620705468
17046.25	0.00095031972578	17046.25	0.00570078268233
17046.3	0.000778268101588	17046.3	0.00557222965544
17046.35	0.000592029177451	17046.35	0.0054548171846
17046.4	0.000404308371854	17046.4	0.00535281448041
17046.45	0.000227768269441	17046.45	0.00527049075346
17046.5	7.5282080227e-005	17046.5	0.00521211521435

17046.55	-4.13435090472e-005	17046.55	0.00518065600697
17046.6	-0.000118322118569	17046.6	0.00517387700846
17046.65	-0.000160138393158	17046.65	0.00518824102927
17046.7	-0.000171058234123	17046.7	0.00522021087983
17046.75	-0.00015550919763	17046.75	0.00526624937061
17046.8	-0.000117875305919	17046.8	0.00532281931203
17046.85	-6.2553062072e-005	17046.85	0.00538638351455
17046.9	6.0674040873e-006	17046.9	0.00545340478861
17046.95	8.35794257017e-005	17046.95	0.00552034594466
17047.0	0.000165442475686	17047.0	0.00558366979313
17047.05	0.00024696540638	17047.05	0.00564048977296
17047.1	0.000323458663058	17047.1	0.005690521837
17047.15	0.000390232147718	17047.15	0.00573413256659
17047.2	0.0004425883943	17047.2	0.00577168854305
17047.25	0.000475859952209	17047.25	0.00580355634771
17047.3	0.000485267089626	17047.3	0.00583010256191
17047.35	0.000466556468128	17047.35	0.00585169376698
17047.4	0.000420662902343	17047.4	0.00586869654425
17047.45	0.000354869789396	17047.45	0.00588147747506
17047.5	0.000276455679812	17047.5	0.00589040314074
17047.55	0.000192799944956	17047.55	0.00589593498875
17047.6	0.00011126168176	17047.6	0.00589891393106
17047.65	3.91802640536e-005	17047.65	0.00590027574579

17047.7	-1.60059816333e-005	17047.7	0.00590095621104
17047.75	-4.7321299928e-005	17047.75	0.00590189110492
17047.8	-5.3733950155e-005	17047.8	0.00590401620552
17047.85	-4.24445247267e-005	17047.85	0.00590826729097
17047.9	-2.08362334187e-005	17047.9	0.00591558013936
17047.95	3.60141525003e-006	17047.95	0.00592689052881
17048.0	2.34022951431e-005	17048.0	0.00594313423741
17048.05	3.11130493492e-005	17048.05	0.00596487431306
17048.1	1.92059625206e-005	17048.1	0.00599118288278
17048.15	-1.94952491169e-005	17048.15	0.00602075934336
17048.2	-8.6512764275e-005	17048.2	0.00605230309162
17048.25	-0.000174880737968	17048.25	0.00608451352434
17048.3	-0.000277297793267	17048.3	0.00611609003834
17048.35	-0.000386372246347	17048.35	0.00614573203042
17048.4	-0.000494734349851	17048.4	0.00617213889737
17048.45	-0.000595016917449	17048.45	0.00619401003599
17048.5	-0.000679820605846	17048.5	0.0062100448431
17048.55	-0.000741906531827	17048.55	0.00621917442128
17048.6	-0.000777487153407	17048.6	0.00622125669633
17048.65	-0.000788382010265	17048.65	0.00621638129981
17048.7	-0.000776739986067	17048.7	0.0062046378633
17048.75	-0.000744755182948	17048.75	0.00618611601838
17048.8	-0.000694609575338	17048.8	0.00616090539664

17048.85	-0.00062848843001	17048.85	0.00612909562964
17048.9	-0.000548575972082	17048.9	0.00609077634897
17048.95	-0.000457057666138	17048.95	0.0060460371862
17049.0	-0.000356162091268	17049.0	0.00599496777291
17049.05	-0.000248196568832	17049.05	0.00593796779945
17049.1	-0.000135475623172	17049.1	0.00587667719124
17049.15	-2.03140550967e-005	17049.15	0.00581304593245
17049.2	9.49734086411e-005	17049.2	0.00574902400728
17049.25	0.000208072021464	17049.25	0.00568656139992
17049.3	0.000316667042106	17049.3	0.00562760809454
17049.35	0.000418450068536	17049.35	0.00557411407535
17049.4	0.000511912526035	17049.4	0.00552802932651
17049.45	0.000597117076603	17049.45	0.00549130383222
17049.5	0.000674309424338	17049.5	0.00546588757667
17049.55	0.000743735273319	17049.55	0.00545292138891
17049.6	0.00080564032763	17049.6	0.00545030947751
17049.65	0.000860270291357	17049.65	0.00545514689588
17049.7	0.000907870868574	17049.7	0.00546452869746
17049.75	0.000948687763368	17049.75	0.00547554993569
17049.8	0.000982966679821	17049.8	0.00548530566397
17049.85	0.00101095332202	17049.85	0.00549089093576
17049.9	0.00103289339404	17049.9	0.00548940080447
17049.95	0.00104903259996	17049.95	0.00547793032354

17050.0	0.00105961664388	17050.0	0.00545357454639
17050.05	0.00106489122986	17050.05	0.00541440886276
17050.1	0.001065102062	17050.1	0.00536243000756
17050.15	0.00106049484438	17050.15	0.00530061505202
17050.2	0.00105131528108	17050.2	0.00523194106737
17050.25	0.00103780907617	17050.25	0.00515938512482
17050.3	0.00102022193375	17050.3	0.00508592429561
17050.35	0.0009987995579	17050.35	0.00501453565095
17050.4	0.000973787652694	17050.4	0.00494819626206
17050.45	0.00094543192222	17050.45	0.00488988320018
17050.5	0.000913978070561	17050.5	0.00484257353652
17050.55	0.000879671801797	17050.55	0.00480874176741
17050.6	0.000842758820012	17050.6	0.00478885208955
17050.65	0.000803484829285	17050.65	0.00478286612477
17050.7	0.000762095533704	17050.7	0.00479074549487
17050.75	0.000718836637349	17050.75	0.00481245182166
17050.8	0.000673953844303	17050.8	0.00484794672696
17050.85	0.000627692858647	17050.85	0.00489719183257
17050.9	0.000580299384461	17050.9	0.00496014876032
17050.95	0.000532019125834	17050.95	0.005036779132
17051.0	0.000483097786845	17051.0	0.00512704456944
17051.05	0.000433781071577	17051.05	0.00522996205485
17051.1	0.000384314684112	17051.1	0.00534077001209

Summary of SCM

eqn	S-OH	CO3	UO2	H+
1	1	1	1	-1
2	1	2	1	-1

eqn	S-OH	CO3	UO2	H+
1	1	1	1	-1

eqn	S-OH	CO3	UO2	H+
2	1	2	1	-1

eqn	S-OH	CO3	UO2	H+
3	1	3	1	-1

eqn	S-OH	H20	UO2	H+
4	1		1	-1

eqn	S-OH	H20	UO2	H+
5	1	1	1	-2

eqn	S-OH	H20	UO2	H+
4	1		1	-1
5	1	1	1	-2

KD2

simulation kd

Eqn	Log K	KD Atm pCO2	KD2% pCO2	Kd Ratio (Atm/2%)
1	10.182	8,034	6	1,281
2	17.22	7,975	291	27
3	23.755	7,909	14,783	1
4	2.64	7,976	0.14	56,620
5	-4.23	8,071	0.14	57,107
1,2	10.15, 16.03	7,985	25	321
4,5	`-2.638,-4.23	8,071	0.14	57,107
4,5	4,9, -4.23	1,518,720	25.77	58,926
Experimentally determined				
n/a	n/a	7985 ± 1024	25 ± 1.8	319

Atmospheric pCO2	Concentration (M)	U distribution among soluble uranium
Soluble non-calcium Uranyl carbonates	2.32E-09	0.25%
Calcium uranyl carbonates	9.32E-07	99.75%
Sorbed uranyl carbonates	1.39E-06	
Total soluble uranyl carbonates	9.34E-07	100.00%
Free uranyl ion	1.26E-11	

Ratio

Soluble Species	U(VI) distribution among soluble uranium at Atmospheric P_{CO2}	2% P_{CO2}
Non-calcium uranyl carbonates	0.2%	0.4%
Calcium uranyl carbonates	99.8%	99.6%

2% PCO2	Concentration (M)	U distribution among soluble uranium
Soluble non-calcium Uranyl carbonates	3.63E-09	0.39%
Calcium uranyl carbonates	9.32E-07	99.61%
Sorbed uranyl carbonates	4.65E-07	
Total soluble uranyl carbonates	9.35E-07	
Free uranyl ion	2.26E-14	

System	KD	% sorbed
Atmospheric	7,984.50	99%
2% PCO2	24.85	33%

Reactions 1 and 2 at 2% P_{CO2}															Sorbed	4.65E-07
															Aquous	9.35E-07
															ratio	0.50
															bacteria concentration (kg/L)	0.02
															Kd L/kg	24.85
No temperature corrections performed																
Temperature (K) = 298.1																
Ionic Strength corrections performed:																
Ionic strength = 0.023 Calculated																
Component	Type	Charge	Total(M)	Log Free	Free Molarity											
Ca+2	Total	2	6.55E-03	-2.341	4.57E-03											
SO4-2	Total	-2	8.00E-03	-2.213	6.13E-03											
CO3-2	Total	-2	3.27E-03	-5.629	2.35E-06											
UO2+2	Total	2	1.40E-06	-13.647	2.26E-14											
WOH	Total	0	5.00E-05	-4.305	4.95E-05											
H+	Free	1	0.00E+00	-7	1.00E-07											
H2O	Free	0	5.55E+01	0	1.00E+00											
Species	Type	Molarity	Log M	Delta H	Delta S	Delta G	Log K	Stoichiometry							[UO2]	UO2 distribu
(UO2)2(OH)2+2	Dissolved	4.85E-20	-19.314	48.9	0	0	-5.62		0	0	0	2	0	-2	2	9.71E-20	0.00%
(UO2)2CO3(OH)3-	Dissolved	1.92E-14	-13.717	0	0	0	-0.859		0	0	1	2	0	-3	3	3.84E-14	0.00%
(UO2)2(OH)+3	Dissolved	1.02E-23	-22.993	0	0	0	-2.7		0	0	0	2	0	-1	1	2.03E-23	0.00%
(UO2)3(CO3)6-6	Dissolved	1.92E-21	-20.716	-62.7	0	0	54		0	0	6	3	0	0	0	5.77E-21	0.00%
(UO2)3(OH)4+2	Dissolved	2.28E-26	-25.641	0	0	0	-11.9		0	0	0	3	0	-4	4	6.85E-26	0.00%
(UO2)3(OH)5+	Dissolved	2.76E-23	-22.559	123	0	0	-15.55		0	0	0	3	0	-5	5	8.29E-23	0.00%
(UO2)3(OH)7-	Dissolved	4.55E-26	-25.342	0	0	0	-32.2		0	0	0	3	0	-7	7	1.36E-25	0.00%
(UO2)4(OH)7+	Dissolved	1.11E-29	-28.956	0	0	0	-21.9		0	0	0	4	0	-7	7	4.42E-29	0.00%
Ca2UO2(CO3)3(aq)	Dissolved	7.60E-07	-6.119	0	0	0	30.7		2	0	3	1	0	0	0	7.60E-07	54.25%
CaCO3(aq)	Dissolved	5.19E-06	-5.285	16	0	0	3.22		1	0	1	0	0	0	0	0.00E+00	0.00%
CaHCO3+	Dissolved	1.06E-04	-3.976	0	0	0	11.529		1	0	1	0	0	1	0	0.00E+00	0.00%
CaOH+	Dissolved	4.96E-09	-8.305	64.1	0	0	-12.697		1	0	0	0	0	-1	1	0.00E+00	0.00%
CaSO4(aq)	Dissolved	1.87E-03	-2.728	7.1	0	0	2.36		1	1	0	0	0	0	0	0.00E+00	0.00%
CaUO2(CO3)3-2	Dissolved	1.72E-07	-6.764	0	0	0	27.18		1	0	3	1	0	0	0	1.72E-07	12.29%
H2CO3*(aq)	Dissolved	4.47E-04	-3.349	-32	0	0	16.681		0	0	1	0	0	2	0	0.00E+00	0.00%
HCO3-	Dissolved	2.71E-03	-2.568	-14.6	0	0	10.329		0	0	1	0	0	1	0	0.00E+00	0.00%
HSO4-	Dissolved	3.24E-08	-7.49	22	0	0	1.99		0	1	0	0	0	1	0	0.00E+00	0.00%
UO2(CO3)2-2	Dissolved	1.48E-09	-8.83	18.5	0	0	16.61		0	0	2	1	0	0	0	1.48E-09	0.11%
UO2(CO3)3-4	Dissolved	2.02E-09	-8.695	-39.2	0	0	21.84		0	0	3	1	0	0	0	2.02E-09	0.14%
UO2(OH)2	Dissolved	6.35E-13	-12.197	0	0	0	-12.15		0	0	0	1	0	-2	2	6.35E-13	0.00%
UO2(OH)3-	Dissolved	5.04E-14	-13.297	0	0	0	-20.25		0	0	0	1	0	-3	3	5.04E-14	0.00%
UO2(OH)4-2	Dissolved	4.86E-19	-18.314	0	0	0	-32.4		0	0	0	1	0	-4	4	4.86E-19	0.00%
UO2(SO4)2-2	Dissolved	3.42E-15	-14.466	35.1	0	0	4.14		0	2	0	1	0	0	0	3.42E-15	0.00%
UO2CO3(aq)	Dissolved	1.35E-10	-9.87	5	0	0	9.94		0	0	1	1	0	0	0	1.35E-10	0.01%
UO2OH+	Dissolved	6.86E-13	-12.164	0.9	0	0	-5.25		0	0	0	1	0	-1	1	6.86E-13	0.00%
UO2(SO4)3-4	Dissolved	5.44E-18	-17.265	0	0	0	3.02		0	3	0	1	0	0	0	5.44E-18	0.00%
UO2SO4(aq)	Dissolved	5.71E-14	-13.244	19.5	0	0	3.15		0	1	0	1	0	0	0	5.71E-14	0.00%
OH-	Dissolved	1.01E-07	-6.997	55.8	0	0	-13.997		0	0	0	0	0	-1	1	0.00E+00	0.00%
WOUO2CO3	Dissolved	1.08E-07	-6.966	0	0	0	10.15		0	0	1	1	1	-1	0	1.08E-07	7.73%
WOUO2(CO3)2	Dissolved	3.57E-07	-6.448	0	0	0	16.03		0	0	2	1	1	-1	0	3.57E-07	25.47%
																	100.00%

Reactions 1 and 2 at atmospheric P_{CO2}																Sorbed	1.39E-06
																Aquous	8.71E-09
																ratio	159.69
																bacteria concentration (kg/L)	0.02
																Kd L/kg	7,984.50
No temperature corrections performed																	
Temperature (K) = 298.1																	
Ionic Strength corrections performed:																	
Ionic strength = 0.021 Calculated																	
Component	Type	Charge	Total(M)	Log Free	Free Molarity												
Ca+2	Total	2	6.55E-03	-2.336	4.61E-03												
SO4-2	Total	-2	8.00E-03	-2.217	6.06E-03												
CO3-2	Total	-2	7.21E-05	-7.303	4.98E-08												
UO2+2	Total	2	1.40E-06	-10.899	1.26E-11												
WOH	Total	0	5.00E-05	-4.313	4.86E-05												
H+	Free	1	0.00E+00	-7	1.00E-07												
H2O	Free	0	5.55E+01	0	1.00E+00												
Species	Type	Molarity	Log M	Delta H	Delta S	Delta G	Log K	Stoichiometry								[UO2]	UO2 distribution
(UO2)2(OH)2+2	Dissolved	1.55E-14	-13.809	48.9	0	0	-5.62		0	0	0	2	0	-2	2	3.11E-14	0.00%
(UO2)2CO3(OH)3-	Dissolved	1.35E-10	-9.87	0	0	0	-0.859		0	0	1	2	0	-3	3	2.70E-10	0.02%
(UO2)2(OH)+3	Dissolved	3.17E-18	-17.499	0	0	0	-2.7		0	0	0	2	0	-1	1	6.34E-18	0.00%
(UO2)3(CO3)6-6	Dissolved	3.05E-23	-22.516	-62.7	0	0	54		0	0	6	3	0	0	0	9.14E-23	0.00%
(UO2)3(OH)4+2	Dissolved	4.19E-18	-17.378	0	0	0	-11.9		0	0	0	3	0	-4	4	1.26E-17	0.00%
(UO2)3(OH)5+	Dissolved	5.16E-15	-14.288	123	0	0	-15.55		0	0	0	3	0	-5	5	1.55E-14	0.00%
(UO2)3(OH)7-	Dissolved	8.56E-18	-17.068	0	0	0	-32.2		0	0	0	3	0	-7	7	2.57E-17	0.00%
(UO2)4(OH)7+	Dissolved	1.18E-18	-17.927	0	0	0	-21.9		0	0	0	4	0	-7	7	4.73E-18	0.00%
Ca2UO2(CO3)3(aq)	Dissolved	4.57E-09	-8.34	0	0	0	30.7		2	0	3	1	0	0	0	4.57E-09	0.33%
CaCO3(aq)	Dissolved	1.15E-07	-6.939	16	0	0	3.22		1	0	1	0	0	0	0	0.00E+00	0.00%
CaHCO3+	Dissolved	2.35E-06	-5.63	0	0	0	11.529		1	0	1	0	0	1	0	0.00E+00	0.00%
CaOH+	Dissolved	5.09E-09	-8.293	64.1	0	0	-12.697		1	0	0	0	0	-1	1	0.00E+00	0.00%
CaSO4(aq)	Dissolved	1.94E-03	-2.713	7.1	0	0	2.36		1	1	0	0	0	0	0	0.00E+00	0.00%
CaUO2(CO3)3-2	Dissolved	9.91E-10	-9.004	0	0	0	27.18		1	0	3	1	0	0	0	9.91E-10	0.07%
H2CO3*(aq)	Dissolved	9.73E-06	-5.012	-32	0	0	16.681		0	0	1	0	0	2	0	0.00E+00	0.00%
HCO3-	Dissolved	5.84E-05	-4.234	-14.6	0	0	10.329		0	0	1	0	0	1	0	0.00E+00	0.00%
HSO4-	Dissolved	3.26E-08	-7.487	22	0	0	1.99		0	1	0	0	0	1	0	0.00E+00	0.00%
UO2(CO3)2-2	Dissolved	3.85E-10	-9.415	18.5	0	0	16.61		0	0	2	1	0	0	0	3.85E-10	0.03%
UO2(CO3)3-4	Dissolved	1.08E-11	-10.968	-39.2	0	0	21.84		0	0	3	1	0	0	0	1.08E-11	0.00%
UO2(OH)2	Dissolved	3.64E-10	-9.439	0	0	0	-12.15		0	0	0	1	0	-2	2	3.64E-10	0.03%
UO2(OH)3-	Dissolved	2.89E-11	-10.539	0	0	0	-20.25		0	0	0	1	0	-3	3	2.89E-11	0.00%
UO2(OH)4-2	Dissolved	2.76E-16	-15.559	0	0	0	-32.4		0	0	0	1	0	-4	4	2.76E-16	0.00%
UO2(SO4)2-2	Dissolved	1.93E-12	-11.714	35.1	0	0	4.14		0	2	0	1	0	0	0	1.93E-12	0.00%
UO2CO3(aq)	Dissolved	1.65E-09	-8.782	5	0	0	9.94		0	0	1	1	0	0	0	1.65E-09	0.12%
UO2OH+	Dissolved	3.90E-10	-9.409	0.9	0	0	-5.25		0	0	0	1	0	-1	1	3.90E-10	0.03%
UO2(SO4)3-4	Dissolved	2.94E-15	-14.531	0	0	0	3.02		0	3	0	1	0	0	0	2.94E-15	0.00%
UO2SO4(aq)	Dissolved	3.26E-11	-10.486	19.5	0	0	3.15		0	1	0	1	0	0	0	3.26E-11	0.00%
OH-	Dissolved	1.01E-07	-6.997	55.8	0	0	-13.997		0	0	0	0	0	-1	1	0.00E+00	0.00%
WOUO2CO3	Dissolved	1.30E-06	-5.885	0	0	0	10.15		0	0	1	1	1	-1	0	1.30E-06	92.93%
WOUO2(CO3)2	Dissolved	8.94E-08	-7.049	0	0	0	16.03		0	0	2	1	1	-1	0	8.94E-08	6.39%
																	99.94%

Reaction 1 at atmospheric P_{CO2}																Sorbed	1.39E-06
																Aquous	8.66E-09
																ratio	160.68
																bacteria concentration (kg/L)	0.02
																Kd L/kg	8,033.99
No temperature corrections performed																	
Temperature (K) = 298.1																	
Ionic Strength corrections performed:																	
Ionic strength = 0.021 Calculated																	
Component	Type	Charge	Total(M)	Log Free	Free Molarity												
Ca+2	Total	2	6.55E-03	-2.336	4.61E-03												
SO4-2	Total	-2	8.00E-03	-2.217	6.06E-03												
CO3-2	Total	-2	7.21E-05	-7.302	4.98E-08												
UO2+2	Total	2	1.40E-06	-10.903	1.25E-11												
WOH	Total	0	5.00E-05	-4.313	4.86E-05												
H+	Free	1	0.00E+00	-7	1.00E-07												
H2O	Free	0	5.55E+01	0	1.00E+00												
Species	Type	Molarity	Log M	Delta H	Delta S	Delta G	Log K	Stoichiometry								[UO2]	UO2 distribution
(UO2)2(OH)2+2	Dissolved	1.53E-14	-13.816	48.9	0	0	-5.62		0	0	0	2	0	-2	2	3.06E-14	0.00%
(UO2)2CO3(OH)3-	Dissolved	1.33E-10	-9.877	0	0	0	-0.859		0	0	1	2	0	-3	3	2.65E-10	0.02%
(UO2)2(OH)+3	Dissolved	3.12E-18	-17.506	0	0	0	-2.7		0	0	0	2	0	-1	1	6.24E-18	0.00%
(UO2)3(CO3)6-6	Dissolved	2.99E-23	-22.524	-62.7	0	0	54		0	0	6	3	0	0	0	8.98E-23	0.00%
(UO2)3(OH)4+2	Dissolved	4.09E-18	-17.389	0	0	0	-11.9		0	0	0	3	0	-4	4	1.23E-17	0.00%
(UO2)3(OH)5+	Dissolved	5.03E-15	-14.299	123	0	0	-15.55		0	0	0	3	0	-5	5	1.51E-14	0.00%
(UO2)3(OH)7-	Dissolved	8.34E-18	-17.079	0	0	0	-32.2		0	0	0	3	0	-7	7	2.50E-17	0.00%
(UO2)4(OH)7+	Dissolved	1.14E-18	-17.942	0	0	0	-21.9		0	0	0	4	0	-7	7	4.57E-18	0.00%
Ca2UO2(CO3)3(aq)	Dissolved	4.55E-09	-8.342	0	0	0	30.7		2	0	3	1	0	0	0	4.55E-09	0.33%
CaCO3(aq)	Dissolved	1.15E-07	-6.938	16	0	0	3.22		1	0	1	0	0	0	0	0.00E+00	0.00%
CaHCO3+	Dissolved	2.35E-06	-5.629	0	0	0	11.529		1	0	1	0	0	1	0	0.00E+00	0.00%
CaOH+	Dissolved	5.09E-09	-8.293	64.1	0	0	-12.697		1	0	0	0	0	-1	1	0.00E+00	0.00%
CaSO4(aq)	Dissolved	1.94E-03	-2.713	7.1	0	0	2.36		1	1	0	0	0	0	0	0.00E+00	0.00%
CaUO2(CO3)3-2	Dissolved	9.86E-10	-9.006	0	0	0	27.18		1	0	3	1	0	0	0	9.86E-10	0.07%
H2CO3*(aq)	Dissolved	9.74E-06	-5.011	-32	0	0	16.681		0	0	1	0	0	2	0	0.00E+00	0.00%
HCO3-	Dissolved	5.84E-05	-4.233	-14.6	0	0	10.329		0	0	1	0	0	1	0	0.00E+00	0.00%
HSO4-	Dissolved	3.26E-08	-7.487	22	0	0	1.99		0	1	0	0	0	1	0	0.00E+00	0.00%
UO2(CO3)2-2	Dissolved	3.82E-10	-9.418	18.5	0	0	16.61		0	0	2	1	0	0	0	3.82E-10	0.03%
UO2(CO3)3-4	Dissolved	1.07E-11	-10.97	-39.2	0	0	21.84		0	0	3	1	0	0	0	1.07E-11	0.00%
UO2(OH)2	Dissolved	3.61E-10	-9.443	0	0	0	-12.15		0	0	0	1	0	-2	2	3.61E-10	0.03%
UO2(OH)3-	Dissolved	2.87E-11	-10.543	0	0	0	-20.25		0	0	0	1	0	-3	3	2.87E-11	0.00%
UO2(OH)4-2	Dissolved	2.74E-16	-15.563	0	0	0	-32.4		0	0	0	1	0	-4	4	2.74E-16	0.00%
UO2(SO4)2-2	Dissolved	1.92E-12	-11.717	35.1	0	0	4.14		0	2	0	1	0	0	0	1.92E-12	0.00%
UO2CO3(aq)	Dissolved	1.64E-09	-8.785	5	0	0	9.94		0	0	1	1	0	0	0	1.64E-09	0.12%
UO2OH+	Dissolved	3.86E-10	-9.413	0.9	0	0	-5.25		0	0	0	1	0	-1	1	3.86E-10	0.03%
UO2(SO4)3-4	Dissolved	2.92E-15	-14.535	0	0	0	3.02		0	3	0	1	0	0	0	2.92E-15	0.00%
UO2SO4(aq)	Dissolved	3.24E-11	-10.49	19.5	0	0	3.15		0	1	0	1	0	0	0	3.24E-11	0.00%
OH-	Dissolved	1.01E-07	-6.997	55.8	0	0	-13.997		0	0	0	0	0	-1	1	0.00E+00	0.00%
WOUO2CO3	Dissolved	1.39E-06	-5.857	0	0	0	10.182		0	0	1	1	1	-1	0	1.39E-06	99.36%
																0.00E+00	0.00%
																	99.97%

Reaction 1 at 2% P_{CO2}																Sorbed	1.56E-07
																Aquous	1.24E-06
																ratio	0.13
																bacteria concentration (kg/L)	0.02
																Kd L/kg	6.27
No temperature corrections performed																	
Temperature (K) = 298.1																	
Ionic Strength corrections performed:																	
Ionic strength = 0.023 Calculated																	
Component	Type	Charge	Total(M)	Log Free	Free Molarity												
Ca+2	Total	2	6.55E-03	-2.341	4.57E-03												
SO4-2	Total	-2	8.00E-03	-2.213	6.13E-03												
CO3-2	Total	-2	3.27E-03	-5.63	2.35E-06												
UO2+2	Total	2	1.40E-06	-13.522	3.00E-14												
WOH	Total	0	5.00E-05	-4.302	4.98E-05												
H+	Free	1	0.00E+00	-7	1.00E-07												
H2O	Free	0	5.55E+01	0	1.00E+00												
Species	Type	Molarity	Log M	Delta H	Delta S	Delta G	Log K	Stoichiometry								[UO2]	UO2 distribution
(UO2)2(OH)2+2	Dissolved	8.60E-20	-19.066	48.9	0	0	-5.62		0	0	0	2	0	-2	2	1.72E-19	0.00%
(UO2)2CO3(OH)3-	Dissolved	3.40E-14	-13.469	0	0	0	-0.859		0	0	1	2	0	-3	3	6.80E-14	0.00%
(UO2)2(OH)+3	Dissolved	1.80E-23	-22.745	0	0	0	-2.7		0	0	0	2	0	-1	1	3.60E-23	0.00%
(UO2)3(CO3)6-6	Dissolved	4.53E-21	-20.344	-62.7	0	0	54		0	0	6	3	0	0	0	1.36E-20	0.00%
(UO2)3(OH)4+2	Dissolved	5.38E-26	-25.269	0	0	0	-11.9		0	0	0	3	0	-4	4	1.61E-25	0.00%
(UO2)3(OH)5+	Dissolved	6.51E-23	-22.186	123	0	0	-15.55		0	0	0	3	0	-5	5	1.95E-22	0.00%
(UO2)3(OH)7-	Dissolved	1.07E-25	-24.97	0	0	0	-32.2		0	0	0	3	0	-7	7	3.22E-25	0.00%
(UO2)4(OH)7+	Dissolved	3.47E-29	-28.459	0	0	0	-21.9		0	0	0	4	0	-7	7	1.39E-28	0.00%
Ca2UO2(CO3)3(aq)	Dissolved	1.01E-06	-5.996	0	0	0	30.7		2	0	3	1	0	0	0	1.01E-06	72.14%
CaCO3(aq)	Dissolved	5.19E-06	-5.285	16	0	0	3.22		1	0	1	0	0	0	0	0.00E+00	0.00%
CaHCO3+	Dissolved	1.06E-04	-3.976	0	0	0	11.529		1	0	1	0	0	1	0	0.00E+00	0.00%
CaOH+	Dissolved	4.96E-09	-8.305	64.1	0	0	-12.697		1	0	0	0	0	-1	1	0.00E+00	0.00%
CaSO4(aq)	Dissolved	1.87E-03	-2.728	7.1	0	0	2.36		1	1	0	0	0	0	0	0.00E+00	0.00%
CaUO2(CO3)3-2	Dissolved	2.29E-07	-6.64	0	0	0	27.18		1	0	3	1	0	0	0	2.29E-07	16.34%
H2CO3*(aq)	Dissolved	4.47E-04	-3.349	-32	0	0	16.681		0	0	1	0	0	2	0	0.00E+00	0.00%
HCO3-	Dissolved	2.71E-03	-2.568	-14.6	0	0	10.329		0	0	1	0	0	1	0	0.00E+00	0.00%
HSO4-	Dissolved	3.24E-08	-7.49	22	0	0	1.99		0	1	0	0	0	1	0	0.00E+00	0.00%
UO2(CO3)2-2	Dissolved	1.97E-09	-8.706	18.5	0	0	16.61		0	0	2	1	0	0	0	1.97E-09	0.14%
UO2(CO3)3-4	Dissolved	2.69E-09	-8.571	-39.2	0	0	21.84		0	0	3	1	0	0	0	2.69E-09	0.19%
UO2(OH)2	Dissolved	8.45E-13	-12.073	0	0	0	-12.15		0	0	0	1	0	-2	2	8.45E-13	0.00%
UO2(OH)3-	Dissolved	6.71E-14	-13.173	0	0	0	-20.25		0	0	0	1	0	-3	3	6.71E-14	0.00%
UO2(OH)4-2	Dissolved	6.46E-19	-18.19	0	0	0	-32.4		0	0	0	1	0	-4	4	6.46E-19	0.00%
UO2(SO4)2-2	Dissolved	4.55E-15	-14.342	35.1	0	0	4.14		0	2	0	1	0	0	0	4.55E-15	0.00%
UO2CO3(aq)	Dissolved	1.79E-10	-9.746	5	0	0	9.94		0	0	1	1	0	0	0	1.79E-10	0.01%
UO2OH+	Dissolved	9.13E-13	-12.04	0.9	0	0	-5.25		0	0	0	1	0	-1	1	9.13E-13	0.00%
UO2(SO4)3-4	Dissolved	7.24E-18	-17.14	0	0	0	3.02		0	3	0	1	0	0	0	7.24E-18	0.00%
UO2SO4(aq)	Dissolved	7.59E-14	-13.12	19.5	0	0	3.15		0	1	0	1	0	0	0	7.59E-14	0.00%
OH-	Dissolved	1.01E-07	-6.997	55.8	0	0	-13.997		0	0	0	0	0	-1	1	0.00E+00	0.00%
WOUO2CO3	Dissolved	1.56E-07	-6.807	0	0	0	10.182		0	0	1	1	1	-1	0	1.56E-07	11.14%
																0.00E+00	0.00%
																	99.97%

Reaction 2 at atmospheric $_{PCO2}$																Sorbed	1.39E-06
																Aquous	8.72E-09
																ratio	159.49
																bacteria concentration (kg/L)	0.02
																Kd L/kg	7,974.73
No temperature corrections performed																	
Temperature (K) = 298.1																	
Ionic Strength corrections performed:																	
Ionic strength = 0.021 Calculated																	
Component	Type	Charge	Total(M)	Log Free	Free Molarity												
Ca+2	Total	2	6.55E-03	-2.336	4.61E-03												
SO4-2	Total	-2	8.00E-03	-2.217	6.06E-03												
CO3-2	Total	-2	7.21E-05	-7.311	4.89E-08												
UO2+2	Total	2	1.40E-06	-10.882	1.31E-11												
WOH	Total	0	5.00E-05	-4.313	4.86E-05												
H+	Free	1	0.00E+00	-7	1.00E-07												
H2O	Free	0	5.55E+01	0	1.00E+00												
Species	Type	Molarity	Log M	Delta H	Delta S	Delta G	Log K	Stoichiometry								[UO2]	UO2 distribution
(UO2)2(OH)2+2	Dissolved	1.69E-14	-13.773	48.9	0	0	-5.62		0	0	0	2	0	-2	2	3.37E-14	0.00%
(UO2)2CO3(OH)3-	Dissolved	1.44E-10	-9.843	0	0	0	-0.859		0	0	1	2	0	-3	3	2.87E-10	0.02%
(UO2)2(OH)+3	Dissolved	3.44E-18	-17.463	0	0	0	-2.7		0	0	0	2	0	-1	1	6.89E-18	0.00%
(UO2)3(CO3)6-6	Dissolved	3.09E-23	-22.51	-62.7	0	0	54		0	0	6	3	0	0	0	9.27E-23	0.00%
(UO2)3(OH)4+2	Dissolved	4.74E-18	-17.324	0	0	0	-11.9		0	0	0	3	0	-4	4	1.42E-17	0.00%
(UO2)3(OH)5+	Dissolved	5.83E-15	-14.234	123	0	0	-15.55		0	0	0	3	0	-5	5	1.75E-14	0.00%
(UO2)3(OH)7-	Dissolved	9.68E-18	-17.014	0	0	0	-32.2		0	0	0	3	0	-7	7	2.90E-17	0.00%
(UO2)4(OH)7+	Dissolved	1.39E-18	-17.856	0	0	0	-21.9		0	0	0	4	0	-7	7	5.57E-18	0.00%
Ca2UO2(CO3)3(aq)	Dissolved	4.51E-09	-8.346	0	0	0	30.7		2	0	3	1	0	0	0	4.51E-09	0.32%
CaCO3(aq)	Dissolved	1.13E-07	-6.947	16	0	0	3.22		1	0	1	0	0	0	0	0.00E+00	0.00%
CaHCO3+	Dissolved	2.30E-06	-5.638	0	0	0	11.529		1	0	1	0	0	1	0	0.00E+00	0.00%
CaOH+	Dissolved	5.09E-09	-8.293	64.1	0	0	-12.697		1	0	0	0	0	-1	1	0.00E+00	0.00%
CaSO4(aq)	Dissolved	1.94E-03	-2.713	7.1	0	0	2.36		1	1	0	0	0	0	0	0.00E+00	0.00%
CaUO2(CO3)3-2	Dissolved	9.77E-10	-9.01	0	0	0	27.18		1	0	3	1	0	0	0	9.77E-10	0.07%
H2CO3*(aq)	Dissolved	9.55E-06	-5.02	-32	0	0	16.681		0	0	1	0	0	2	0	0.00E+00	0.00%
HCO3-	Dissolved	5.73E-05	-4.242	-14.6	0	0	10.329		0	0	1	0	0	1	0	0.00E+00	0.00%
HSO4-	Dissolved	3.26E-08	-7.487	22	0	0	1.99		0	1	0	0	0	1	0	0.00E+00	0.00%
UO2(CO3)2-2	Dissolved	3.86E-10	-9.413	18.5	0	0	16.61		0	0	2	1	0	0	0	3.86E-10	0.03%
UO2(CO3)3-4	Dissolved	1.06E-11	-10.974	-39.2	0	0	21.84		0	0	3	1	0	0	0	1.06E-11	0.00%
UO2(OH)2	Dissolved	3.79E-10	-9.421	0	0	0	-12.15		0	0	0	1	0	-2	2	3.79E-10	0.03%
UO2(OH)3-	Dissolved	3.01E-11	-10.521	0	0	0	-20.25		0	0	0	1	0	-3	3	3.01E-11	0.00%
UO2(OH)4-2	Dissolved	2.87E-16	-15.541	0	0	0	-32.4		0	0	0	1	0	-4	4	2.87E-16	0.00%
UO2(SO4)2-2	Dissolved	2.01E-12	-11.696	35.1	0	0	4.14		0	2	0	1	0	0	0	2.01E-12	0.00%
UO2CO3(aq)	Dissolved	1.69E-09	-8.772	5	0	0	9.94		0	0	1	1	0	0	0	1.69E-09	0.12%
UO2OH+	Dissolved	4.06E-10	-9.391	0.9	0	0	-5.25		0	0	0	1	0	-1	1	4.06E-10	0.03%
UO2(SO4)3-4	Dissolved	3.07E-15	-14.513	0	0	0	3.02		0	3	0	1	0	0	0	3.07E-15	0.00%
UO2SO4(aq)	Dissolved	3.40E-11	-10.469	19.5	0	0	3.15		0	1	0	1	0	0	0	3.40E-11	0.00%
OH-	Dissolved	1.01E-07	-6.997	55.8	0	0	-13.997		0	0	0	0	0	-1	1	0.00E+00	0.00%
WOUO2(CO3)2	Dissolved	1.39E-06	-5.857	0	0	0	17.22		0	0	2	1	1	-1	0	1.39E-06	99.36%
																0.00E+00	0.00%
																	99.98%

Reaction 2 at 2% P_{CO2}																Sorbed	1.19E-06
																Aquous	2.05E-07
																ratio	5.81
																bacteria concentration (kg/L)	0.02
																Kd L/kg	290.70
No temperature corrections performed																	
Temperature (K) = 298.1																	
Ionic Strength corrections performed:																	
Ionic strength = 0.023 Calculated																	
Component	Type	Charge	Total(M)	Log Free	Free Molarity												
Ca+2	Total	2	6.55E-03	-2.34	4.57E-03												
SO4-2	Total	-2	8.00E-03	-2.213	6.13E-03												
CO3-2	Total	-2	3.27E-03	-5.629	2.35E-06												
UO2+2	Total	2	1.40E-06	-14.305	4.95E-15												
WOH	Total	0	5.00E-05	-4.312	4.88E-05												
H+	Free	1	0.00E+00	-7	1.00E-07												
H2O	Free	0	5.55E+01	0	1.00E+00												
Species	Type	Molarity	Log M	Delta H	Delta S	Delta G	Log K	Stoichiometry								[UO2]	UO2 distribution
(UO2)2(OH)2+2	Dissolved	2.34E-21	-20.631	48.9	0	0	-5.62		0	0	0	2	0	-2	2	4.67E-21	0.00%
(UO2)2CO3(OH)3-	Dissolved	9.24E-16	-15.034	0	0	0	-0.859		0	0	1	2	0	-3	3	1.85E-15	0.00%
(UO2)2(OH)+3	Dissolved	4.89E-25	-24.31	0	0	0	-2.7		0	0	0	2	0	-1	1	9.79E-25	0.00%
(UO2)3(CO3)6-6	Dissolved	2.03E-23	-22.692	-62.7	0	0	54		0	0	6	3	0	0	0	6.10E-23	0.00%
(UO2)3(OH)4+2	Dissolved	2.41E-28	-27.618	0	0	0	-11.9		0	0	0	3	0	-4	4	7.24E-28	0.00%
(UO2)3(OH)5+	Dissolved	2.92E-25	-24.535	123	0	0	-15.55		0	0	0	3	0	-5	5	8.76E-25	0.00%
(UO2)3(OH)7-	Dissolved	4.80E-28	-27.318	0	0	0	-32.2		0	0	0	3	0	-7	7	1.44E-27	0.00%
(UO2)4(OH)7+	Dissolved	2.57E-32	-31.591	0	0	0	-21.9		0	0	0	4	0	-7	7	1.03E-31	0.00%
Ca2UO2(CO3)3(aq)	Dissolved	1.67E-07	-6.778	0	0	0	30.7		2	0	3	1	0	0	0	1.67E-07	11.91%
CaCO3(aq)	Dissolved	5.20E-06	-5.284	16	0	0	3.22		1	0	1	0	0	0	0	0.00E+00	0.00%
CaHCO3+	Dissolved	1.06E-04	-3.975	0	0	0	11.529		1	0	1	0	0	1	0	0.00E+00	0.00%
CaOH+	Dissolved	4.96E-09	-8.305	64.1	0	0	-12.697		1	0	0	0	0	-1	1	0.00E+00	0.00%
CaSO4(aq)	Dissolved	1.87E-03	-2.728	7.1	0	0	2.36		1	1	0	0	0	0	0	0.00E+00	0.00%
CaUO2(CO3)3-2	Dissolved	3.78E-08	-7.423	0	0	0	27.18		1	0	3	1	0	0	0	3.78E-08	2.70%
H2CO3*(aq)	Dissolved	4.47E-04	-3.349	-32	0	0	16.681		0	0	1	0	0	2	0	0.00E+00	0.00%
HCO3-	Dissolved	2.71E-03	-2.568	-14.6	0	0	10.329		0	0	1	0	0	1	0	0.00E+00	0.00%
HSO4-	Dissolved	3.24E-08	-7.49	22	0	0	1.99		0	1	0	0	0	1	0	0.00E+00	0.00%
UO2(CO3)2-2	Dissolved	3.25E-10	-9.489	18.5	0	0	16.61		0	0	2	1	0	0	0	3.25E-10	0.02%
UO2(CO3)3-4	Dissolved	4.43E-10	-9.353	-39.2	0	0	21.84		0	0	3	1	0	0	0	4.43E-10	0.03%
UO2(OH)2	Dissolved	1.39E-13	-12.856	0	0	0	-12.15		0	0	0	1	0	-2	2	1.39E-13	0.00%
UO2(OH)3-	Dissolved	1.11E-14	-13.956	0	0	0	-20.25		0	0	0	1	0	-3	3	1.11E-14	0.00%
UO2(OH)4-2	Dissolved	1.07E-19	-18.973	0	0	0	-32.4		0	0	0	1	0	-4	4	1.07E-19	0.00%
UO2(SO4)2-2	Dissolved	7.50E-16	-15.125	35.1	0	0	4.14		0	2	0	1	0	0	0	7.50E-16	0.00%
UO2CO3(aq)	Dissolved	2.96E-11	-10.529	5	0	0	9.94		0	0	1	1	0	0	0	2.96E-11	0.00%
UO2OH+	Dissolved	1.51E-13	-12.823	0.9	0	0	-5.25		0	0	0	1	0	-1	1	1.51E-13	0.00%
UO2(SO4)3-4	Dissolved	1.19E-18	-17.923	0	0	0	3.02		0	3	0	1	0	0	0	1.19E-18	0.00%
UO2SO4(aq)	Dissolved	1.25E-14	-13.902	19.5	0	0	3.15		0	1	0	1	0	0	0	1.25E-14	0.00%
OH-	Dissolved	1.01E-07	-6.997	55.8	0	0	-13.997		0	0	0	0	0	-1	1	0.00E+00	0.00%
WOUO2(CO3)2	Dissolved	1.19E-06	-5.923	0	0	0	17.22		0	0	2	1	1	-1	0	1.19E-06	85.29%
																0.00E+00	0.00%
																	99.95%

Reaction 3 at atmospheric P_{CO2}																Sorbed	1.39E-06
																Aquous	8.79E-09
																ratio	158.19
																bacteria concentration (kg/L)	0.02
																Kd L/kg	7,909.48
No temperature corrections performed																	
Temperature (K) = 298.1																	
Ionic Strength corrections performed:																	
Ionic strength = 0.021 Calculated																	
Component	Type	Charge	Total(M)	Log Free	Free Molarity												
Ca+2	Total	2	6.55E-03	-2.336	4.61E-03												
SO4-2	Total	-2	8.00E-03	-2.217	6.07E-03												
CO3-2	Total	-2	7.21E-05	-7.32	4.79E-08												
UO2+2	Total	2	1.40E-06	-10.859	1.38E-11												
WOH	Total	0	5.00E-05	-4.313	4.86E-05												
H+	Free	1	0.00E+00	-7	1.00E-07												
H2O	Free	0	5.55E+01	0	1.00E+00												
Species	Type	Molarity	Log M	Delta H	Delta S	Delta G	Log K	Stoichiometry								[UO2]	UO2 distribution
(UO2)2(OH)2+2	Dissolved	1.87E-14	-13.729	48.9	0	0	-5.62		0	0	0	2	0	-2	2	3.74E-14	0.00%
(UO2)2CO3(OH)3-	Dissolved	1.56E-10	-9.807	0	0	0	-0.859		0	0	1	2	0	-3	3	3.12E-10	0.02%
(UO2)2(OH)+3	Dissolved	3.81E-18	-17.419	0	0	0	-2.7		0	0	0	2	0	-1	1	7.63E-18	0.00%
(UO2)3(CO3)6-6	Dissolved	3.19E-23	-22.496	-62.7	0	0	54		0	0	6	3	0	0	0	9.58E-23	0.00%
(UO2)3(OH)4+2	Dissolved	5.52E-18	-17.258	0	0	0	-11.9		0	0	0	3	0	-4	4	1.66E-17	0.00%
(UO2)3(OH)5+	Dissolved	6.79E-15	-14.168	123	0	0	-15.55		0	0	0	3	0	-5	5	2.04E-14	0.00%
(UO2)3(OH)7-	Dissolved	1.13E-17	-16.948	0	0	0	-32.2		0	0	0	3	0	-7	7	3.38E-17	0.00%
(UO2)4(OH)7+	Dissolved	1.71E-18	-17.767	0	0	0	-21.9		0	0	0	4	0	-7	7	6.83E-18	0.00%
Ca2UO2(CO3)3(aq)	Dissolved	4.46E-09	-8.35	0	0	0	30.7		2	0	3	1	0	0	0	4.46E-09	0.32%
CaCO3(aq)	Dissolved	1.11E-07	-6.956	16	0	0	3.22		1	0	1	0	0	0	0	0.00E+00	0.00%
CaHCO3+	Dissolved	2.26E-06	-5.647	0	0	0	11.529		1	0	1	0	0	1	0	0.00E+00	0.00%
CaOH+	Dissolved	5.09E-09	-8.293	64.1	0	0	-12.697		1	0	0	0	0	-1	1	0.00E+00	0.00%
CaSO4(aq)	Dissolved	1.94E-03	-2.713	7.1	0	0	2.36		1	1	0	0	0	0	0	0.00E+00	0.00%
CaUO2(CO3)3-2	Dissolved	9.67E-10	-9.014	0	0	0	27.18		1	0	3	1	0	0	0	9.67E-10	0.07%
H2CO3*(aq)	Dissolved	9.36E-06	-5.029	-32	0	0	16.681		0	0	1	0	0	2	0	0.00E+00	0.00%
HCO3-	Dissolved	5.62E-05	-4.251	-14.6	0	0	10.329		0	0	1	0	0	1	0	0.00E+00	0.00%
HSO4-	Dissolved	3.26E-08	-7.487	22	0	0	1.99		0	1	0	0	0	1	0	0.00E+00	0.00%
UO2(CO3)2-2	Dissolved	3.90E-10	-9.409	18.5	0	0	16.61		0	0	2	1	0	0	0	3.90E-10	0.03%
UO2(CO3)3-4	Dissolved	1.05E-11	-10.978	-39.2	0	0	21.84		0	0	3	1	0	0	0	1.05E-11	0.00%
UO2(OH)2	Dissolved	3.99E-10	-9.399	0	0	0	-12.15		0	0	0	1	0	-2	2	3.99E-10	0.03%
UO2(OH)3-	Dissolved	3.17E-11	-10.499	0	0	0	-20.25		0	0	0	1	0	-3	3	3.17E-11	0.00%
UO2(OH)4-2	Dissolved	3.02E-16	-15.519	0	0	0	-32.4		0	0	0	1	0	-4	4	3.02E-16	0.00%
UO2(SO4)2-2	Dissolved	2.12E-12	-11.674	35.1	0	0	4.14		0	2	0	1	0	0	0	2.12E-12	0.00%
UO2CO3(aq)	Dissolved	1.74E-09	-8.759	5	0	0	9.94		0	0	1	1	0	0	0	1.74E-09	0.12%
UO2OH+	Dissolved	4.27E-10	-9.369	0.9	0	0	-5.25		0	0	0	1	0	-1	1	4.27E-10	0.03%
UO2(SO4)3-4	Dissolved	3.23E-15	-14.491	0	0	0	3.02		0	3	0	1	0	0	0	3.23E-15	0.00%
UO2SO4(aq)	Dissolved	3.58E-11	-10.447	19.5	0	0	3.15		0	1	0	1	0	0	0	3.58E-11	0.00%
OH-	Dissolved	1.01E-07	-6.997	55.8	0	0	-13.997		0	0	0	0	0	-1	1	0.00E+00	0.00%
WOUO2(CO3)3	Dissolved	1.39E-06	-5.857	0	0	0	23.755		0	0	3	1	1	-1	0	1.39E-06	99.36%
																0.00E+00	0.00%
																1.40E-06	99.98%

Reaction 3 at 2% P_{CO2}																Sorbed	1.40E-06
																Aquous	4.72E-09
																ratio	295.65
																bacteria concentration (kg/L)	0.02
																Kd L/kg	14,782.73
No temperature corrections performed																	
Temperature (K) = 298.1																	
Ionic Strength corrections performed:																	
Ionic strength = 0.023 Calculated																	
Component	Type	Charge	Total(M)	Log Free	Free Molarity												
Ca+2	Total	2	6.55E-03	-2.34	4.57E-03												
SO4-2	Total	-2	8.00E-03	-2.213	6.13E-03												
CO3-2	Total	-2	3.27E-03	-5.629	2.35E-06												
UO2+2	Total	2	1.40E-06	-15.943	1.14E-16												
WOH	Total	0	5.00E-05	-4.313	4.86E-05												
H+	Free	1	0.00E+00	-7	1.00E-07												
H2O	Free	0	5.55E+01	0	1.00E+00												
Species	Type	Molarity	Log M	Delta H	Delta S	Delta G	Log K	Stoichiometry								[UO2]	UO2 distribution
(UO2)2(OH)2+2	Dissolved	1.24E-24	-23.908	48.9	0	0	-5.62		0	0	0	2	0	-2	2	2.47E-24	0.00%
(UO2)2CO3(OH)3-	Dissolved	4.89E-19	-18.311	0	0	0	-0.859		0	0	1	2	0	-3	3	9.78E-19	0.00%
(UO2)2(OH)+3	Dissolved	2.59E-28	-27.587	0	0	0	-2.7		0	0	0	2	0	-1	1	5.18E-28	0.00%
(UO2)3(CO3)6-6	Dissolved	2.47E-28	-27.607	-62.7	0	0	54		0	0	6	3	0	0	0	7.42E-28	0.00%
(UO2)3(OH)4+2	Dissolved	2.94E-33	-32.532	0	0	0	-11.9		0	0	0	3	0	-4	4	8.81E-33	0.00%
(UO2)3(OH)5+	Dissolved	3.55E-30	-29.45	123	0	0	-15.55		0	0	0	3	0	-5	5	1.07E-29	0.00%
(UO2)3(OH)7-	Dissolved	5.85E-33	-32.233	0	0	0	-32.2		0	0	0	3	0	-7	7	1.75E-32	0.00%
(UO2)4(OH)7+	Dissolved	7.18E-39	-38.144	0	0	0	-21.9		0	0	0	4	0	-7	7	2.87E-38	0.00%
Ca2UO2(CO3)3(aq)	Dissolved	3.83E-09	-8.417	0	0	0	30.7		2	0	3	1	0	0	0	3.83E-09	0.27%
CaCO3(aq)	Dissolved	5.19E-06	-5.285	16	0	0	3.22		1	0	1	0	0	0	0	0.00E+00	0.00%
CaHCO3+	Dissolved	1.06E-04	-3.976	0	0	0	11.529		1	0	1	0	0	1	0	0.00E+00	0.00%
CaOH+	Dissolved	4.96E-09	-8.305	64.1	0	0	-12.697		1	0	0	0	0	-1	1	0.00E+00	0.00%
CaSO4(aq)	Dissolved	1.87E-03	-2.728	7.1	0	0	2.36		1	1	0	0	0	0	0	0.00E+00	0.00%
CaUO2(CO3)3-2	Dissolved	8.68E-10	-9.061	0	0	0	27.18		1	0	3	1	0	0	0	8.68E-10	0.06%
H2CO3*(aq)	Dissolved	4.47E-04	-3.349	-32	0	0	16.681		0	0	1	0	0	2	0	0.00E+00	0.00%
HCO3-	Dissolved	2.71E-03	-2.568	-14.6	0	0	10.329		0	0	1	0	0	1	0	0.00E+00	0.00%
HSO4-	Dissolved	3.24E-08	-7.49	22	0	0	1.99		0	1	0	0	0	1	0	0.00E+00	0.00%
UO2(CO3)2-2	Dissolved	7.47E-12	-11.127	18.5	0	0	16.61		0	0	2	1	0	0	0	7.47E-12	0.00%
UO2(CO3)3-4	Dissolved	1.02E-11	-10.992	-39.2	0	0	21.84		0	0	3	1	0	0	0	1.02E-11	0.00%
UO2(OH)2	Dissolved	3.20E-15	-14.494	0	0	0	-12.15		0	0	0	1	0	-2	2	3.20E-15	0.00%
UO2(OH)3-	Dissolved	2.54E-16	-15.594	0	0	0	-20.25		0	0	0	1	0	-3	3	2.54E-16	0.00%
UO2(OH)4-2	Dissolved	2.45E-21	-20.611	0	0	0	-32.4		0	0	0	1	0	-4	4	2.45E-21	0.00%
UO2(SO4)2-2	Dissolved	1.72E-17	-16.763	35.1	0	0	4.14		0	2	0	1	0	0	0	1.72E-17	0.00%
UO2CO3(aq)	Dissolved	6.80E-13	-12.168	5	0	0	9.94		0	0	1	1	0	0	0	6.80E-13	0.00%
UO2OH+	Dissolved	3.46E-15	-14.461	0.9	0	0	-5.25		0	0	0	1	0	-1	1	3.46E-15	0.00%
UO2(SO4)3-4	Dissolved	2.75E-20	-19.561	0	0	0	3.02		0	3	0	1	0	0	0	2.75E-20	0.00%
UO2SO4(aq)	Dissolved	2.88E-16	-15.541	19.5	0	0	3.15		0	1	0	1	0	0	0	2.88E-16	0.00%
OH-	Dissolved	1.01E-07	-6.997	55.8	0	0	-13.997		0	0	0	0	0	-1	1	0.00E+00	0.00%
WOUO2(CO3)3	Dissolved	1.40E-06	-5.855	0	0	0	23.755		0	0	3	1	1	-1	0	1.40E-06	99.64%
																0.00E+00	0.00%
																1.40E-06	99.98%

Reaction 4 at atmospheric P_{CO2}																Sorbed	1.39E-06
																Aquous	8.72E-09
																ratio	159.52
																bacteria concentration (kg/L)	0.02
																Kd L/kg	7,976.20
No temperature corrections performed																	
Temperature (K) = 298.1																	
Ionic Strength corrections performed:																	
Ionic strength = 0.021 Calculated																	
Component	Type	Charge	Total(M)	Log Free	Free Molarity												
Ca+2	Total	2	6.55E-03	-2.336	4.61E-03												
SO4-2	Total	-2	8.00E-03	-2.217	6.06E-03												
CO3-2	Total	-2	7.21E-05	-7.294	5.08E-08												
UO2+2	Total	2	1.40E-06	-10.918	1.21E-11												
WOH	Total	0	5.00E-05	-4.313	4.86E-05												
H+	Free	1	0.00E+00	-7	1.00E-07												
H2O	Free	0	5.55E+01	0	1.00E+00												
Species	Type	Molarity	Log M	Delta H	Delta S	Delta G	Log K	Stoichiometry								[UO2]	UO2 distribution
(UO2)2(OH)2+2	Dissolved	1.42E-14	-13.847	48.9	0	0	-5.62		0	0	0	2	0	-2	2	2.85E-14	0.00%
(UO2)2CO3(OH)3-	Dissolved	1.26E-10	-9.899	0	0	0	-0.859		0	0	1	2	0	-3	3	2.52E-10	0.02%
(UO2)2(OH)+3	Dissolved	2.91E-18	-17.537	0	0	0	-2.7		0	0	0	2	0	-1	1	5.81E-18	0.00%
(UO2)3(CO3)6-6	Dissolved	3.03E-23	-22.519	-62.7	0	0	54		0	0	6	3	0	0	0	9.08E-23	0.00%
(UO2)3(OH)4+2	Dissolved	3.67E-18	-17.435	0	0	0	-11.9		0	0	0	3	0	-4	4	1.10E-17	0.00%
(UO2)3(OH)5+	Dissolved	4.52E-15	-14.345	123	0	0	-15.55		0	0	0	3	0	-5	5	1.36E-14	0.00%
(UO2)3(OH)7-	Dissolved	7.50E-18	-17.125	0	0	0	-32.2		0	0	0	3	0	-7	7	2.25E-17	0.00%
(UO2)4(OH)7+	Dissolved	9.93E-19	-18.003	0	0	0	-21.9		0	0	0	4	0	-7	7	3.97E-18	0.00%
Ca2UO2(CO3)3(aq)	Dissolved	4.66E-09	-8.332	0	0	0	30.7		2	0	3	1	0	0	0	4.66E-09	0.33%
CaCO3(aq)	Dissolved	1.18E-07	-6.93	16	0	0	3.22		1	0	1	0	0	0	0	0.00E+00	0.00%
CaHCO3+	Dissolved	2.39E-06	-5.621	0	0	0	11.529		1	0	1	0	0	1	0	0.00E+00	0.00%
CaOH+	Dissolved	5.09E-09	-8.293	64.1	0	0	-12.697		1	0	0	0	0	-1	1	0.00E+00	0.00%
CaSO4(aq)	Dissolved	1.94E-03	-2.713	7.1	0	0	2.36		1	1	0	0	0	0	0	0.00E+00	0.00%
CaUO2(CO3)3-2	Dissolved	1.01E-09	-8.996	0	0	0	27.18		1	0	3	1	0	0	0	1.01E-09	0.07%
H2CO3*(aq)	Dissolved	9.94E-06	-5.003	-32	0	0	16.681		0	0	1	0	0	2	0	0.00E+00	0.00%
HCO3-	Dissolved	5.96E-05	-4.225	-14.6	0	0	10.329		0	0	1	0	0	1	0	0.00E+00	0.00%
HSO4-	Dissolved	3.26E-08	-7.487	22	0	0	1.99		0	1	0	0	0	1	0	0.00E+00	0.00%
UO2(CO3)2-2	Dissolved	3.84E-10	-9.416	18.5	0	0	16.61		0	0	2	1	0	0	0	3.84E-10	0.03%
UO2(CO3)3-4	Dissolved	1.10E-11	-10.96	-39.2	0	0	21.84		0	0	3	1	0	0	0	1.10E-11	0.00%
UO2(OH)2	Dissolved	3.48E-10	-9.458	0	0	0	-12.15		0	0	0	1	0	-2	2	3.48E-10	0.02%
UO2(OH)3-	Dissolved	2.77E-11	-10.558	0	0	0	-20.25		0	0	0	1	0	-3	3	2.77E-11	0.00%
UO2(OH)4-2	Dissolved	2.64E-16	-15.578	0	0	0	-32.4		0	0	0	1	0	-4	4	2.64E-16	0.00%
UO2(SO4)2-2	Dissolved	1.85E-12	-11.733	35.1	0	0	4.14		0	2	0	1	0	0	0	1.85E-12	0.00%
UO2CO3(aq)	Dissolved	1.61E-09	-8.792	5	0	0	9.94		0	0	1	1	0	0	0	1.61E-09	0.12%
UO2OH+	Dissolved	3.73E-10	-9.428	0.9	0	0	-5.25		0	0	0	1	0	-1	1	3.73E-10	0.03%
UO2(SO4)3-4	Dissolved	2.82E-15	-14.55	0	0	0	3.02		0	3	0	1	0	0	0	2.82E-15	0.00%
UO2SO4(aq)	Dissolved	3.12E-11	-10.505	19.5	0	0	3.15		0	1	0	1	0	0	0	3.12E-11	0.00%
OH-	Dissolved	1.01E-07	-6.997	55.8	0	0	-13.997		0	0	0	0	0	-1	1	0.00E+00	0.00%
WOU2	Dissolved	1.39E-06	-5.857	0	0	0	2.635		0	0	0	1	1	-1	0	1.39E-06	99.36%
																0.00E+00	0.00%
																	99.98%

Reaction 4 at 2% P_{CO2}																Sorbed	3.93E-09
																Aquous	1.40E-06
																ratio	0.00
																bacteria concentration (kg/L)	0.02
																Kd L/kg	0.14
No temperature corrections performed																	
Temperature (K) = 298.1																	
Ionic Strength corrections performed:																	
Ionic strength = 0.023 Calculated																	
Component	Type	Charge	Total(M)	Log Free	Free Molarity												
Ca+2	Total	2	6.55E-03	-2.341	4.57E-03												
SO4-2	Total	-2	8.00E-03	-2.213	6.13E-03												
CO3-2	Total	-2	3.27E-03	-5.63	2.35E-06												
UO2+2	Total	2	1.40E-06	-13.472	3.37E-14												
WOH	Total	0	5.00E-05	-4.301	5.00E-05												
H+	Free	1	0.00E+00	-7	1.00E-07												
H2O	Free	0	5.55E+01	0	1.00E+00												
Species	Type	Molarity	Log M	Delta H	Delta S	Delta G	Log K	Stoichiometry								[UO2]	UO2 distrib
(UO2)2(OH)2+2	Dissolved	1.08E-19	-18.965	48.9	0	0	-5.62		0	0	0	2	0	-2	2	2.17E-19	0.00%
(UO2)2CO3(OH)3-	Dissolved	4.28E-14	-13.368	0	0	0	-0.859		0	0	1	2	0	-3	3	8.57E-14	0.00%
(UO2)2(OH)+3	Dissolved	2.27E-23	-22.644	0	0	0	-2.7		0	0	0	2	0	-1	1	4.54E-23	0.00%
(UO2)3(CO3)6-6	Dissolved	6.40E-21	-20.194	-62.7	0	0	54		0	0	6	3	0	0	0	1.92E-20	0.00%
(UO2)3(OH)4+2	Dissolved	7.62E-26	-25.118	0	0	0	-11.9		0	0	0	3	0	-4	4	2.29E-25	0.00%
(UO2)3(OH)5+	Dissolved	9.22E-23	-22.035	123	0	0	-15.55		0	0	0	3	0	-5	5	2.76E-22	0.00%
(UO2)3(OH)7-	Dissolved	1.52E-25	-24.819	0	0	0	-32.2		0	0	0	3	0	-7	7	4.55E-25	0.00%
(UO2)4(OH)7+	Dissolved	5.52E-29	-28.258	0	0	0	-21.9		0	0	0	4	0	-7	7	2.21E-28	0.00%
Ca2UO2(CO3)3(aq)	Dissolved	1.13E-06	-5.945	0	0	0	30.7		2	0	3	1	0	0	0	1.13E-06	80.93%
CaCO3(aq)	Dissolved	5.19E-06	-5.285	16	0	0	3.22		1	0	1	0	0	0	0	0.00E+00	0.00%
CaHCO3+	Dissolved	1.06E-04	-3.976	0	0	0	11.529		1	0	1	0	0	1	0	0.00E+00	0.00%
CaOH+	Dissolved	4.96E-09	-8.305	64.1	0	0	-12.697		1	0	0	0	0	-1	1	0.00E+00	0.00%
CaSO4(aq)	Dissolved	1.87E-03	-2.728	7.1	0	0	2.36		1	1	0	0	0	0	0	0.00E+00	0.00%
CaUO2(CO3)3-2	Dissolved	2.57E-07	-6.59	0	0	0	27.18		1	0	3	1	0	0	0	2.57E-07	18.34%
H2CO3*(aq)	Dissolved	4.47E-04	-3.349	-32	0	0	16.681		0	0	1	0	0	2	0	0.00E+00	0.00%
HCO3-	Dissolved	2.71E-03	-2.568	-14.6	0	0	10.329		0	0	1	0	0	1	0	0.00E+00	0.00%
HSO4-	Dissolved	3.24E-08	-7.49	22	0	0	1.99		0	1	0	0	0	1	0	0.00E+00	0.00%
UO2(CO3)2-2	Dissolved	2.21E-09	-8.656	18.5	0	0	16.61		0	0	2	1	0	0	0	2.21E-09	0.16%
UO2(CO3)3-4	Dissolved	3.01E-09	-8.521	-39.2	0	0	21.84		0	0	3	1	0	0	0	3.01E-09	0.22%
UO2(OH)2	Dissolved	9.48E-13	-12.023	0	0	0	-12.15		0	0	0	1	0	-2	2	9.48E-13	0.00%
UO2(OH)3-	Dissolved	7.53E-14	-13.123	0	0	0	-20.25		0	0	0	1	0	-3	3	7.53E-14	0.00%
UO2(OH)4-2	Dissolved	7.25E-19	-18.139	0	0	0	-32.4		0	0	0	1	0	-4	4	7.25E-19	0.00%
UO2(SO4)2-2	Dissolved	5.11E-15	-14.292	35.1	0	0	4.14		0	2	0	1	0	0	0	5.11E-15	0.00%
UO2CO3(aq)	Dissolved	2.01E-10	-9.696	5	0	0	9.94		0	0	1	1	0	0	0	2.01E-10	0.01%
UO2OH+	Dissolved	1.02E-12	-11.989	0.9	0	0	-5.25		0	0	0	1	0	-1	1	1.02E-12	0.00%
UO2(SO4)3-4	Dissolved	8.13E-18	-17.09	0	0	0	3.02		0	3	0	1	0	0	0	8.13E-18	0.00%
UO2SO4(aq)	Dissolved	8.53E-14	-13.069	19.5	0	0	3.15		0	1	0	1	0	0	0	8.53E-14	0.00%
OH-	Dissolved	1.01E-07	-6.997	55.8	0	0	-13.997		0	0	0	0	0	-1	1	0.00E+00	0.00%
WOU2	Dissolved	3.93E-09	-8.405	0	0	0	2.635		0	0	0	1	1	-1	0	3.93E-09	0.28%
																0.00E+00	0.00%
																	99.94%

Reaction 5 at atmospheric P_{CO2}															Sorbed	1.39E-06
															Aquous	8.62E-09
															ratio	161.43
															bacteria concentration (kg/L)	0.02
															Kd L/kg	8,071.41
No temperature corrections performed																
Temperature (K) = 298.1																
Ionic Strength corrections performed:																
Ionic strength = 0.021 Calculated																
Component	Type	Charge	Total(M)	Log Free	Free Molarity											
Ca+2	Total	2	6.55E-03	-2.336	4.61E-03											
SO4-2	Total	-2	8.00E-03	-2.217	6.06E-03											
CO3-2	Total	-2	7.21E-05	-7.294	5.08E-08											
UO2+2	Total	2	1.40E-06	-10.923	1.19E-11											
WOH	Total	0	5.00E-05	-4.313	4.86E-05											
H+	Free	1	0.00E+00	-7	1.00E-07											
H2O	Free	0	5.55E+01	0	1.00E+00											
Species	Type	Molarity	Log M	Delta H	Delta S	Delta G	Log K	Stoichiometry							[UO2]	UO2 distribution
(UO2)2(OH)2+2	Dissolved	1.39E-14	-13.857	48.9	0	0	-5.62		0	0	0	2	0	-2	2	2.78E-14	0.00%
(UO2)2CO3(OH)3-	Dissolved	1.23E-10	-9.909	0	0	0	-0.859		0	0	1	2	0	-3	3	2.46E-10	0.02%
(UO2)2(OH)+3	Dissolved	2.84E-18	-17.547	0	0	0	-2.7		0	0	0	2	0	-1	1	5.68E-18	0.00%
(UO2)3(CO3)6-6	Dissolved	2.92E-23	-22.534	-62.7	0	0	54		0	0	6	3	0	0	0	8.77E-23	0.00%
(UO2)3(OH)4+2	Dissolved	3.55E-18	-17.45	0	0	0	-11.9		0	0	0	3	0	-4	4	1.06E-17	0.00%
(UO2)3(OH)5+	Dissolved	4.37E-15	-14.36	123	0	0	-15.55		0	0	0	3	0	-5	5	1.31E-14	0.00%
(UO2)3(OH)7-	Dissolved	7.25E-18	-17.14	0	0	0	-32.2		0	0	0	3	0	-7	7	2.17E-17	0.00%
(UO2)4(OH)7+	Dissolved	9.48E-19	-18.023	0	0	0	-21.9		0	0	0	4	0	-7	7	3.79E-18	0.00%
Ca2UO2(CO3)3(aq)	Dissolved	4.60E-09	-8.337	0	0	0	30.7		2	0	3	1	0	0	0	4.60E-09	0.33%
CaCO3(aq)	Dissolved	1.18E-07	-6.93	16	0	0	3.22		1	0	1	0	0	0	0	0.00E+00	0.00%
CaHCO3+	Dissolved	2.39E-06	-5.621	0	0	0	11.529		1	0	1	0	0	1	0	0.00E+00	0.00%
CaOH+	Dissolved	5.09E-09	-8.293	64.1	0	0	-12.697		1	0	0	0	0	-1	1	0.00E+00	0.00%
CaSO4(aq)	Dissolved	1.94E-03	-2.713	7.1	0	0	2.36		1	1	0	0	0	0	0	0.00E+00	0.00%
CaUO2(CO3)3-2	Dissolved	9.98E-10	-9.001	0	0	0	27.18		1	0	3	1	0	0	0	9.98E-10	0.07%
H2CO3*(aq)	Dissolved	9.94E-06	-5.003	-32	0	0	16.681		0	0	1	0	0	2	0	0.00E+00	0.00%
HCO3-	Dissolved	5.96E-05	-4.225	-14.6	0	0	10.329		0	0	1	0	0	1	0	0.00E+00	0.00%
HSO4-	Dissolved	3.26E-08	-7.487	22	0	0	1.99		0	1	0	0	0	1	0	0.00E+00	0.00%
UO2(CO3)2-2	Dissolved	3.79E-10	-9.421	18.5	0	0	16.61		0	0	2	1	0	0	0	3.79E-10	0.03%
UO2(CO3)3-4	Dissolved	1.08E-11	-10.965	-39.2	0	0	21.84		0	0	3	1	0	0	0	1.08E-11	0.00%
UO2(OH)2	Dissolved	3.44E-10	-9.463	0	0	0	-12.15		0	0	0	1	0	-2	2	3.44E-10	0.02%
UO2(OH)3-	Dissolved	2.73E-11	-10.563	0	0	0	-20.25		0	0	0	1	0	-3	3	2.73E-11	0.00%
UO2(OH)4-2	Dissolved	2.61E-16	-15.583	0	0	0	-32.4		0	0	0	1	0	-4	4	2.61E-16	0.00%
UO2(SO4)2-2	Dissolved	1.83E-12	-11.738	35.1	0	0	4.14		0	2	0	1	0	0	0	1.83E-12	0.00%
UO2CO3(aq)	Dissolved	1.60E-09	-8.797	5	0	0	9.94		0	0	1	1	0	0	0	1.60E-09	0.11%
UO2OH+	Dissolved	3.69E-10	-9.433	0.9	0	0	-5.25		0	0	0	1	0	-1	1	3.69E-10	0.03%
UO2(SO4)3-4	Dissolved	2.79E-15	-14.555	0	0	0	3.02		0	3	0	1	0	0	0	2.79E-15	0.00%
UO2SO4(aq)	Dissolved	3.09E-11	-10.51	19.5	0	0	3.15		0	1	0	1	0	0	0	3.09E-11	0.00%
OH-	Dissolved	1.01E-07	-6.997	55.8	0	0	-13.997		0	0	0	0	0	-1	1	0.00E+00	0.00%
WOUOOH	Dissolved	1.39E-06	-5.857	0	0	0	-4.23		0	0	0	1	1	-2	1	1.39E-06	99.36%
																	99.97%

Reaction 5at 2% P_{CO2}															Sorbed	3.94E-09
															Aquous	1.40E-06
															ratio	0.00
															bacteria concentration (kg/L)	0.02
															Kd L/kg	0.14
No temperature corrections performed																
Temperature (K) = 298.1																
Ionic Strength corrections performed:																
Ionic strength = 0.023 Calculated																
Component	Type	Charge	Total(M)	Log Free	Free Molarity											
Ca+2	Total	2	6.55E-03	-2.341	4.57E-03											
SO4-2	Total	-2	8.00E-03	-2.213	6.13E-03											
CO3-2	Total	-2	3.27E-03	-5.63	2.35E-06											
UO2+2	Total	2	1.40E-06	-13.472	3.37E-14											
WOH	Total	0	5.00E-05	-4.301	5.00E-05											
H+	Free	1	0.00E+00	-7	1.00E-07											
H2O	Free	0	5.55E+01	0	1.00E+00											
Species	Type	Molarity	Log M	Delta H	Delta S	Delta G	Log K	Stoichiometry							[UO2]	UO2 distribution
(UO2)2(OH)2+2	Dissolved	1.08E-19	-18.965	48.9	0	0	-5.62		0	0	0	2	0	-2	2	2.17E-19	0.00%
(UO2)2CO3(OH)3-	Dissolved	4.28E-14	-13.368	0	0	0	-0.859		0	0	1	2	0	-3	3	8.57E-14	0.00%
(UO2)2(OH)+3	Dissolved	2.27E-23	-22.644	0	0	0	-2.7		0	0	0	2	0	-1	1	4.54E-23	0.00%
(UO2)3(CO3)6-6	Dissolved	6.40E-21	-20.194	-62.7	0	0	54		0	0	6	3	0	0	0	1.92E-20	0.00%
(UO2)3(OH)4+2	Dissolved	7.62E-26	-25.118	0	0	0	-11.9		0	0	0	3	0	-4	4	2.29E-25	0.00%
(UO2)3(OH)5+	Dissolved	9.22E-23	-22.035	123	0	0	-15.55		0	0	0	3	0	-5	5	2.76E-22	0.00%
(UO2)3(OH)7-	Dissolved	1.52E-25	-24.819	0	0	0	-32.2		0	0	0	3	0	-7	7	4.55E-25	0.00%
(UO2)4(OH)7+	Dissolved	5.52E-29	-28.258	0	0	0	-21.9		0	0	0	4	0	-7	7	2.21E-28	0.00%
Ca2UO2(CO3)3(aq)	Dissolved	1.13E-06	-5.945	0	0	0	30.7		2	0	3	1	0	0	0	1.13E-06	80.93%
CaCO3(aq)	Dissolved	5.19E-06	-5.285	16	0	0	3.22		1	0	1	0	0	0	0	0.00E+00	0.00%
CaHCO3+	Dissolved	1.06E-04	-3.976	0	0	0	11.529		1	0	1	0	0	1	0	0.00E+00	0.00%
CaOH+	Dissolved	4.96E-09	-8.305	64.1	0	0	-12.697		1	0	0	0	0	-1	1	0.00E+00	0.00%
CaSO4(aq)	Dissolved	1.87E-03	-2.728	7.1	0	0	2.36		1	1	0	0	0	0	0	0.00E+00	0.00%
CaUO2(CO3)3-2	Dissolved	2.57E-07	-6.59	0	0	0	27.18		1	0	3	1	0	0	0	2.57E-07	18.34%
H2CO3*(aq)	Dissolved	4.47E-04	-3.349	-32	0	0	16.681		0	0	1	0	0	2	0	0.00E+00	0.00%
HCO3-	Dissolved	2.71E-03	-2.568	-14.6	0	0	10.329		0	0	1	0	0	1	0	0.00E+00	0.00%
HSO4-	Dissolved	3.24E-08	-7.49	22	0	0	1.99		0	1	0	0	0	1	0	0.00E+00	0.00%
UO2(CO3)2-2	Dissolved	2.21E-09	-8.656	18.5	0	0	16.61		0	0	2	1	0	0	0	2.21E-09	0.16%
UO2(CO3)3-4	Dissolved	3.01E-09	-8.521	-39.2	0	0	21.84		0	0	3	1	0	0	0	3.01E-09	0.22%
UO2(OH)2	Dissolved	9.48E-13	-12.023	0	0	0	-12.15		0	0	0	1	0	-2	2	9.48E-13	0.00%
UO2(OH)3-	Dissolved	7.53E-14	-13.123	0	0	0	-20.25		0	0	0	1	0	-3	3	7.53E-14	0.00%
UO2(OH)4-2	Dissolved	7.25E-19	-18.139	0	0	0	-32.4		0	0	0	1	0	-4	4	7.25E-19	0.00%
UO2(SO4)2-2	Dissolved	5.11E-15	-14.292	35.1	0	0	4.14		0	2	0	1	0	0	0	5.11E-15	0.00%
UO2CO3(aq)	Dissolved	2.01E-10	-9.696	5	0	0	9.94		0	0	1	1	0	0	0	2.01E-10	0.01%
UO2OH+	Dissolved	1.02E-12	-11.989	0.9	0	0	-5.25		0	0	0	1	0	-1	1	1.02E-12	0.00%
UO2(SO4)3-4	Dissolved	8.13E-18	-17.09	0	0	0	3.02		0	3	0	1	0	0	0	8.13E-18	0.00%
UO2SO4(aq)	Dissolved	8.53E-14	-13.069	19.5	0	0	3.15		0	1	0	1	0	0	0	8.53E-14	0.00%
OH-	Dissolved	1.01E-07	-6.997	55.8	0	0	-13.997		0	0	0	0	0	-1	1	0.00E+00	0.00%
WOUOOH	Dissolved	3.94E-09	-8.404	0	0	0	-4.23		0	0	0	1	1	-2	1	3.94E-09	0.28%
																0.00E+00	0.00%
																	99.94%

Reactions 4 and 5 at atmospheric P_{CO2}															Sorbed	1.39E-06
															Aquous	8.62E-09
															ratio	161.43
															bacteria concentration (kg/L)	0.02
															Kd L/kg	8071.45
No temperature corrections performed																
Temperature (K) = 298.1																
Ionic Strength corrections performed:																
Ionic strength = 0.021 Calculated																
Component	Type	Charge	Total(M)	Log Free	Free Molarity											
Ca+2	Total	2	6.55E-03	-2.336	4.61E-03											
SO4-2	Total	-2	8.00E-03	-2.217	6.06E-03											
CO3-2	Total	-2	7.21E-05	-7.294	5.08E-08											
UO2+2	Total	2	1.40E-06	-10.923	1.19E-11											
WOH	Total	0	5.00E-05	-4.313	4.86E-05											
H+	Free	1	0.00E+00	-7	1.00E-07											
H2O	Free	0	5.55E+01	0	1.00E+00											
Species	Type	Molarity	Log M	Delta H	Delta S	Delta G	Log K	Stoichiometry							[UO2]	UO2 distribution
(UO2)2(OH)2+2	Dissolved	1.39E-14	-13.857	48.9	0	0	-5.62		0	0	0	2	0	-2	2	2.78E-14	0.00%
(UO2)2CO3(OH)3-	Dissolved	1.23E-10	-9.909	0	0	0	-0.859		0	0	1	2	0	-3	3	2.46E-10	0.02%
(UO2)2(OH)+3	Dissolved	2.84E-18	-17.547	0	0	0	-2.7		0	0	0	2	0	-1	1	5.68E-18	0.00%
(UO2)3(CO3)6-6	Dissolved	2.92E-23	-22.534	-62.7	0	0	54		0	0	6	3	0	0	0	8.77E-23	0.00%
(UO2)3(OH)4+2	Dissolved	3.55E-18	-17.45	0	0	0	-11.9		0	0	0	3	0	-4	4	1.06E-17	0.00%
(UO2)3(OH)5+	Dissolved	4.37E-15	-14.36	123	0	0	-15.55		0	0	0	3	0	-5	5	1.31E-14	0.00%
(UO2)3(OH)7-	Dissolved	7.25E-18	-17.14	0	0	0	-32.2		0	0	0	3	0	-7	7	2.17E-17	0.00%
(UO2)4(OH)7+	Dissolved	9.48E-19	-18.023	0	0	0	-21.9		0	0	0	4	0	-7	7	3.79E-18	0.00%
Ca2UO2(CO3)3(aq)	Dissolved	4.60E-09	-8.337	0	0	0	30.7		2	0	3	1	0	0	0	4.60E-09	0.33%
CaCO3(aq)	Dissolved	1.18E-07	-6.93	16	0	0	3.22		1	0	1	0	0	0	0	0.00E+00	0.00%
CaHCO3+	Dissolved	2.39E-06	-5.621	0	0	0	11.529		1	0	1	0	0	1	0	0.00E+00	0.00%
CaOH+	Dissolved	5.09E-09	-8.293	64.1	0	0	-12.697		1	0	0	0	0	-1	1	0.00E+00	0.00%
CaSO4(aq)	Dissolved	1.94E-03	-2.713	7.1	0	0	2.36		1	1	0	0	0	0	0	0.00E+00	0.00%
CaUO2(CO3)3-2	Dissolved	9.98E-10	-9.001	0	0	0	27.18		1	0	3	1	0	0	0	9.98E-10	0.07%
H2CO3*(aq)	Dissolved	9.94E-06	-5.003	-32	0	0	16.681		0	0	1	0	0	2	0	0.00E+00	0.00%
HCO3-	Dissolved	5.96E-05	-4.225	-14.6	0	0	10.329		0	0	1	0	0	1	0	0.00E+00	0.00%
HSO4-	Dissolved	3.26E-08	-7.487	22	0	0	1.99		0	1	0	0	0	1	0	0.00E+00	0.00%
UO2(CO3)2-2	Dissolved	3.79E-10	-9.421	18.5	0	0	16.61		0	0	2	1	0	0	0	3.79E-10	0.03%
UO2(CO3)3-4	Dissolved	1.08E-11	-10.965	-39.2	0	0	21.84		0	0	3	1	0	0	0	1.08E-11	0.00%
UO2(OH)2	Dissolved	3.44E-10	-9.463	0	0	0	-12.15		0	0	0	1	0	-2	2	3.44E-10	0.02%
UO2(OH)3-	Dissolved	2.73E-11	-10.563	0	0	0	-20.25		0	0	0	1	0	-3	3	2.73E-11	0.00%
UO2(OH)4-2	Dissolved	2.61E-16	-15.583	0	0	0	-32.4		0	0	0	1	0	-4	4	2.61E-16	0.00%
UO2(SO4)2-2	Dissolved	1.83E-12	-11.738	35.1	0	0	4.14		0	2	0	1	0	0	0	1.83E-12	0.00%
UO2CO3(aq)	Dissolved	1.60E-09	-8.797	5	0	0	9.94		0	0	1	1	0	0	0	1.60E-09	0.11%
UO2OH+	Dissolved	3.69E-10	-9.433	0.9	0	0	-5.25		0	0	0	1	0	-1	1	3.69E-10	0.03%
UO2(SO4)3-4	Dissolved	2.79E-15	-14.555	0	0	0	3.02		0	3	0	1	0	0	0	2.79E-15	0.00%
UO2SO4(aq)	Dissolved	3.09E-11	-10.51	19.5	0	0	3.15		0	1	0	1	0	0	0	3.09E-11	0.00%
OH-	Dissolved	1.01E-07	-6.997	55.8	0	0	-13.997		0	0	0	0	0	-1	1	0.00E+00	0.00%
WOUOOH	Dissolved	1.39E-06	-5.857	0	0	0	-4.23		0	0	0	1	1	-2	1	1.39E-06	99.36%
WOU2	Dissolved	7.34E-12	-11.134	0	0	0	-2.638		0	0	0	1	1	-1	0	7.34E-12	0.00%
																1.40E-06	99.97%

Reactions 4 and 5 at 2% P_{CO2}															Sorbed	3.94E-09
															Aquous	1.40E-06
															ratio	0.00
															bacteria concentration (kg/L)	0.02
															Kd L/kg	0.14
No temperature corrections performed																
Temperature (K) = 298.1																
Ionic Strength corrections performed:																
Ionic strength = 0.023 Calculated																
Component	Type	Charge	Total(M)	Log Free	Free Molarity											
Ca+2	Total	2	6.55E-03	-2.341	4.57E-03											
SO4-2	Total	-2	8.00E-03	-2.213	6.13E-03											
CO3-2	Total	-2	3.27E-03	-5.63	2.35E-06											
UO2+2	Total	2	1.40E-06	-13.472	3.37E-14											
WOH	Total	0	5.00E-05	-4.301	5.00E-05											
H+	Free	1	0.00E+00	-7	1.00E-07											
H2O	Free	0	5.55E+01	0	1.00E+00											
Species	Type	Molarity	Log M	Delta H	Delta S	Delta G	Log K	Stoichiometry							[UO2]	UO2 distribution
(UO2)2(OH)2+2	Dissolved	1.08E-19	-18.965	48.9	0	0	-5.62		0	0	0	2	0	-2	2	2.17E-19	0.00%
(UO2)2CO3(OH)3-	Dissolved	4.28E-14	-13.368	0	0	0	-0.859		0	0	1	2	0	-3	3	8.57E-14	0.00%
(UO2)2(OH)+3	Dissolved	2.27E-23	-22.644	0	0	0	-2.7		0	0	0	2	0	-1	1	4.54E-23	0.00%
(UO2)3(CO3)6-6	Dissolved	6.40E-21	-20.194	-62.7	0	0	54		0	0	6	3	0	0	0	1.92E-20	0.00%
(UO2)3(OH)4+2	Dissolved	7.62E-26	-25.118	0	0	0	-11.9		0	0	0	3	0	-4	4	2.29E-25	0.00%
(UO2)3(OH)5+	Dissolved	9.22E-23	-22.035	123	0	0	-15.55		0	0	0	3	0	-5	5	2.76E-22	0.00%
(UO2)3(OH)7-	Dissolved	1.52E-25	-24.819	0	0	0	-32.2		0	0	0	3	0	-7	7	4.55E-25	0.00%
(UO2)4(OH)7+	Dissolved	5.52E-29	-28.258	0	0	0	-21.9		0	0	0	4	0	-7	7	2.21E-28	0.00%
Ca2UO2(CO3)3(aq)	Dissolved	1.13E-06	-5.945	0	0	0	30.7		2	0	3	1	0	0	0	1.13E-06	80.93%
CaCO3(aq)	Dissolved	5.19E-06	-5.285	16	0	0	3.22		1	0	1	0	0	0	0	0.00E+00	0.00%
CaHCO3+	Dissolved	1.06E-04	-3.976	0	0	0	11.529		1	0	1	0	0	1	0	0.00E+00	0.00%
CaOH+	Dissolved	4.96E-09	-8.305	64.1	0	0	-12.697		1	0	0	0	0	-1	1	0.00E+00	0.00%
CaSO4(aq)	Dissolved	1.87E-03	-2.728	7.1	0	0	2.36		1	1	0	0	0	0	0	0.00E+00	0.00%
CaUO2(CO3)3-2	Dissolved	2.57E-07	-6.59	0	0	0	27.18		1	0	3	1	0	0	0	2.57E-07	18.34%
H2CO3*(aq)	Dissolved	4.47E-04	-3.349	-32	0	0	16.681		0	0	1	0	0	2	0	0.00E+00	0.00%
HCO3-	Dissolved	2.71E-03	-2.568	-14.6	0	0	10.329		0	0	1	0	0	1	0	0.00E+00	0.00%
HSO4-	Dissolved	3.24E-08	-7.49	22	0	0	1.99		0	1	0	0	0	1	0	0.00E+00	0.00%
UO2(CO3)2-2	Dissolved	2.21E-09	-8.656	18.5	0	0	16.61		0	0	2	1	0	0	0	2.21E-09	0.16%
UO2(CO3)3-4	Dissolved	3.01E-09	-8.521	-39.2	0	0	21.84		0	0	3	1	0	0	0	3.01E-09	0.22%
UO2(OH)2	Dissolved	9.48E-13	-12.023	0	0	0	-12.15		0	0	0	1	0	-2	2	9.48E-13	0.00%
UO2(OH)3-	Dissolved	7.53E-14	-13.123	0	0	0	-20.25		0	0	0	1	0	-3	3	7.53E-14	0.00%
UO2(OH)4-2	Dissolved	7.25E-19	-18.139	0	0	0	-32.4		0	0	0	1	0	-4	4	7.25E-19	0.00%
UO2(SO4)2-2	Dissolved	5.11E-15	-14.292	35.1	0	0	4.14		0	2	0	1	0	0	0	5.11E-15	0.00%
UO2CO3(aq)	Dissolved	2.01E-10	-9.696	5	0	0	9.94		0	0	1	1	0	0	0	2.01E-10	0.01%
UO2OH+	Dissolved	1.02E-12	-11.989	0.9	0	0	-5.25		0	0	0	1	0	-1	1	1.02E-12	0.00%
UO2(SO4)3-4	Dissolved	8.13E-18	-17.09	0	0	0	3.02		0	3	0	1	0	0	0	8.13E-18	0.00%
UO2SO4(aq)	Dissolved	8.53E-14	-13.069	19.5	0	0	3.15		0	1	0	1	0	0	0	8.53E-14	0.00%
OH-	Dissolved	1.01E-07	-6.997	55.8	0	0	-13.997		0	0	0	0	0	-1	1	0.00E+00	0.00%
WOUOOH	Dissolved	3.94E-09	-8.404	0	0	0	-4.23		0	0	0	1	1	-2	1	3.94E-09	0.28%
WOU2	Dissolved	2.10E-14	-13.678	0	0	0	-2.638		0	0	0	1	1	-1	0	2.10E-14	0.00%
																1.40E-06	99.94%

Reactions 4 and 5 at 2% P_{CO2} fixing Log K again to match experimental conditions																Sorbed	4.76E-07
																Aquous	9.24E-07
																ratio	0.52
																bacteria concentration (kg/L)	0.02
																Kd L/kg	25.77
No temperature corrections performed																	
Temperature (K) = 298.1																	
Ionic Strength corrections performed:																	
Ionic strength = 0.023 Calculated																	
Component	Type	Charge	Total(M)	Log Free	Free Molarity												
Ca+2	Total	2	6.55E-03	-2.341	4.57E-03												
SO4-2	Total	-2	8.00E-03	-2.213	6.13E-03												
CO3-2	Total	-2	3.27E-03	-5.629	2.35E-06												
UO2+2	Total	2	1.40E-06	-13.652	2.23E-14												
WOH	Total	0	5.00E-05	-4.305	4.95E-05												
H+	Free	1	0.00E+00	-7	1.00E-07												
H2O	Free	0	5.55E+01	0	1.00E+00												
Species	Type	Molarity	Log M	Delta H	Delta S	Delta G	Log K	Stoichiometry								[UO2]	UO2 distribution
(UO2)2(OH)2+2	Dissolved	4.73E-20	-19.325	48.9	0	0	-5.62		0	0	0	2	0	-2	2	9.46E-20	0.00%
(UO2)2CO3(OH)3-	Dissolved	1.87E-14	-13.728	0	0	0	-0.859		0	0	1	2	0	-3	3	3.74E-14	0.00%
(UO2)2(OH)+3	Dissolved	9.90E-24	-23.004	0	0	0	-2.7		0	0	0	2	0	-1	1	1.98E-23	0.00%
(UO2)3(CO3)6-6	Dissolved	1.85E-21	-20.733	-62.7	0	0	54		0	0	6	3	0	0	0	5.55E-21	0.00%
(UO2)3(OH)4+2	Dissolved	2.20E-26	-25.658	0	0	0	-11.9		0	0	0	3	0	-4	4	6.59E-26	0.00%
(UO2)3(OH)5+	Dissolved	2.66E-23	-22.575	123	0	0	-15.55		0	0	0	3	0	-5	5	7.97E-23	0.00%
(UO2)3(OH)7-	Dissolved	4.38E-26	-25.359	0	0	0	-32.2		0	0	0	3	0	-7	7	1.31E-25	0.00%
(UO2)4(OH)7+	Dissolved	1.05E-29	-28.978	0	0	0	-21.9		0	0	0	4	0	-7	7	4.20E-29	0.00%
Ca2UO2(CO3)3(aq)	Dissolved	7.50E-07	-6.125	0	0	0	30.7		2	0	3	1	0	0	0	7.50E-07	53.59%
CaCO3(aq)	Dissolved	5.20E-06	-5.284	16	0	0	3.22		1	0	1	0	0	0	0	0.00E+00	0.00%
CaHCO3+	Dissolved	1.06E-04	-3.975	0	0	0	11.529		1	0	1	0	0	1	0	0.00E+00	0.00%
CaOH+	Dissolved	4.96E-09	-8.305	64.1	0	0	-12.697		1	0	0	0	0	-1	1	0.00E+00	0.00%
CaSO4(aq)	Dissolved	1.87E-03	-2.728	7.1	0	0	2.36		1	1	0	0	0	0	0	0.00E+00	0.00%
CaUO2(CO3)3-2	Dissolved	1.70E-07	-6.77	0	0	0	27.18		1	0	3	1	0	0	0	1.70E-07	12.14%
H2CO3*(aq)	Dissolved	4.48E-04	-3.349	-32	0	0	16.681		0	0	1	0	0	2	0	0.00E+00	0.00%
HCO3-	Dissolved	2.71E-03	-2.568	-14.6	0	0	10.329		0	0	1	0	0	1	0	0.00E+00	0.00%
HSO4-	Dissolved	3.24E-08	-7.49	22	0	0	1.99		0	1	0	0	0	1	0	0.00E+00	0.00%
UO2(CO3)2-2	Dissolved	1.46E-09	-8.835	18.5	0	0	16.61		0	0	2	1	0	0	0	1.46E-09	0.10%
UO2(CO3)3-4	Dissolved	1.99E-09	-8.7	-39.2	0	0	21.84		0	0	3	1	0	0	0	1.99E-09	0.14%
UO2(OH)2	Dissolved	6.27E-13	-12.203	0	0	0	-12.15		0	0	0	1	0	-2	2	6.27E-13	0.00%
UO2(OH)3-	Dissolved	4.98E-14	-13.303	0	0	0	-20.25		0	0	0	1	0	-3	3	4.98E-14	0.00%
UO2(OH)4-2	Dissolved	4.79E-19	-18.319	0	0	0	-32.4		0	0	0	1	0	-4	4	4.79E-19	0.00%
UO2(SO4)2-2	Dissolved	3.37E-15	-14.472	35.1	0	0	4.14		0	2	0	1	0	0	0	3.37E-15	0.00%
UO2CO3(aq)	Dissolved	1.33E-10	-9.876	5	0	0	9.94		0	0	1	1	0	0	0	1.33E-10	0.01%
UO2OH+	Dissolved	6.77E-13	-12.169	0.9	0	0	-5.25		0	0	0	1	0	-1	1	6.77E-13	0.00%
UO2(SO4)3-4	Dissolved	5.37E-18	-17.27	0	0	0	3.02		0	3	0	1	0	0	0	5.37E-18	0.00%
UO2SO4(aq)	Dissolved	5.63E-14	-13.249	19.5	0	0	3.15		0	1	0	1	0	0	0	5.63E-14	0.00%
OH-	Dissolved	1.01E-07	-6.997	55.8	0	0	-13.997		0	0	0	0	0	-1	1	0.00E+00	0.00%
WOUOOH	Dissolved	2.58E-09	-8.588	0	0	0	-4.23		0	0	0	1	1	-2	1	2.58E-09	0.18%
WOU2	Dissolved	4.74E-07	-6.325	0	0	0	4.9		0	0	0	1	1	-1	0	4.74E-07	33.83%
																1.40E-06	100.00%

Reactions 4 and 5 at atm P_{CO2} using Log K changed at 2% match experimental conditions																Sorbed	1.40E-06
																Aquous	4.61E-11
																ratio	30,374.41
																bacteria concentration (kg/L)	0.02
																Kd L/kg	1518720.42
No temperature corrections performed																	
Temperature (K) = 298.1																	
Ionic Strength corrections performed:																	
Ionic strength = 0.021 Calculated																	
Component	Type	Charge	Total(M)	Log Free	Free Molarity												
Ca+2	Total	2	6.55E-03	-2.336	4.61E-03												
SO4-2	Total	-2	8.00E-03	-2.217	6.06E-03												
CO3-2	Total	-2	7.21E-05	-7.294	5.08E-08												
UO2+2	Total	2	1.40E-06	-13.183	6.56E-14												
WOH	Total	0	5.00E-05	-4.313	4.86E-05												
H+	Free	1	0.00E+00	-7	1.00E-07												
H2O	Free	0	5.55E+01	0	1.00E+00												
Species	Type	Molarity	Log M	Delta H	Delta S	Delta G	Log K	Stoichiometry								[UO2]	UO2 distribution
(UO2)2(OH)2+2	Dissolved	4.21E-19	-18.376	48.9	0	0	-5.62		0	0	0	2	0	-2	2	8.42E-19	0.00%
(UO2)2CO3(OH)3-	Dissolved	3.73E-15	-14.428	0	0	0	-0.859		0	0	1	2	0	-3	3	7.46E-15	0.00%
(UO2)2(OH)+3	Dissolved	8.59E-23	-22.066	0	0	0	-2.7		0	0	0	2	0	-1	1	1.72E-22	0.00%
(UO2)3(CO3)6-6	Dissolved	4.87E-30	-29.312	-62.7	0	0	54		0	0	6	3	0	0	0	1.46E-29	0.00%
(UO2)3(OH)4+2	Dissolved	5.91E-25	-24.229	0	0	0	-11.9		0	0	0	3	0	-4	4	1.77E-24	0.00%
(UO2)3(OH)5+	Dissolved	7.27E-22	-21.139	123	0	0	-15.55		0	0	0	3	0	-5	5	2.18E-21	0.00%
(UO2)3(OH)7-	Dissolved	1.21E-24	-23.919	0	0	0	-32.2		0	0	0	3	0	-7	7	3.62E-24	0.00%
(UO2)4(OH)7+	Dissolved	8.68E-28	-27.061	0	0	0	-21.9		0	0	0	4	0	-7	7	3.47E-27	0.00%
Ca2UO2(CO3)3(aq)	Dissolved	2.53E-11	-10.596	0	0	0	30.7		2	0	3	1	0	0	0	2.53E-11	0.00%
CaCO3(aq)	Dissolved	1.18E-07	-6.93	16	0	0	3.22		1	0	1	0	0	0	0	0.00E+00	0.00%
CaHCO3+	Dissolved	2.40E-06	-5.621	0	0	0	11.529		1	0	1	0	0	1	0	0.00E+00	0.00%
CaOH+	Dissolved	5.09E-09	-8.293	64.1	0	0	-12.697		1	0	0	0	0	-1	1	0.00E+00	0.00%
CaSO4(aq)	Dissolved	1.94E-03	-2.713	7.1	0	0	2.36		1	1	0	0	0	0	0	0.00E+00	0.00%
CaUO2(CO3)3-2	Dissolved	5.49E-12	-11.26	0	0	0	27.18		1	0	3	1	0	0	0	5.49E-12	0.00%
H2CO3*(aq)	Dissolved	9.94E-06	-5.003	-32	0	0	16.681		0	0	1	0	0	2	0	0.00E+00	0.00%
HCO3-	Dissolved	5.96E-05	-4.225	-14.6	0	0	10.329		0	0	1	0	0	1	0	0.00E+00	0.00%
HSO4-	Dissolved	3.26E-08	-7.487	22	0	0	1.99		0	1	0	0	0	1	0	0.00E+00	0.00%
UO2(CO3)2-2	Dissolved	2.09E-12	-11.68	18.5	0	0	16.61		0	0	2	1	0	0	0	2.09E-12	0.00%
UO2(CO3)3-4	Dissolved	5.96E-14	-13.225	-39.2	0	0	21.84		0	0	3	1	0	0	0	5.96E-14	0.00%
UO2(OH)2	Dissolved	1.89E-12	-11.723	0	0	0	-12.15		0	0	0	1	0	-2	2	1.89E-12	0.00%
UO2(OH)3-	Dissolved	1.50E-13	-12.823	0	0	0	-20.25		0	0	0	1	0	-3	3	1.50E-13	0.00%
UO2(OH)4-2	Dissolved	1.44E-18	-17.843	0	0	0	-32.4		0	0	0	1	0	-4	4	1.44E-18	0.00%
UO2(SO4)2-2	Dissolved	1.01E-14	-13.997	35.1	0	0	4.14		0	2	0	1	0	0	0	1.01E-14	0.00%
UO2CO3(aq)	Dissolved	8.78E-12	-11.057	5	0	0	9.94		0	0	1	1	0	0	0	8.78E-12	0.00%
UO2OH+	Dissolved	2.03E-12	-11.693	0.9	0	0	-5.25		0	0	0	1	0	-1	1	2.03E-12	0.00%
UO2(SO4)3-4	Dissolved	1.53E-17	-16.815	0	0	0	3.02		0	3	0	1	0	0	0	1.53E-17	0.00%
UO2SO4(aq)	Dissolved	1.70E-13	-12.77	19.5	0	0	3.15		0	1	0	1	0	0	0	1.70E-13	0.00%
OH-	Dissolved	1.01E-07	-6.997	55.8	0	0	-13.997		0	0	0	0	0	-1	1	0.00E+00	0.00%
WOUOOH	Dissolved	7.65E-09	-8.116	0	0	0	-4.23		0	0	0	1	1	-2	1	7.65E-09	0.55%
WOU2	Dissolved	1.39E-06	-5.856	0	0	0	4.9		0	0	0	1	1	-1	0	1.39E-06	99.43%
																1.40E-06	99.98%

Reactions 1 and 2 at pH 6 and 2% PCO2 to determine if the model fits experimental condtions																	% Sorbed	85.19%	
																	%Aquous	14.81%	
No temperature corrections performed																			
Temperature (K) = 298.1																			
Ionic Strength corrections performed:																			
Ionic strength = 0.022 Calculated																			
Component	Type	Charge	Total(M)	Log Free	Free Molarity														
Ca+2	Total	2	6.55E-03	-2.338	4.59E-03														
SO4-2	Total	-2	8.00E-03	-2.215	6.09E-03														
CO3-2	Total	-2	3.27E-03	-6.983	1.04E-07														
UO2+2	Total	2	1.40E-06	-10.311	4.89E-11														
WOH	Total	0	5.00E-05	-4.312	4.88E-05														
H+	Free	1	0.00E+00	-6	1.00E-06														
H2O	Free	0	5.55E+01	0	1.00E+00														
Species	Type	Molarity	Log M	Delta H	Delta S	Delta G	Log K	Stoichiometry								[UO2]	UO2 distribution		
(UO2)2(OH)2+2	Dissolved	2.31E-15	-14.637	48.9	0	0	-5.62		0	0	0	2	0	-2	2	4.61E-15	0.00%		
(UO2)2CO3(OH)3-	Dissolved	4.12E-12	-11.385	0	0	0	-0.859		0	0	1	2	0	-3	3	8.24E-12	0.00%		
(UO2)2(OH)+3	Dissolved	4.76E-18	-17.322	0	0	0	-2.7		0	0	0	2	0	-1	1	9.52E-18	0.00%		
(UO2)3(CO3)6-6	Dissolved	1.47E-19	-18.832	-62.7	0	0	54		0	0	6	3	0	0	0	4.42E-19	0.00%		
(UO2)3(OH)4+2	Dissolved	2.38E-20	-19.623	0	0	0	-11.9		0	0	0	3	0	-4	4	7.15E-20	0.00%		
(UO2)3(OH)5+	Dissolved	2.91E-18	-17.536	123	0	0	-15.55		0	0	0	3	0	-5	5	8.73E-18	0.00%		
(UO2)3(OH)7-	Dissolved	4.81E-23	-22.318	0	0	0	-32.2		0	0	0	3	0	-7	7	1.44E-22	0.00%		
(UO2)4(OH)7+	Dissolved	2.56E-23	-22.592	0	0	0	-21.9		0	0	0	4	0	-7	7	1.02E-22	0.00%		
Ca2UO2(CO3)3(aq)	Dissolved	1.53E-07	-6.815	0	0	0	30.7		2	0	3	1	0	0	0	1.53E-07	10.94%		
CaCO3(aq)	Dissolved	2.36E-07	-6.627	16	0	0	3.22		1	0	1	0	0	0	0	0.00E+00	0.00%		
CaHCO3+	Dissolved	4.81E-05	-4.318	0	0	0	11.529		1	0	1	0	0	1	0	0.00E+00	0.00%		
CaOH+	Dissolved	5.04E-10	-9.298	64.1	0	0	-12.697		1	0	0	0	0	-1	1	0.00E+00	0.00%		
CaSO4(aq)	Dissolved	1.91E-03	-2.719	7.1	0	0	2.36		1	1	0	0	0	0	0	0.00E+00	0.00%		
CaUO2(CO3)3-2	Dissolved	3.38E-08	-7.471	0	0	0	27.18		1	0	3	1	0	0	0	3.38E-08	2.42%		
H2CO3*(aq)	Dissolved	2.01E-03	-2.697	-32	0	0	16.681		0	0	1	0	0	2	0	0.00E+00	0.00%		
HCO3-	Dissolved	1.21E-03	-2.917	-14.6	0	0	10.329		0	0	1	0	0	1	0	0.00E+00	0.00%		
HSO4-	Dissolved	3.25E-07	-6.488	22	0	0	1.99		0	1	0	0	0	1	0	0.00E+00	0.00%		
UO2(CO3)2-2	Dissolved	6.40E-09	-8.194	18.5	0	0	16.61		0	0	2	1	0	0	0	6.40E-09	0.46%		
UO2(CO3)3-4	Dissolved	3.80E-10	-9.421	-39.2	0	0	21.84		0	0	3	1	0	0	0	3.80E-10	0.03%		
UO2(OH)2	Dissolved	1.39E-11	-10.856	0	0	0	-12.15		0	0	0	1	0	-2	2	1.39E-11	0.00%		
UO2(OH)3-	Dissolved	1.11E-13	-12.956	0	0	0	-20.25		0	0	0	1	0	-3	3	1.11E-13	0.00%		
UO2(OH)4-2	Dissolved	1.06E-19	-18.974	0	0	0	-32.4		0	0	0	1	0	-4	4	1.06E-19	0.00%		
UO2(SO4)2-2	Dissolved	7.45E-12	-11.128	35.1	0	0	4.14		0	2	0	1	0	0	0	7.45E-12	0.00%		
UO2CO3(aq)	Dissolved	1.32E-08	-7.881	5	0	0	9.94		0	0	1	1	0	0	0	1.32E-08	0.94%		
UO2OH+	Dissolved	1.50E-10	-9.824	0.9	0	0	-5.25		0	0	0	1	0	-1	1	1.50E-10	0.01%		
UO2(SO4)3-4	Dissolved	1.16E-14	-13.937	0	0	0	3.02		0	3	0	1	0	0	0	1.16E-14	0.00%		
UO2SO4(aq)	Dissolved	1.25E-10	-9.903	19.5	0	0	3.15		0	1	0	1	0	0	0	1.25E-10	0.01%		
OH-	Dissolved	1.01E-08	-7.997	55.8	0	0	-13.997		0	0	0	0	0	-1	1	0.00E+00	0.00%		
WOUO2CO3	Dissolved	1.04E-06	-5.982	0	0	0	10.15		0	0	1	1	1	-1	0	1.04E-06	74.43%	85.19%	
WOUO2(CO3)2	Dissolved	1.51E-07	-6.822	0	0	0	16.03		0	0	2	1	1	-1	0	1.51E-07	10.76%		
																	99.98%		